S. Schlorholtz, K.L. Bergeson

Final Report

Investigation of Rapid Thermal Analysis Procedures for Prediction of the Service Life of PCCP Carbonate Coarse Aggregate

June 1993

Sponsored by the Iowa Department of Transportation,
Highway Division, and the
Iowa Highway Research Board

Iowa Dot Project HR-337
ERI Project 3473
ISU-ERI-Ames 93-412

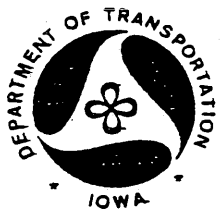

Iowa Department
of Transportation

report

College of
Engineering
Iowa State University

S. Schlorholtz, K.L. Bergeson

Final Report

Investigation of Rapid Thermal Analysis Procedures for Prediction of the Service Life of PCCP Carbonate Coarse Aggregate

Sponsored by the Iowa Department of Transportation,
Highway Division, and the
Iowa Highway Research Board

Iowa Dot Project HR-337
ERI Project 3473
ISU-ERI-Ames 93-412

Civil and Construction Engineering Department

engineering
research institute
iowa state university

TABLE OF CONTENTS

ABSTRACT

The major objective of this research project was to use thermal analysis techniques in conjunction with x-ray analysis methods to identify and explain chemical reactions that promote aggregate related deterioration in portland cement concrete.

Twenty-two different carbonate aggregate samples were subjected to a chemical testing scheme that included:

- bulk chemistry (major, minor and selected trace elements)
- bulk mineralogy (minor phases concentrated by acid extraction)
- solid-solution in the major carbonate phases
- crystallite size determinations for the major carbonate phases
- a salt treatment study to evaluate the impact of deicer salts

Test results from these different studies were then compared to information that had been obtained using thermogravimetric analysis techniques. Since many of the limestones and dolomites that were used in the study had extensive field service records it was possible to correlate many of the variables with service life.

The results of this study have indicated that thermogravimetric analysis can play an important role in categorizing carbonate aggregates. In fact, with modern automated thermal analysis systems it should be possible to utilize such methods on a quality control basis.

Strong correlations were found between several of the variables that were monitored in this study. In fact, several of the variables exhibited significant correlations to concrete service life. When the full data set was utilized (n = 18), the significant correlations to service life can be summarized as follows (α = 5% level):

- Correlation coefficient, r, = -0.73 for premature TG loss versus service life.
- Correlation coefficient, r, = 0.74 for relative crystallite size versus service life.
- Correlation coefficient, r, = 0.53 for ASTM C666 durability factor versus service life.
- Correlation coefficient, r, = -0.52 for acid-insoluble residue versus service life.

Separation of the carbonate aggregates into their mineralogical categories (i.e., calcites and dolomites) tended to increase the correlation coefficients for some specific variables (r sometimes approached 0.90); however, the reliability of such correlations was questionable because of the small number of samples that were present in this study.

INTRODUCTION

The following report summarizes research activities conducted on Iowa Department of Transportation (IDOT) Project HR-337, for the period May 1, 1991 through June 30, 1993. The objective of this research project was to investigate if thermal analysis techniques could be used in conjunction with x-ray analysis techniques to identify and explain chemical reactions that promote aggregate related deterioration in portland cement concrete.

BACKGROUND AND DEFINITION OF THE PROBLEM

Highway engineers have always desired to specify concrete pavement mixes that exhibit excellent durability characteristics. However, both early and recent studies have clearly indicated that durability can be a difficult property to define explicitly. Much of the difficulty arises from the fact that concrete is a composite material; and hence, it may fail through the action of a variety of different mechanisms that may act individually or in unison.

Water plays a major role in the durability of portland cement concrete pavements. This is not only due to the fact that water promotes freeze-thaw deterioration. One must also remember that water acts as the major transport medium for other time dependent degradation processes. For instance, both sulfate attack and alkali-aggregate reaction are strongly dependent on the moisture content of the concrete and the relative humidity of the local environment. Without adequate moisture these various degradation processes would have little influence on the durability of portland cement concrete. Hence, the key to avoiding durability related problems hinges on the engineers knowledge of the various materials that will be used to proportion the concrete mix and the environment that the concrete will be subjected to. This sounds like a relatively easy task but a number of practical details tend to complicate the design criteria.

First, it is important to understand that no single test method currently exists that can be used to accurately predict the durability of portland cement concrete. Field service record is the only true measurement of durability that is available.

Popovics [1] has expressed this fact as follows:

> "Considering everything, at the present time the service record is the engineer's most reliable criterion for predicting the aggregate performance concerning durability of concrete. Existing methods for testing the frost resistance of aggregates can show, at best, the relative frost resistance of aggregates, but they cannot predict the performance of a concrete made with an aggregate under specific field conditions."

Field service record is only roughly quantitative (i.e., measurable only to about 5 to 10 year increments) and is strongly dependent on both materials and environmental factors. Hence, service record may not be quick to respond to changes in the quality of cement or other additives that are routinely added to modern concretes. Obviously, it takes a very long time for an aggregate source to obtain a reliable field service record.

And secondly, these difficulties have caused engineers to create a wide variety of different accelerated test methods that can be used to estimate the durability of concrete. Some of the test methods that have been developed focus on the individual constituents present in concrete, while other methods have been constructed to probe the durability of laboratory concrete specimens. A summary of the different tests that are commonly used to predict the freeze-thaw durability of a given test specimen is given in Table 1. It is pertinent to add that all of the accelerated tests attempt to predict service life by directly (or indirectly) categorizing materials (or concretes) using a relative performance rating scheme or a maximum allowable criterion; however, none of the tests has been found to be very reliable. Some of the test methods correlate to service life better than others but none of the tests produce absolute durability information. Hence, the search for the "perfect" durability test still continues.

The purpose of this study was to investigate if thermal analysis techniques could be used to predict the freeze-thaw durability of coarse aggregates commonly found in (or near) Iowa. Thermal analysis techniques were investigated because the tests can be conducted relatively fast (in minutes or hours), the tests can be automated and they have excellent precision and accuracy.

Table 1. Durability tests that are commonly used for aggregates and/or concrete materials.

Type	Method	Description	Time to Complete
A	ASTM C 88	Soundness of Aggregates by use of Sodium Sulfate or Magnesium Sulfate	days
A	ASTM C 295	Petrographic Examination of Aggregates for Concrete	days
A	IDOT	Pore Index test	days
A	SHRP (AASHTO)	Washington Hydraulic Fracture Test	days
C	ASTM C 666	Resistance of Concrete to Rapid Freezing and Thawing	weeks to months
C	ASTM C 671	Critical Dilation of Concrete Specimens Subjected to Freezing	weeks to months
C	ASTM C 682	Evaluation of Frost Resistance of Coarse Aggregates in Air-Entrained Concrete by Critical Dilation Procedures	weeks to months

A = Aggregate test; C = Concrete test

RESEARCH APPROACH

Sampling Scheme

Twenty coarse aggregate samples were selected for the first phase of this study. The samples were selected based on availability, homogeneity and service record. A summary of the samples that were selected is given in Table 2. The table also lists the aggregates service record and durability factor (ASTM C 666, method B) when used in IDOT C-3 concrete mixes.

A sample size of 200 to 300 pounds of crushed stone was taken from the various quarries. One third of the sample (about 100 pounds) was crushed in a jaw mill to obtain a maximum particle size of about 1/4 inch. A representative sub-sample of this crushed material was then obtained by

Table 2. Summary of the coarse aggregate samples studied in this project.

Sample Identification	Quarry Location	Service Record, Years to Visible Deterioration	C 666 Durability Factor
Eldorado	SW17 T095 R08W	40	97
Maryville	SE24 T091 R07W	40	96
Alden (tan, bed 3)	NW20 T089 R21W	40	96
Crescent (beds 25 d, e)	35 T076 R44W	07	75
Menlo (bed 15)	SE17 T077 R31W	10	88
Montour (beds 1-7)	NW09 T083 R16W	40	84
Garrison (beds 12-16)	NE33 T085 R11W	15	100
Pesky (bed 5)	SW01 T088 R12W	15	90
Lamont (bed 4)	NW14 T090 R07W	40	96
Cedar Rapids South-Gray	NW07 T082 R07W	N/A	N/A
Cedar Rapids South-Tan	NW07 T082 R07W	40	99
Plower (beds 1-9)	SE36 T086 R06W	10	88
Early Chapel (bed 15)	NW10 T076 R29W	10	65
Linwood	SW13 T077 R02E	30	94
Bryan	Minnesota	15	93
Conklin (beds 6-9)	NW33 T080 R06W	30	88
Skyline (beds 1-3)	SE10 T098 R08W	25-30	92
Gassman	SE07 T088 R03E	40?	N/A
Huntington	Missouri	20-25	92
Le Claire	NW35 T079 R05E	25	98
Landis	SE12 T093 R08W	?	?
Lisbon	NW24 T082 R05W	20?	?

N/A = Not Available ? = Questionable

riffle splitting. This sample was used for the chemical and physical tests conducted in this research project. The remaining (uncrushed) sample was placed in storage.

Two additional aggregate sources were added to the study during phase II. These samples were delivered to the laboratory as hand specimens (approximately 10 to 15 pound chunks of

material) and they were included in the research program because Mr. Wendell Dubberke had observed some strange trends in the thermal analysis testing that had been conducted by the Iowa Department of Transportation in research project HR-336.

Hand specimens of a selected number of the phase I samples were also obtained for the second year of this project. These hand specimens included Maryville, Lamont, Alden, Plower, Garrison, Crescent, Early Chapel, Montour, Linwood, LeClaire, Gassman, Skyline, South Cedar Rapids (Gray), Pesky, Conklin, and Eldorado stones.

Equipment and Methods

All of the aggregate samples were subjected to detailed chemical and mineralogical analysis. X-ray methods were utilized for bulk composition (both bulk chemistry and bulk mineralogy). Also, thermal analytical techniques and both light microscopy and scanning electron microscopy were used to study the thermal stability and morphology, respectively, of the various stone samples. The aggregate samples were also subjected to salt solutions (10 percent NaCl and 10 percent $CaCl_2$) and then re-analyzed. This salt treatment study was conducted to evaluate the influence of deicing salts on the various aggregates.

X-ray diffraction (XRD) was used to identify the major and minor crystalline compounds present in each sample. The identification of minor constituents was enhanced by an acid digestion process which removed the major (carbonate) minerals from the test specimen. These tests were performed in a manner similar to the standard procedure described in ASTM D 3042 [2]; however, the bulk samples were ground to a small particle size (passing a #100 mesh sieve) to reduce the time that was needed to dissolve the carbonate fraction of the various samples. The acid-insoluble residue was thoroughly washed with deionized water and then dried at 50° C (rather than 110° C). This was done to allow for the identification of the clay minerals that were present in the acid-insoluble fraction of the carbonate stones. The acid-insoluble residue was subjected to X-ray diffraction analysis using both side-loaded specimens and oriented aggregate specimens.

The side-loading technique helps to minimize preferred orientation, this was important for the proper identification of the various feldspar minerals that were present in the acid-insoluble residue.

The oriented aggregate specimens were made using a procedure described by Pollastro [3]. This procedure consists of a series of treatments that help to simplify the identification of clay minerals. The treatments that were used in this study were {1} air-dry (50 percent relative humidity) to identify the location of the major clay mineral peaks; {2} glycolation to expand any swelling minerals present in the sample (1 day @ 50° C in a desiccator filled with ethylene glycol vapor, see Carroll [4] for explicit details); and {3} heat treatment (1 hour at 550° C) to collapse or destroy the clay minerals present in the acid-insoluble residue. This experimental program was not as rigorous as the procedures that are commonly used for the identification of clay minerals [4,5]; however the procedure was adequate for the purpose of this research project.

A Siemens D 500 x-ray diffractometer was used throughout this study. The diffractometer was controlled by a PDP 11/23 computer via an LC 500 interface. A copper x-ray tube was used for all diffraction work. The diffractometer was equipped with a diffracted beam monochromator. Normally the diffractometer was operated with the various slits in a medium resolution configuration; however, the slits were placed in a high resolution configuration for some of the crystallite size measurements.

X-ray fluorescence (XRF) analysis was used to quantify the major, minor and selected trace elements present in the various samples. A Siemens SRS 200 sequential x-ray spectrometer was used for all the analyses. The spectrometer was fully computer controlled via an IBM compatible microcomputer and a LC 200 interface. The spectrometer was operated in vacuum mode, and, depending on the element of interest, employed either a chromium or tungsten x-ray tube.

Test specimens for XRF analysis were prepared using two different sample preparation techniques. The first technique that was used was a loose powder method. This method allows samples to be prepared very quickly since they only need to be ground to a fine particle size (passing #200 mesh sieve) and then loaded into disposable specimen cups. The major drawback to this sample preparation technique is that plastic (prolene, 4 microns thick) film must be used to seal the sample in the specimen cups. The film attenuates much of the fluorescent x-radiation from light elements. This causes the method to have poor sensitivity to light elements like Na, Mg and Al, or to

elements present in low quantities (i.e., trace elements). The second sample preparation technique used pressed pellets. The basic recipe that was used can be summarized as follows:

{1} The bulk sample was ground in a shatterbox for two minutes to homogenize the sample.

{2} Eight (8.00) grams of sample was mixed with 0.80 grams of x-ray mix powder and two boric acid tablets.

{3} The mixture was then ground in a shatterbox for two minutes to create an intimate mixture.

{4} Eight grams (8.0) of the ground-up mixture was then pressed into a 40 mm pellet using a sample press. All pellets were compacted using 26 tons of load.

The second sample preparation method was much slower than the first method; however, the use of pressed pellet specimens nearly doubled the analyte intensity that was observed for sodium and magnesium. Hence, analysis time was reduced and the detection limit of the technique was substantially improved.

The thermal analysis studies utilized a TA Instruments 2000 thermal analysis system. The system employed a TA Hi-Res. TGA 2950 thermogravimetric analyzer module, and a high temperature (1500° C), simultaneous DTA/TGA module (STD 2960). The Hi-Res. TGA system was equipped with a 16 sample carousel. A typical TGA experiment used the following analytical parameters: {1} a scanning rate of 40° per minute, resolution = 5; {2} a sample mass of 55 ± 2 milligrams for powder specimens and a mass of about 50 to 130 mg for chip specimens; {3} a dynamic nitrogen or carbon dioxide atmosphere (depending on the goal of the experiment), purged at 100 ml per minute; {4} test specimens were heated from 100° C to about 970° C in platinum sample cups.

A typical experiment that was run on the simultaneous DTA/TGA module (STD 2960) used the following analytical parameters: {1} a scanning rate of 10°/minute; {2} a sample mass of about 20 milligrams (depending on the type of experiment that was being performed); {3} a carbon dioxide or air atmosphere that was purged at 100 ml per minute; {4} test specimens were heated from room temperature to 1400° C in corundum specimen holders.

A JEOL JSM-840 scanning electron microscope (SEM) was used to examine the morphology of the coarse aggregate samples. The SEM is interfaced to both a KEVEX Delta V Microanalyzer and a WDX-2A wavelength dispersive x-ray spectrometer, this allows researchers to supplement morphological features with detailed chemical information.

All of the pulverized carbonate stones were subjected to particle size separation by using an Allen-Bradley Sonic sifter (model L3P). The apparatus uses waves of sonic frequency to agitate particles on the sieves and thus, produces relatively quick and accurate size separation. Electroformed nickel metal sieves with nominal sizes of 105, 45 and 20 microns were used throughout this study. The particles passing through all of the sieves were also collected for subsequent analysis. Hence, four particle size fractions were obtained from the sonic sifter: {1} particles greater than 105 microns (denoted as +105); {2} particles smaller than 105 but larger than 45 microns (denoted as +45); {3} particles smaller than 45 but greater than 20 microns (denoted as +20); {4} particles smaller than 20 microns in diameter (denoted as fines or -20).

RESULTS AND DISCUSSION

X-Ray Studies

Bulk properties

The results of the bulk XRD scans are summarized in Table 3. X-ray diffractograms of all the samples can be found in Appendix I. The JCPDS database information that was used to identify the minerals that were present in the various diffractograms has also been placed in Appendix I.

Semi-quantitative estimates of the amounts of calcite and dolomite are also listed in Table 3. These values refer only to the carbonate fraction of the various samples (i.e., % calcite + % dolomite = 100). The acid insoluble residue column gives an indication of the amount of noncarbonate material that was present in the samples.

The results of x-ray diffraction analysis of the acid-insoluble residue tests are summarized in Table 4. The removal of the carbonate fraction simplified the identification of the minor and trace minerals that were present in the various samples. Hence, one should rely on the test results listed in

Table 3. Minerals identified in the bulk specimens by using XRD analysis.

⇐ Limestones ⇒							
	Minerals				Rough QXRD (carbonates only)		
Sample	Calcite	Dolomite	Quartz	Pyrite	%Calcite	%Dolomite	Acid Insoluble Residue (wt %)
Alden	M	-	-	-	100	0	0.38
Crescent	M	T	m	-	100	0	3.07
Conklin	M	-	-	-	100	0	0.90
Early Chapel	M	m	m	-	96	4	3.76
Eldorado	M	-	T	-	100	0	1.01
Linwood	M	T	m	-	100	0	1.83
Menlo	M	-	m	-	100	0	4.46
Montour	M	T	-	T	99	1	1.48
Skyline	M	M	m	-	71	29	2.66
Huntington	M	m	m	-	88	12	2.13
⇐ Dolomites ⇒							
	Minerals				Rough QXRD (carbonates only)		
Sample	Calcite	Dolomite	Quartz	Pyrite	%Calcite	%Dolomite	Acid Insoluble Residue (wt %)
Maryville	m	M	T	-	10	90	3.25
Bryan	m	M	m	-	4	96	10.3
C. Rapids-Gray	T	M	m	T	1	99	2.94
C. Rapids-Tan	T	M	T	-	1	99	1.29
Garrison	m	M	T	T	9	91	3.73
Gassman	m	M	m	-	1	99	2.34
Lamont	T	M	T	-	1	99	1.59
LeClaire	T	M	T	-	2	98	3.87
Pesky	m	M	T	-	11	89	2.15
Plower	M	M	m	-	14	86	2.47
Landis	T	M	m	-	1	99	5.30
Lisbon	T	M	m	-	1	99	2.55

M = major component; m = minor component; T = trace/uncertain

Table 4. Minerals identified in the acid-insoluble residue of the various carbonate stones.

⇐ Limestones ⇒								
	Minerals							
			Feldspar		Clay			
Sample	Quartz	Pyrite	Orthoclase	Albite	Kaolinite	Illite	Montmorillonite	Other
Alden	M	-	-	-	M	M	-	? mixed layer clay
Crescent	M	T	m	-	-	M	-	-
Conklin	M	m	T	-	-	m	-	-
Early Chapel	M	T	-	m	T	m	-	-
Eldorado	M	m	m	-	T	m	-	? mixed layer clay
Linwood	M	m	-	-	T	m	-	? feldspar
Menlo	M	-	-	m	T	m	T	-
Montour	M	M	-	-	-	-	-	? feldspar
Skyline	M	-	m	-	-	m	-	-
Huntington	M	m	-	-	-	T	-	? feldspar
⇐ Dolomites ⇒								
	Minerals							
			Feldspar		Clay			
Sample	Quartz	Pyrite	Orthoclase	Albite	Kaolinite	Illite	Montmorillonite	Other
Maryville	M	-	m	-	m	m	-	-
Bryan	M	-	m	-	-	T	-	-
C.Rapids-Gray	M	m	m	-	-	T	-	-
C.Rapids-Tan	M	-	m	-	-	T	-	? hematite
Garrison	M	m	m	-	-	T	-	? gypsum
Gassman	M	-	m	-	-	m	-	-
Lamont	M	-	T	-	m	m	-	-
LeClaire	M	-	m	-	m	m	-	-
Pesky	M	m	m	-	-	m	-	-
Plower	M	-	m	-	-	m	-	? mixed layer clay
Landis	M	-	T	-	-	m	-	-
Lisbon	m	-	M	-	-	m	-	-

M = major component; m = minor component; T = trace; ? = questionable

Table 4 for the most accurate identification of minor minerals (noncarbonates) that were present in the samples. However, one must remember that all acid soluble materials, in addition to the carbonate minerals, would have been removed by the acid treatment. Also, there was a chance that the clay mineral fraction could have been altered by the acid extraction [6], although this alteration would have been minimal for the clays that were identified in this study.

The results of the bulk XRF tests using the loose powder specimen preparation technique are summarized in Table 5. The loss-on-ignition (LOI) values listed in the table were obtained from bulk LOI tests (1 gram samples, ignited @ 950 ± 25° C for 1 hour). All of the assays have been expressed as oxides. This allows one to quickly check the overall reliability of the analyses since the oxide totals should approach 100 percent. Also, the reliability of the XRF test method was evaluated by inserting standards into the spectrometer along with the test specimens. Two of the standards were certified reference materials of National Institute of Standards and Technology (NIST, previously known as the NBS) or British Chemical Society (BCS) quality. The remaining standard was high purity calcite from Fisher Scientific Company. One of the standards (NBS 1c) had been included in the original development of the calibration curves for the various elements; and hence, cannot be used to estimate the bias in the method. This standard was used only to monitor drift in the XRF spectrometer. The remaining standards (BCS 368 and Fisher Calcite) had not been used in the calibration procedure and can be used to estimate the potential bias in the analytical method. The test results obtained from the various standards are summarized in Table 6. The measured values are in reasonably good agreement with the certified (or specified) values.

The results of the bulk and trace element XRF tests using the pressed pellet specimen preparation technique are summarized in Table 7. In general, the results are very similar to those that were obtained using the loose powder technique (compare Tables 5 and 7). However, there are a few discrepancies that must be noted.

First, the Si values, expressed as SiO_2 in this instance, appear to diverge with increasing Si content. This trend was most evident in the dolomite specimens and was partially due to the fact that few standards were available for calibration. Most well characterized standards (i.e., NIST quality or

Table 5. Results of bulk XRF analyses on the carbonate stone specimens (loose powder technique).

⟸ Limestones ⟹										
Oxide (wt.%)	Early Chapel	Menlo	Conklin	Montour	Crescent	Eldorado	Skyline	Huntington	Linwood	Alden
SiO_2	2.77	3.99	0.62	0.27	2.41	1.20	1.87	1.50	0.79	0.16
Fe_2O_3	0.60	0.33	0.19	0.60	0.18	0.16	0.31	0.12	0.22	0.20
Al_2O_3	0.40	0.37	0.12	0.05	0.25	0.26	0.28	0.13	0.16	0.06
TiO_2	0.02	0.02	0.01	<0.01	0.02	0.02	0.02	0.01	0.01	0.01
P_2O_5	0.02	0.02	<0.01	<0.01	0.01	<0.01	0.03	0.04	<0.01	0.01
MnO	0.04	0.03	0.05	0.02	0.02	0.01	0.02	0.02	0.05	0.02
CaO	52.39	52.56	53.44	53.13	52.94	54.89	47.40	52.72	52.96	53.75
SrO	0.04	0.04	0.02	0.02	0.04	0.02	0.02	0.02	0.02	0.03
MgO	0.71	0.35	0.44	0.41	0.42	0.29	4.34	1.18	0.32	0.30
K_2O	0.08	0.08	0.04	0.01	0.06	0.08	0.14	0.04	0.04	0.01
SO_3	0.04	<0.01	0.04	0.20	0.05	0.03	<0.01	0.04	0.09	<0.01
LOI+mc	42.6	42.3	43.7	43.6	42.9	43.4	44.0	43.6	43.2	44.1
SUM	99.7	100.1	98.7	98.3	99.3	100.4	98.4	99.4	97.9	98.6
⟸ Dolomites ⟹										
Oxide (wt.%)	Maryville	Gassman	Ced. Rapids-Gray	Bryan	LeClaire	Lamont	Garrison	Plower	Pesky	Ced. Rapids-Tan
SiO_2	2.16	2.07	2.83	7.67	1.46	1.46	2.27	2.56	1.69	0.76
Fe_2O_3	0.27	0.93	0.30	2.74	0.35	0.20	0.84	0.94	0.46	0.53
Al_2O_3	0.42	0.42	0.24	0.77	0.33	0.23	0.48	0.44	0.31	0.16
TiO_2	0.03	0.03	0.02	0.04	0.03	0.02	0.03	0.03	0.02	0.01
P_2O_5	0.01	0.07	0.01	0.08	0.01	<0.01	0.02	0.02	<0.01	0.01
MnO	0.02	0.05	0.03	0.20	0.04	0.02	0.04	0.04	0.02	0.03
CaO	32.13	29.76	30.34	28.92	30.08	30.34	32.39	31.91	34.38	30.12
SrO	0.02	0.01	0.02	0.02	0.02	0.02	0.02	0.02	0.02	0.02
MgO	16.22	17.93	18.84	15.72	18.43	18.52	15.62	16.72	13.18	18.54
K_2O	0.10	0.18	0.11	0.31	0.09	0.07	0.15	0.16	0.10	0.06
SO_3	<0.01	<0.01	0.06	<0.01	<0.01	<0.01	0.27	0.01	0.21	<0.01
LOI+mc	46.0	46.5	45.8	42.0	46.4	46.8	45.0	45.4	45.9	46.7
SUM	97.4	97.9	98.6	98.5	97.2	97.7	97.1	98.3	96.3	97.0

LOI = loss-on-ignition @ 950°C, mc = moisture content @ 105°C, all samples had moisture contents less than 0.3%

Table 6. Comparison of measured (by XRF) and certified values for three standards (loose powder technique).

	NBS 1c*		BCS 368		Fisher Calcite	
Oxide (wt.%)	Measured	Certified	Measured	Certified	Measured	Certified
SiO_2	6.90	6.84	0.86	0.92	0.02	N/M
Fe_2O_3	0.57	0.55	0.25	0.23	0.00	<0.005
Al_2O_3	1.20	1.30	0.10	0.17	0.02	N/M
TiO_2	0.07	0.07	0.01	<0.01	0.01	N/M
P_2O_5	0.04	0.04	0.01	-	0.00	N/M
MnO	0.02	0.025	0.05	0.06	0.01	N/M
CaO	50.68	50.3	30.85	30.8	55.01	56
SrO	0.025	0.03	0.017	<0.01	0.021	0.02
MgO	0.45	0.42	20.80	20.9	0.23	0.01
K_2O	0.27	0.28	0.02	<0.01	0.00	<0.01
Na_2O	N/M	0.02	N/M	<0.01	N/M	<0.01
LOI + mc	40.11	39.9	46.84	46.7	43.8	44
SUM	100.3	99.8	99.8	99.8	99.1	100.0

*** This standard was used in the calibration process for the elements (oxides) measured in this study.**
N/M = not measured

better) that were available tended to approximate the composition of pure dolomite; and hence, did not encompass the range of Si that was observed in the samples. This error was compounded by the fact that the intensity of the background radiation for Si was strongly dependent on the calcium content of the specimen matrix (see Figure 1). This made it difficult to use calcite standards to extend the calibration range of the XRF spectrometer. Several other elements were also influenced in a similar manner (see the bottom half of Figure 1). This particular problem is always present in XRF analysis but it becomes most important when analyte concentrations drop to the trace element level (i.e., when the background intensity is nearly equivalent to the analyte intensity) or when the sensitivity of the analyte line is low (i.e., when the counts-per-second/percent of analyte is a small number).

Table 7. Results of bulk XRF analyses on the carbonate stone specimens (pressed pellet technique).

⟸ Limestones (major/minor elements, all values in wt. %) ⟹										
Oxide/ Element	**Early Chapel**	**Menlo**	**Conklin**	**Montour**	**Crescent**	**Eldorado**	**Skyline**	**Huntington**	**Linwood**	**Alden**
SiO_2	2.45	3.33	0.58	0.26	2.01	0.93	1.60	1.34	0.65	0.15
Fe_2O_3	0.55	0.33	0.18	0.58	0.19	0.15	0.30	0.15	0.24	0.19
Al_2O_3	0.38	0.36	0.11	0.01	0.24	0.22	0.24	0.09	0.13	0.03
TiO_2	0.02	0.02	0.01	<0.01	<0.01	0.01	0.02	0.01	0.01	0.01
P_2O_5	0.03	0.02	<0.01	<0.01	0.01	<0.01	0.02	0.05	0.01	0.02
MnO	0.03	0.03	0.05	0.02	0.03	0.01	0.02	0.02	0.04	0.02
CaO	52.16	52.07	54.28	53.88	53.17	53.92	49.54	52.25	53.67	54.14
SrO	0.06	0.05	0.02	0.02	0.06	0.01	0.02	0.02	0.02	0.03
MgO	0.62	0.29	0.35	0.27	0.26	0.23	3.54	0.90	0.19	0.18
K_2O	0.08	0.08	0.04	0.01	0.06	0.08	0.15	0.04	0.04	0.01
Na_2O	0.02	0.01	0.02	0.01	0.03	0.01	0.02	0.03	0.02	0.04
SO_3	0.09	0.01	0.08	0.44	0.10	0.05	0.01	0.07	0.21	0.01
LOI+mc	42.46	42.13	43.57	43.60	42.73	43.09	43.56	43.14	43.11	43.50
SUM	98.95	98.73	99.28	99.10	98.88	98.72	99.03	98.09	98.34	98.33
⟸ Trace Elements (all values in parts-per-million (i.e., $\mu g/_g$)) ⟹										
Oxide/ Element	**Early Chapel**	**Menlo**	**Conklin**	**Montour**	**Crescent**	**Eldorado**	**Skyline**	**Huntington**	**Linwood**	**Alden**
Ba	21	42	<5	<5	11	61	16	<5	<5	<5
Cd	<5	<5	<5	<5	<5	<5	<5	<5	<5	<5
Cl	60	82	82	67	89	89	163	116	62	171
Cr	<10	15	<10	<10	<10	10	<10	<10	<10	15
Cu	8	6	8	12	8	<5	<5	8	<5	<5
Ni	9	8	8	7	<5	<5	6	<5	<5	<5
Pb	<5	12	8	6	6	6	8	9	<5	8
Zn	6	18	<5	<5	6	<5	7	<5	<5	5

Table 7. Results of bulk XRF analyses on the carbonate stone specimens (pressed pellet technique) - (continued).

⟸ Dolomites (major/minor elements, all values in wt. %) ⟹												
Oxide/ Element	Maryville	Gassman	Ced.Rapids -Gray	Bryan	LeClaire	Lamont	Garrison	Plower	Pesky	Ced. Rapids-Tan	Landis	Lisbon
SiO_2	1.61	1.68	2.39	6.82	1.16	1.19	1.99	2.15	1.42	0.68	2.95	0.13
Fe_2O_3	0.27	0.90	0.31	2.64	0.34	0.21	0.80	0.90	0.44	0.49	0.31	0.23
Al_2O_3	0.44	0.46	0.26	0.73	0.37	0.23	0.62	0.51	0.38	0.15	1.25	<0.02
TiO_2	0.03	0.04	0.02	0.04	0.03	0.02	0.04	0.03	0.02	0.01	0.09	0.01
P_2O_5	<0.01	0.06	<0.01	0.06	0.01	<0.01	0.03	0.01	<0.01	0.01	<0.01	<0.01
MnO	0.02	0.04	0.03	0.16	0.04	0.02	0.04	0.04	0.04	0.03	0.02	0.03
CaO	30.99	29.59	28.92	26.67	29.57	29.88	31.68	31.51	34.47	29.99	27.73	30.48
SrO	0.01	<0.01	0.01	0.01	0.01	0.01	0.01	0.01	0.01	0.01	0.01	0.01
MgO	20.0	21.0	20.1	18.5	19.4	20.9	16.3	18.6	14.0	21.6	18.2	20.6
K_2O	0.12	0.24	0.14	0.45	0.12	0.09	0.23	0.22	0.14	0.07	0.36	<0.01
Na_2O	0.06	0.08	0.04	0.02	0.04	0.06	0.07	0.04	0.05	0.03	0.14	0.09
SO_3	<0.01	0.01	0.09	0.01	0.01	<0.01	0.52	0.02	0.36	0.03	0.02	0.02
LOI+mc	46.01	46.47	45.80	42.00	46.45	46.81	45.04	45.37	45.91	46.74	45.78	47.48
SUM	99.6	100.4	98.1	98.0	97.5	99.4	97.3	99.3	97.2	99.7	96.7	98.9
⟸ Trace Elements (all values in parts-per-million (i.e., $\mu g/_g$)) ⟹												
Oxide/ Element	Maryville	Gassman	Ced.Rapids -Gray	Bryan	LeClaire	Lamont	Garrison	Plower	Pesky	Ced. Rapids-Tan	Landis	Lisbon
Ba	12	40	16	82	20	<5	28	57	30	33	44	9
Cd	<5	<5	<5	<5	<5	<5	<5	<5	<5	<5	<5	<5
Cl	699	791	412	221	173	875	275	264	354	300	1175	1131
Cr	10	12	<10	23	<10	10	<10	<10	13	6	23	13
Cu	14	25	8	17	<5	<5	13	8	<5	9	12	6
Ni	<5	<5	7	7	<5	<5	<5	<5	6	<5	<5	8
Pb	<5	5	6	9	8	8	<5	11	11	14	<5	8
Zn	22	8	12	15	14	28	11	25	11	42	8	38

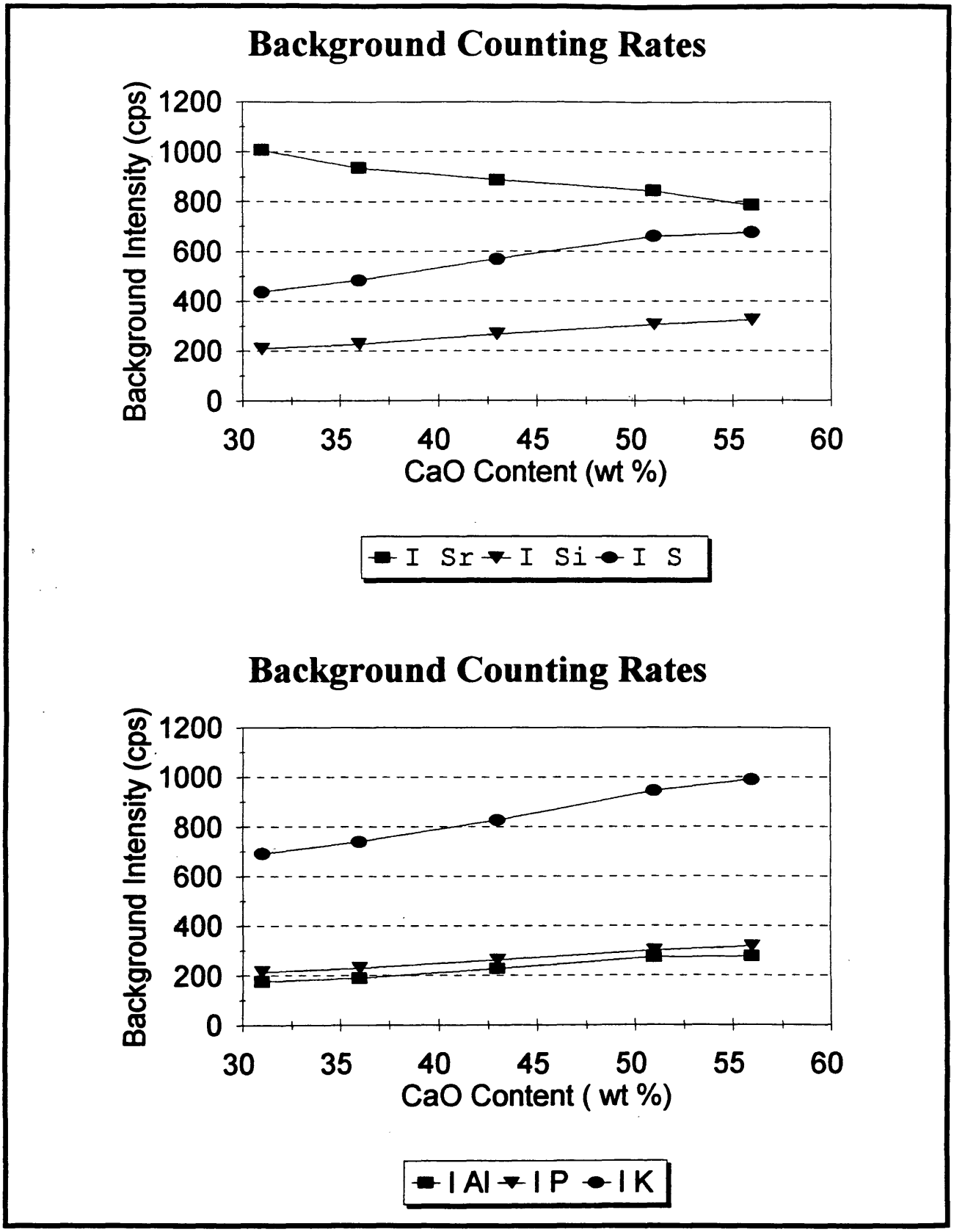

Figure 1. Influence of CaO content on the background intensity of several elements monitored in this study.

Secondly, the Mg contents that are listed in Tables 5 and 7 are considerably different in some cases. For most cases the pressed pellet technique appeared to provide a more reliable estimate of the Mg content. This was basically due to the fact that the analyte intensity for Mg radiation was much higher in the pressed pellets than in the loose powder specimens.

And finally, the S content of the pressed pellet specimens were different than the loose powder specimens because different calibration methods were used. The S content of the pressed pellet specimens was estimated by spiking Lamont and Alden samples with pure pyrite. This process yielded the S content of these two samples plus additional calibration specimens containing known amounts of pyrite. This process was necessary because few of the certified reference materials had known (certified) S concentrations.

The trace elements that were determined in the various carbonate stones are also summarized in Table 7. The most notable contrast between the calcites and the dolomites is that the Cl contents can vary by about an order of magnitude. Also, the Na content of the dolomites is strongly correlated to the Cl content, perhaps this suggests the presence of minor to trace amounts of NaCl. Most often, however, many of the elements that were determined remained below a concentration of about 20 ppm.

Since much of the discussion that will continue later in this report is dependent on the conversion of various elements to oxides or carbonates, the pertinent gravimetric factors for these conversions have been summarized in Table 8. Also, Table 8 contains the formula weights of the various constituents so they can be expressed on a molar basis. These factors greatly simplify the chemical computations that will be conducted later in this report.

Solid solution and crystallite size studies

Goldsmith et al. [7,8,9,10] firmly documented the existence of solid solution in the calcium-magnesium carbonates. Their work indicated that the volume of the unit cell of rhombohedral carbonates varied smoothly (nearly linearly) from its two endmembers (calcite and magnesite). This trend is illustrated in Figure 2. The explanation for the trend is commonly attributed to the size difference between the cations (i.e., most commonly Ca^{2+}, Mg^{2+}, Fe^{2+}, and Mn^{2+} for geological

Table 8. Gravimetric factors and formula weights for the elements and compounds of interest in this study.

Carbonates - Gravimetric factors				
Element	**Multiply by to get —>**	**Oxide**	**Multiply by to get —>**	**Carbonate**
Ca	1.3992	CaO	1.7848	$CaCO_3$
Mg	1.6579	MgO	2.0915	$MgCO_3$
Fe	1.2865	FeO	1.6125	$FeCO_3$
Mn	1.2913	MnO	1.6205	$MnCO_3$
Ba	1.1165	BaO	1.2870	$BaCO_3$
Sr	1.1826	SrO	1.4247	$SrCO_3$
element	<— divide by to get	oxide	<— divide by to get	carbonate

Others - Gravimetric factors		
Element	**Multiply by to get —>**	**Oxide/sulfide**
Fe	1.4297	Fe_2O_3
Fe	2.1483	FeS_2
Al	1.8899	Al_2O_3
K	1.2046	K_2O
S	2.4969	SO_3
S	1.8711	FeS_2
Ti	1.6681	TiO_2
Si	2.1404	SiO_2
P	2.2912	P_2O_5
Na	1.3479	Na_2O
element	<— divide by to get	oxide

Formula Weights	
Item	**Grams/mole**
CaO	56.08
MgO	40.32
K_2O	94.19
Na_2O	61.99
TiO_2	79.90
Al_2O_3	101.94
SiO_2	60.06
CO_2	44.01
P_2O_5	141.96
MnO	70.93
SrO	103.63
$CaCO_3$	100.09
$MgCO_3$	84.32
$MnCO_3$	114.94
$SrCO_3$	147.64
$CaMg(CO_3)_2$	184.41

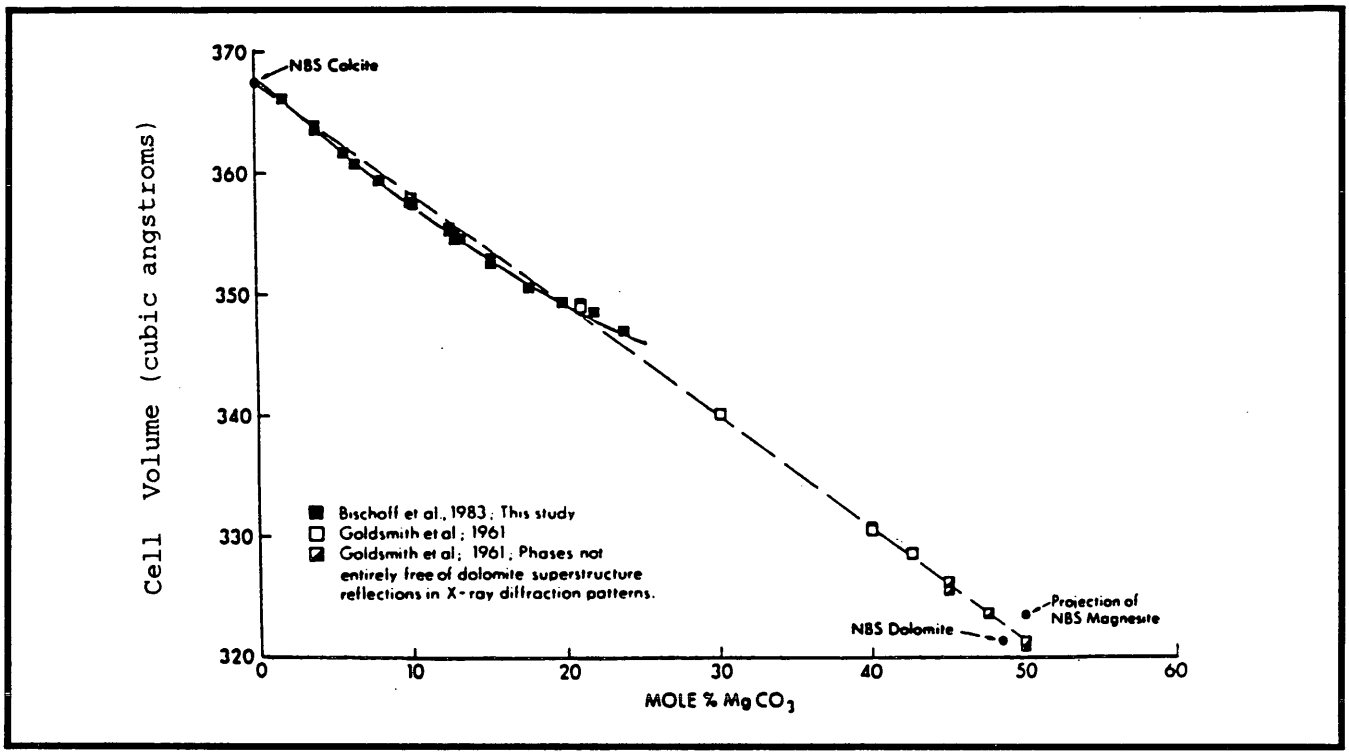

Figure 2. Relationship between percent $MgCO_3$ content and cell volume for carbonates. (adapted from reference 11)

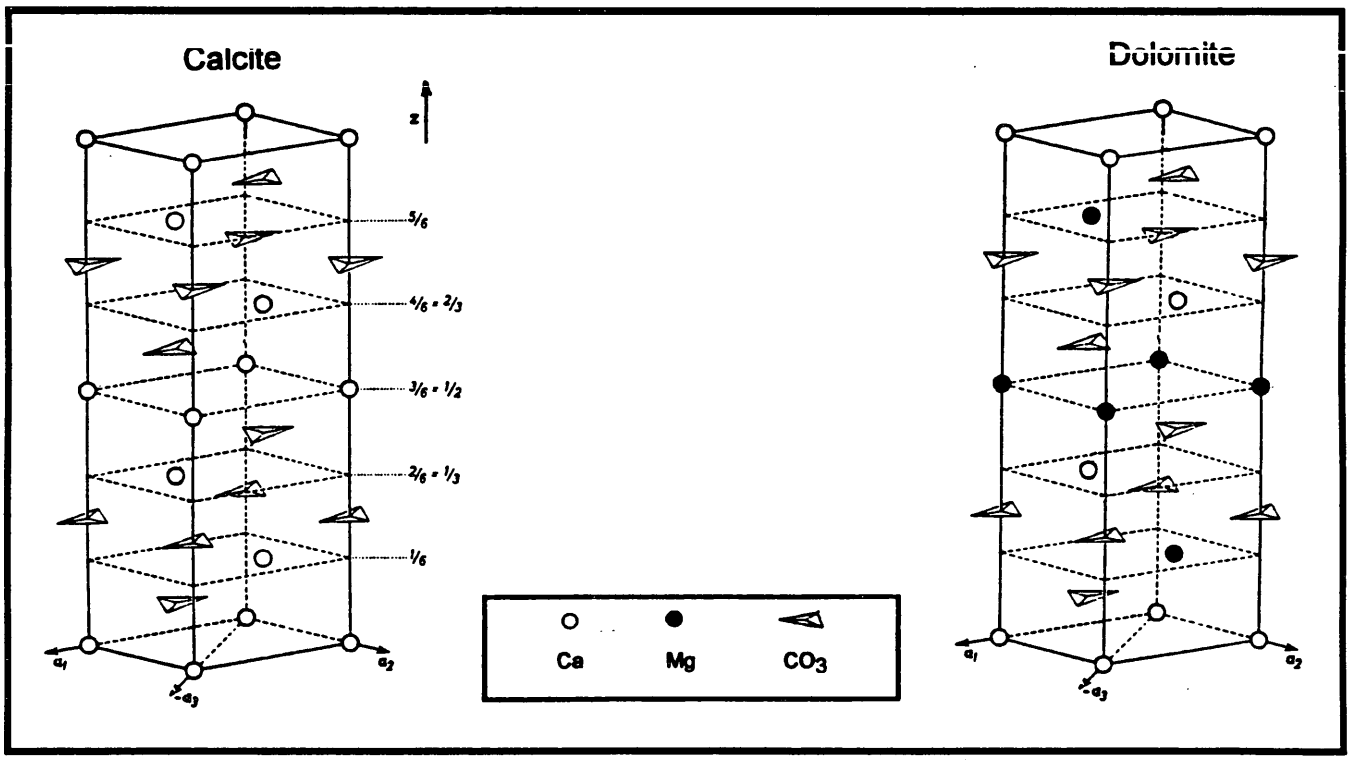

Figure 3. Crystal structures for calcite and dolomite. (adapted from reference 11)

systems) present in the crystal structure. The crystal structures for calcite and dolomite are illustrated in Figure 3.

For the purpose of illustration one can consider the crystal structures of calcite and dolomite to be close packed spheres that represent cations and anions (see Figure 4). This drastically simplifies the explanation that is needed to address the concept of solid solution and how one quantifies such a phenomenon using x-ray diffraction. In perfectly ordered systems the cations and anions sit uniformly in the crystal lattice. This is the case for both the calcite and dolomite illustrated in Figure 3. However, if one atom of calcium (Ca^{2+}, ionic radius = 1.00Å) is replaced with one atom of magnesium (Mg^{2+}, ionic radius = 0.78Å) then the structure is no longer ideal because a substitutional solid solution has occurred (see the bottom half of Figure 4). Note that the cations are both divalent, this satisfies the condition that the structure should remain electrically neutral; however, the size difference causes a distortion in the crystal lattice. Solid solution can likewise occur in the magnesium layers of dolomite. The distortion of the crystal lattice can easily be measured using x-ray diffraction techniques. Portions of the x-ray diffractograms for pure calcite (Fisher, reagent grade) and nearly pure dolomite (NBS 88a) are shown in Figure 5. The diffraction peaks that arise from identical crystallographic planes have been labeled in the figure. Since a dolomite crystal has less symmetry than a calcite crystal (i.e., it contains both Mg and Ca atoms) it produces a series of weak reflections that are commonly referred to as "order reflections" [9]. Hence, these reflections can be used to assess how closely the crystal structure approaches that of an "ideal" dolomite. Also, the angular location of the various diffraction peaks of rhombohedral carbonates tend to shift as a function composition, this fact was alluded to in Figure 2. Reeder [11] has suggested that it is best to conduct a total structural refinement of any given carbonate sample to assess the ideality of the structure; however, such an approach would be time consuming and would not be applicable on a quality control basis. Hence, for the purpose of this study the method described by Hutchinson [12] was used to estimate the Mg - Ca solid solution in Iowa carbonate stones.

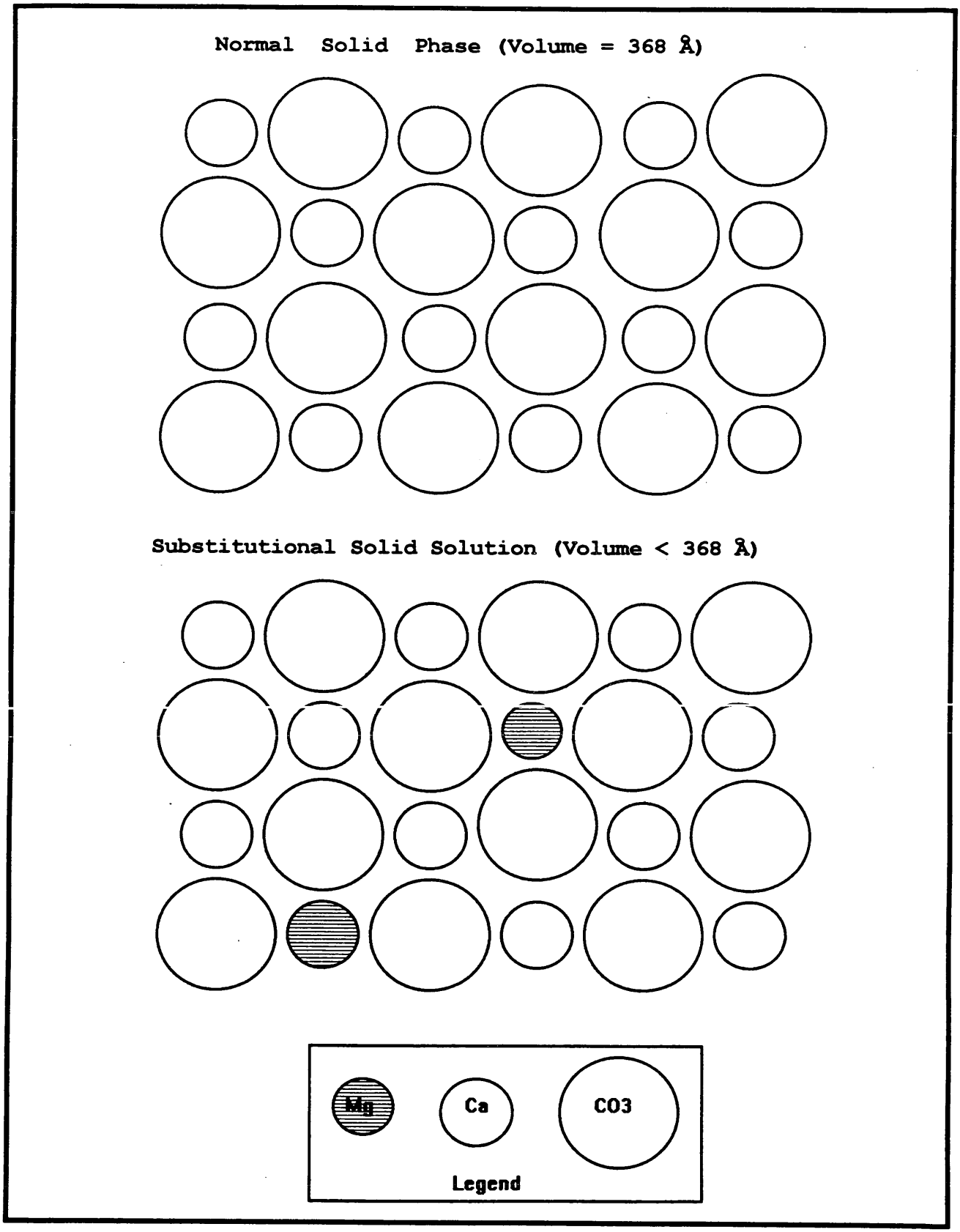

Figure 4. Example of a substitutional solid solution.

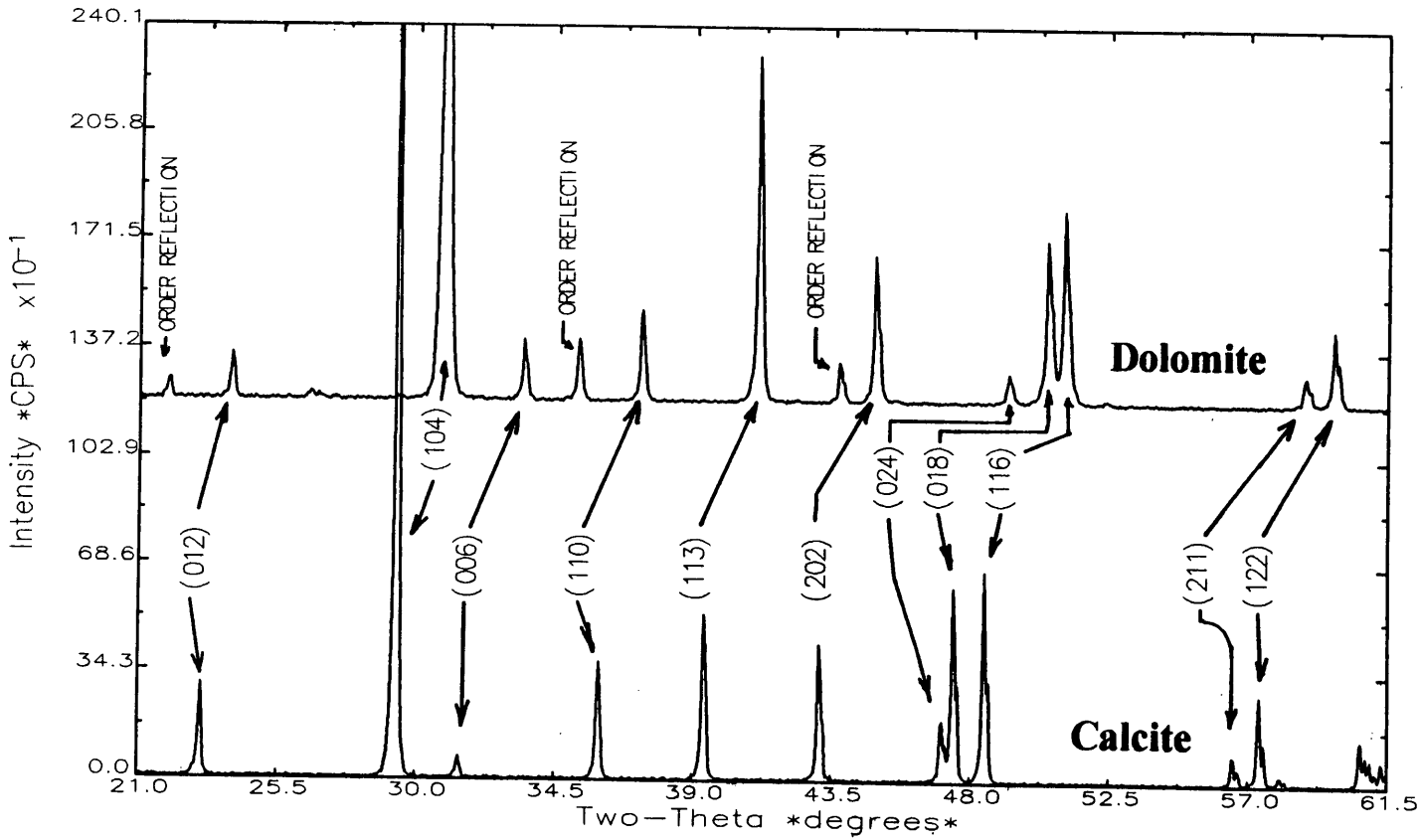

Figure 5. X-ray diffractograms of calcite and dolomite.

Briefly, this method consists of mixing a small amount (10 weight percent) of an internal standard (Si, electrical grade, passing a 20 micron sieve) with each carbonate sample. Then the test specimen was dusted onto a single crystal, inserted into the diffractometer and then scanned from 28 to 32 degrees two-theta. This angular scan encompassed the primary diffraction peaks for Si, calcite and dolomite (assuming a Cu x-ray tube was used in the experiments). The scanning speed was very slow (0.02° steps, 4 seconds counting time at each step), this allowed the peak positions to be determined within about 0.01° two-theta (standard deviation of Si (111) reflection = ± 0.009°; coefficient of variation = 0.03 percent; based on the analysis of 31 samples). The difference between the calcite or dolomite (104) diffraction peak and the Si (111) diffraction peak, which will be referred to as $\Delta 2\theta$, was then used to calculate the mole percent of $MgCO_3$. The relationship between $MgCO_3$ content and $\Delta 2\theta$ is shown in the top half of Figure 6. This relationship was adapted from Brown [13], who based his information on that reported by Goldsmith et al [10] and Graf [14]. Note, that the relationship depicted in Figure 6 was extended to 100 percent $MgCO_3$ (i.e., magnesite) with only a slight change in the regression coefficients. Also, it was found to be advantageous to use only the first four data points (0 - 30 percent $MgCO_3$) to evaluate the amount of Mg substituted into the calcites (see the lower half of Figure 6) because this produced better regression intercepts at low values of $MgCO_3$.

The results of the solid solution study are summarized in Table 9. The results have been expressed to the nearest 0.1 percent for the purpose of comparison only. The absolute accuracy of the method is difficult to estimate because the information was taken from the literature (which has been subjected to some scrutiny because of inconsistencies [10]); however, the precision of the method allows it to differentiate between samples with $MgCO_3$ contents within ± 0.5 percent. A series of standards were also included with the study but none of the standards had been certified for mole % $MgCO_3$. Hence, one must keep in mind that we are searching for trends rather than trying to quantify the absolute amount of solid solution present in the carbonate rocks.

The results for the limestones that are summarized in Table 9, are in reasonably good agreement with those that were obtained by Dubberke [15] in an earlier study (see Table 10).

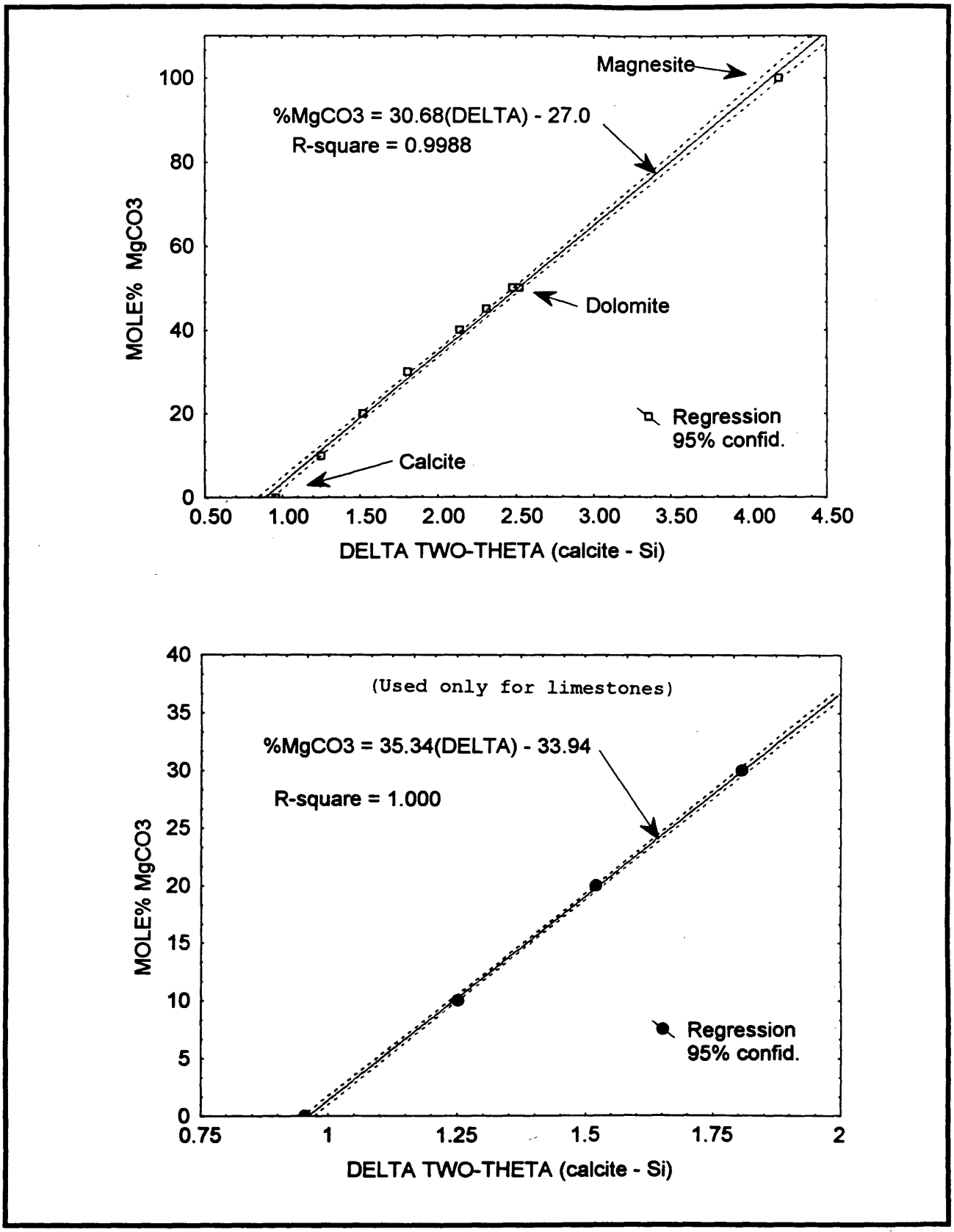

Figure 6. Relationships between percent $MgCO_3$ and relative peak position that were used in this study.

Table 9. Results of the solid solution study.

Sample	Calcite $MgCO_3$ (mole %)	Dolomite $MgCO_3$ (mole %)
Limestones		
Skyline	0.6	48.7
Cresent	0.8	-
Montour	0.7	-
Huntington	0.5	49.8
Alden	0.6	-
Early Chapel	0.8	43.6
Conklin	0.8	-
Eldorado	0.4	-
Menlo	1.0	-
Linwood	0.6	-
Dolomites		
Gassman	4.5	49.7
Cedar Rapids-Tan	0.0	49.5
Plower	0.7	49.1
Landis	0.0	49.6
Bryan	4.4	49.3
Pesky	1.3	44.6
LeClaire	3.8	49.5
Lisbon	1.9	49.7
Garrison	0.5	45.1
Lamont	0.2	49.8
Maryville	1.2	49.5
Cedar Rapids-Grey	1.1	49.5
Standards		
FSCO Calcite	0.0	-
Wards Calcite	0.4	-
BCS 393 Calcite	0.6	-
NBS 1C Calcite	0.8	-
NBS 88A Dolomite	0.0	49.9
BCS 368 Dolomite	1.4	50.0
Wards Fe Dolomite	0.6	49.8
Wards Dolomite	0.7	48.6

In general, one can conclude that few of the limestones contained calcite fractions that exhibited Mg solid solution in excess of approximately 2 percent (mole % $MgCO_3$). Some of the samples that had poor service records appeared to contain more Mg than the other limestones; however, there was a high amount of overlap between "good" and "bad" samples. Most of the dolomite samples also contained minor amounts of calcite and several of the calcite fractions tended to contain a

Table 10. Results of the solid solution study by Dubberke.

Sample	Calcite $MgCO_3$ (mole %)	Service Record
Calcite - Pure	0.0	Not Known
Linwood	0.5	Good
Montour	0.6	Good
Elkader	0.7	Poor
Gilmore City	0.8	Good
Alden	0.8	Good
Ullin	0.8	Poor
Menlo - Rerun	0.9	Poor
Elkader	0.9	Poor
Menlo	1.0	Poor
Logan/Clark	1.1	Poor
LeGrand - E C	1.2	Poor
Ames - Pit	1.6	Poor
Kingston	1.6	Poor
Lemley	1.9	Poor

considerable amount of Mg (note results for Gassman, Bryan (could also be Fe or Mn in this instance), and LeClaire).

The results of the solid solution study for the dolomite fraction of the limestones and dolomites is also summarized in Table 9. Several of the samples had $MgCO_3$ contents that deviated significantly from the composition of an ideal dolomite (i.e., 50 percent $MgCO_3$). Several of these samples, most notably Early Chapel, Pesky and Garrison, also have very poor service records.

The crystallite size of the various carbonate samples was measured using XRD techniques. Crystallite size is important because it may influence both the sample decomposition temperature that is observed in the thermal analysis experiments, and the solubility of the bulk phase in the salt treatment studies.

The term "crystallite size" refers to the fact that in reality all crystals contain imperfections. These imperfections cause the formation of substructure or "mosaic structure" in the bulk material. This concept is illustrated in Figure 7. Hence, the crystallite size (t) can be interpreted as the average dimensions of the small crystal fragments shown in Figure 7. These imperfections cause the x-ray

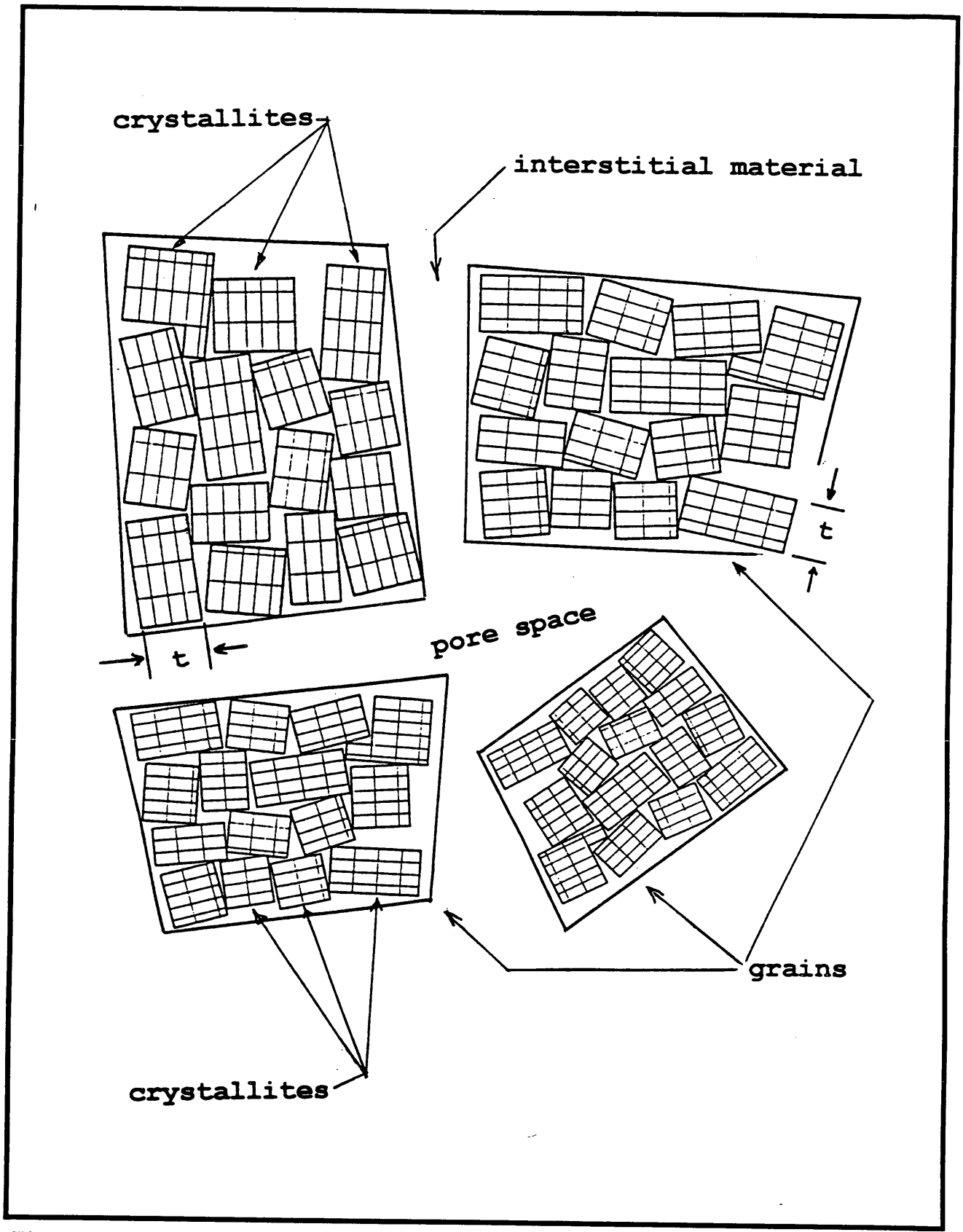

Figure 7. Illustration of the mosaic structure of real crystals (adapted from reference 16).

diffraction profiles of the crystals to broaden as the crystallite size decreases (see Figure 8). Obviously, since the x-ray powder diffraction technique is a bulk analytical method (i.e., the x-ray beam impinges on many crystals all at the same time) the method yields only an average value for the crystallite size. The crystallite size is often determined using the Scherrer equation [18, 19]:

$$t = \frac{0.9\,\lambda}{\beta \cos\theta} \qquad (1)$$

Where: t = average crystallite size in Å
λ = wavelength of the radiation source (1.54056 Å in this case)
β = peak breadth in radians (specimen broadening)
θ = peak location in degrees

It is important to note that the peak breadth (β) in equation 1 can sometimes be rather difficult to obtain. This is because x-ray diffraction profiles consist of the convolution of two parts. Part of the profile is due to the specimen while the other part of the profile is due to the instrument on which the diffraction data is being collected (see Figure 8). Hence, accurate measurements require that a profile standard is used to define the contribution of the instrument to the observed diffraction profile. For the purpose of this study NIST 660 (LaB_6, profile shape standard) was used to compensate for the peak broadening that was caused by the instrument.

Several different crystallite size studies were conducted over the duration of this project. All of the studies, with the exception of the last one, utilized samples that had been pulverized in a shatterbox employing a wet grinding technique (i.e., isopropyl alcohol) to help minimize the strain broadening of the samples.

The first study consisted of slow, high resolution scans over the calcite or dolomite (104) peak. This peak is the most intense peak in both the calcite or dolomite pattern and is located at about 3.04Å and about 2.88Å, respectively. The NIST 660 standard conveniently contained a strong diffraction peak at 2.94Å, this peak was scanned to provide the instrument broadening correction for

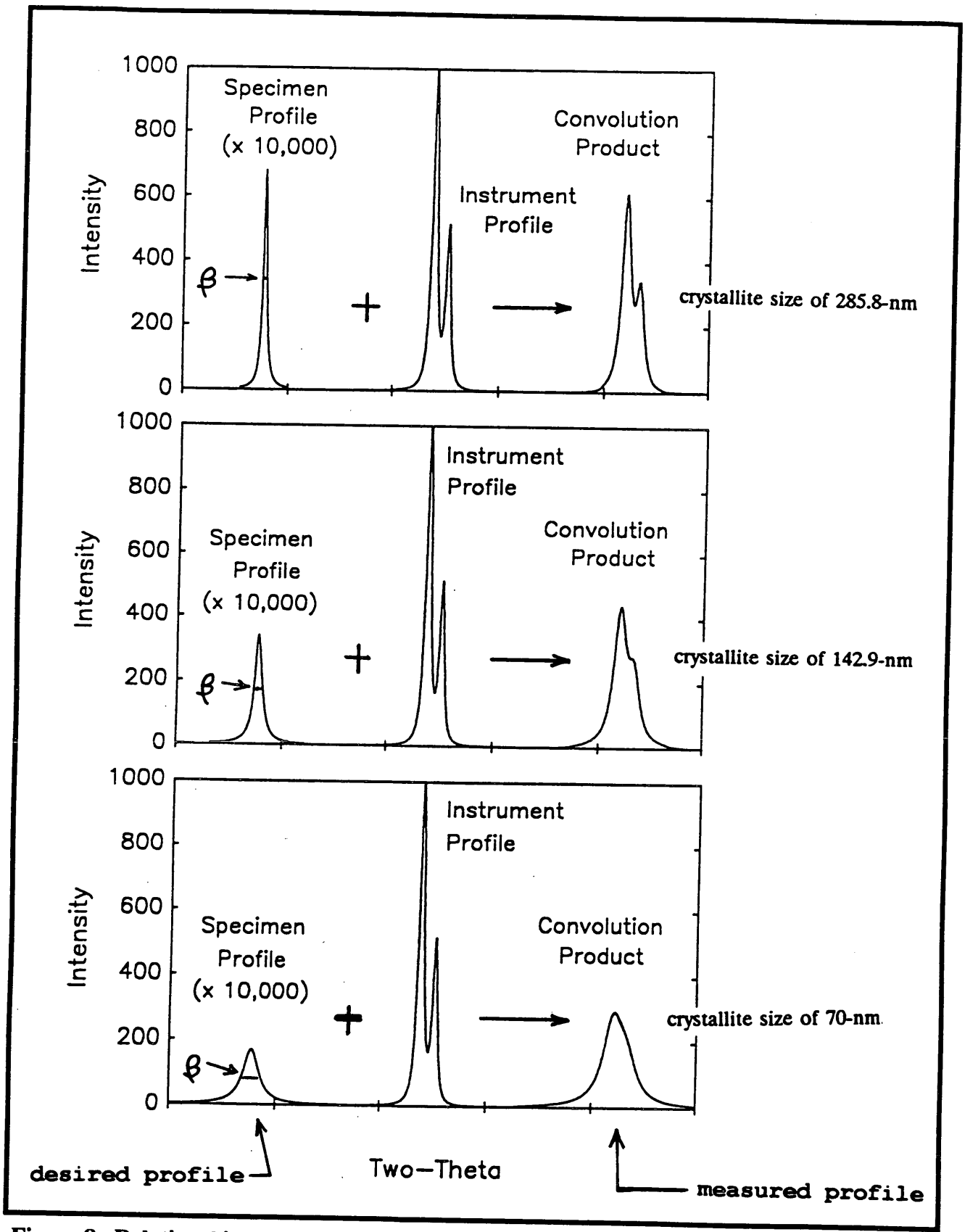

Figure 8. Relationship between the XRD specimen profile and the average crystallite size (adapted from reference 17).

the crystallite size determinations. The diffraction profiles were assumed to have a Gaussian shape; and hence, the instrument broadening was corrected using equation 2.

$$\beta^2 = B^2 - b^2 \qquad (2)$$

Where: β = specimen broadening
B = measured profile broadening (specimen + instrument)
b = instrument broadening

The results of this study are denoted as "Study #1" in Table 11. It is important to note that typically one would desire to measure peaks that are located at higher two-theta locations because this would provide additional resolution (i.e., larger measured values). This in turn would help to reduce the error in the measurements. However, the purpose of this phase of the experimental program was to provide a technique that could be used by the Iowa Department of Transportation to produce crystallite size measurements using data that had accumulated over approximately the last ten years. Since their x-ray diffraction scans were limited to the region of about 26 to 33 degrees two-theta (i.e., the major carbonate peaks) this particular phase of the research was also restricted to that range.

The second crystallite size study consisted of slow scans (0.02° step, 4 second counting time) over several different diffraction peaks in each carbonate sample. The diffraction peaks that were chosen for the study spanned a range from about 29 degrees two-theta to about 51 degrees two-theta, this included the (104), (110), (113), the (202) and the (116) diffraction lines (refer to Figure 5 for an idea where the various peaks are located). The crystallite size of each sample was determined by using a diffraction profile fitting method (SHADOW program) that has been described in detail by Howard [17, 20]. Again, the NIST 660 profile shape standard was used to establish the instrument broadening function for the diffractometer. The results of this study are denoted as "Study #2" in Table 11. Please note in Table 11, that the results reported for Study #2 only pertain to the (104) diffraction peak. This was done so that one can make a direct comparison to the test results that were obtained from Study #1. The other four diffraction peaks that were measured tended to indicate

Table 11. Results of the crystallite size studies conducted on the carbonate stones.

⇐ Limestones ⇒				
	Study #1		Study #2	
Sample	Avg. Crystallite Size (Angstroms)	Relative Size (Relative to Alden)	Avg. Crystallite Size (Angstroms)	Relative Size (Relative to Alden)
Montour	1500	0.47	1470	0.40
Skyline	1990	0.62	1605	0.44
Menlo	1300	0.40	1420	0.39
Linwood	2400	0.75	2280	0.63
Eldorado	3210	1.00	3220	0.89
Early Chapel	1210	0.38	1420	0.39
Conklin	1500	0.47	1380	0.38
Crescent	1730	0.54	1700	0.47
Huntington	1900	0.59	1420	0.39
Alden	3210	1.00	3630	1.00
⇐ Dolomites ⇒				
	Study #1		Study #2	
Sample	Avg. Crystallite Size (Angstroms)	Relative Size (Relative to Maryville)	Avg. Crystallite Size (Angstroms)	Relative Size (Relative to Maryville)
C. Rapids-Gray	1760	0.57	1460	0.75
Maryville	3060	1.00	1950	1.00
Lamont	1940	0.63	1950	1.00
Garrison	730	0.24	770	0.39
Lisbon	1550	0.51	1750	0.90
LeClaire	1570	0.51	1380	0.71
Pesky	740	0.24	610	0.31
Bryan	1440	0.47	1300	0.67
Landis	1050	0.34	1370	0.70
Plower	1025	0.33	1000	0.51
C. Rapids-Tan	2010	0.66	1720	0.88
Gassman	2280	0.74	1950	1.00

that the crystallite size varied in different crystallographic dimensions; and hence, indicated that one should also investigate the crystallite shape of the various carbonate samples (i.e., a two or three dimensional size). However, such an undertaking was clearly outside of the scope of this research project. The results obtained from the two different studies are in general agreement with each other.

The crystallite sizes that are summarized in Table 11 indicate that the limestone samples tended to have larger crystallites than the dolomite samples. Also, it is important to mention that when the crystallite size exceeds about 2000 to 2500 Å the size calculations can become unstable. This is due to the fact that the peak breadth term is in the denominator of the Scherrer equation (see

equation 1). When the measured diffraction profile approaches the same breadth as the instrument profile this essentially causes the denominator of equation 1 to approach zero. Obviously, this causes the crystallite size to approach infinity. Hence, it is important to realize that several of the determinations listed in Table 11, namely those for Alden, Eldorado and Linwood, are less accurate than the other values. It is therefore important to again stress that the purpose of the study was to distinguish relative trends rather than absolute size estimates.

The last crystallite size study was conducted on calcite samples that had been subjected to a series of heat treatments in a carbon dioxide atmosphere. For the purpose of discussion the results obtained from a good limestone (Montour, 40 year service life), a poor limestone (Crescent, 7 year service life), and a standard calcite sample (Fisher calcite; used as a control specimen) will be discussed in detail.

The experimental procedure was as follows: {1} a one gram portion of each test specimen was weighed into a porcelain crucible; {2} the crucible was placed in a warm muffle furnace (temperature about 200°C) that was continuously purged with carbon dioxide; {3} the temperature was increased to the desired temperature (440, 550 or 810) and held constant (± 20°C) for 15 ± 1 hours; {4} after treatment the crucibles were covered with lids and then removed from the muffle furnace; {5} the various samples were cooled to room temperature and then subjected to a series of tests (i.e., weight loss, XRD, crystallite size, etc.).

The results of the weight loss and XRD tests are summarized in Table 12. The general trend indicated by the test results suggests that the full-width-at-half-maximum (FWHM, a rough estimate of the peak breadth, β) tends to decrease during the heat treatments. The decrease was very small for the Fisher calcite but quite measurable for either the Crescent or Montour samples. Recall that a decrease in β indicates an <u>increase</u> in average crystallite size. Also, the change in FWHM appeared to take place even at the lowest temperature used in this study (440°C). All three of the calcite specimens had very similar FWHM values (about 0.18° 2θ) after the heat treatment at 810°C. This indicates that heat treatment tends to increase the average crystallite size of the calcium carbonate crystals.

Table 12. Results of heat treatment tests conducted on several limestone specimens.

Sample	Treatment Temperature (°C)			
	Initial (25)	440	550	810
Crescent				
Weight loss, %	0.00	0.24	0.14	2.93
3.04Å FWHM, °2θ	0.241	0.209	0.214	0.176
2.28Å FWHM, °2θ	0.269	0.255	0.245	0.207
Montour				
Weight Loss, %	0.00	0.23	0.07	0.71
3.04Å FWHM, °2θ	0.214	0.193	0.208	0.177
2.28Å FWHM, °2θ	0.264	0.241	0.236	0.189
Fisher Calcite				
Weight Loss, %	0.00	0.02	0.03	0.03
3.04Å FWHM, °2θ	0.187	0.169	0.173	0.167
2.28Å FWHM, °2θ	0.191	0.183	0.200	0.183

Thermal Analysis Studies

Preliminary experiments

The results of the thermogravimetric analysis (referred to as TGA or TG throughout this report) studies have been summarized in Tables 13 and 14. The various parameters listed in the two tables are defined in Figures 9 and 10. Note, that each table contains information pertaining to tests that were conducted in either a carbon dioxide or a nitrogen atmosphere. The parameters for the samples tested in a nitrogen atmosphere were similar to those shown in Figure 9. However, the calcite and dolomite decompositions were not resolved by the tests and only an average decomposition temperature, denoted as DT_{Both} in Tables 13 and 14, has been listed for each of the test specimens. The thermal curves that were observed for the various test specimens can be found in Appendix II.

Table 13. Results of TGA tests conducted on limestones.

Sample	CO_2 Atmosphere			N_2 Atmosphere		
	DT_{CAL}	Loss from 825°C to DT_{CAL}	Residue	DT_{CAL}	Loss from 400° to 650° C	Residue
Alden	930.5	0.18	55.55	688.9	0.76	55.94
Crescent	922.2	1.10	56.86	700.5	0.34	57.11
Conklin	923.0	0.31	56.33	694.2	0.36	56.33
Early Chapel	919.0	1.20	57.06	700.4	0.38	57.44
Eldorado	928.5	0.41	56.44	696.5	0.35	56.58
Linwood	925.4	0.35	56.42	702.3	0.33	56.79
Menlo	919.9	1.80	58.00	696.3	0.50	57.71
Montour	927.8	0.16	56.64	704.0	0.59	57.11
Skyline	919.0	0.67	55.60	688.5	1.02	55.98
Huntington	925.2	0.50	56.22	696.0	1.18	56.43
FSCO	947.1	0.00	56.19 ± 0.14*	684.8	0.43	56.06
Wards-Calcite	933.7	0.08	56.14	681.8	0.49	56.00
Synthetic- Calcite	911.0	0.65	55.98	N/M	N/M	N/M

*** test result based on 5 repetitions**
N/M = not measured

Table 14. Results of TGA tests conducted on dolomites.

Sample	CO_2 Atmosphere					N_2 Atmosphere		
	DT_{DOL}	DT_{CAL}	Residue	Loss from 400° to 700°C	Loss from 825° to DT_{CAL}	DT_{Both}	Residue	Loss from 400° to 650°C
Maryville	743.3	916.2	49.09	9.71	0.86	676.1	48.71	10.65
Bryan	730.6	916.1	53.77	7.51	1.66	682.9	57.01	3.15
Cedar Rapids-Gray	733.4	916.0	52.60	3.93	0.84	678.4	52.80	3.39
Cedar Rapids-Tan	738.2	917.1	52.26	2.38	0.72	679.4	52.46	1.95
Garrison	724.8	911.9	54.21	2.23	2.04	684.5	54.71	1.60
Gassman	724.2	913.3	47.92	14.19	1.07	676.5	48.11	12.67
Lamont	726.6	917.2	45.93	15.67	0.65	673.2	46.81	14.1
LeClaire	736.5	916.2	52.51	2.61	0.93	678.9	52.90	2.20
Pesky	728.1	911.7	53.90	2.16	1.35	684.0	53.97	1.29
Plower	736.5	914.8	54.54	1.44	1.01	683.1	54.26	1.35

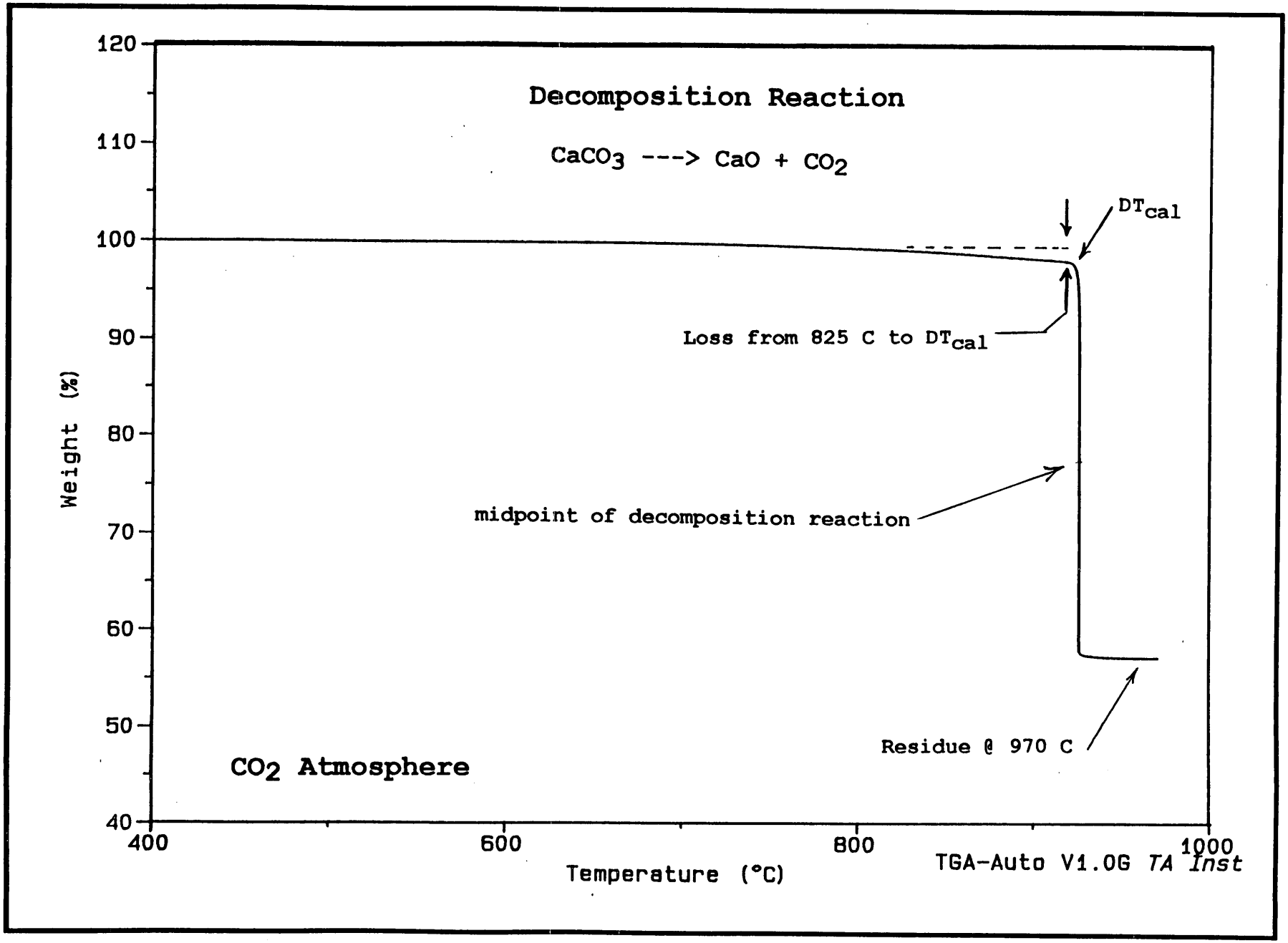

Figure 9. Definition of the pertinent aspects of the thermogravimetric (TG) analysis curves for limestones.

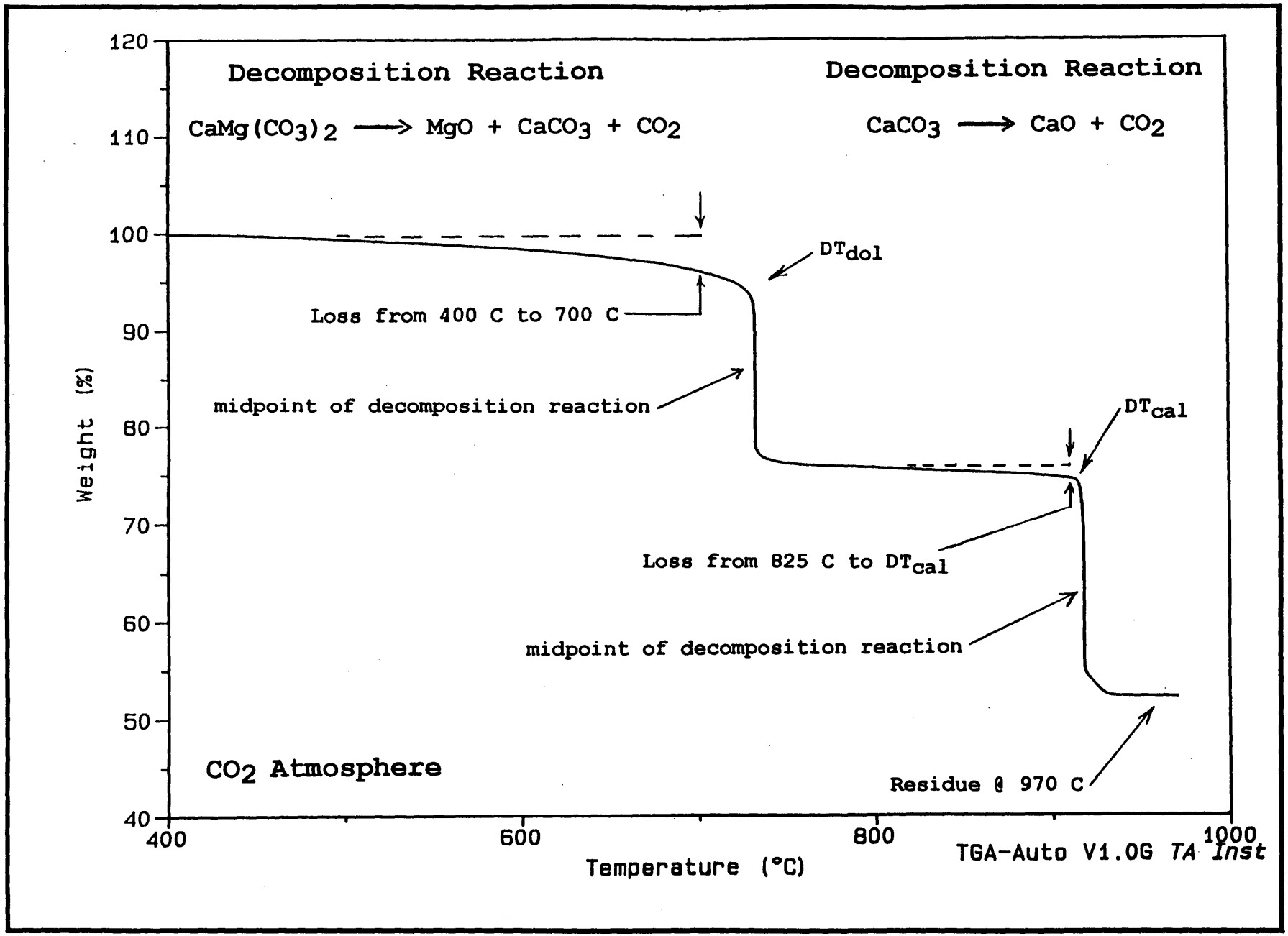

Figure 10. Definition of the pertinent aspects of the thermogravimetric (TG) analysis curves for dolomites.

There are several trends that are readily apparent in Tables 13 and 14, and also in the thermal curves listed in Appendix II. First, the carbon dioxide atmosphere was essential for distinguishing calcite samples from dolomite samples in the TGA tests. Without the carbon dioxide atmosphere (i.e., see test results in nitrogen) both calcites and dolomites decomposed within a temperature range of about 25° C, although the calcite samples tended to decompose closer to 700° C than did the dolomite samples. Secondly, the residue values obtained for calcite samples tested in a nitrogen atmosphere tended to be slightly larger than those observed from the same samples that had been tested in a carbon dioxide atmosphere. This trend was also observed for many of the dolomite samples. And finally, several of the dolomite samples (Lamont, Maryville, Gassman, and to some extent, Bryan) exhibited a very gradual weight loss during early stages of the TGA scans. The purge gas had only a minor influence on this decomposition reaction because neither the onset nor the weight loss of the reaction changed dramatically when carbon dioxide gas was substituted for nitrogen gas (see Figure 11).

After the preliminary TG runs of the various carbonate specimens had been completed, several experimental parameters were identified that needed to be investigated in detail. This is not meant to trivialize the vast amount of research that had already been conducted on the thermal decomposition of carbonate stones; however, much of the early research [21, 22] had concentrated on differential thermal analysis (DTA) techniques rather than TG techniques. Also, recent literature [23, 24, 25, 26] has not yet addressed the Hi-Res. TGA method that has been used in this study. Hence, several experiments were conducted to: {1} study the influence of sample size and instrument parameters on the decomposition temperature and residue values; {2} estimate the absolute accuracy of the method when using certified reference materials; {3} to evaluate how the loss on ignition values obtained from the TG method (55 milligram sample weight) correlated to those obtained from bulk samples (1 gram sample weight); and {4} evaluate the influence of clay minerals on the shape of the thermal curves.

Dubberke and Marks [27] have already conducted a brief study of the influence of sample size on the test results obtained from Hi-Res. TGA scans. Their study consisted of comparing test

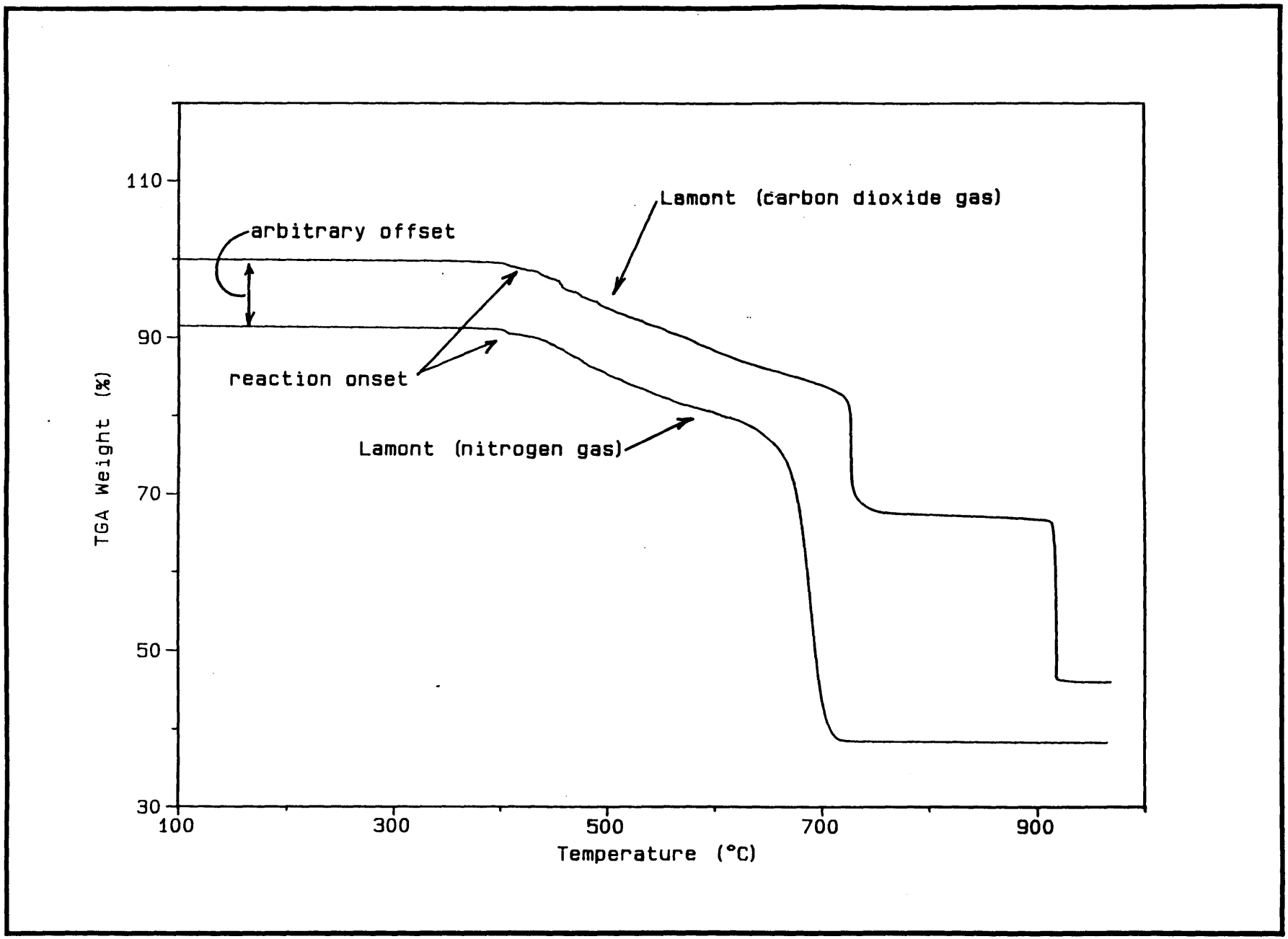

Figure 11. Example of how furnace atmosphere (N_2 versus CO_2) influences the behavior of the TG curve for a dolomite specimen.

results that were obtained from using nominal sample sizes of 20 milligrams and 55 milligrams, respectively, of Lisbon dolomite. All of their tests were conducted in a CO_2 atmosphere and employed a Hi-Res. TGA scanning rate of 40°C/minute at a resolution of 5. The results of the study are summarized in Table 15. In general, both samples sizes produced test results that were highly precise. However, their study also indicated that an increase in sample size tended to increase the precision of the residue determinations, but also tended to decrease the precision of the decomposition temperatures.

Since the previous precision study only dealt with a dolomite sample another study was performed that used a calcite sample (Fisher reagent grade calcium carbonate). In this study the sample mass was varied from 0.5 milligrams to 55 milligrams, to define better trends between it and the observed values for decomposition temperature and residue. Again, all of the experiments were performed in a CO_2 atmosphere, using a scanning rate of 40°C/minute and a resolution = 5. The results of the study are summarized in Table 16. The only major change in the procedure was that the determination of the residue value was moved up to 970°C (from 950°C). This was done to make sure that the decomposition reaction was completed before attempting to define a value for the residue. In general, the study indicated that the calcite decomposition temperature decreased significantly with decreasing sample size. Also, the study indicated that for accurate residue determinations a sample size of about 25 to 55 milligrams was best; smaller sample sizes greatly reduced the accuracy of the residue measurements.

A companion study was also conducted to evaluate how test results obtained from the Hi-Res. TGA mode compared to similar tests conducted using normal (constant scanning rate) TG techniques. This was done so that the test results summarized in this report can be more easily compared to those already reported in the thermal analysis literature. Again, the study used the reagent grade calcite sample, a nominal sample mass of 55 milligrams, and a CO_2 atmosphere. The scanning rate and resolution were varied to see how these parameters influenced the results of any given experiment. However, it must be noted that while the scanning rate was allowed to vary between 5 and 40°C/minute, the resolution was set to either 0 (zero, normal constant scanning rate

Table 15. Precision values generated during a repetitive analysis of Lisbon dolomite [adapted from 27].

Run Number	Sample Size (mg)	DT_{DOL} (°C)	Residue @ 800°C (mg)	DT_{DOL} (°C)	Residue @ 950°C (mg)
1	20.591	714.53	75.92	920.64	51.49
2	20.431	713.86	76.05	920.57	51.65
3	20.127	714.17	75.60	920.38	50.77
4	20.457	714.40	76.02	920.27	51.63
5	20.466	714.53	76.28	920.23	51.78
	Standard Deviation	0.29	0.25	0.18	0.40
	Mean	714.30	75.97	920.42	51.46
	Coefficient of Variation (%)	0.04%	0.33%	0.02%	0.78%
1	55.812	720.00	76.70	919.89	52.07
2	55.195	717.74	76.74	920.12	52.15
3	55.314	718.48	76.75	919.91	52.12
4	54.892	719.14	76.55	919.67	51.95
5	55.304	719.20	76.57	919.52	51.82
6	55.351	717.33	76.58	918.98	51.98
7	55.612	719.88	76.65	918.55	52.02
	Standard Deviation	1.02	0.08	0.56	0.11
	Mean	718.82	76.65	919.38	52.02
	Coefficient of Variation (%)	0.14%	0.10%	0.06%	0.21%

Table 16. Results of the study to see how sample mass influenced experimental values.

Sample Mass (mg)	DT_{CAL} (°C)	Residue @ 975°C (%)	Residue Yield* (% Error from theoretical)
55.5	947.1	56.19	+0.29
25.1	945.6	56.08	+0.09
5.0	939.6	55.51	-0.93
1.10	935.6	53.52	-4.48
0.53	931.2	51.97	-7.25

* **theoretically, the residue should be 56.03%**

TG method) or 5. Hence, no intermediate resolution settings will be described in this study.

The results of the scanning rate/resolution study are summarized in Table 17. One of the major benefits of the Hi-Res. TGA method that is apparent in Table 17, is the time efficiency of the

Table 17. Influence of scanning rate and resolution on the results of TG tests.

Sample Mass (mg)	Mode	Scanning Rate (°C/minute)	Resolution	DT_{CAL} (onset)	DT_{CAL} (midpoint)	Residue (%)	Run Time (minutes)
55.5	Normal	5	0	929.6	941.2	56.11	190
55.3	Normal	10	0	935.4	950.7	56.15	95
55.5	Normal	20	0	940.5	960.8	58.3*	47
55.4	Hi-Res	10	5	931.0	931.1	56.09	115
55.6	Hi-Res	20	5	938.0	938.1	56.14	58
55.4	Hi-Res	30	5	943.6	943.8	56.15	42
55.5	Hi-Res	40	5	947.1	948.5	56.19	30

***decomposition reaction had not reached completion by the end of the run (about 980°C)**

method. Typically, one can conduct a Hi-Res. scan in considerably less time than a normal TG scan, with only a small loss of information concerning the decomposition temperature. Also, once the decomposition temperature is reached the Hi-Res. TGA mode tends to stop heating the sample until the decomposition is complete (note the small difference between DT(onset) and DT(midpoint) in Table 17). This helps to separate adjacent decomposition reactions and also tends to make the thermal curves appear sharper or more ideal. However, one can also argue that the decomposition temperature observed in the Hi-Res. TGA mode is still influenced by the many factors associated with normal TG methods (i.e., sample thermal conductivity, sample cooling, etc.), and this tends to suggest that at high scanning rates (say above about 20°C/minute, resolution = 5) the observed decomposition temperature has little thermodynamical significance. One should not interpret the preceding statement to mean that the information obtained from Hi-Res. TGA tests that employ fast scanning rates is wrong. Instead, one must simply be aware that the value obtained for the decomposition temperature is still strongly dependent on the sample size, the scanning rate and the resolution setting. The previous tables have all clearly indicated that if one defines an experimental

procedure, and then strictly follows that procedure, the Hi-Res. TGA method will produce very precise relative decomposition temperatures. This is typically all that is needed when one desires to compare materials with similar compositions.

An example of the ability of the Hi-Res. TGA mode to separate close decomposition reactions is illustrated in Figure 12. The Hi-Res. TGA mode forces the decomposition reactions to approach their theoretical shapes (i.e., have square edges, see the curve labeled NBS 88a in Figure 12). When the curves deviate from their theoretical shapes, one may surmise that another decomposition reaction is occurring at a slightly higher temperature (see the curve labeled BCS 368 in Figure 12). This phenomenon is most clearly evident if one plots the derivative of the TG data (see the lower half of Figure 12). The low temperature decomposition reaction appears to be related to the amount secondary calcite present in the sample. The secondary calcite was formed through the decomposition of the dolomite crystals. The secondary calcite typically decomposed at temperatures between 910°C and 920°C. The higher temperature decomposition reaction appears to be related to the amount of primary calcite that was present in the sample. The primary calcite was initially present in the bulk sample and normally decomposed at temperatures above 920°C.

The accuracy of the Hi-Res. TGA method was assessed by using five different certified reference materials. All standards were carbonate stones of NIST (NBS) or equivalent quality. The results of this study are summarized in Table 18. Typically, the method produced very accurate

Table 18. Summary of the results of the accuracy study.

Standard	Certified Values		Observed Values	Relative Error (%)
	LOI (%) mean value	Std. Deviation	LOI (%) = 100 - Residue (corrected for moisture content)	
NBS 88a	46.7	not available	46.79	0.19
BCS 368	46.7	0.11	46.75	0.11
NBS 1c	39.88	0.06	40.01	0.33
BCS 393	43.44	0.13	43.46	0.05
NBS 1a	34.55	0.03	34.29	-0.75

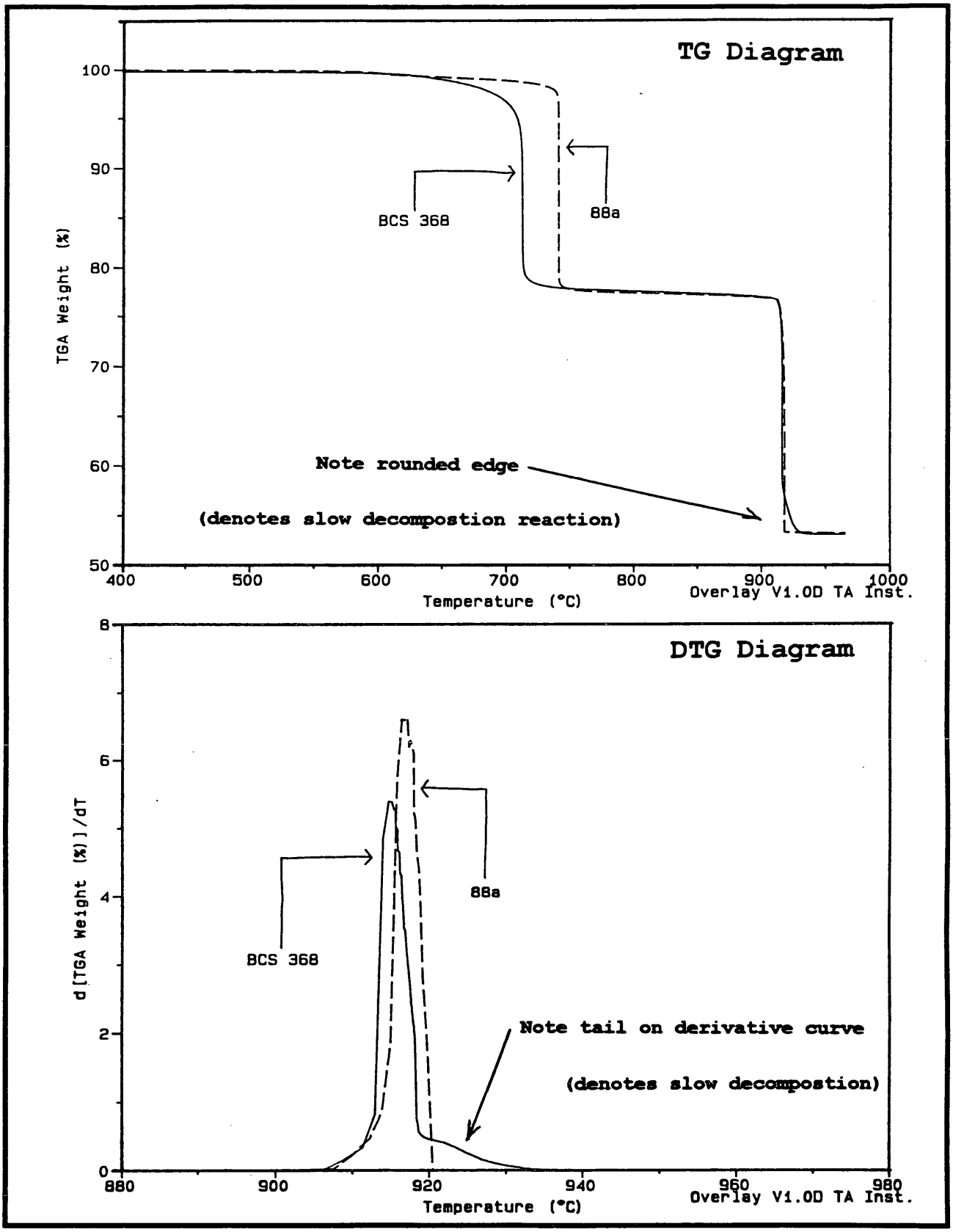

Figure 12. Example of how the Hi-Res. TG method enhances the ability to separate closely spaced decomposition reactions.

measurements because all test results except one were within ±0.2 percent (absolute) of the certified values. When experimental error in the standards and the samples was taken into consideration only one determination (NBS 1a) was statistically different from its certified value. Hence, one may conclude that the residue values determined by the Hi-Res. TGA method are in excellent agreement with values that have been determined in many other laboratories.

A series of blended standards (denoted as "mixtures" later in this text) were proportioned to estimate the detection limits of the analytical method and the potential magnitude of the decomposition temperature error that could be expected in any given sample. Two certified reference materials, BCS 393 (a calcite) and BCS 368 (a dolomite), were blended together to make five different mixtures. The mixtures had the calculated (theoretical) compositions that are tabulated in Table 19. The theoretically calculated values account for the fact that the BCS 368 dolomite contained about 2.5 percent calcite; however, no attempt was made to incorporate the 0.3 percent $MgCO_3$ present in the BCS 393 limestone into the theoretical calculations. It was reassuring to note that the certified value for MgO (0.3 percent expressed as $MgCO_3$) present in the BCS 393 limestone, was in reasonable agreement with the solid solution value listed in Table 9 (0.6 percent $MgCO_3$ determined by XRD). The mixture studies were conducted using a nominal sample size of 55 milligrams, a dynamic CO_2 atmosphere and a Hi-Res. scanning rate of 40°C/minute at a resolution of 5.

The results of a typical TG experiment are illustrated in Figure 13. Figure 13 also illustrates how the concentrations of calcite, dolomite and insoluble material that are present in a given carbonate stone can be estimated using the TG technique. The calculations were based on the assumptions that the carbonates were initially stoichiometric and contained a negligible amount of clays. These assumptions are only partially true as was indicated in the x-ray study section of this report. However, the results of these simple calculations appear to be in reasonably good agreement with the theoretical values (see Table 19). The details of the calculations are listed in Table 19, these calculations are very similar to those listed earlier by Dubberke and Marks [27]. The calculations were conducted by starting at the dolomite endmember and then progressing towards the calcite

Table 19. Comparison of calculated and empirically determined compositions of the various standard mixtures.

Sample	Theoretical (calculated, wt. %)			DT_{DOL} (°C)	Residue @ 825°C (%)	DT_{CAL} (°C)	Residue @ 970°C (%)	Predicted (wt. %)		
	Dolomite	Calcite	Insoluble					Dolomite	Calcite	Insoluble
BCS 368	96.2	2.5	1.3	712.7	77.48	915.8	53.12	94.4	4.2	1.4
MIX 1	93.8	4.9	1.3	713.1	78.04	915.5	53.37	92.0	6.2	1.8
MIX 2	77.0	21.8	1.3	716.9	81.96	917.5	54.91	75.6	20.5	3.9
MIX 3	48.1	50.7	1.3	726.2	88.66	919.6	54.93	47.5	50.9	1.6
MIX 4	19.3	79.5	1.2	740.9	95.34	922.9	55.83	19.5	79.3	1.2
MIX 5	2.5	96.3	1.2	768.6	99.13	928.1	56.38	3.7	95.2	1.1
BCS 393	0.0	98.8	0.9	-	99.70	938.7	56.49	1.3	97.6	1.2

Calculation of Predicted compositions using TG results		
Step #	**Description**	**Example**
1	LOI_M = 100 - (Residue @ 825°C)	100 - 77.48 = 22.52
2	Convert to $MgCO_3$: LOI_M x 1.915928 = % $MgCO_3$	22.52 x 1.9159 = 43.15
3	Convert to moles $MgCO_3$: % $MgCO_3$ / 84.32 = moles $MgCO_3$	$43.15/84.32$ = 0.5117
4	LOI_C = (Residue @ 825°C) - (Residue @ 970°C)	77.48 - 53.12 = 24.36
5	Convert to $CaCO_3$: LOI_C x 2.274256 = % $CaCO_3$	24.36 x 2.274 = 55.40
6	Convert to moles $CaCO_3$: % $CaCO_3$ / 100.09 = moles $CaCO_3$	$55.40/100.09$ = 0.5535
7	Determine molar excess: moles $CaCO_3$ - moles $MgCO_3$ = excess $CaCO_3$	0.5535 - 0.5117 = 0.0418
8	Dolomite (%) = 2.187026 x % $MgCO_3$	43.15 x 2.187 = 94.4
9	Calcite (%) = moles excess $CaCO_3$ x 100.09	0.0418 x 100.09 = 4.2
10	Insoluble (%) = 100 - Dolomite - Calcite = 100 - (LOI_M x 1.9159) - (LOI_C x 2.274)	100 - 94.4 - 4.2 = 1.4

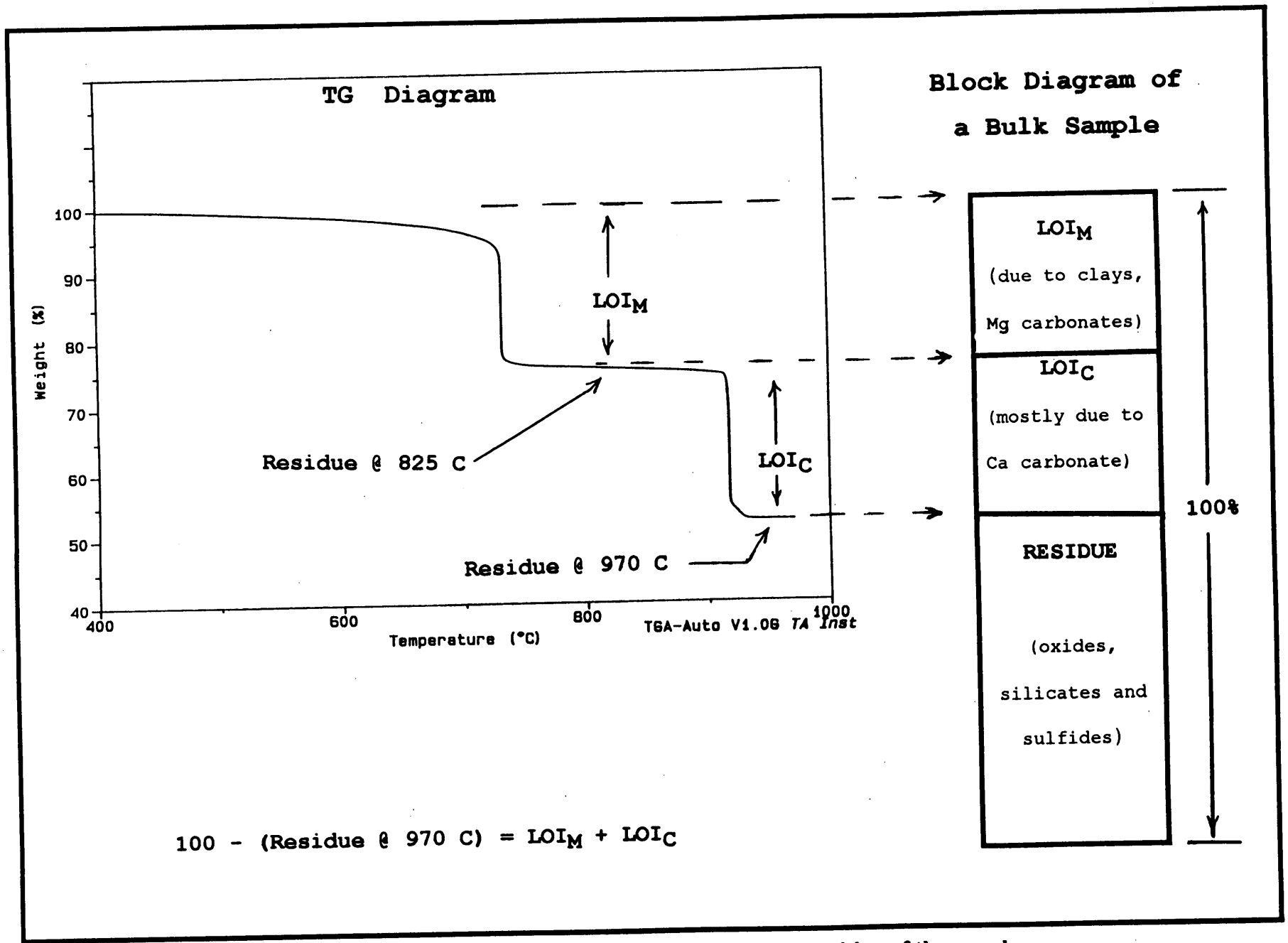

Figure 13. Description of how the various TG parameters correspond to the composition of the sample.

endmember. However, better results can be obtained for specimens with compositions near the calcite endmember if one ignores the dolomite calculation and simply assumes that the Mg is present as a solid solution with calcite. This type of calculation can be performed by simply skipping the calculation of the amount of excess calcite (steps 3, 6, 7 and 9 in Table 19) and the amount of dolomite (step 8 in Table 19) present in the sample.

The mixture study also clearly indicated the previously mentioned trend of increasing decomposition temperature with decreasing concentration. This trend, which is illustrated in Figure 14, was caused by the fast scanning rate that was employed in the study. A slower scanning rate or an increase in the sensitivity setting would have helped to eliminate this anomaly; however, such a change would have definitely increased the time required for any given run.

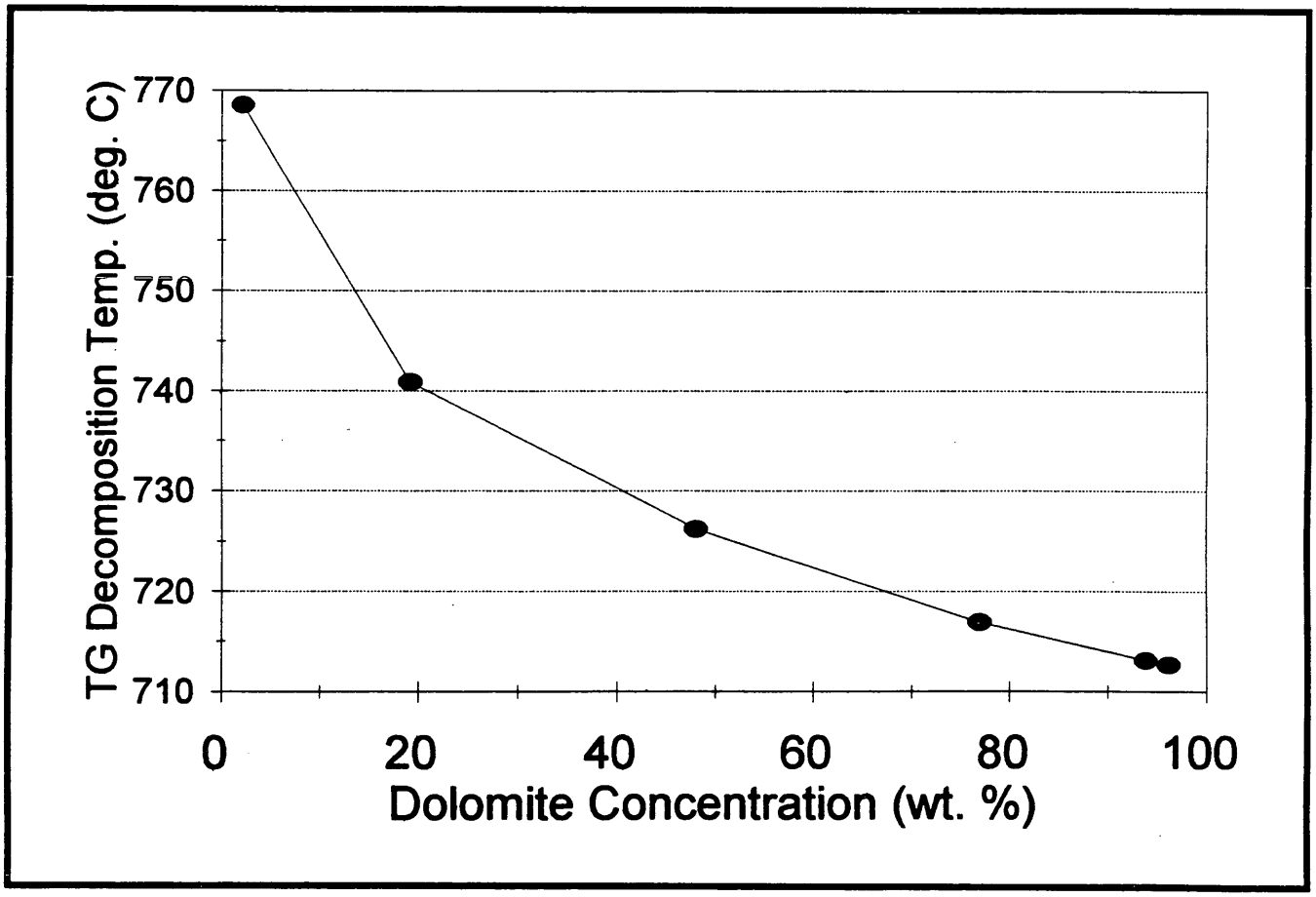

Figure 14. Relationship between the decomposition temperature (DT_{DOL}) and the concentration of dolomite in a series of standard mixtures.

So far one would conclude that the Hi-Res. TGA method exhibits excellent precision and accuracy; however, one must remember the majority of the tests have been conducted on certified reference materials that were extremely homogeneous and well behaved. Would such precision and accuracy be obtained on "real" samples? The precision portion of this question has already been answered (refer to Table 15). A partial answer to the accuracy portion of this question can be assessed by comparing the results of the Hi-Res. TGA tests to standard (bulk, 1 gram samples) loss-on-ignition (LOI) tests. Obviously, the bulk LOI tests were conducted in a normal (air) atmosphere so the comparison to tests conducted in inert atmospheres (N_2 or CO_2) is not as simple as one would desire. However, few of the samples contained significant amounts of reduced species (i.e., pyrite, ankerite, etc.) so the comparison should be roughly valid. Figure 15 illustrates the comparison between LOI values determined from the Hi-Res. TGA method and the bulk LOI determinations. In general, the results were in good agreement for the calcites but poor agreement for the dolomites. The type of atmosphere had a small (but significant) influence on the trends for the dolomite samples. Typically the coarse-grained dolomites caused the largest discrepancies when analyzed using a carbon dioxide atmosphere. This anomaly was investigated in detail and will be discussed later in the particle size section of this report.

Clay minerals can also cause difficulty when attempting to interpret the results of the TG experiments. A short study was conducted to assess how the clay content would affect the results of the composition calculations listed in Table 19. Two different clays, an illite and a kaolinite, were blended with a calcite standard (BCS 393) and a dolomite standard (BCS 368). Six different mixtures were prepared that ranged in clay content from about 7 percent to 11 percent. The results of the clay study are summarized in Table 20. The thermal curves for the two clay samples are shown in the top half of Figure 16. The thermal curves for several of the clay-calcite mixtures are shown in the bottom half of Figure 16. The presence of clay in the carbonate stone tends to decrease the accuracy of the predicted values, this becomes quite noticable at higher clay contents. Also, the presence of clay minerals tends to increase the magnitude of the slope of the thermal curve (i.e., weight loss versus temperature curve). Numerical corrections could be used to obtain better

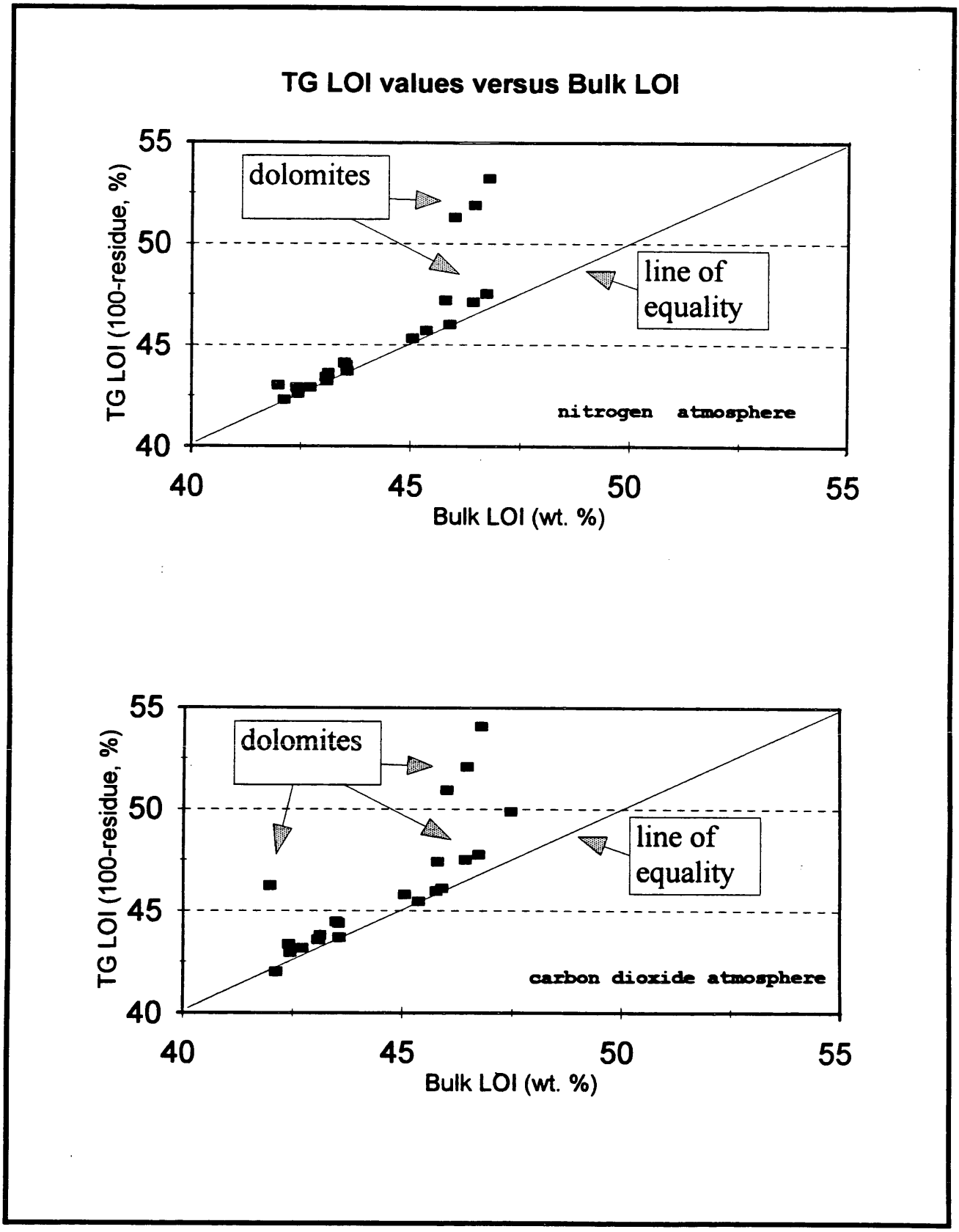

Figure 15. Relationship between loss-on-ignition calculated from TG tests and those determined from bulk samples.

Table 20. Results of the clay study.

BCS 393 + Clay			Results via TG method			
					Predicted	
Sample	% Clay	% Calcite	Residue @ 825°C	Residue @ 970°C	Calcite (%)	% Insoluble
1	0	98.8	99.70	56.49	98.3	1.2
2	6.97 kaolinite	91.8	98.37	58.58	90.5	6.4
3	7.06 illite	91.7	98.58	58.87	90.3	7.0
4	11.11 illite	87.7	97.79	60.24	85.4	10.4

BCS 368 + Clay				Results via TG method				
						Predicted		
Sample	% Clay	% Calcite	% Dolomite	Residue @ 825°C	Residue @ 970°C	Calcite (%)	Dolomite (%)	% Insoluble
1	0	2.5	96.2	77.48	53.12	4.2	94.4	1.4
2	6.97 kaolinite	2.3	89.4	78.00	55.38	1.4	92.2	6.4
3	7.02 illite	2.3	89.4	78.30	55.83	1.8	90.9	7.3
4	11.15 illite	2.2	85.3	78.79	57.40	0.4	88.9	10.7

estimates of the calcite content of the various carbonate stones since most clay minerals decompose at temperatures below 900°C. However, such corrections would not be directly applicable to the dolomite samples because they decompose over a wide range of temperatures. It is interesting to note in Figure 16 (see the bottom half of the figure), that the Hi-Res. TGA method can distinguish a carbonate stone that contains an illite clay from one that contain a kaolinite clay. The rounded corner on the tail end of the decomposition event clearly indicates that at least two minerals are decomposing simultaneously. Inspection of the top half of Figure 16 shows that kaolinite has reached a stable mass by about 700°C; however, the illite clay was still in the process of decomposing. Hence, one may conclude that in this instance, the rounded tail of the decomposition event indicates the presence of an illitic clay mineral.

Particle size study

By the end of the first year of this study a considerable amount of evidence indicated that certain types of dolomites tended to exhibit very odd decomposition reactions. Most of these dolomites tended to have medium to coarsely grained textures. The odd behavior that was observed

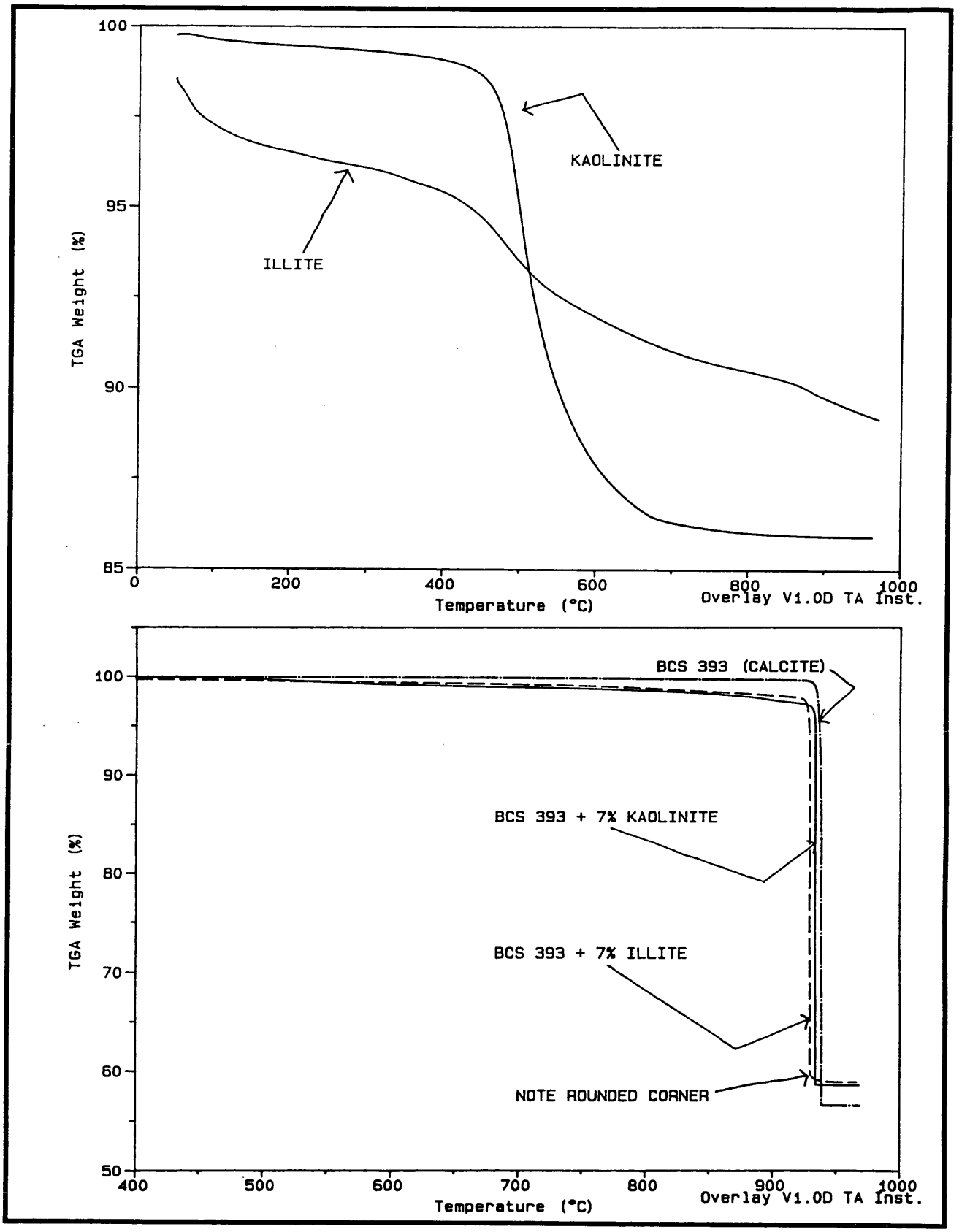

Figure 16. Typical test results that were obtained from mixtures of two different clays with a standard limestone sample.

is illustrated in Figure 17. The major features that deviate from normality can be summarized as follows.

First, a very sluggish decomposition reaction commonly began at approximately 400 to 500°C. This decomposition reaction could not initially be attributed to any specific mineral phase and it often continued up to the decomposition temperature of the dolomite crystals (DT_{DOL}). Secondly, as mentioned earlier in this report (refer to Figure 11), the sluggish decomposition reaction did not appear to be drastically altered by changing the atmosphere that was used in the various experiments. And finally, the residue value that was measured at 970°C appeared to be too low (i.e., the LOI values were too high for stoichiometric (or nearly so) carbonate stones). These strange experimental results tended to cause the results of the TG tests to deviate significantly from those obtained from the x-ray studies (both x-ray diffraction and x-ray fluorescence). Hence, additional experimental programs were conducted to investigate potential explanations for this odd behavior.

The first experimental parameter that was investigated was sample grinding time. Previous researchers had already established that particle size can have a significant influence on the results of thermal analysis tests (mostly DTA tests) [21, 22, 23, and 26]. Hence, Lamont dolomite was subjected to grinding in a shatterbox using three different time durations (3, 10, and 15 minutes). The results of TG tests that were conducted on the three samples are shown in Figure 18. The figure indicates that grinding times in excess of 3 minutes helped to smooth out the noise in low temperature decomposition reaction and also increased the amount of residue at 970°C. However, the low temperature decomposition reaction did not disappear. In fact, it became more prominent and tended to occur at about 580°C (well below the decomposition temperature for dolomite, regardless if the atmosphere was composed of nitrogen or carbon dioxide). Hence, one may conclude that this brief study indicated that particle size was an important variable but it could not explain the anomalous decomposition reaction that occurred at about 580°C.

The second particle size study was designed to investigate how specific particle size fractions of various dolomite and limestone samples influenced the results of the TG tests. Six carbonate stones were used in the study (limestones consisted of Alden, Huntington and Early Chapel;

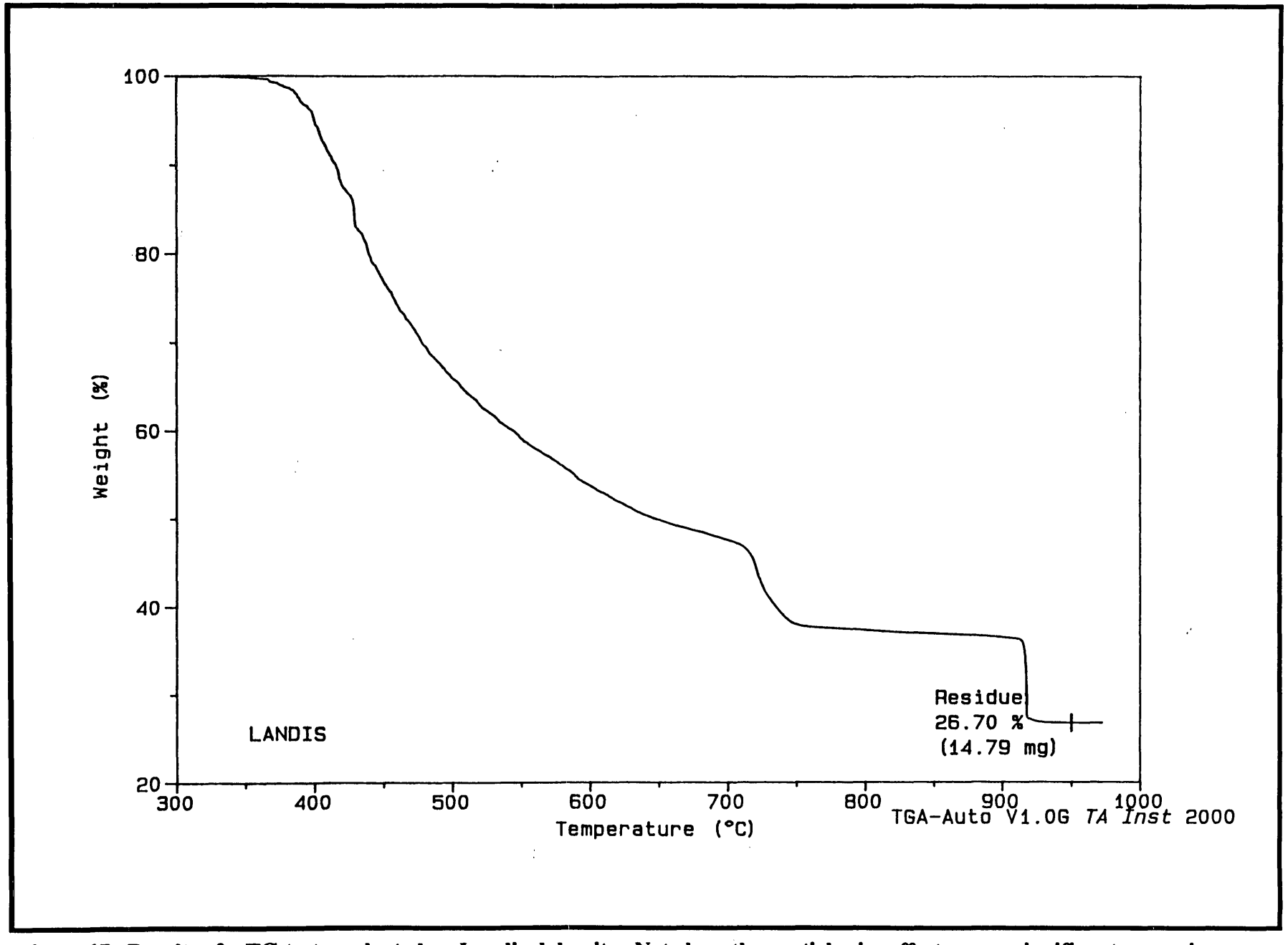

Figure 17. Results of a TG test conducted on Landis dolomite. Note how the particle size effect causes significant errors in decomposition temperature and residue values.

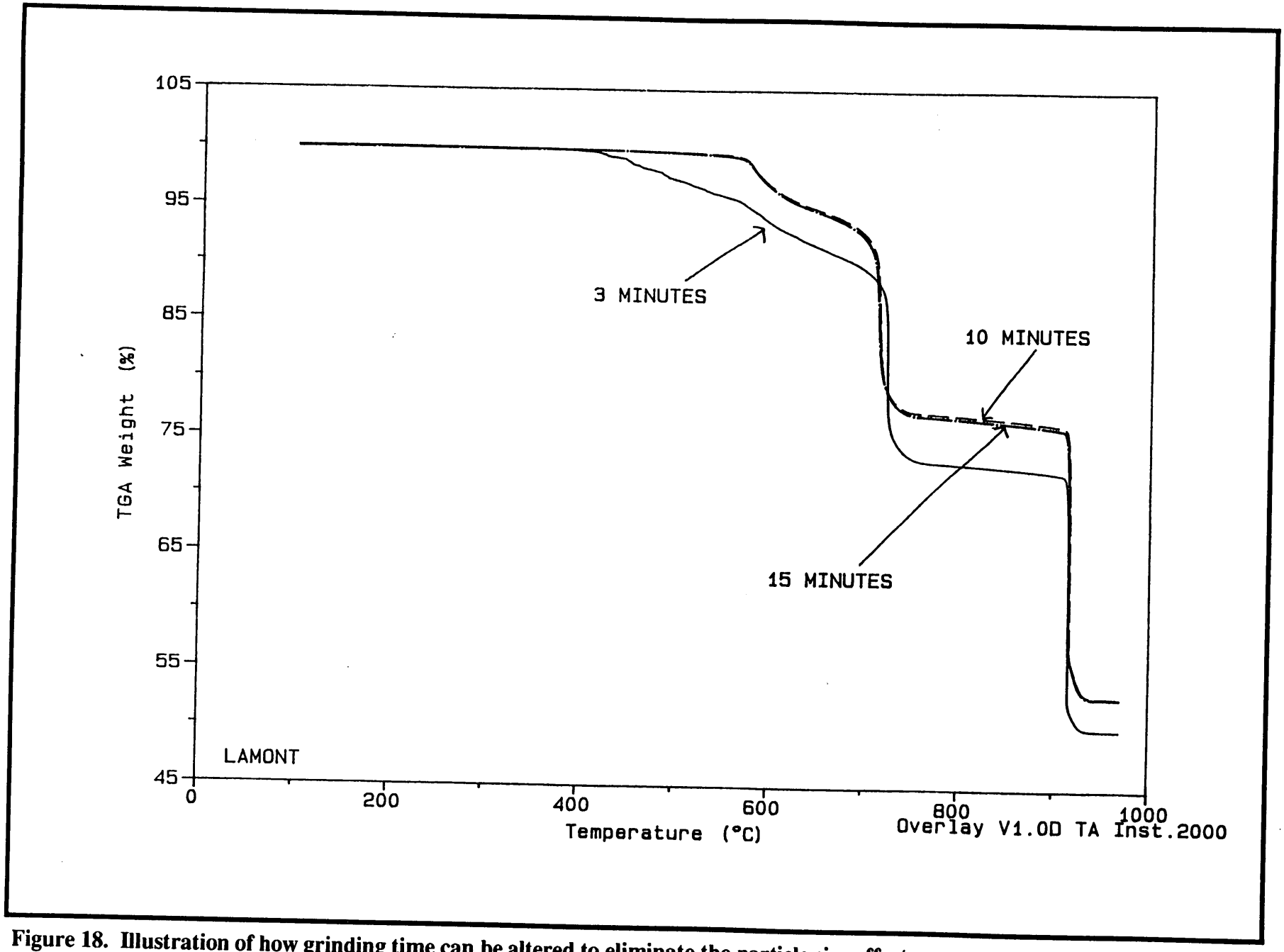

Figure 18. Illustration of how grinding time can be altered to eliminate the particle size effect.

dolomites consisted of Maryville, LeClaire and Garrison). Each bulk carbonate sample was ground in a shatterbox for three minutes and then subjected to sonic sifting. The various particle size fractions (i.e., $^{+}$105 microns, $^{-}$105 but $^{+}$45 microns, $^{-}$45 microns but $^{+}$20 microns, and $^{-}$20 microns or fines) were collected and then subjected to TG testing using the standard test parameters (40°C/min, resolution = 5; CO_2 atmosphere, 55 milligram sample).

Typical results from the study are shown in Figures 19 and 20. The test results suggest that the various carbonate samples should contain a maximum particle diameter of about 45 microns if one wants to obtain accurate quantitative information from the sample. Particles larger than 45 microns tended to cause erroneous weight losses that varied from small discrepancies for Garrison or Early Chapel, to a very large discrepancy for Maryville. Note in the top half of Figure 20, that larger particles can cause the residues measurement (at 970°C) to be in error by approximately 25 percent (absolute!). This magnitude of error drastically influences the results of calculating the dolomite or calcite content of the sample using the technique listed in Table 19.

One may argue that the particle size effect may not be the only variable present in the particle size study because of the potential for mineral segregation during the sieving process. However, mineral segregation did not appear to play a major role in the particle size effect because when the coarse particles size fractions ($^{+}$105 microns) were ground up they tended to produce results very similar to those obtained from the small particle size fractions (see Figure 21).

Hence, it was concluded that the particle size effect could mainly be attributed to inadequate grinding. Poor grinding tended to produce significant quantities of larger particles that appeared to decompose at lower temperatures because of the restricted access of CO_2 purge gas to the interior of the particles. The decomposition reactions occurred violently (similar to popcorn?) and this caused the sample mass to change abruptly. The abrupt mass changes are evident as "noise" in the thermal curves (see Figures 21 and 22). An attempt was made to remedy this situation by simply increasing the depth of the sample pan used in the TG experiments; however, this attempt was not totally satisfactory (see Figure 22) because the thermal curves still deviated significantly from the ideal (i.e., small particle size) curve.

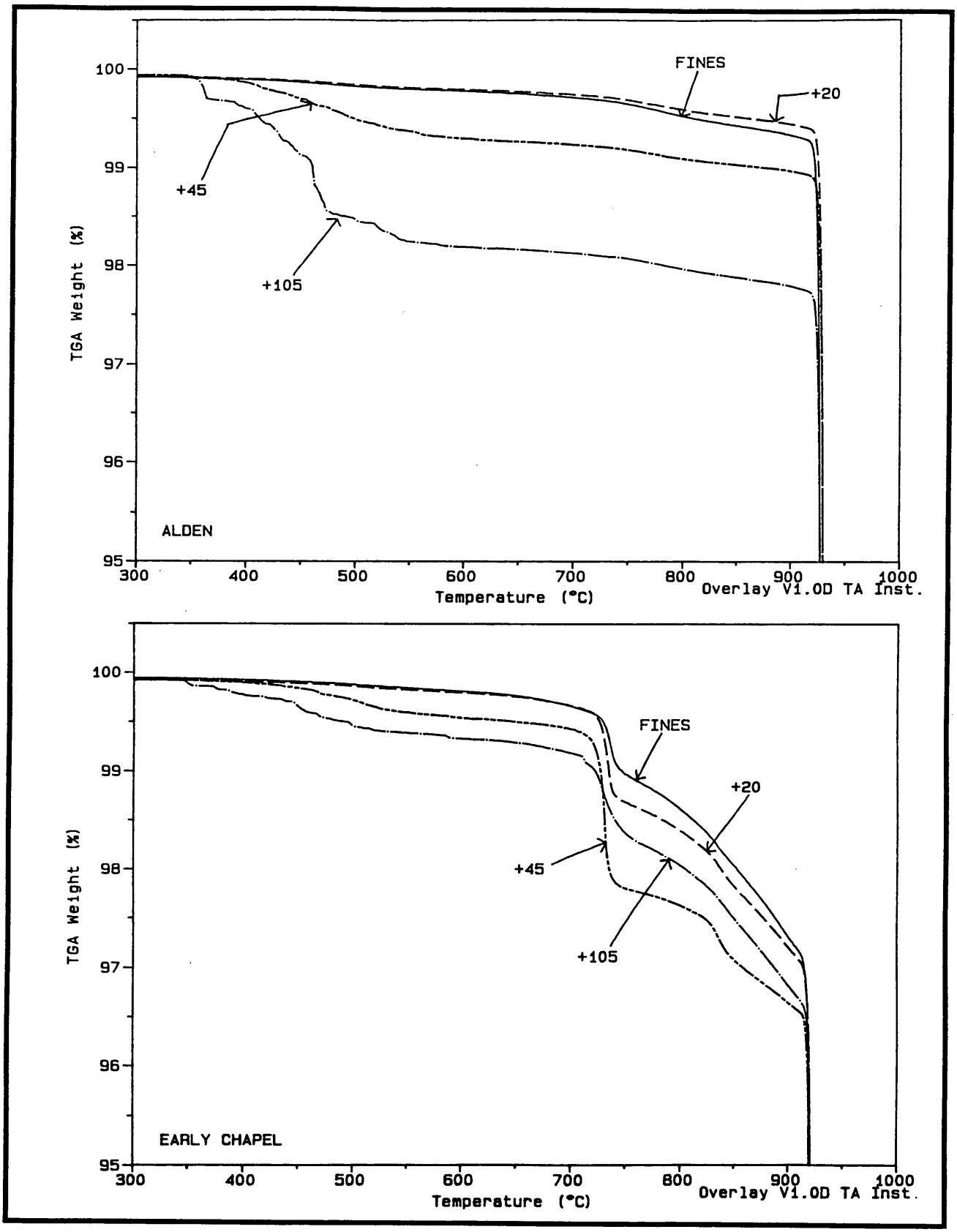

Figure 19. Illustration of how different particle sizes of limestones can influence the results of TG tests.

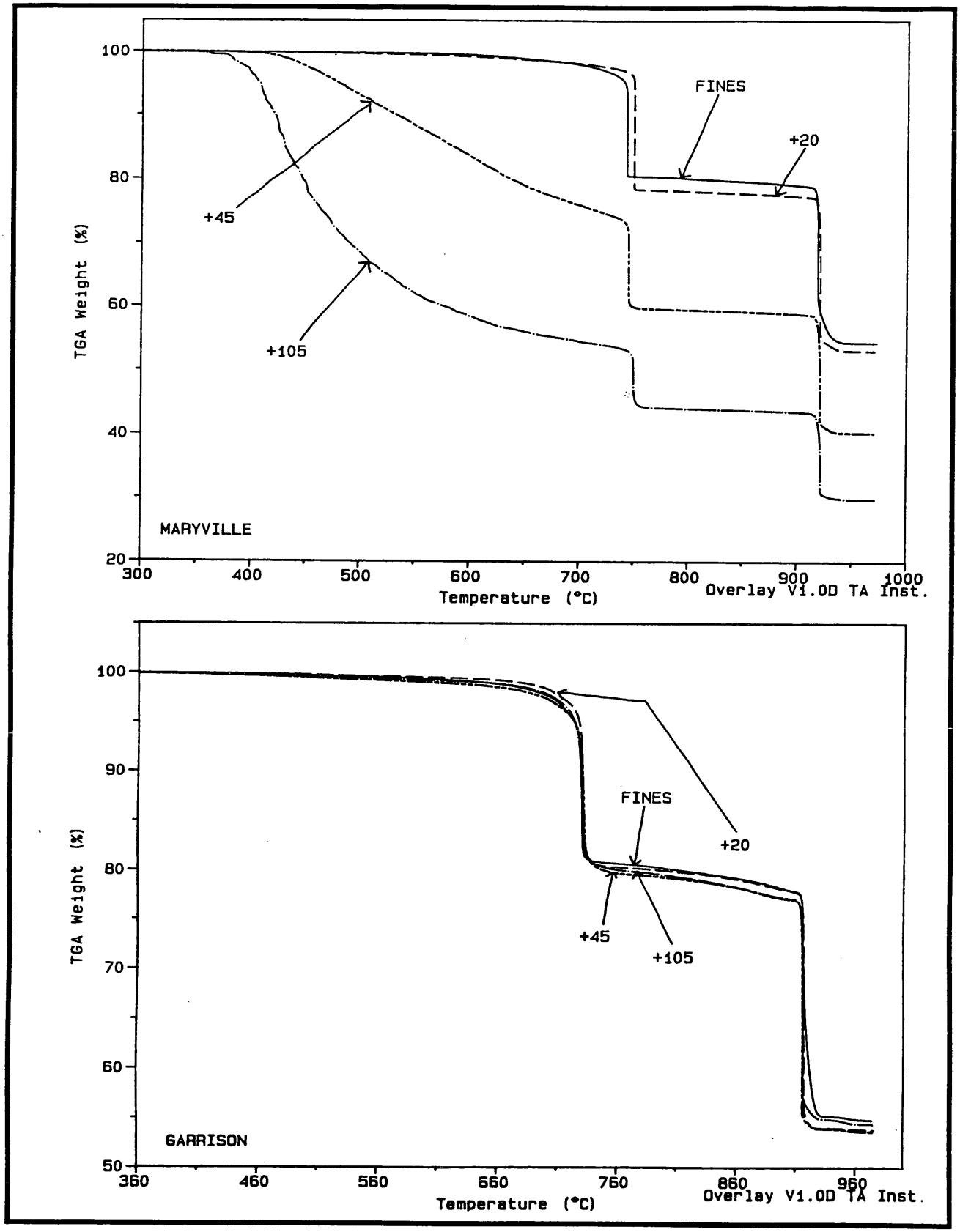

Figure 20. Illustration of how different particle sizes of dolomites can influence the results of TG tests.

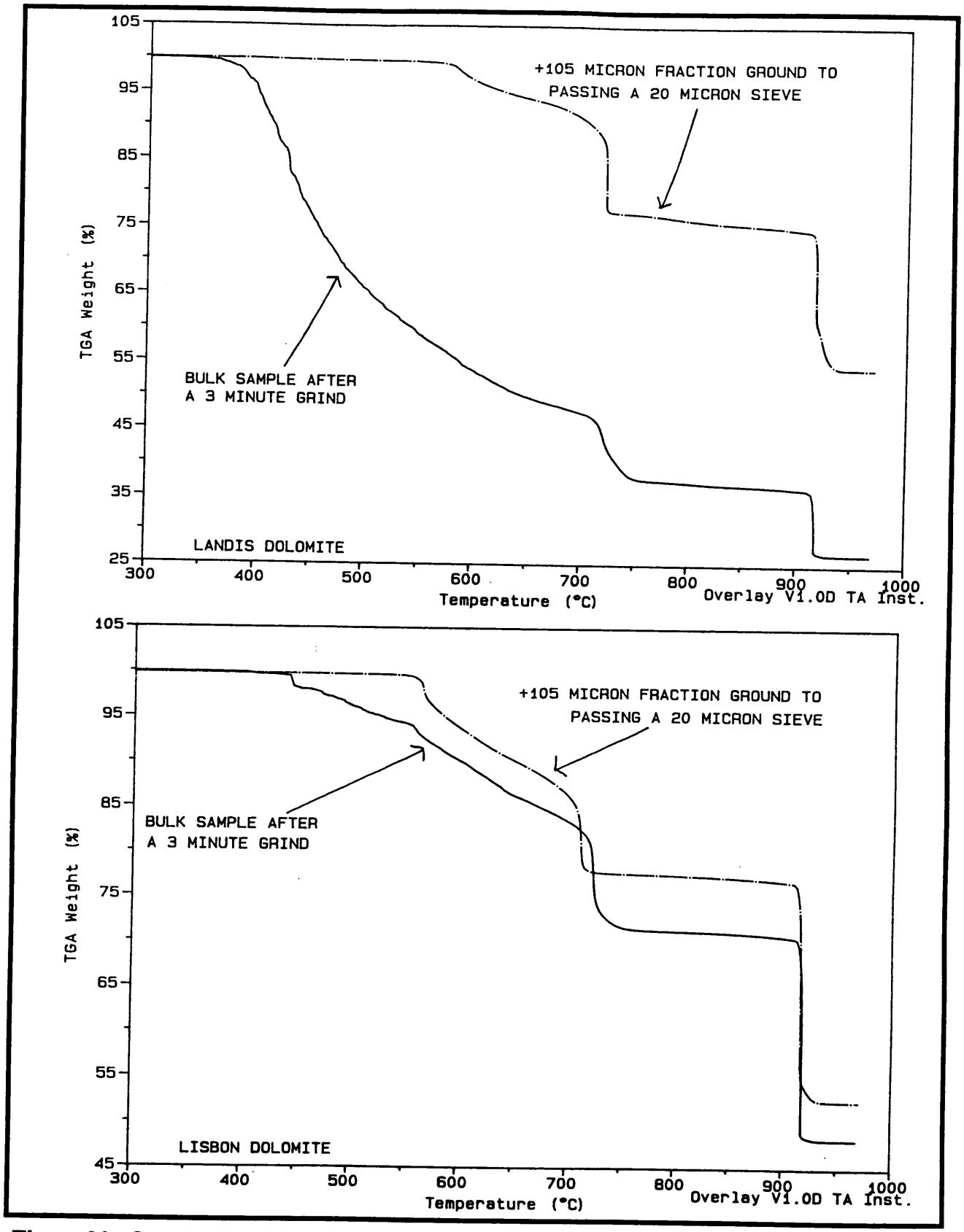

Figure 21. Comparison of TG results before and after grinding the coarse particle fraction of Lisbon and Landis dolomites.

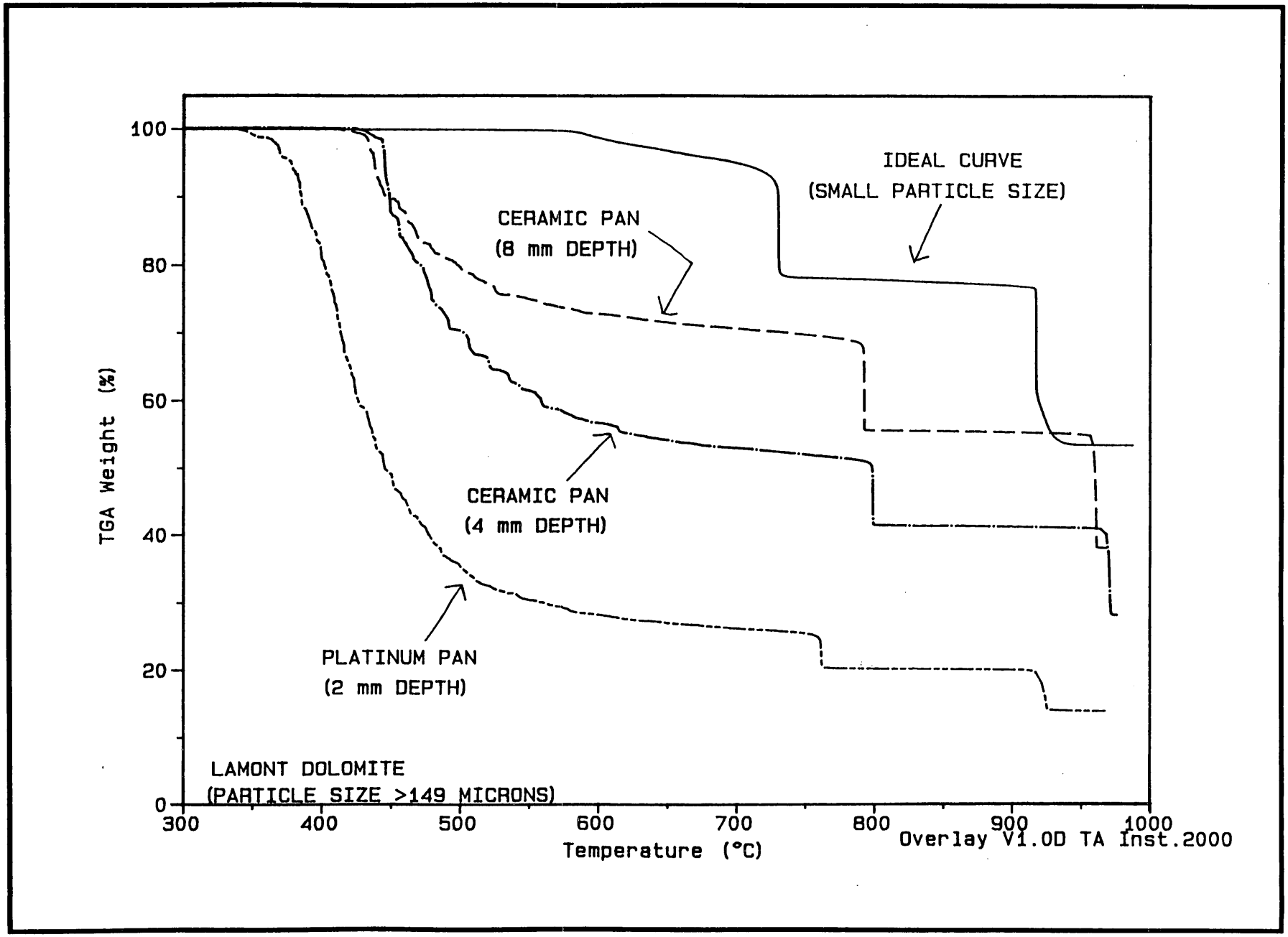

Figure 22. Illustration of how sample pan depth influences the results of TG experiments conducted on coarse particles of dolomite.

The thermal curves from several of the dolomite samples (Landis, Lisbon, Lamont, Gassman, and Maryville to some degree) still exhibited a significant premature decomposition reaction (located approximately at 580°C) even after precautions had been taken to avoid any type of particle size problems. This decomposition temperature is near that of magnesite ($MgCO_3$); however, XRD indicated that the samples were dolomites. Hence, another reason was needed to explain why these particular samples deviated from the ideal dolomite decomposition reaction. A DTA study of several of the samples also indicated that the decomposition reaction occurred over a rather broad range of temperature (see Figure 23). Other researchers have reported similar DTA test results and have attributed such behavior to excessive grinding during the sample preparation process [28, 29] or the presence of soluble salts (most commonly sodium chloride) [21, 22, 30]. The latter explanation appears to be the most probable reason for the behavior of some of the dolomites investigated in this research project.

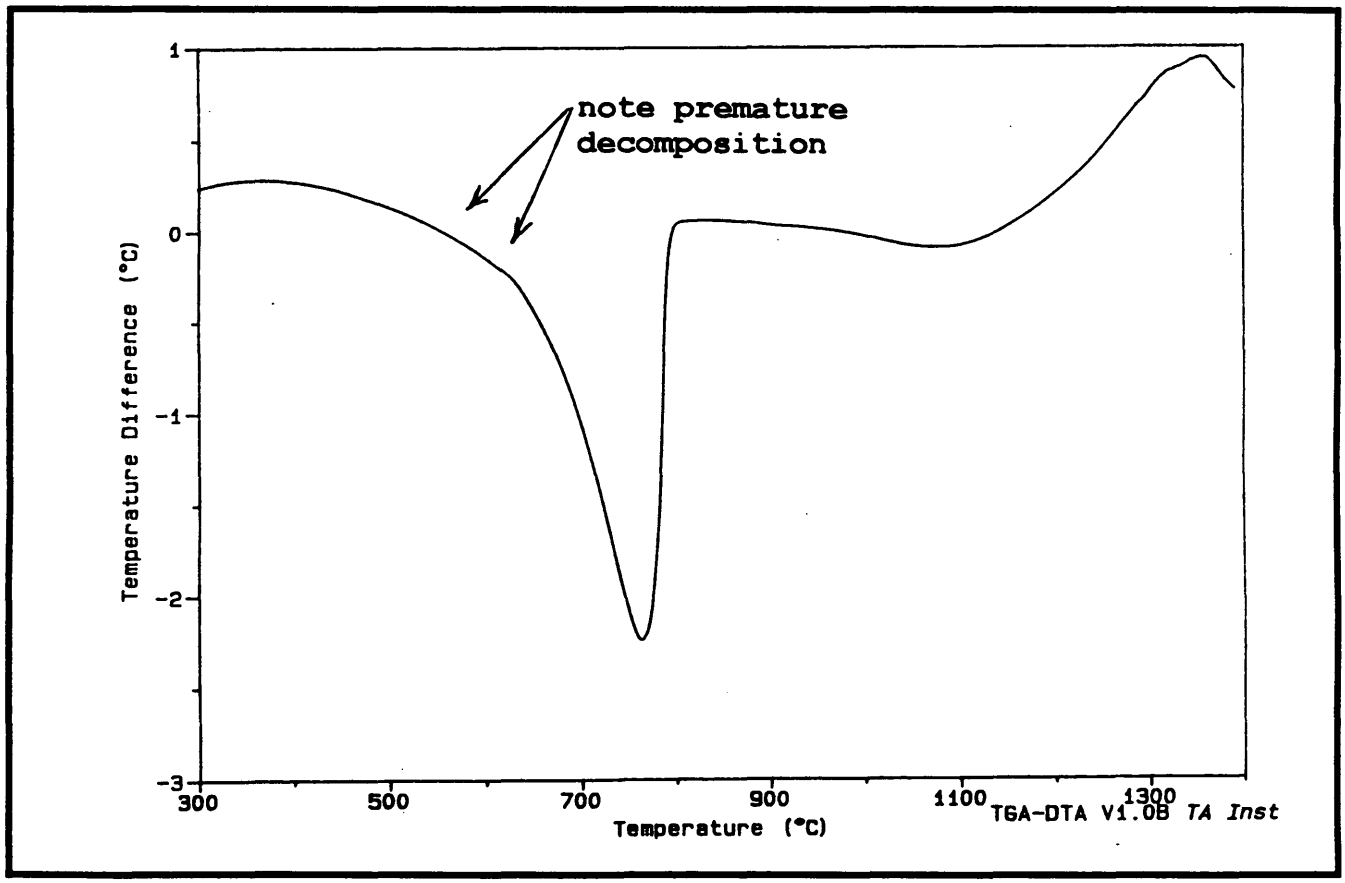

Figure 23. Results of differential thermal analysis (DTA) testing of the Lamont dolomite.

The soluble salt theory fits the premature dolomite decomposition behavior best because washing the various carbonate stones eliminated (or minimized) the odd decomposition reaction (see Figures 24 and 25). Washing should have had little influence on the degradation induced by excessive grinding. Also, the chemical assays, listed in Table 7, clearly indicate that the chlorine (Cl) content was generally above approximately 500 ppm (i.e., 0.05%) in the specimens that exhibited the premature dolomite decomposition reaction. Hence, the chloride salt concentration of the dolomite specimens tends to lower the decomposition temperature of the dolomite crystals. Note, that sodium, magnesium or potassium chloride (i.e., NaCl, $MgCl_2$ and KCl, respectively) do not decompose below about 700°C, and this has caused some researchers to conclude that trace amounts of soluble salts have a catalytic effect on the decomposition of dolomite [30]. Could chloride salts from external sources cause similar behavior in carbonate stones that contain only low concentrations of soluble salts? That was the basis for conducting a detailed study on the influence of sodium chloride and calcium chloride on the decomposition reactions of carbonate stones.

Salt treatment studies

The salt treatment studies consisted of exposing the finely ground limestone and dolomite samples to solutions containing sodium chloride or calcium chloride (10% solutions by weight). All of the solutions were prepared from reagent grade chemicals and distilled water that had been boiled to minimize the amount of CO_2 gas dissolved in the solution. The samples were subjected to two treatment times (one day and three days) and three treatment temperatures (5°C, 38°C and 96°C). All treatments were conducted using 3 grams of sample and 90 ml of solution.

A series of blanks (i.e., no salt treatment, specimens subjected only to CO_2 free water) were conducted in unison with the majority of the samples that were investigated. However, the 38°C treatment temperature and some specific samples were eliminated from the blank runs to reduce the total number of samples present in the study.

After the treatment each sample was filtered to remove the fluid phase. Then the residue was washed at least three times using CO_2 free water, and then dried to a constant weight at 96°C. The samples were then scraped from the filter paper and subjected to thermal analysis and x-ray analysis.

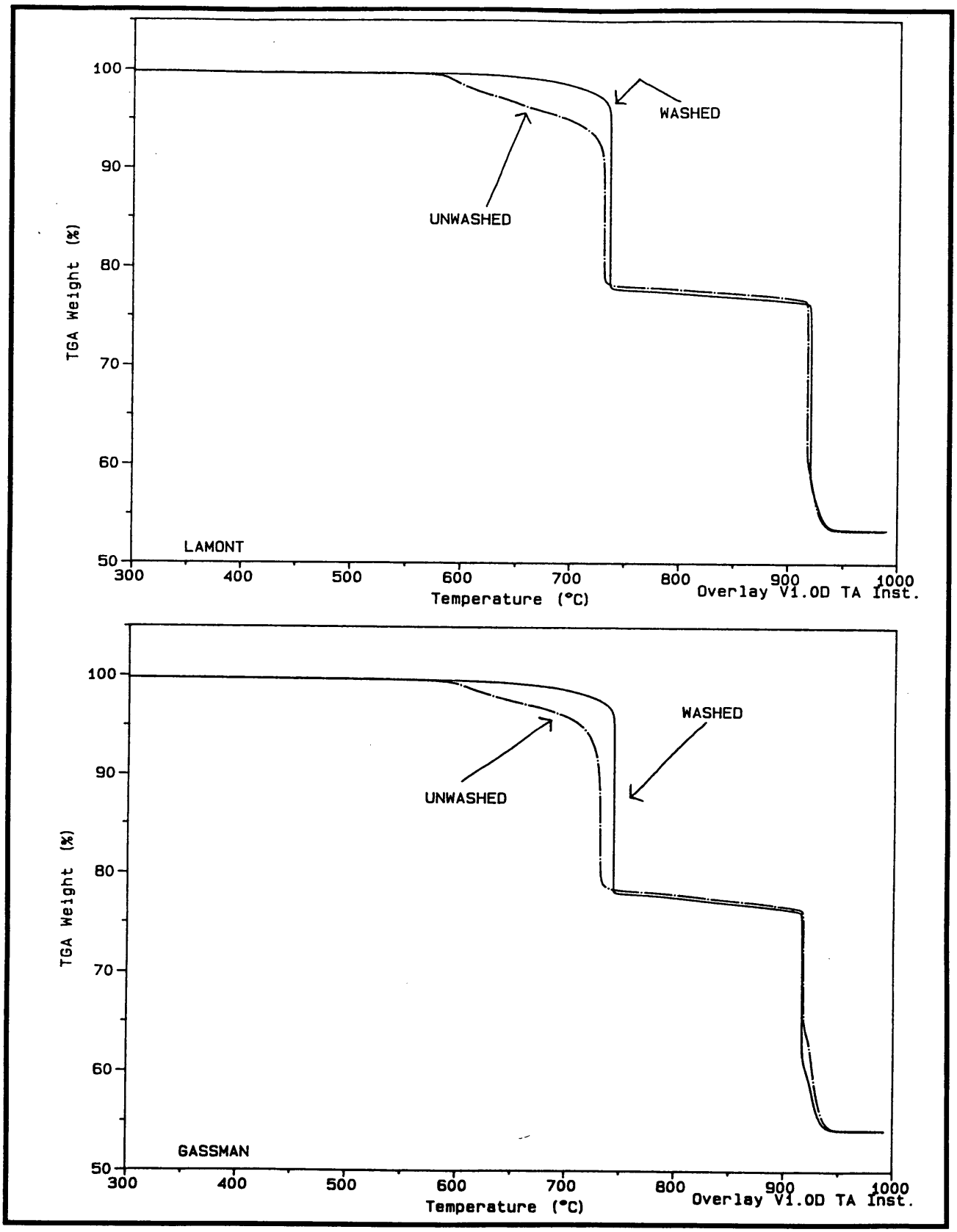

Figure 24. Illustration of how washing Lamont and Gassman dolomites influences the results of a TG experiment.

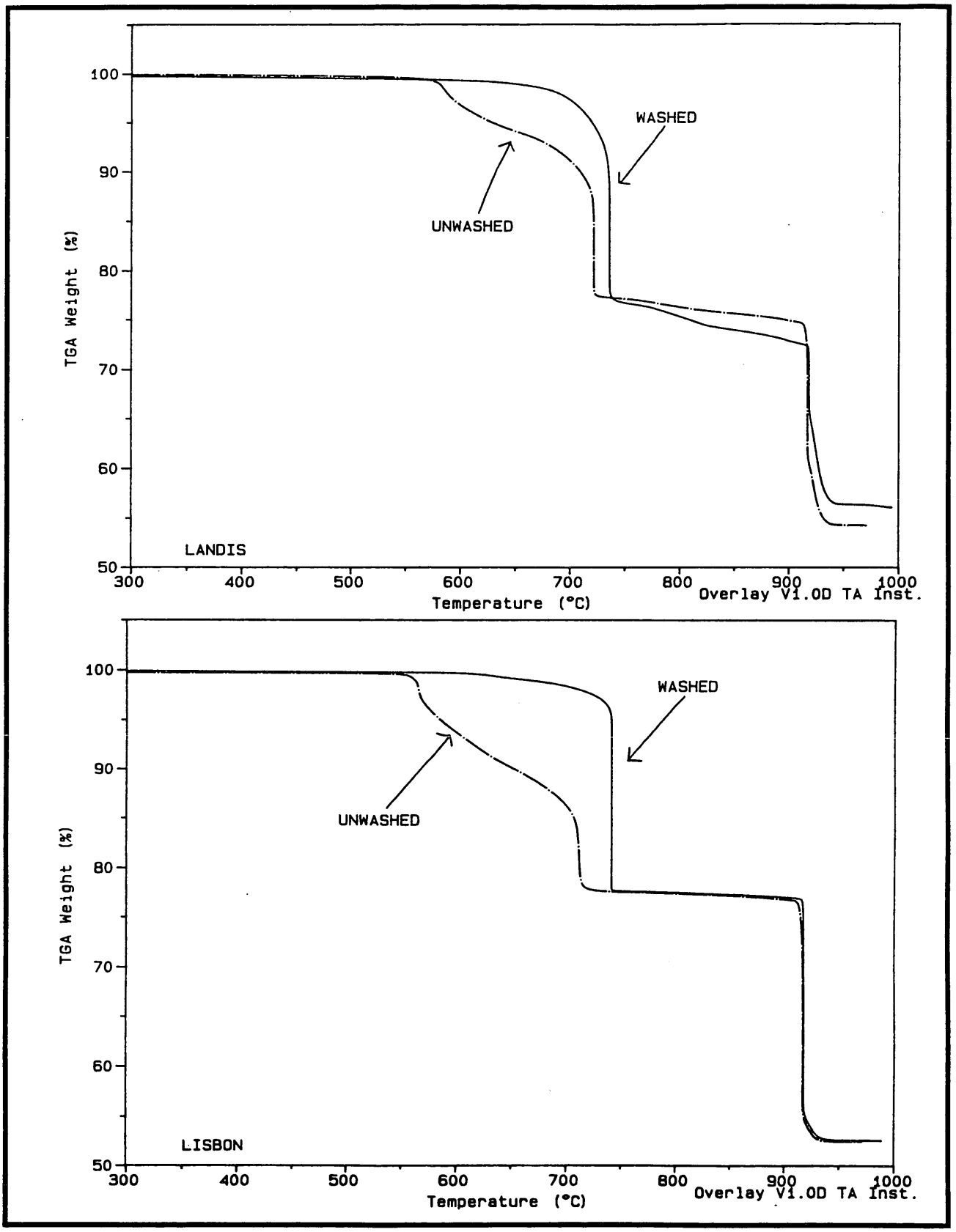

Figure 25. Illustration of how washing Landis and Lisbon dolomites influences the results of a TG experiment.

The results of the TG studies are summarized in Tables 21 through 23 for the limestones (mostly calcites), and Tables 24 through 26 for the dolomites. In general, the limestone (calcite) samples that were subjected to the salt treatments showed only very subtle changes in thermal decomposition behavior. The chemistry and mineralogy of the limestone specimens was nearly identical to the control specimens. However, the dolomite samples were severely altered by the calcium chloride treatment and partially altered by the sodium chloride treatment. Hence, the limestones and dolomites will be considered separately throughout the remainder of this discussion.

For the purpose of illustration, the behavior of three different limestone samples will be discussed in detail, the majority of the other limestone samples exhibited similar trends during the salt treatment study. The limestone aggregates that will be discussed consist of Alden (40 year service record), Linwood (30 year service record) and Crescent (10 year service record).

Thermal analysis studies on the Crescent, Linwood and Alden limestones indicated that the salt treatment had little influence on the residue observed at 825°C, the decomposition temperature (DT_{CAL}) or the residue observed at 970°C. In fact, most of these values were easily within approximately 0.5 percent of the control samples. However, a subtle trend was observed in the decomposition behavior of the Crescent limestone. The trend is shown in Figure 26. The top half of Figure 26 illustrates how the TG curve changed slightly with the salt treatments. The bottom half of Figure 26 simply illustrates how the slope of the TG curve from 825°C to DT_{CAL}, changes as a function of temperature. Both salt treatments (i.e., NaCl and $CaCl_2$) caused the slope to decrease with increasing temperature. The changes were subtle but they were consistent. In fact, one could claim that similar trends were found in the data for Linwood and Alden limestones; however, due to the very small magnitude of the decomposition events (0.29 percent for Linwood and 0.15 percent for Alden) the TG test results could not be considered statistically significant.

X-ray diffraction studies indicated that the sodium chloride salt treatment tended to increase the average crystallite size of the Crescent limestone by 13 percent and the Linwood limestone by about 7 percent. The crystallite size of the Alden limestone remained unchanged by the salt treatment.

Table 21. Results of TG analysis on the control specimens (water solution) for the salt treatment study (powder samples).

⇐ Limestones (all samples 55 ± 2 mg, CO_2 atmosphere) ⇒						
Sample	1 day treatment			3 day treatment		
	Residue @ 825°C (%)	DT_{CAL} (°C)	Residue @ 970°C (%)	Residue @ 825°C (%)	DT_{CAL} (°C)	Residue @ 970°C (%)
Treatment temperature = 5°C						
Eldorado	-	-	-	99.09	927.7	56.60
Alden	99.33	930.1	56.04	99.31	927.2	56.02
Crescent	98.83	924.6	56.99	98.80	925.3	56.92
Menlo	-	-	-	98.45	923.0	57.77
Montour	99.22	931.1	56.41	99.17	930.4	56.43
Early Chapel	97.96	921.5	57.38	97.96	921.9	57.42
Linwood	-	-	-	99.25	924.0	56.46
Skyline	93.45	921.1	55.97	93.37	921.3	56.00
Huntington	97.66	926.2	56.59	97.63	925.5	56.57
Conklin	-	-	-	99.13	923.4	56.29
Treatment temperature = 96°C						
Eldorado	-	-	-	99.04	927.7	56.56
Alden	99.25	931.9	55.97	99.19	930.7	55.95
Crescent	98.93	925.6	57.10	98.86	927.4	56.88
Menlo	-	-	-	98.43	923.2	57.62
Montour	99.27	932.9	56.39	99.28	932.1	56.42
Early Chapel	98.02	921.7	57.36	97.83	923.2	57.46
Linwood	-	-	-	99.27	925.5	56.46
Skyline	93.32	921.8	55.91	93.45	921.5	56.03
Huntington	97.88	926.3	56.61	97.63	925.0	56.60
Conklin	-	-	-	99.12	924.5	56.31

Table 22. Results of TG analysis on the 10% NaCl treated specimens for the salt treatment study (powder specimens).

⇐ Limestones (all samples 55 ± 2 mg, CO_2 atmosphere) ⇒						
Sample	1 day treatment			3 day treatment		
	Residue @ 825°C (%)	DT_{CAL} (°C)	Residue @ 970°C (%)	Residue @ 825°C (%)	DT_{CAL} (°C)	Residue @ 970°C (%)
Treatment temperature = 5°C						
Eldorado	99.10	927.5	56.59	98.97	926.4	56.54
Alden	99.20	928.7	55.97	99.06	920.4*	55.90
Crescent	98.92	923.9	57.02	98.92	925.6	57.02
Menlo	98.22	924.7	57.72	98.40	922.9	57.73
Montour	99.19	928.8	56.41	99.22	930.2	56.38
Early Chapel	97.83	923.0	57.36	97.84	921.3	57.38
Linwood	99.15	921.1	56.46	99.21	922.8	56.46
Skyline	93.37	921.4	55.92	93.39	920.3	55.93
Huntington	97.61	926.2	56.54	97.50	924.8	56.52
Conklin	99.10	921.0	56.37	99.08	919.7	56.31
Treatment temperature = 38°C						
Eldorado	99.07	926.1	56.57	99.05	926.6	56.56
Alden	99.14	930.6	55.93	99.22	929.1	55.97
Crescent	98.82	924.2	57.05	98.81	925.8	56.93
Menlo	98.22	923.4	57.67	98.37	922.8	57.72
Montour	99.24	928.9	56.42	99.14	929.9	56.38
Early Chapel	97.88	921.8	57.37	97.75	920.7	57.42
Linwood	99.19	923.4	56.45	99.15	923.1	56.41
Skyline	93.37	921.4	55.94	93.16	921.2	55.78
Huntington	97.70	923.1	56.57	97.72	925.0	56.53
Conklin	99.10	921.5	56.30	99.10	922.7	56.29
Treatment temperature = 96°C						
Eldorado	99.08	927.5	56.56	98.99	928.7	56.55
Alden	99.38	931.3	56.04	99.10	929.0	55.91
Crescent	98.81	926.3	56.98	98.85	927.0	56.91
Menlo	98.11	920.2	57.88	98.24	923.2	57.73
Montour	99.22	926.9	56.54	99.24	930.9	56.39
Early Chapel	98.00	923.3	57.46	97.73	923.1	57.47
Linwood	99.26	923.4	56.46	99.25	924.7	56.45
Skyline	93.94	922.6	55.89	93.23	921.3	55.99
Huntington	97.65	927.3	56.51	97.35	924.9	56.53
Conklin	99.12	923.0	56.30	99.11	922.3	56.30

* this TG curve had a strange tail on the decomposition reaction

Table 23. Results of TG analysis on the 10% $CaCl_2$ treated specimens for the salt treatment study (powder specimens).

⇐ Limestones (all samples 55 ± 2 mg, CO_2 atmosphere) ⇒						
	1 day treatment			3 day treatment		
Sample	Residue @ 825°C (%)	DT_{CAL} (°C)	Residue @ 970°C (%)	Residue @ 825°C (%)	DT_{CAL} (°C)	Residue @ 970°C (%)
Treatment temperature = 5°C						
Eldorado	99.06	928.4	56.56	99.07	929.6	56.59
Alden	99.15	931.1	55.94	99.12	929.3	55.92
Crescent	98.94	925.9	57.03	98.92	925.2	57.00
Menlo	98.39	923.6	57.70	98.41	922.7	57.80
Montour	99.06	930.2	56.35	99.18	930.5	56.38
Early Chapel	97.98	922.2	57.38	97.90	921.4	57.36
Linwood	99.22	925.3	56.46	99.29	925.5	56.48
Skyline	93.35	921.7	55.88	93.34	921.7	55.89
Huntington	97.72	926.3	56.58	97.79	925.5	56.57
Conklin	99.18	922.8	56.35	99.16	925.7	56.32
Treatment temperature = 38°C						
Eldorado	99.10	926.2	56.59	99.01	930.3	56.57
Alden	99.28	932.6	56.01	99.27	931.1	56.00
Crescent	98.80	925.4	57.01	98.89	924.6	57.04
Menlo	98.45	923.0	57.76	98.44	923.4	57.56
Montour	99.14	930.9	56.36	99.18	931.2	56.42
Early Chapel	97.97	922.2	57.42	97.95	921.9	57.41
Linwood	99.23	924.2	56.52	99.26	925.7	56.53
Skyline	93.60	921.9	55.96	93.62	920.9	55.91
Huntington	97.90	927.1	56.60	97.87	925.5	56.67
Conklin	99.14	923.1	56.32	99.08	923.7	56.28
Treatment temperature = 96°C						
Eldorado	99.12	928.1	56.57	99.12	930.3	56.58
Alden	99.27	931.8	55.98	99.38	932.0	56.07
Crescent	98.90	927.2	57.03	98.66	926.3	56.90
Menlo	98.23	922.7	57.64	98.34	923.3	57.84
Montour	99.27	933.9	56.42	99.35	933.2	56.4[illegible]
Early Chapel	98.44	923.4	57.55	98.55	923.7	57.59
Linwood	99.33	926.7	56.49	99.38	925.5	56.51
Skyline	96.74	922.3	56.57	97.58	923.0	56.61
Huntington	98.57	928.3	56.67	98.93	928.9	56.82
Conklin	99.24	925.5	56.35	99.20	924.8	56.29

Table 24. Results of TG analysis on the control specimens (water solution) for the salt treatment study (powder specimens).

⇐ Dolomites (all samples 55 ± 2 mg, CO_2 atmosphere) ⇒								
Sample	1 day treatment				3 day treatmemt			
	DT_{DOL} (°C)	Residue @ 825°C (%)	DT_{CAL} (°C)	Residue @ 970°C (%)	DT_{DOL} (°C)	Residue @ 825°C (%)	DT_{CAL} (°C)	Residue @ 970°C (%)
Treatment temperature = 5°C								
Maryville	737.6	69.67	920.4	47.41	737.8	68.68	921.2	46.77
Gassman	731.9	70.56	913.9	49.00	733.0	70.04	914.5	48.65
Ced.Rapids-Gray	730.6	75.28	918.1	52.22	731.3	75.32	918.2	52.28
Ced. Rapids-Tan	733.9	76.62	919.2	52.49	733.9	76.43	917.4	52.37
Bryan	718.4	77.71	917.3	57.24	739.9	77.34	918.0	57.00
LeClaire	732.4	75.29	918.0	52.08	732.4	75.31	918.0	52.08
Lamont	731.3	71.23	919.3	49.01	731.0	70.70	919.6	48.63
Garrison	730.8	79.52	915.5	54.26	-	-	-	-
Plower	731.9	79.41	917.4	54.11	730.6	79.38	917.6	54.09
Pesky	732.5	81.31	915.8	53.52	731.2	81.16	914.4	53.45
Lisbon	-	-	-	-	729.3	74.09	917.5	50.13
Landis	-	-	-	-	723.5	75.56	913.8	54.05
Treatment temperature = 96°C								
Maryville	738.4	73.16	920.1	49.88	741.9	71.44	920.1	48.83
Gassman	738.2	68.15	913.7	47.36	744.8	70.87	915.2	49.34
Ced.Rapids-Gray	732.0	75.78	918.3	52.69	742.3	75.15	917.9	52.47
Ced. Rapids-Tan	737.5	76.27	920.0	52.24	741.1	76.53	918.9	52.46
Bryan	722.8	77.70	917.9	57.34	726.0	77.45	918.5	57.30
LeClaire	731.3	75.91	918.0	52.61	733.4	75.56	917.8	52.37
Lamont	735.2	70.83	918.2	48.80	739.3	71.97	920.4	49.65
Garrison	730.6	79.52	915.0	54.25	-	-	-	-
Plower	732.8	79.29	917.3	54.10	734.1	79.23	917.3	54.21
Pesky	735.4	81.83	914.6	53.56	737.0	81.28	914.8	53.53
Lisbon	-	-	-	-	731.2	73.00	917.1	49.43
Landis	-	-	-	-	721.5	75.50	913.0	54.28

Table 25. Results of TG analysis on the 10% NaCl treated specimens for the salt treatment study (powder specimens).

⇐ Dolomites (all samples 55 ± 2 mg, CO_2 atmosphere) ⇒								
Sample	1 day treatment				3 day treatmemt			
	DT_{DOL} (°C)	Residue @ 825°C (%)	DT_{CAL} (°C)	Residue @ 970°C (%)	DT_{DOL} (°C)	Residue @ 825°C (%)	DT_{CAL} (°C)	Residue @ 970°C (%)
Treatment temperature = 5°C								
Maryville	732.8	71.32	919.2	48.63	733.2	71.19	920.7	48.51
Gassman	727.5	67.83	914.4	47.03	726.6	70.29	913.6	48.84
Ced.Rapids-Gray	731.6	75.17	918.2	52.19	728.8	74.16	917.3	51.43
Ced. Rapids-Tan	734.0	76.19	919.9	52.18	734.7	76.31	917.7	52.28
Bryan	726.6	77.83	917.5	57.28	740.0	77.60	918.3	57.07
LeClaire	733.0	75.82	918.6	52.47	731.8	75.80	917.9	52.45
Lamont	726.4	70.56	918.7	48.56	729.9	70.54	919.6	48.52
Garrison	729.7	79.37	915.6	54.14	731.1	79.46	915.7	54.25
Plower	733.8	79.33	917.1	54.04	732.0	79.29	917.8	53.90
Pesky	731.7	81.42	915.2	53.60	731.2	81.15	914.5	53.43
Lisbon	727.3	72.58	918.6	49.09	718.2	76.09	916.1	51.49
Landis	716.2	75.46	914.4	54.06	722.1	75.61	910.6	54.13
Treatment temperature = 38°C								
Maryville	735.5	70.89	919.8	48.27	736.6	72.45	920.0	49.35
Gassman	727.6	69.24	913.0	48.04	732.4	68.94	913.7	47.89
Ced.Rapids-Gray	732.5	75.48	918.5	52.37	732.2	75.79	917.9	52.58
Ced. Rapids-Tan	733.2	76.27	919.2	52.22	732.7	76.45	917.5	52.37
Bryan	728.0	77.40	917.4	56.98	724.0	77.49	918.2	57.03
LeClaire	732.4	75.28	919.2	52.05	731.9	75.97	918.1	52.55
Lamont	729.3	69.82	918.7	48.02	732.2	69.71	917.5	47.96
Garrison	728.9	79.46	915.6	54.22	729.7	79.29	916.6	54.12
Plower	735.6	79.36	917.6	54.09	734.1	79.32	917.4	54.05
Pesky	730.7	81.38	915.3	53.59	732.7	81.32	915.9	53.51
Lisbon	725.0	73.69	917.0	49.82	720.2	74.27	917.1	50.24
Landis	709.8	75.50	914.8	54.23	724.5	75.59	911.7	54.04
Treatment temperature = 96°C								
Maryville	739.6	72.32	919.7	49.25	744.4	73.86	918.8	50.60
Gassman	626.0	69.54	914.6	48.96	747.7	69.87	913.3	48.77
Ced.Rapids-Gray	733.5	75.63	917.1	52.64	746.8	75.29	917.4	52.76
Ced. Rapids-Tan	718.8	76.47	918.2	52.39	744.1	76.25	917.4	52.36
Bryan	724.2	77.49	916.9	57.45	738.6	77.17	919.0	57.28
LeClaire	728.2	75.82	918.1	52.53	722.8	75.69	918.1	52.54
Lamont	734.7	71.29	915.0	49.20	738.5	71.72	918.8	49.60
Garrison	729.7	79.39	914.7	54.16	734.3	79.34	916.2	54.33
Plower	739.3	79.38	917.1	54.22	739.6	78.95	916.5	54.11
Pesky	733.9	81.50	915.6	53.69	739.0	81.32	914.8	53.65
Lisbon	719.0	74.76	916.1	50.55	722.5	75.34	916.3	50.99
Landis	720.6	75.65	914.2	53.72	719.8	75.56	911.0	53.92

Table 26. Results of TG analysis on the 10% $CaCl_2$ treated specimens for the salt treatment study (powder specimens).

⇐ Dolomites (all samples 55 ± 2 mg, CO_2 atmosphere) ⇒								
Sample	1 day treatment				3 day treatmemt			
	DT_{DOL} (°C)	Residue @ 825°C (%)	DT_{CAL} (°C)	Residue @ 970°C (%)	DT_{DOL} (°C)	Residue @ 825°C (%)	DT_{CAL} (°C)	Residue @ 970°C (%)
Treatment temperature = 5°C								
Maryville	741.9	71.66	919.6	48.77	741.8	68.00	921.4	46.25
Gassman	736.2	68.66	914.4	47.58	737.5	68.22	914.5	47.29
Ced.Rapids-Gray	733.5	75.30	918.1	52.14	734.4	75.87	916.7	52.54
Ced. Rapids-Tan	736.5	76.36	919.0	52.26	737.4	75.80	917.3	51.86
Bryan	721.3	77.83	917.5	57.28	723.4	77.75	918.2	57.12
LeClaire	736.6	75.32	918.5	51.99	734.8	75.73	918.0	52.29
Lamont	734.9	69.51	918.6	47.77	735.8	69.61	919.7	47.80
Garrison	729.6	79.58	915.4	54.26	732.4	79.67	917.5	54.29
Plower	738.1	79.50	916.9	54.13	733.5	79.51	917.3	54.12
Pesky	732.5	81.43	914.7	53.57	733.2	81.34	915.0	53.47
Lisbon	733.4	72.81	918.5	49.17	731.8	75.11	917.1	50.68
Landis	728.4	75.69	914.0	54.09	743.9	75.33	915.4	53.77
Treatment temperature = 38°C								
Maryville	748.3	73.79	919.6	49.93	752.1	74.71	920.8	50.23
Gassman	743.1	70.24	914.7	48.51	747.1	70.86	914.7	48.70
Ced.Rapids-Gray	740.0	76.03	918.2	52.44	743.2	76.86	918.0	52.69
Ced. Rapids-Tan	745.5	76.92	920.0	52.46	747.2	77.12	918.3	52.46
Bryan	729.9	78.34	917.7	57.31	740.1	78.90	916.9	57.37
LeClaire	741.8	76.04	917.7	52.26	745.2	77.36	918.5	52.77
Lamont	745.1	69.73	918.8	47.67	748.4	71.60	918.9	48.60
Garrison	732.2	79.87	914.9	54.36	733.1	80.08	916.1	54.42
Plower	740.3	79.71	916.7	54.02	748.8	80.69	918.3	54.26
Pesky	732.4	81.56	914.9	53.49	735.9	82.28	915.2	53.87
Lisbon	741.3	74.76	918.6	50.19	748.4	77.34	918.4	51.36
Landis	735.3	76.54	914.6	54.29	738.9	77.35	912.2	54.48
Treatment temperature = 96°C								
Maryville	761.3	81.97	919.8	52.48	766.3	83.25	920.7	52.30
Gassman	757.0	77.20	914.7	50.62	763.3	83.78	916.3	52.84
Ced.Rapids-Gray	751.9	82.67	917.9	93.91	761.7	85.43	916.8	54.52
Ced. Rapids-Tan	758.6	83.87	919.3	53.68	762.3	87.23	920.2	54.29
Bryan	755.7	84.91	916.4	58.41	753.1	89.58	918.0	59.39
LeClaire	757.3	83.92	919.7	54.00	764.4	87.61	920.0	54.81
Lamont	763.0	78.24	919.2	50.84	764.1	84.04	919.8	52.82
Garrison	738.5	84.82	914.7	55.43	745.9	87.98	916.7	56.24
Plower	757.0	86.42	918.2	55.26	765.4	90.22	918.0	55.94
Pesky	745.6	86.18	915.3	54.65	751.9	88.73	915.9	55.12
Lisbon	753.8	82.68	919.8	51.93	759.3	87.38	919.7	53.58
Landis	747.7	83.94	916.1	55.33	753.5	87.64	916.9	55.81

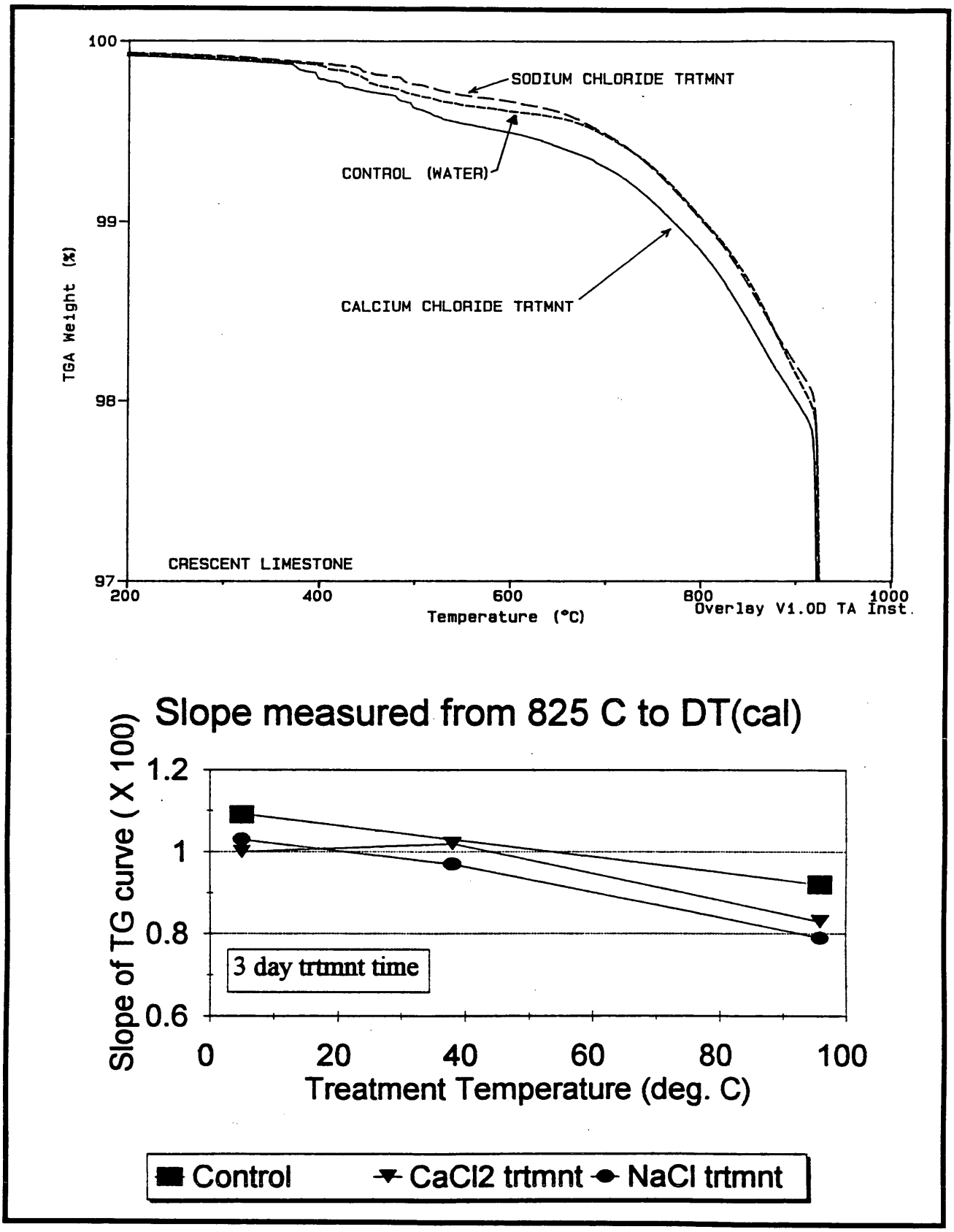

Figure 26. Influence of the two different salt treatments on the TG curve for Crescent limestone.

The results of the TG and XRD studies suggest that the chloride salts tend to attack the small crystallites present in the limestone samples. Since the small crystallites were preferentially removed from the bulk solid, this tended to increase the average crystallite size of the salt treated samples. These test results appear to be in good agreement with those obtained by other researchers [31], who have proposed that carbonate dissolution is controlled by the presence of "active sites" in the bulk solid. The active sites are generally located at defects, boundaries or edges of adjacent crystals. The solubility is enhanced because of a local increase in surface area. The theoretical relationship between solubility and surface area is illustrated in Figure 27. It is evident in Figure 27 that small crystals can be many times more soluble than large crystals; and hence, they tend to dominate the dissolution behavior of the carbonate samples.

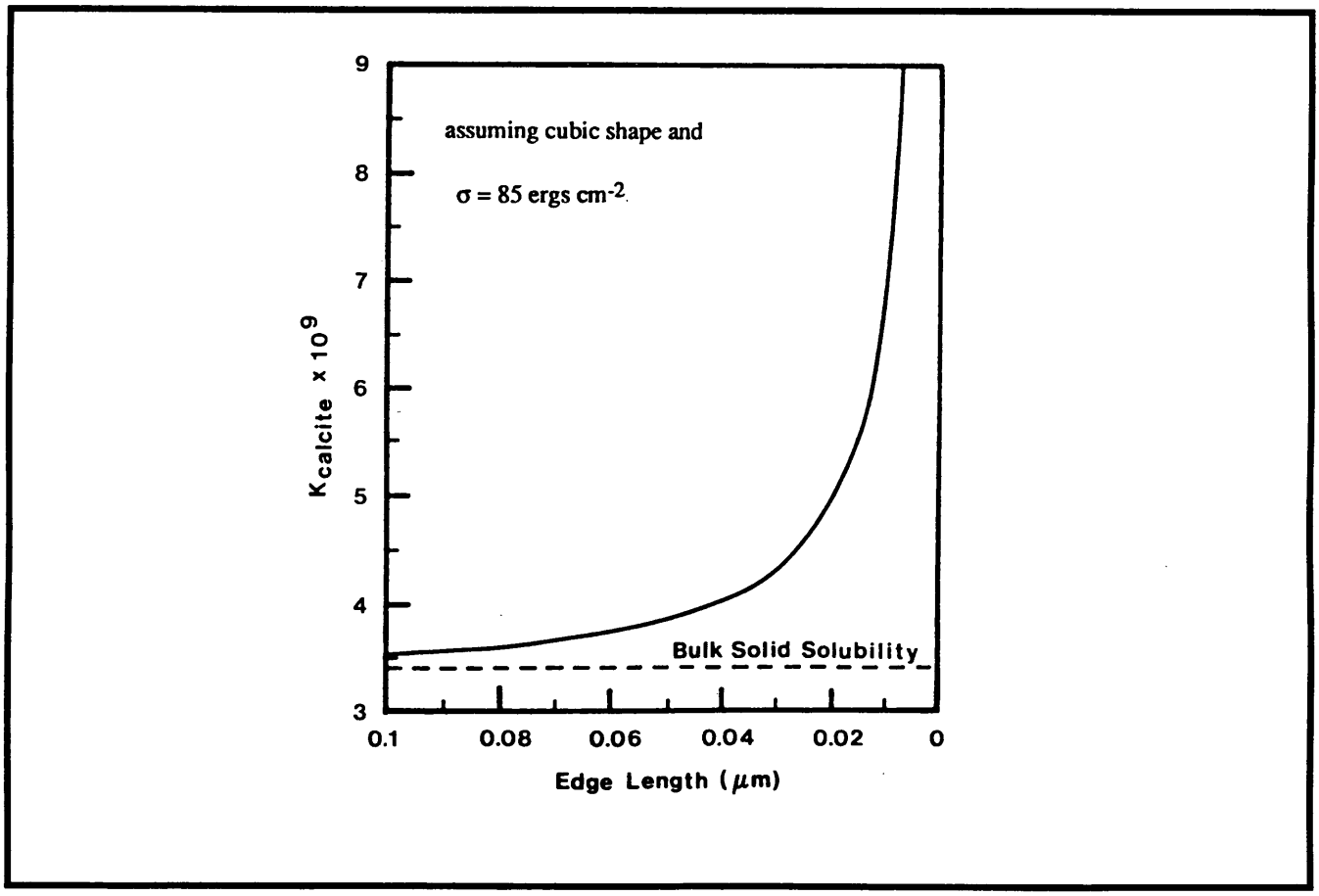

Figure 27. Theoretical relationship between apparent solubility and particle size (adapted from reference 31).

The dolomite samples tended to exhibit a much larger response to the salt treatments. In fact, many of the samples were extensively decomposed during just three days of exposure to a 10 percent calcium chloride solution. The results of TG tests that were conducted after the various treatments (i.e., water solution, sodium chloride solution and calcium chloride solution) are summarized in Tables 24, 25 and 26, respectively. It is important to describe two discrepancies that were noted when tabulating the data summarized in the three tables. First, some of the samples exhibited premature decomposition behavior that surely can be attributed to the "particle size" effect described earlier in this report. This behavior was probably caused by the agglomeration of particles during the experiments (i.e., washing and drying procedures). And secondly, several of the samples had to be subjected to the washing process twice because it was difficult to remove all traces of the salt from them. Typically this occurred during the sodium chloride treatment and it was most notable in the Landis samples. The exact reason why the dolomite samples were so difficult to wash clean of the sodium chloride salt is currently not known. However, as was explained earlier in this report, the presence of soluble salts drastically alters the early decomposition behavior of the $MgCO_3$ fraction of dolomites. This phenomenon is again illustrated in Figure 28.

All of the dolomite samples reacted with both the sodium chloride and the calcium chloride solutions; however, the calcium chloride solution tended to attack the samples much faster, especially at the highest treatment temperature (96°C). X-ray diffraction studies and bulk chemistry obtained by x-ray fluorescence spectrometry were in qualitative agreement with the results of the thermal analysis. A comparison of the test results obtained from the three different methods is illustrated in Figures 29 and 30.

The sodium chloride treatment had a relatively small influence on the dissolution of the dolomite samples; and hence, the sodium chloride treatment curves (see Figures 29 and 30) tended to run nearly parallel to the x-axis (i.e., little or no apparent slope). Often these curves had a slight positive slope that tends to suggest that the dolomite crystals were being subjected to only slight alteration during the duration of the three day study. As expected the 5°C treatment had a negligible influence on most samples.

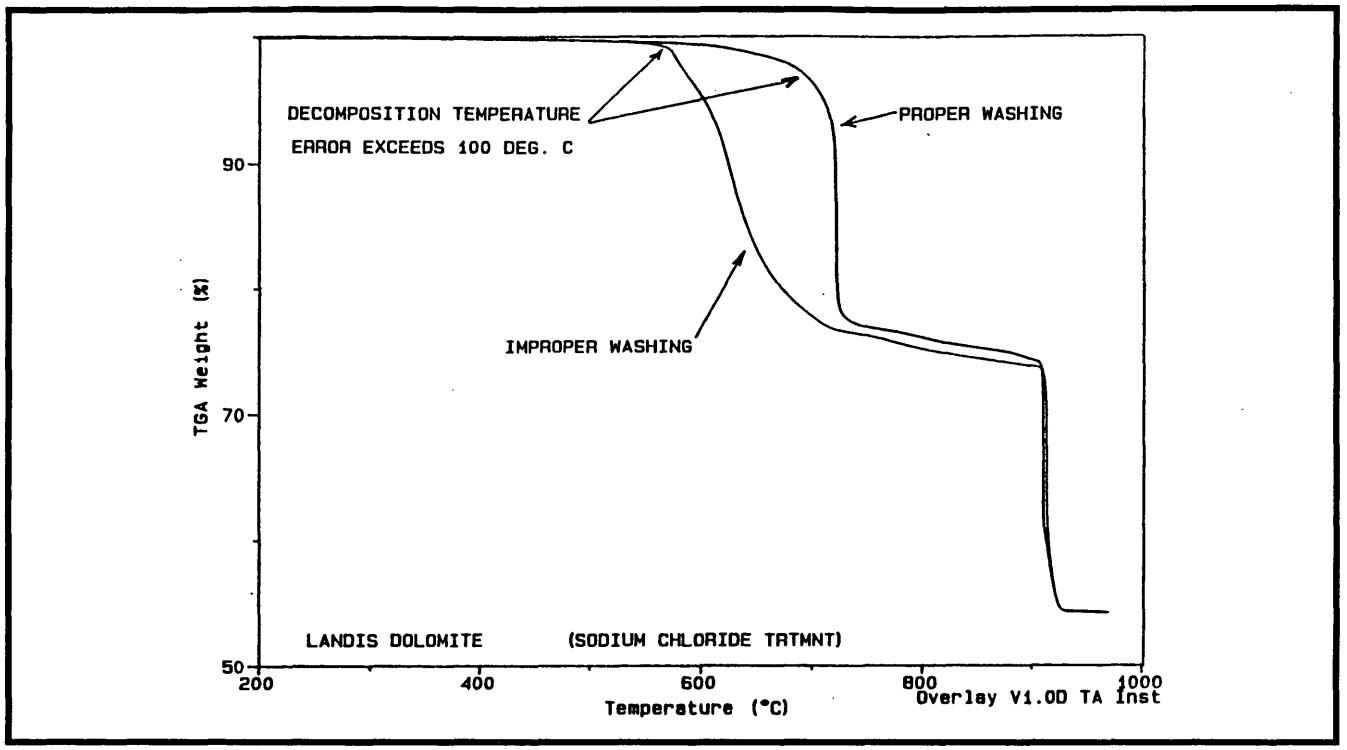

Figure 28. Influence of excess salt (NaCl) on the early decomposition behavior of dolomites.

In contrast, the calcium chloride treatment always caused dolomite dissolution and calcite formation in the test specimens. This trend was evident in all three different modes of analysis (i.e., XRD, XRF and TG tests); however it was disappointing that the trends were only qualitative and not quantitative. The desire of this phase of the research program was to develop quantitative methods for the study of carbonate dissolution kinetics but this goal was not attained.

The study has clearly indicated that the chemistry of dolomite dissolution in a calcium chloride solution can be described by equation 3.

$$MgCa(CO_3)_2 + CaCl_2 \longrightarrow 2CaCO_3 + MgCl_2 \qquad (3)$$

This fact becomes very obvious when one considers Figures 31 and 32 which depict the decomposition of dolomite and subsequent formation of calcite in the various test specimens. Figure 31 was constructed using x-ray diffraction data (normalized, integrated intensities for the (104) peaks)

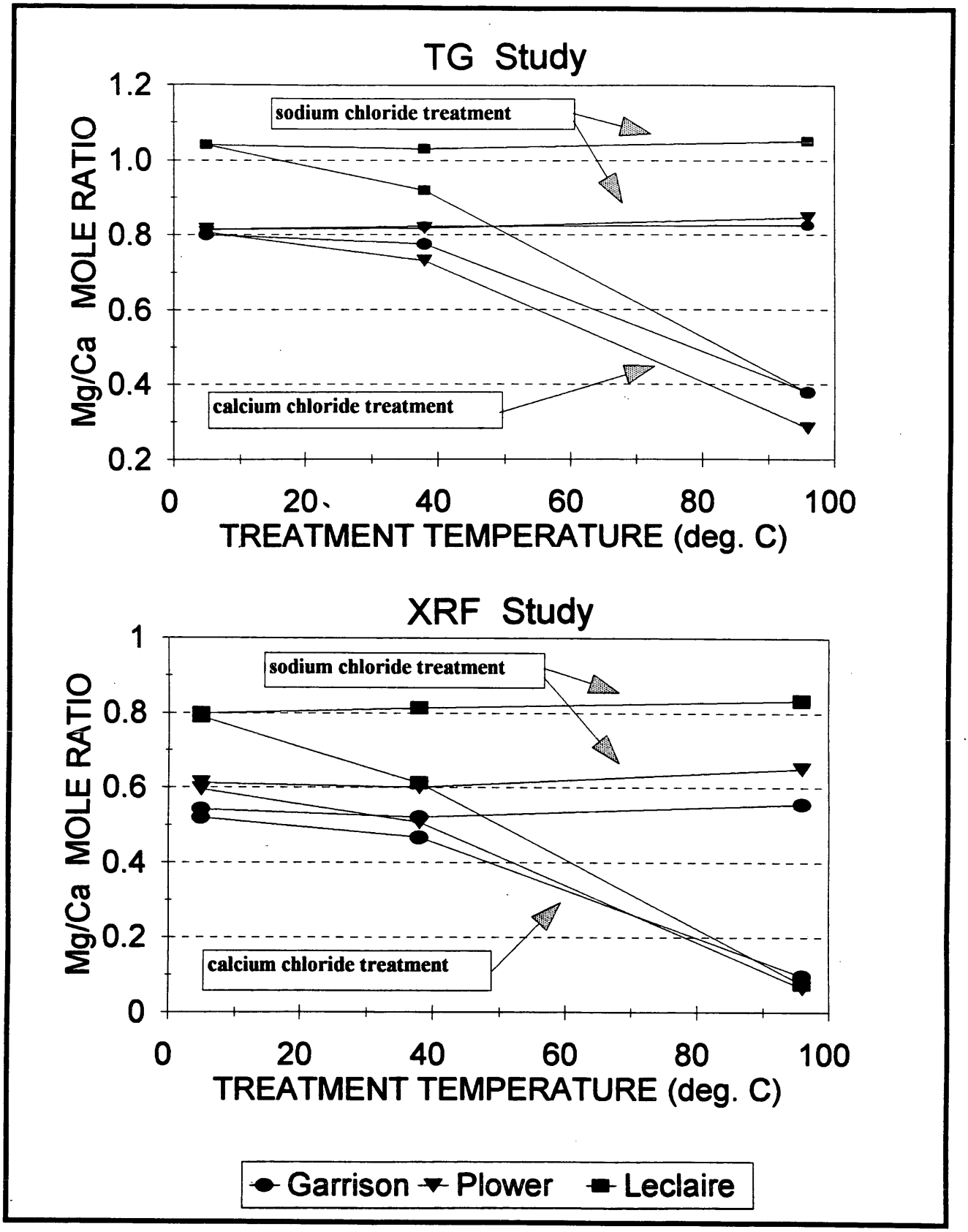

Figure 29. Comparison of TG and XRF test results obtained from the salt treatment study.

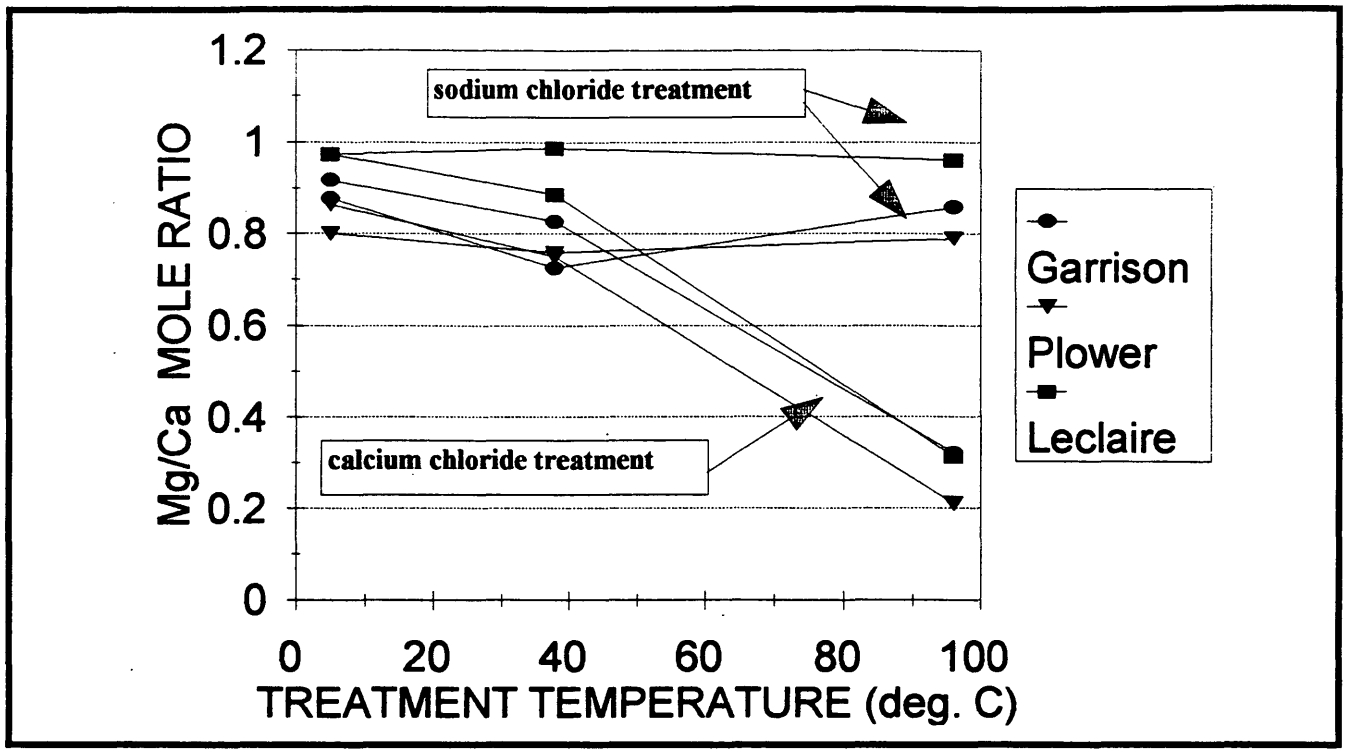

Figure 30. Ilustration of how the salt treatment influenced the XRD test results for dolomite samples.

which depicts the various samples after three days of exposure to the calcium chloride treatment. Temperature played a significant role in the reaction, this is most clearly illustrated in Figure 32. Figure 32 was constructed by using the TG data and the proper gravimetric factors as described in Table 19. The dissolution rate was negligible at 5°C, small (but significant) at 38°C, and rather large at the 96°C treatment temperature.

The time-concentration data did not allow for an unambiguous classification of the order of the decomposition reaction. Hence, it was not possible to calculate reliable equilibrium constants or to estimate the activation energy of the reaction. However, it was obvious that the dolomite decomposition reaction proceeded at a rather large rate for all of the test specimens, especially when the treatment temperature approached 100°C. This suggested that it would be advantageous to perform an additional dissolution study that did not utilize powder specimens. Hence, a short experimental program was designed to evaluate if bulk dolomite specimens would react with chloride salts.

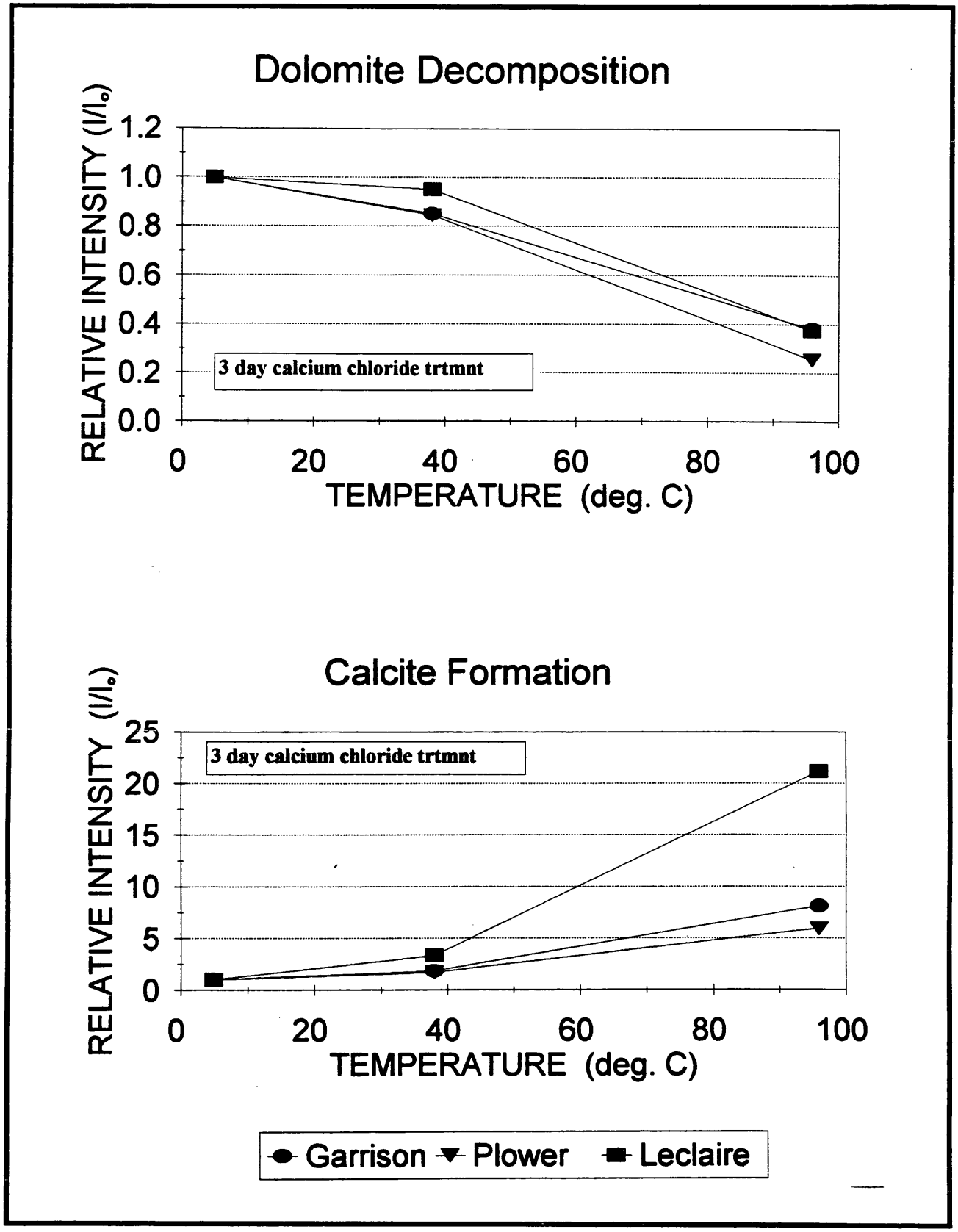

Figure 31. Influence of temperature on the dissolution of dolomite and formation of calcite in the salt treatment studies (XRD data).

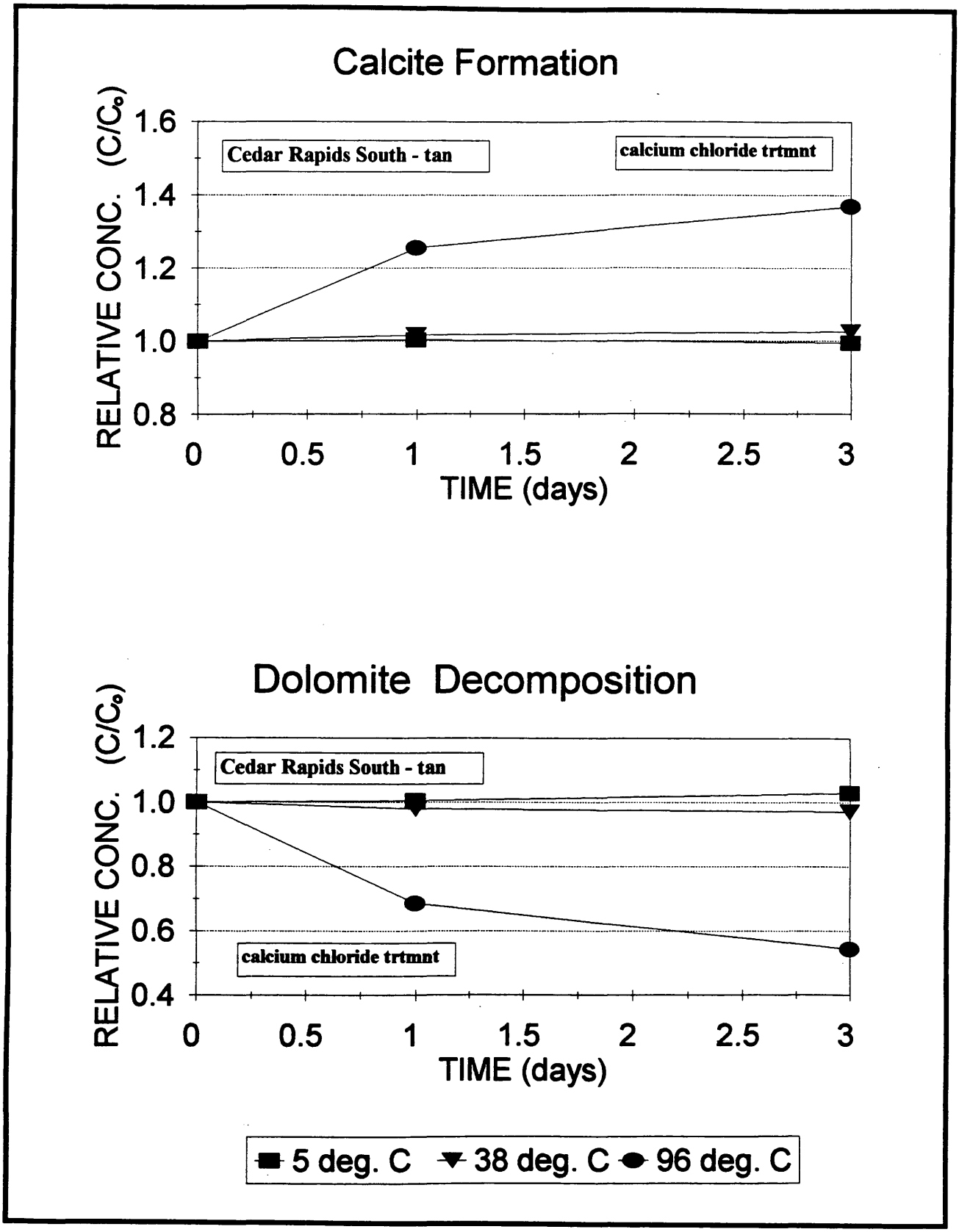

Figure 32. Illustration of the rate of dolomite decomposition and calcite formation in the salt treatment study (TG data).

Briefly, the experimental program used dolomite slices that were approximately 0.2" square by 0.1" thick, these sections will be called "chips" throughout the rest of this report. Specimens were cut from Garrison, Pesky, Lamont and Maryville dolomites. The chips were subjected to the same salt treatments as in the previous experiments; however the duration of exposure was lengthened to five days to allow more time for the reaction to proceed. After the salt treatments at the three different temperatures, the chip specimens were washed, dried and then subjected to TG analysis. The specimens were not pulverized prior to the TG tests. The results of the brief study are summarized in Tables 27, 28 and 29.

In general, the chip study indicated that the dolomite decomposition reaction had proceeded at a very small to negligible rate in most of the salt treated specimens. The low and moderate temperature test results were generally inconclusive, especially when one considers the potential variation in composition between different specimens that were cut from the same chunk of dolomite. Again, the 96°C calcium chloride treatment appeared to produce the most decomposition. This was most notable in the Garrison and Pesky samples. Both the Maryville and the Pesky samples exhibited strange trends when placed in the water (control solution) and the sodium chloride solution. In fact, the Maryville chip specimens tended to produce TG results that were in very poor agreement with the previous chemical determinations that have been summarized in this report. The bulk chemistry, XRD and TG (conducted on powder specimens) tests have indicated that Maryville can be classified as a reasonably pure dolomite (approximately 90 percent or more dolomite). However, the chip study suggests that the Maryville contains only about 70 percent dolomite. The TG results from the other three dolomites agree with the previous determinations to within ± 5 percent. Hence, it may be wise to disregard the test results for the Maryville chip specimens. The exact reason for the erratic behavior of the Pesky specimens could not be pinpointed.

The experimental difficulties and inconsistencies that were encountered during the chip study tended to indicate that the technique will probably need considerable refinement before it can be used on a routine basis. However, one must not forget the purpose of the chip study, which was simply to compare the dissolution rate of bulk dolomite specimens to the powder specimens.

Table 27. Results of TG analysis on the control specimens (water treatment, chip specimens).

⇐ Dolomites (5 day treatment, TG test run in CO_2 atmosphere) ⇒					
Sample	**Mass (mg)**	**DT_{DOL} (°C)**	**Residue @ 825°C (%)**	**DT_{CAL} (°C)**	**Residue @ 970°C (%)**
Treatment temperature = 5°C					
Lamont	64.2	758.6	76.00	921.4	52.17
Maryville	143.9	765.5	82.96	923.0	53.61
Garrison	53.7	735.2	78.39	919.0	54.51
Pesky	56.0	746.1	80.95	918.7	53.46
Treatment temperature = 96°C					
Lamont	80.3	758.9	76.32	921.2	52.47
Maryville	71.8	763.6	83.54	922.0	53.98
Garrison	75.8	737.6	78.55	922.3	54.98
Pesky	49.9	748.4	82.61	919.7	53.57

Table 28. Results of TG analysis on the 10% NaCl treated specimens (chip specimens).

⇐ Dolomites (5 day treatment, TG test run in CO_2 atmosphere) ⇒					
Sample	**Mass (mg)**	**DT_{DOL} (°C)**	**Residue @ 825°C (%)**	**DT_{CAL} (°C)**	**Residue @ 970°C (%)**
Treatment temperature = 5°C					
Lamont	103.0	749.4	75.78	921.9	52.08
Maryville	137.5	760.9	84.04	922.4	54.58
Garrison	112.9	740.3	78.33	921.4	54.76
Pesky	37.7	746.4	82.41	920.6	53.49
Treatment temperature = 38°C					
Lamont	83.3	752.2	75.89	920.2	52.15
Maryville	91.4	764.2	84.63	922.6	53.83
Garrison	58.0	735.6	78.44	920.0	54.53
Pesky	73.2	749.8	83.40	920.0	53.68
Treatment temperature =96°C					
Lamont	80.4	757.0	76.05	921.3	52.33
Maryville	157.3	760.1	85.39	923.3	53.88
Garrison	54.0	736.4	78.24	919.8	54.56
Pesky	37.4	748.1	81.89	919.4	53.46

Table 29. Results of TG analysis on the 10% $CaCl_2$ treated specimens (chip specimens).

⇐ Dolomites (5 day treatment, TG test run in CO_2 atmosphere) ⇒					
Sample	Mass (mg)	DT_{DOL} (°C)	Residue @ 825°C (%)	DT_{CAL} (°C)	Residue @ 970°C (%)
Treatment temperature = 5°C					
Lamont	68.0	746.8	75.54	919.0	51.80
Maryville	119.9	763.1	83.67	921.3	53.75
Garrison	51.8	735.8	78.34	920.2	54.56
Pesky	66.5	750.2	81.11	920.4	53.43
Treatment temperature = 38°C					
Lamont	124.8	746.9	76.15	921.8	52.05
Maryville	122.6	764.1	82.82	923.6	53.79
Garrison	37.9	733.1	78.14	919.1	54.67
Pesky	53.3	746.0	81.30	920.8	53.43
Treatment temperature =96°C					
Lamont	69.7	761.8	76.16	920.3	52.21
Maryville	127.7	767.0	82.63	924.9	53.73
Garrison	52.4	741.6	79.20	918.9	55.21
Pesky	58.2	751.4	83.34	921.4	53.72

The chip experiment indicated that typically less than about 5 to 10 percent of the dolomite had decomposed after five days of salt treatment. This was considerably less than the value of 40 to 50 percent that had been obtained from the powder study (only a three day treatment duration). Hence, one must weigh both the particle size and porosity factors when attempting to apply the various experimental results to real life situations (i.e., coarse aggregates in a concrete pavement structure).

One may question why so much time has been spent trying to determine if different dolomites are stable in the presence of chloride salt solutions. The reason for the apparent digression can be attributed to the fact that concrete aggregates are generally exposed to an environment saturated with hydroxyl anions (i.e., a pore fluid consisting of calcium, sodium and potassium hydroxides, pH above 12). If dolomites tend to donate Mg^{2+} ions to the pore solution then they surely must promote the formation of brucite ($Mg(OH)_2$) in the pore water system. This proposed reaction is denoted as equation 4.

$$Mg^{2+} + Ca(OH)_2 \longrightarrow Mg(OH)_2 + Ca^{2+} \quad (4)$$

Since brucite is insoluble in a basic solution it must precipitate from the pore solution. This causes pore filling and may ultimately contribute to the disruption of the cement matrix because of the net increase in the solid volume of the products relative to the reactants [32]. Hence, a dolomite chemical attack mechanism may make a significant contribution to the early deterioration that is commonly attributed to physical degradation processes like freeze-thaw attack.

SUMMARY AND FURTHER DISCUSSION

In summary, a series of experiments have been conducted to evaluate the use of thermal analysis techniques (especially Hi-Res. TGA) for predicting the service life of portland cement concrete pavement aggregates. At this time, it is important to review the compositions of the various aggregates that were included in the study. This is most easily done by referring to the ternary diagram shown in Figure 33. Figure 33, which was constructed from the bulk chemical information (XRF and acid-insoluble residue), indicates that the study was restricted to relatively pure (typically less than about 5 percent impurities) limestones and dolomites (15 out of 22 samples). The study also included one dolomitic limestone and six calcareous dolomites. Hence, it is wise to keep such information in mind when attempting to apply the test results to carbonate stones of different compositions.

The major thrust of the study was to evaluate the relationship between chemical characteristics of the various carbonate aggregates and their thermal curves as defined by TG methods. The chemical characteristics that were studied included the solid solution and average crystallite size of the major carbonate minerals, amount and mineralogy of the major impurities, plus a study to evaluate the potential for dissolution of limestones and dolomites in the presence of chloride salts.

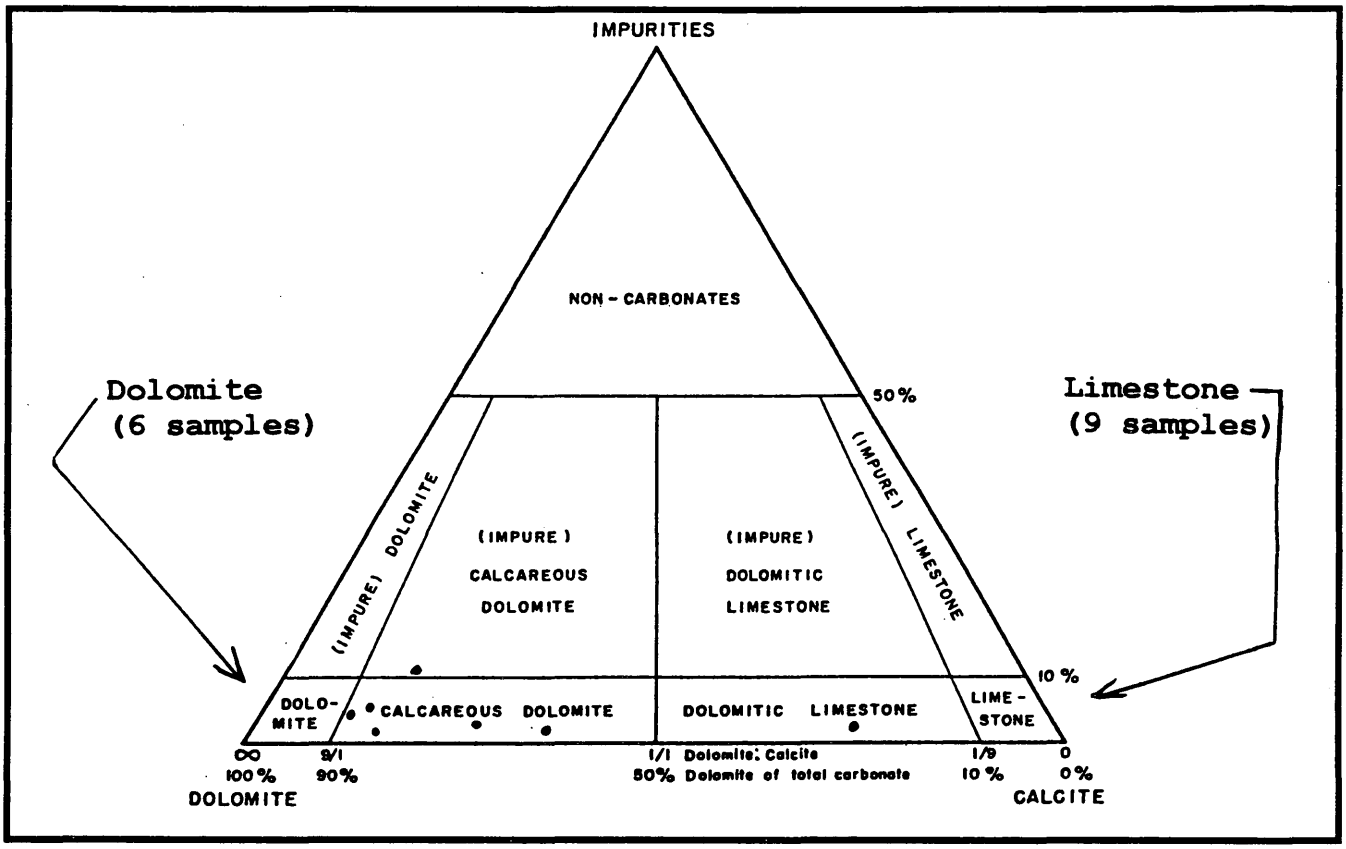

Figure 33. Compositional terminology for the carbonate rocks that were used in this study (adapted from reference 33).

One of the first questions that needed to be addressed was to evaluate how well the TG results correlated to the bulk chemistry information obtained from XRF. In general, this study has found a good correlation between the information provided by these two different test methods. The trends that were observed are illustrated in Figure 34. The TG and XRF information was converted to a carbonate format by using the procedure outlined in Table 19 and the gravimetric factors listed in Table 8, respectively. Test results for limestones were strongly correlated (see the top half of Figure 34), while the dolomites tended to exhibit a little more scatter (see the bottom half of Figure 34). The major factor that contributed to the poor correlation between the XRF results and the TG results for dolomites, appeared to be related to the amount of impurities (especially clay minerals) present in the carbonate stones. This tends to overestimate the amount of dolomite present in any given sample. Refinement of position selected for the $MgCO_3$ residue determination helped to

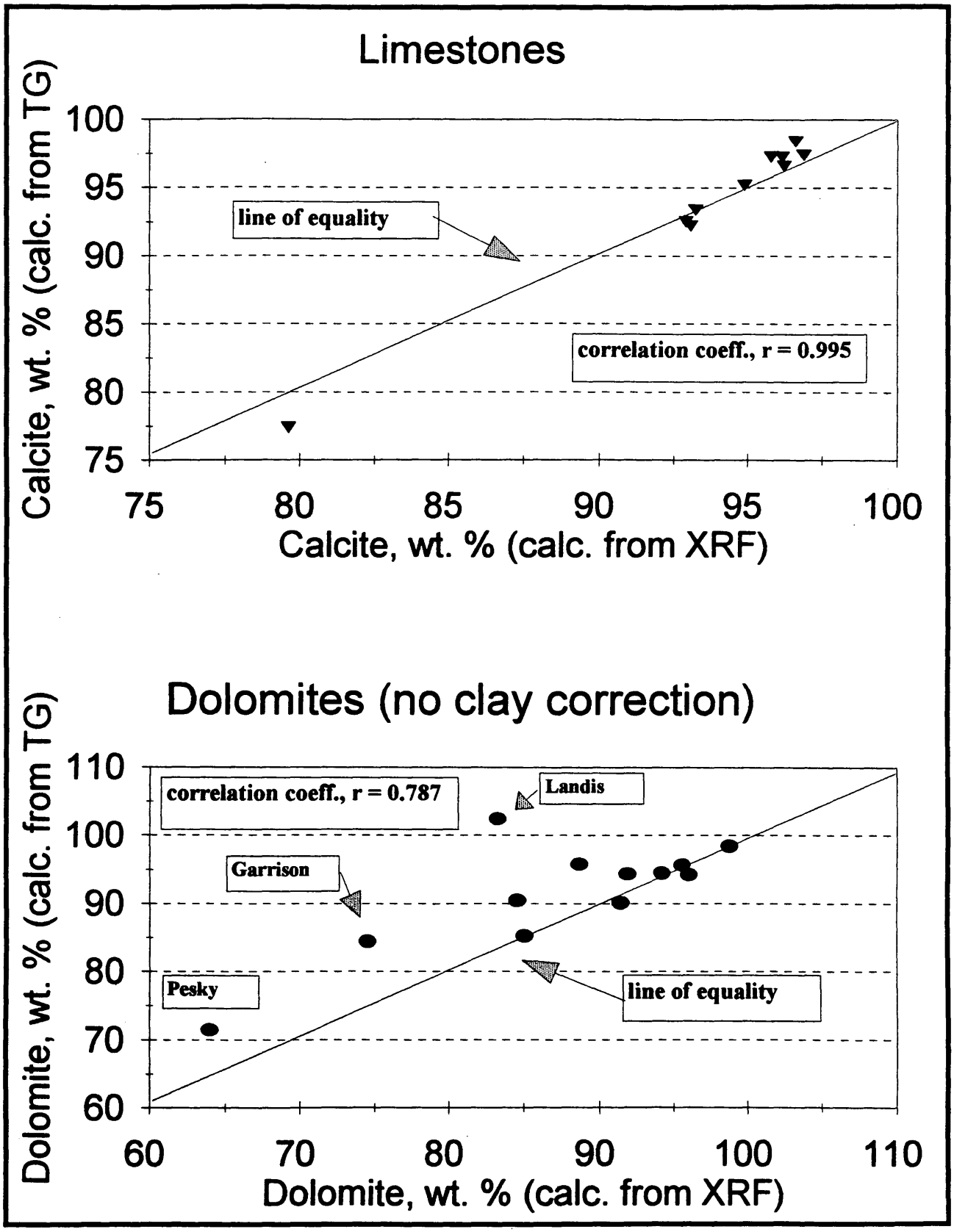

Figure 34. Correlations between bulk compositions calculated by XRF and TG methods.

improve the dolomite correlation to $r = 0.880$. Inspection of the TG curves on a sample-by-sample basis, eliminates many of the assumptions that need to be made concerning the appropriate region for the residue measurement; however, this also tends to require a considerable amount of operator intervention. Hence, one can be reasonably sure that the XRF and TG methods produce complementary information if one takes the proper precautions.

How well can the TG test results predict the service life of the various carbonate stones? This question will be answered in several stages because there are several interrelated variables that need to be discussed. First, however, it is interesting to evaluate how the durability factor (ASTM C 666, procedure B) correlates to service life. This is pertinent because the rapid freeze-thaw method is probably one of the most commonly used physical test methods for evaluating the relative durability of concrete specimens.

A plot of durability factor versus service life is shown in Figure 35. This is simply a graphical portrayal of the data listed in Table 2. The plot indicates that a general trend does exist between durability factor and service life (linear correlation coefficient, r, = 0.53). However, the relationship is of little use for predicting service life because it fails to adequately distinguish between "good" and "bad" aggregates. This is especially true for dolomite aggregates. More rigorous modeling methods could be employed to refine the relationship between durability factor and service life; however, such a task would be highly questionable in this particular instance since we only have 18 reliable samples in our study. Hence, throughout the rest of this report we will be using simple models (i.e., linear correlation coefficients) to evaluate relationships between several of the variables that were monitored in this study.

Correlation matrices for the various studies are summarized in Appendix III. The correlation studies were conducted on both the whole sample population (i.e., both limestones and dolomites combined as a single data set, see Table 1, Appendix III) and the individual limestone and dolomite populations. This was done to identify correlations that may not be evident in the combined dataset. For the most part, however, the discussion will stay focused on information obtained from the whole dataset. The variables that were used in the study included: {1} service life; {2} durability factor;

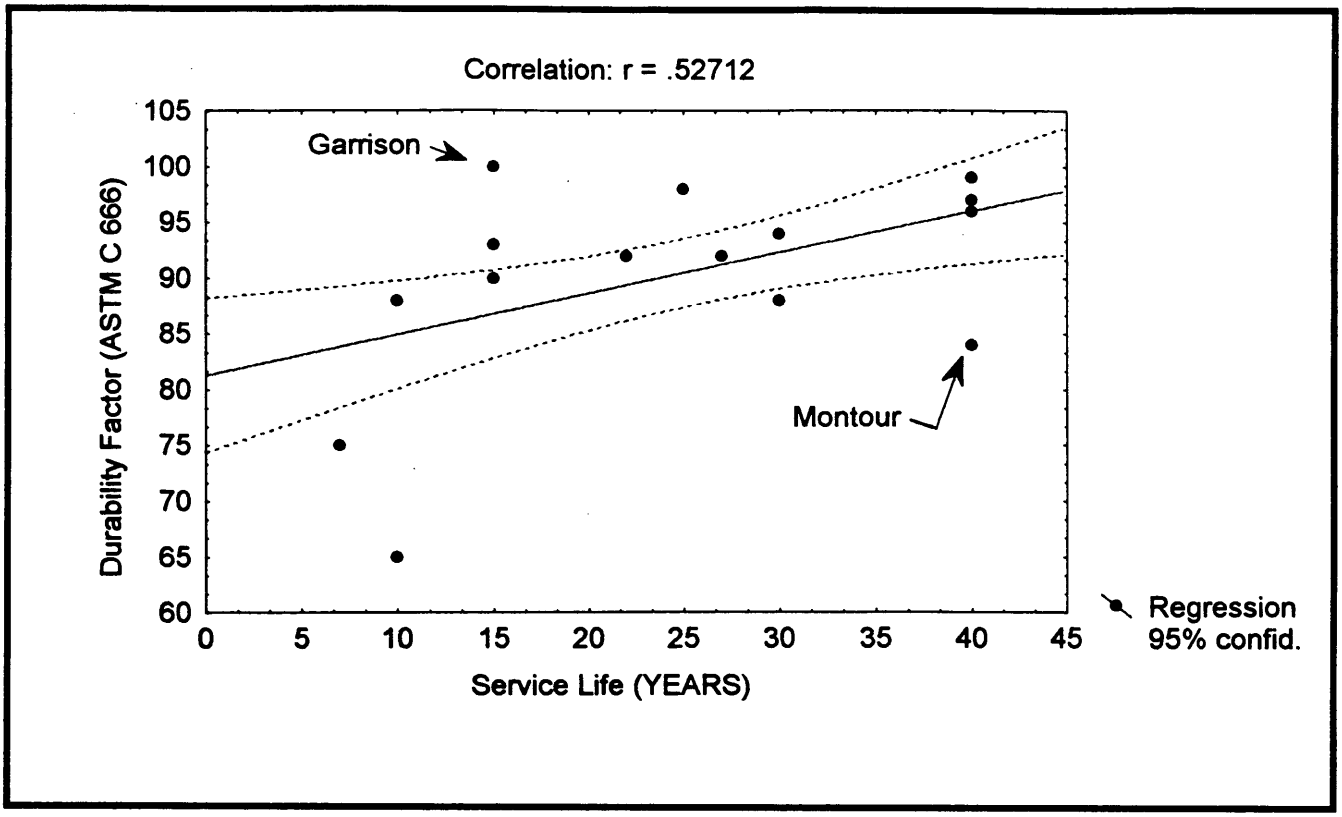

Figure 35. Correlation between service life and ASTM C 666 durability factor for the samples used in this study.

{3} acid-insoluble residue; {4} relative crystallite size; {5} decomposition temperature for calcite, DT_{CAL}; {6} premature TG loss, which has been defined as the weight loss from 825°C to the decomposition temperature; and {7} decomposition temperature for dolomite, DT_{DOL} (this variable only applies to dolomite aggregates).

Several variables exhibited good correlations with concrete pavement service life. For the total dataset (limestone + dolomites) significant correlations were found between service life and premature TG loss, service life and relative crystallite size, service life and durability factor, and service life and acid-insoluble residue. The scatter plots for the two strongest correlations are shown in Figures 36 and 37. The correlation between premature TG loss and service life (see Figure 37) would probably be the simplest to convert into a categorization scheme that separates "good" carbonate aggregates from "bad" aggregates. This research has indicated that if the premature TG loss exceeds about 1.0 percent then the service life will probably be 15 years or less. Note, that this

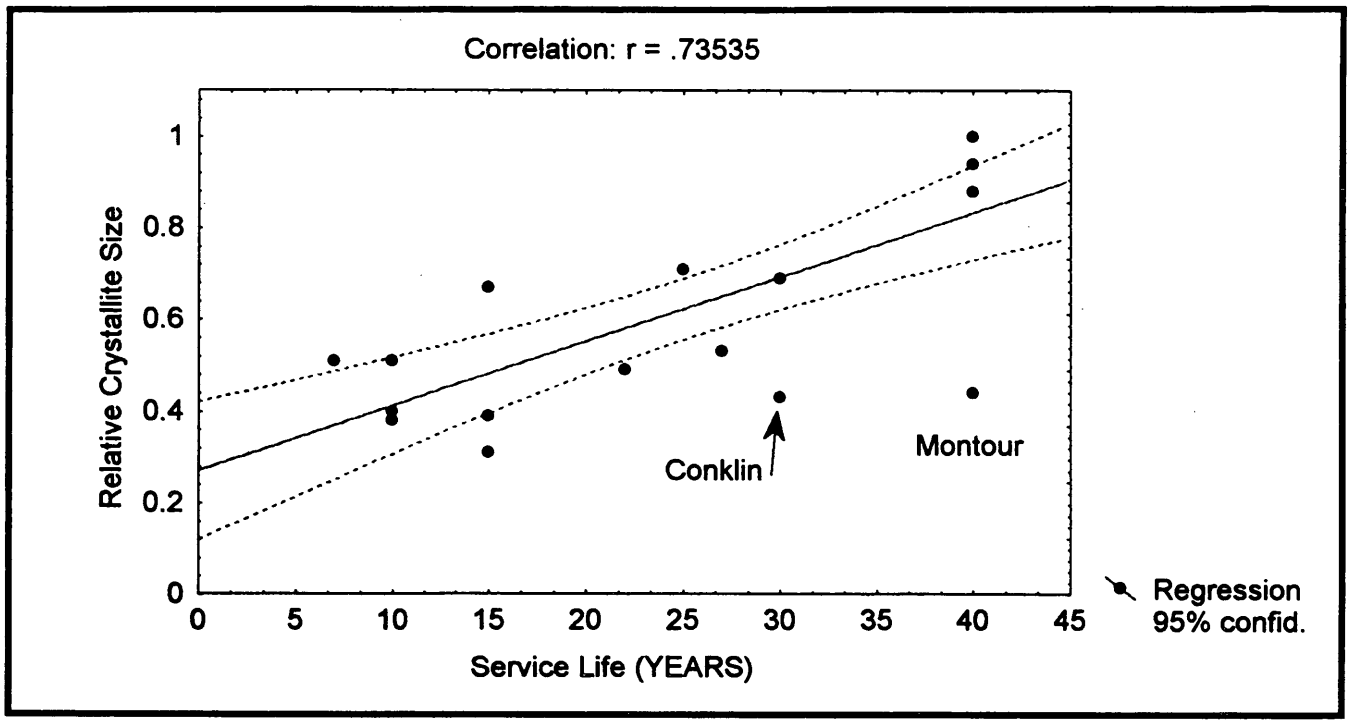

Figure 36. Correlation between service life and relative crystallite size for the samples used in this study.

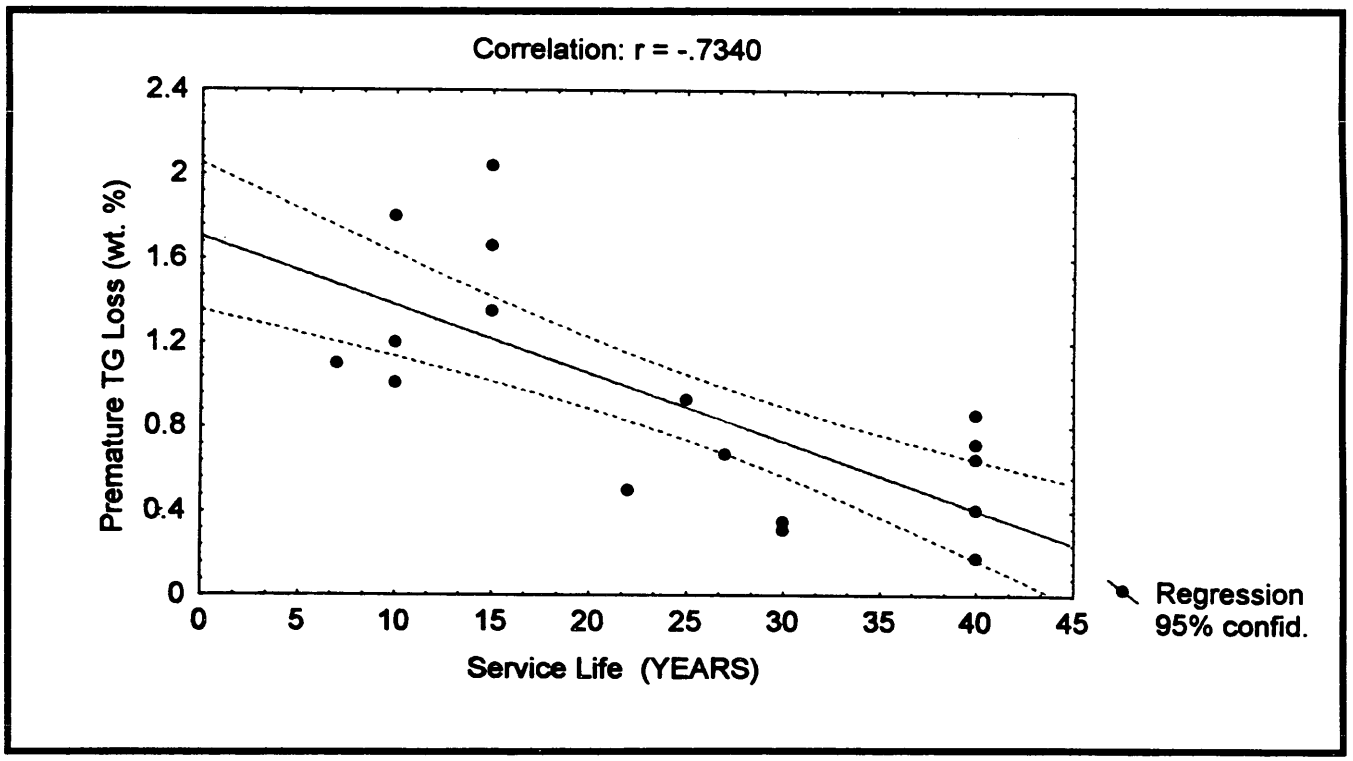

Figure 37. Correlation between service life and premature TG loss (calcite decomposition reaction) for the samples used in this study.

particular variable (premature TG loss) pertains only to the calcite decomposition reaction in a normal TG experiment. The variable could also be expressed as the slope of the TG curve prior to the decomposition event, this slope can be estimated from the existing data by dividing by approximately 100 (i.e., slope = $\Delta y/\Delta x$; Δy = premature TG loss; $\Delta x = DT_{CAL}$ - 825 $\cong$ 100 to a rough approximation). This helps to explain why the correlation coefficient (r) decreases when limestone samples are removed from the dataset. Obviously, one would like to include a correlation variable that pertains to the first step of the dolomite TG decomposition reaction; however, as was explained earlier in this report, both trace amounts of salts and minor amounts of clays can severely influence the shape of that decomposition reaction. Actually, it is interesting to note that strong correlations between premature TG loss and acid insoluble residue (see Figure 38), and between premature TG loss and calcite decomposition temperature (see Figure 39). These correlations suggest that even the calcite decomposition event is strongly correlated to the impurity content of the carbonate stones. Since clays would be the most common impurities that exhibit a significant weight loss in the TG tests, one may speculate that clays plus the particle size (?crystallite size) distribution, must dominate the shape of the decomposition reaction in the vicinity of the decomposition temperature. This research project has had little success in producing a quantitative method that can be used to isolate these two variables from each other.

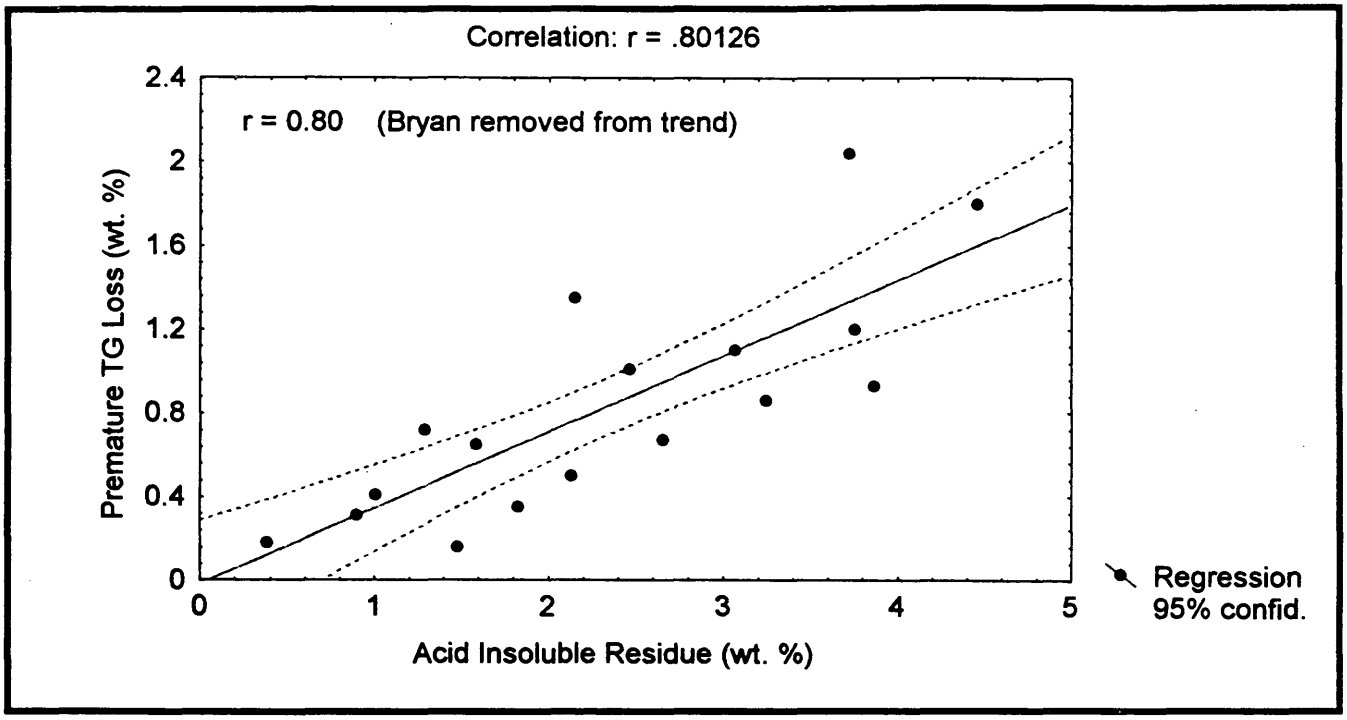

Figure 38. Correlation between acid-insoluble residue and premature TG loss (calcite decomposition reaction) for the samples used in this study.

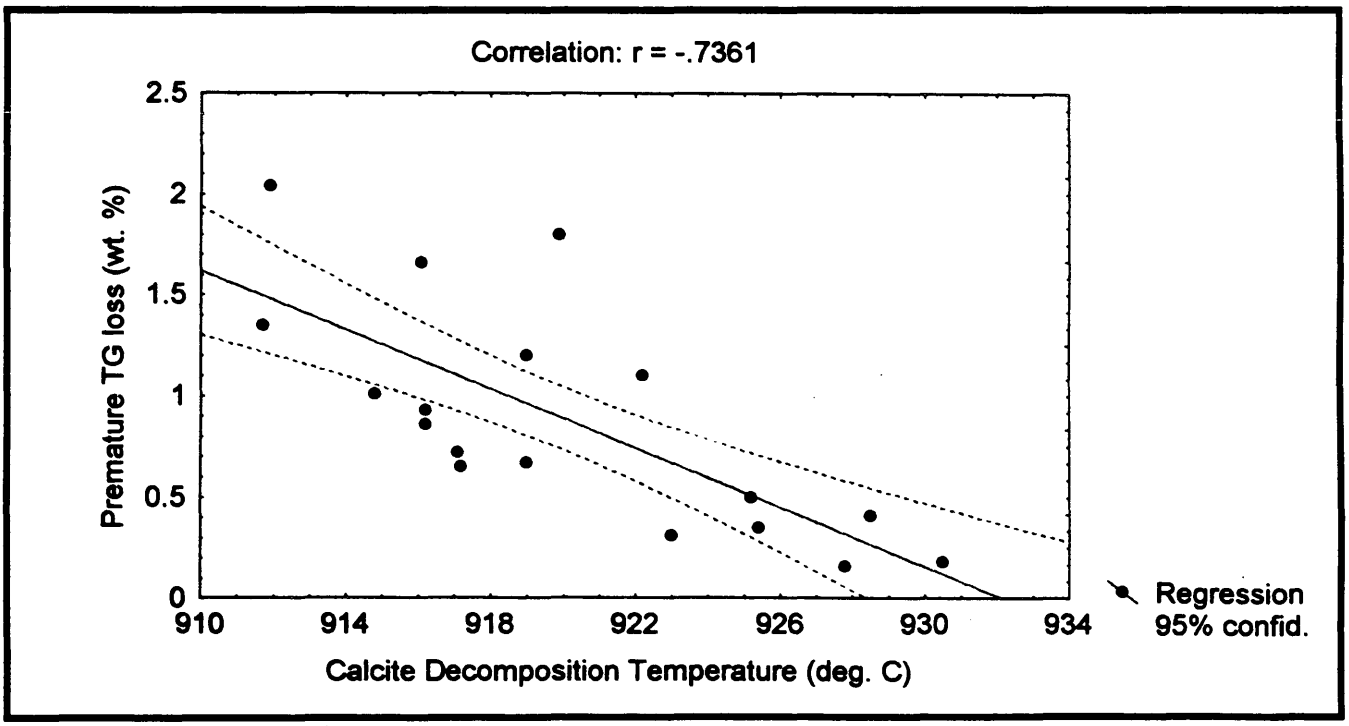

Figure 39. Correlation between calcite decomposition temperature and premature TG loss for the samples used in this study.

CONCLUSIONS AND OBSERVATIONS

After careful interpretation of the test results that were presented in the main body of this research report, the following conclusions can be made.

1. The bulk chemical information that was calculated from the results of the thermogravimetric (TG) tests was in good agreement with the test results obtained from x-ray fluorescence (XRF) techniques. Hence, the aggregate samples can be categorized as follows.

    - Limestones, 9 samples out of 22.
    - Dolomitic Limestone, 1 sample out of 22.
    - Calcareous Dolomites, 6 samples out of 22.
    - Dolomites, 6 samples out of 22.

    Qualitative x-ray diffraction (XRD) scans were also in reasonable agreement with these classifications. The only carbonate minerals identified in the diffractograms were calcite and dolomite.

2. Acid-insoluble residue tests indicated that nearly all of the samples were relatively pure carbonate stones. Only one sample (Bryan Dolomite) had an acid-insoluble residue that exceeded 10 percent (by weight). The large majority of the carbonate stone samples had insoluble residues of less than 4 percent.

3. The minor mineral phases (non-carbonates) that were identified in the samples can be summarized as follows.

    - Quartz (low or α variety) - by far the most common mineral present in all the samples.
    - Clay minerals - illite was the most common clay mineral identified in the various samples. Kaolinite was also identified occasionally, as was a mixed layer clay mineral (?illite - smectite) that exhibited slight expansive tendencies.
    - Feldspars - difficult to identify distinctly because they were commonly present in small concentrations. Most likely a potassium feldspar (orthoclase) in most of the samples.
    - Pyrite - a common impurity that was most evident in the limestones; however, it was also identified in the dolomite and calcareous dolomite samples.

4. The trace element study indicated that most of the samples contained only very small concentrations of Cd, Cr, Cu, Ni, Pb and Zn. Barium (Ba) and Chlorine (Cl) tended to fluctuate considerably between the different samples. The Cl content of several of the dolomite samples exceeded 500 parts-per-million.

5. The solid-solution study indicated that:

   - The calcite crystals in the limestone samples contained only a small amount of Mg; typically less than one (1) mole % $MgCO_3$.

   - The dolomite crystals in the limestone samples contained a nearly stoichiometric Ca : Mg ratio for the Huntington sample. However, the Skyline and Early Chapel aggregates both contained dolomite crystals that were deficient in Mg.

   - The calcite crystals in the dolomite samples occasionally contained a considerable amount of Mg (or Fe) solid solution. In some samples this exceeded 4 percent $MgCO_3$.

   - The dolomite crystals in the dolomite samples, typically contained approximately 50 mole % $MgCO_3$ (i.e.., most were nearly stoichiometric). However, the samples with poor service records (i.e., Garrison, Pesky and Plower) tended to contain dolomite crystals that were deficient in Mg.

     It is important to note that nearly all of the dolomites in this study can be considered to be low-iron dolomites. This is based on the fact that after one corrects the bulk iron content for the iron that is present as pyrite, typically less than one atom (mole) of iron remains for each 100 atoms (moles) of magnesium.

6. The crystallite size determinations indicated that:

   - Calcites tended to have larger crystallites than the dolomites. This conclusion is based on the data that was obtained from a single diffraction peak; and hence, may change in the future when more detailed studies (i.e., determination of crystallite shape) can be conducted.

   - The larger crystallites that were measured for several calcites and dolomites tended to approach the upper limit of reliability for the x-ray diffraction measurements.

   - The crystallite size determinations that were conducted using the profile fitting technique were in good agreement with the alternative procedure that relied on very time consuming high-resolution scans.

7. The results of the thermogravimetric (TG) tests indicated that:

   - The Hi-Res. TGA method produces thermal curves that exhibit sharper, more ideal decomposition reactions than traditional TG methods. This helps to resolve adjacent decomposition reactions (i.e., reactions that occur at nearly the same temperature). Also, the Hi-Res. TGA data can normally be obtained in about half to two-thirds the time that is required for a conventional TG test.

   - The decomposition temperatures that were measured for carbonate stones using the Hi-Res. TGA method appear to have little thermodynamic

significance. This is due to the variable scanning rate that is used in the Hi-Res. TGA method. A slight adjustment of specific test parameters, such as scanning rate, resolution setting, etc., can significantly alter the decomposition temperature of any given experiment. Hence, it is imperative to evaluate a series of alternative experimental conditions to optimize the Hi-Res. TGA method. Once the experimental details have been adequately defined the Hi-Res. TGA method has been found to be highly precise.

If one desires to obtain accurate decomposition temperatures then it is best to perform the experiments with small samples (roughly 1 to 10 milligrams) and very slow scanning rates. In contrast, if one desires to obtain accurate mass change determinations then samples sizes greater than 20 milligrams appear to function best.

- Particle size of the sample has a very significant influence on the thermal curves that were observed for the limestone and dolomite aggregates. This problem was most noticeable for coarse-grained dolomite specimens that had particle sizes (diameter) greater than 45 microns. Tests conducted on fine-grained dolomites, and both coarse and fine-grained limestones were also sensitive to this particle size effect; however, to a much smaller degree. The particle size effect can destroy the accuracy of the mass loss events in the thermal curves.

- The presence of chloride salts in specific dolomite samples caused the TG test specimens to begin to decompose at about 580°C (i.e., roughly the decomposition temperature for magnesite, $MgCO_3$). This premature decomposition event occurs at approximately 100°C less than the "normal" decomposition temperature for dolomite. Washing the finely ground dolomite sample with a large excess of water (100 milligrams sample to 2 liters water) eliminates this premature decomposition reaction.

8. The results of the salt treatment study indicated that:

   - Limestone samples (specifically the calcite fraction of the bulk samples) were only slightly altered by the sodium chloride and calcium chloride treatments. The salt treatments tended to remove small crystallites from the bulk solid.

   - Dolomite samples were slightly altered by the sodium chloride treatment but drastically altered by the calcium chloride treatment. The calcium chloride treatment caused almost half of the dolomite crystals to decompose in only 3 days (powder specimens, 96°C temperature). Similar trends were suggested in the decomposition study that used chip specimens rather than fine powders. However, the chip study was too limited to produce quantitative information concerning the rate of dolomite decomposition in bulk aggregate samples that were exposed to the salt treatments.

9. Strong correlations were found between several of the variables that were monitored in this study. In fact, several of the variables showed significant correlations to concrete service life. The significant correlations (α = 5 percent level) to service life can be summarized as follows.

- Correlation between service life and premature TG loss (calcite decomposition reaction); correlation coeff., r, = - 0.73.
- Correlation between service life and relative crystallite size; correlation coeff., r, = 0.74.
- Correlation between service life and ASTM C 666 durability factor; correlation coeff., r, = 0.53.
- Correlation between service life and acid-insoluble residue; correlation coeff., r, = - 0.52.

RECOMMENDATIONS

This research program has indicated that thermogravimetric (TG) analysis can provide very important information about the fundamental properties of carbonate aggregates in Iowa. In fact, the results of this study suggest that the TG method may prove to be a better predictor of concrete service life than is the currently accepted method of rapid freezing and thawing of concrete specimens. However, this study was limited to the investigation of only 22 samples, and only 18 of the 22 samples had reliable service records. Hence, it is imperative that this projects findings are verified using a larger set of samples. This can easily be done by evaluating the test results that were obtained from research project HR 336, which was the companion project to this basic research project.

The following general recommendations can be made to help eliminate experimental discrepancies and to provide enhanced precision in the empirical methods that were used in this research project.

1. Bulk chemical methods (XRF) can be improved by obtaining (or making) additional standards that better reflect the compositions of "real" limestones and dolomites.
   - Chlorine (Cl) should be added to the list of elements that are routinely measured in carbonate aggregates.
   - Barium (Ba) and sodium (Na) could also be added to the element list.

The Materials Analysis and Research Laboratory will pursue the acquisition of new XRF algorithms that will simplify data reduction and provide more robust interelement corrections.

2. The routine x-ray diffraction studies that are conducted on carbonate aggregates could be improved by:

    - Mixing a small amount (~ 10 percent) of an internal standard (perhaps Si metal) into the diffraction specimens. This would eliminate many of the errors that are commonly observed in x-ray diffraction measurements. It would also allow one to make routine quantitative estimates of the concentrations of calcite, dolomite and quartz in each sample. An alternative to this suggestion would be to use a silicon zero background sample holder for all diffraction studies. This would provide an external standard correction factor that can be applied to all diffraction measurements.

3. The crystallite size calculations should be performed on the existing database of carbonate stones that have been collected by the Iowa Department of Transportation. The profile fitting technique would be the simplest method available that can be used to estimate crystallite size.

    An additional crystallite size study should be conducted to evaluate the shape of crystallites that are present in Iowa carbonate aggregates.

4. The current TG studies that are routinely conducted by the Iowa Department of Transportation are adequate for most needs. However, it is important to stress the need for proper particle size control in most experiments, and the need for washing the coarse-grained dolomite samples if it is desired to obtain reliable dolomite decomposition temperatures.

5. The salt treatment study has indicated that the dolomite samples tended to decompose in rather short periods of time. Since this decomposition reaction has the potential to release magnesium chloride to the concrete pore solution, which may be extremely detrimental to the durability of the concrete system, it is recommended that further studies should be conducted to quantify the rate at which such an attack could occur in real concrete aggregates. This recommendation has been partially addressed by Iowa Department of Transportation research project HR-355, but further basic studies would be of benefit.

RAW DATA

The complete dataset for this project is available in a variety of computer readable formats. This was done to reduce the printing costs for the final report. The data can be obtained from:

Scott Schlorholtz
Room 46 Town Engr. Bldg.
Iowa State University
Ames, IA 50011

The information that is available consists of x-ray diffraction data (~ 3 MB), x-ray fluorescence data (~ 1 MB) and thermogravimetric analysis data (~ 10 MB). The information is available on $3^1/_2$" or $5^1/_4$" media, please specify high or low density format. At this time only IBM compatible formats are available.

ACKNOWLEDGMENTS

We would like to thank all of the many people who made significant contributions to this research project. A special thanks to Iowa Department of Transportation personnel who have contributed materials and time for this project. The participation and support of this project by the Iowa Highway Research Board is gratefully acknowledged. And finally, we would like to thank the personnel (both students and staff) at the Materials Analysis and Research Laboratory, for their tremendous efforts in collecting the data for this research project. Without their diligent efforts this research project would not have been possible.

REFERENCES

1. Popovics, S., Concrete Materials, Properties, Specifications and Testing, 2nd Edition, Noyes Publications, New Jersey, 1992.

2. American Society for Testing and Materials. 1992 Annual Book of ASTM Standards. Vol. 4.02, Concrete and Aggregates, ASTM, Philadelphia, 1992.

3. Pollastro, R.M., "A Recommended Procedure for the Preparation of Oriented Clay-Mineral Specimens for X-ray Diffraction Analysis: Modifications to Drever's Filter-Membrane Peel Technique," United States Dept. of the Interior, Geological Survey, Open File Report 82-71, 1982.

4. Carroll, D., "Clay Minerals: A Guide to Their X-ray Identification," The Geological Society of America, Special Paper 126, 1970.

5. Starkey, H.C., P.D. Blackmon and P.L. Hauff, "The Routine Mineralogical Analysis of Clay-Bearing Samples," USGS Bull. 1563, 1984.

6. Ostrom, M.E., "Separation of Clay Minerals from Carbonate Rocks Using Acid," Journal of Sedimentary Petrology, Vol. 31, No. 1, 1961, pp. 123-129.

7. Goldsmith, J.R., D.L. Graf and O.I. Joensuu, "The Occurence of Magnesian Calcites in Nature," Geochim. Cosmochim. acta, Vol. 5, 1955.

8. Goldsmith, J.R., and D.L. Graf, "Relation Between Lattice Constants and Composition of the Ca-Mg Carbonates," American Mineralogist, Vol. 43, 1958, pp. 84-101.

9. Goldsmith, J.R., and D.L. Graf, "Structural and Compositional Variations in Some Natural Dolomites," Journal of Geology, Vol. 66, 1958, pp. 678-693.

10. Goldsmith, J.R., D.L. Graf and H.C. Heard, "Lattice Constants of the Calcium-Magnesium Carbonates," American Mineralogist, Vol. 46, 1961, pp. 453-457.

11. Reeder, R.J., Chapter 1, in Carbonates: Mineralogy and Chemistry, R.J. Reeder Editor, Mineralogical Society of America, 1983.

12. Hutchison, C.S., Laboratory Handbook of Petrographic Techniques, John Wiley & Sons, New York, 1974.

13. Brown, G., Chapter 8, pp. 389-391, in Crystal Structures of Clay Minerals and their X-ray Identification, Edited by G.W. Brindley and G. Brown, Mineralogical Society Monograph No. 5, London, 1980.

14. Graf, D.L., "Crystallographic Tables for the Rhombohedral Carbonates," American Mineralogist, Vol. 46, 1961, pp. 1283-1316.

15. Dubberke, W., Personal Communication, 1987.

16. Cullity, B.D., Element of X-ray Diffraction, Addison-Wesley, Inc.: Massachusetts, 1978.

17. Howard, S.A. and K.D. Preston, "Profile Fitting of Powder Diffraction Patterns," in Modern Powder Diffraction, editors D.L. Bish and J.E. Post, Mineralogical Society of America: Washington, D.C., 1989, pp. 217-275.

18. Warren, B.E., X-Ray Diffraction, Dover Books: New York, 1990.

19 Azaroff, L.V., Elements of X-ray Crystallography, McGraw-Hill Books: New York, 1968.

20. Howard, S.A. and Materials Data, Inc., SHADOW, A System for X-ray Powder Diffraction Pattern Analysis, Materials Data, Inc.: Livermore, CA, 1992.

21. Webb, T.L. and J.E. Kruger, "Carbonates", pp. 303-341, in Differential Thermal Analysis, Vol 1, edited by R.C. Mackenzie, Academic Press: New York, 1970.

22. Graf, D.L., "Preliminary Report on the Variations in Differential Thermal Curves of Low-Iron Dolomites," American Mineralogist, Vol. 37, No. 1, 1952, pp. 1-27.

23. Fazeli, A.R. and J.A.K. Tareen, "Thermal Decomposition of Rhombohedral Double Carbonates of Dolomite Type," Journal of Thermal Analysis, Vol. 37, 1991, pp. 2605-2611.

24. Criado, J.M. and A. Ortega, "A study of the influence of particle size on the thermal decomposition of $CaCO_3$ by means of constant rate thermal analysis," Thermochimica Acta, Vol. 195, 1992, pp. 163-167.

25. Wilburn, F.W., J.H. Sharp, D.M. Tinsley and R.M. McIntosh, "The Effect of Procedural Variables on TG, DTG and DTA Curves of Calcium Carbonate," Journal of Thermal Analysis, Vol. 37, 1991, pp. 2003-2019.

26. Sharp, J.H., F.W. Wilburn, and R.M. McIntosh, "The Effect of Procedural Variables on TG, DTG and DTA Curves of Magnesite and Dolomite," Journal of Thermal Analysis, Vol. 37, 1991, pp. 2021-2029.

27. Dubberke, W. and V.J. Marks, "Thermogravimetric Analysis of Carbonate Aggregates," Paper No. 920325, presented at the 71st Annual Meeting of the Transportation Research Board, Jan. 1992.

28. Bradley, W.F., J.F. Burst and D.L. Graf, "Crystal Chemistry and Differential Thermal Effects of Dolomite," Illinois State Geol. Survey Report of Investigations No. 167, 1953, pp. 207-217.

29. Jamieson, J.C., and J.R. Goldsmith, "Some Reactions Produced in Carbonates by Grinding," American Mineralogist, Vol. 45, July-August, 1960, pp. 818-827.

30. Bandi, W.R., and G. Krapf, "The Effect of CO_2 Pressure and Alkali Salt on the Mechanism of Decomposition of Dolomite," Thermochimica Acta, Vol. 14, 1976, pp. 221-243.

31. Morse, J.W. and F.T. Mackenzie, Geochemistry of Sedimentary Carbonates, Developments in Sedimentology, Vol. 48, Elsevier: New York, 1990.

32. Oberste-Padtberg, R., "Degradation of Cements by Magnesium Brines -- A Microscopic Study," pp. 24-32, in Proceedings of The Seventh International Conference on Cement Microscopy, March 25-28, 1985.

33. Leighton, M.W. and C. Pendexter, "Carbonate Rock Types," pp. 33-61, in Classification of Carbonate Rocks, Memoir 1, The American Association of Petroleum Geologists, George Banta Co., Inc.: Menasha, Wisconsin (1962).

APPENDIX I

5-0586 JCPDS-ICDD Copyright 1988 Quality: i

CaCO3

Calcium Carbonate Calcite, syn

Rad: CuKα1 wl: 1.5405 Filter: Ni d-sp:
Cutoff: Int: Diffractometer I/Icor: 2.00
Ref: Swanson, Fuyat, Natl. Bur. Stand. (U.S.), Circ. 539, II 51 (1953)

Sys: Rhombohedral (Hex) Space Group: R-3c (167)
a: 4.989 b: c: 17.062 A: C: 3.4199
α: ß: v: Z: 6
Ref: Ibid.
mp: Dx: 2.71 Dm: 2.71 SS/FOM: F(30)=49.9(.0163,37)

εα: 1.487 nwß: 1.659 εv: Sign: - 2v:
Ref: Dana's System of Mineralogy, 7th Ed., 2 142

Color: Colorless
X-ray pattern at 26 C. Sample from Mallinckrodt Chemical Works. CAS RN: 13397-26-7. Spectroscopic analysis: <0.1% Sr; <0.01% Ba; <0.001% Al, B, Cs, Cu, K, Mg, Na, Si, Sn; <0.0001% Ag, Cr, Fe, Li, Mn. Merck Index, 8th Ed., p. 190. Other form: aragonite. PSC: hR10.

---

*Not permitted by space group

d A	Int	h	k	l	d A	Int	h	k	l
3.86	12	0	1	2	1.1538	3	1	3	4
3.035	100	1	0	4	1.1425	1	2	2	6
2.845	3	0	0	6	1.1244	<1	1	2	11
2.495	14	1	1	0	1.0613	1	2	0	14
2.285	18	1	1	3	1.0473	3	4	0	4
2.095	18	2	0	2	1.0447	4	3	1	8
1.927	5	0	2	4	1.0352	2	1	0	16
1.913	17	0	1	8	1.0234	<1	2	1	13
1.875	17	1	1	6	1.0118	2	3	0	12
1.626	4	2	1	1	0.9895	<1	3	2	1
1.604	8	1	2	2	0.9846	1	2	3	2
1.587	2	1	0	10	0.9782	1	[1	3	10]
1.525	5	2	1	4	0.9767	3	1	2	14
1.518	4	2	0	8	0.9655	2	3	2	4
1.510	3	1	1	9	0.9636	4	4	0	8*
1.473	2	1	2	5	0.9562	<1	2	0	16*
1.440	5	3	0	0	0.9429	2	4	1	0
1.422	3	0	0	12	0.9376	2	2	2	12
1.356	1	2	1	7					
1.339	2	0	2	10					
1.297	2	1	2	8					
1.284	1	3	0	6					
1.247	1	2	2	0					
1.235	2	1	1	12					
1.1795	3	2	1	10					

36-0426 JCPDS-ICDD Copyright 1988 Quality: *

CaMg(CO3)2

Calcium Magnesium Carbonate Dolomit

Rad: CuKα wl: 1.54178 Filter: Graph Mono. d-sp: Diffractometer
Cutoff: Int: Diffractometer I/Icor:
Ref: Keller, L., McCarthy, G., North Dakota State University, Fargo, North Dakota, USA, JCPDS Grant-in-Aid Report (1985)

Sys: Rhombohedral (Hex) Space Group: R-3 (148)
a: 4.8092(2) b: c: 16.020(5) A: C: 3.3311
α: ß: v: Z: 3
Ref: Ibid.
mp: Dx: 2.86 Dm: 2.86 SS/FOM: F(30)=148.1(.0063,32)

εα: nwß: 1.680 εv:1.503 Sign: - 2v:
Ref: Howie, Broadhurst, Am. Mineral., 43 1210 (1958)

Color: Tan
Specimen from Baxter Springs, Arkansas, USA. Chemical analysis by EDX at University of North Dakota (wt.%): CaO 30.18, MgO 21.10, FeO 0.44, MnO 0.11, CO2 47.18, Na2O 0.17, Al2O3 0.13, SiO2 0.47 (chiefly from traces of quartz an plagioclase); Ca(Mg0.977Fe0.011Na0.005Mn0.003Ca0.004) (CO3)2. Optical data o specimen from Haley, Ross Township, Ontario, Canada. Silicon used as internal standard. PSC: hR10. To replace 11-78.

d A	Int	h	k	l	d A	Int	h	k	l
4.033	1	1	0	1	1.3350	1	0	0	12
3.699	4	0	1	2	1.2970	1	2	1	7
2.888	100	1	0	4	1.2698	1	0	2	10
2.670	4	0	0	6	1.2374	1	1	2	8
2.539	3	0	1	5	1.2318	<1	3	0	6
2.404	7	1	1	0	1.2022	1	2	2	0
2.193	19	1	1	3	1.1935	<1	2	0	11
2.065	3	0	2	1	1.1817	<1	1	0	13
2.015	10	2	0	2	1.1729	<1	2	2	3
2.006	1	1	0	7	1.1672	1	1	1	12
1.8473	3	0	2	4	1.1433	<1	3	1	2
1.8049	10	0	1	8	1.1228	1	2	1	10
1.7870	13	1	1	6	1.1099	<1	1	3	4
1.7800	2	0	0	9	1.1034	<1	0	1	14
1.7461	<1	2	0	5	1.0963	1	2	2	6
1.5667	2	2	1	1	1.0947	<1	3	0	9
1.5446	4	1	2	2					
1.5403	<1	0	2	7					
1.4955	<1	1	0	10					
1.4652	2	2	1	4					
1.4435	2	2	0	8					
1.4308	1	1	1	9					
1.4129	1	1	2	5					
1.3885	2	3	0	0					
1.3436	<1	3	0	3					

33-1161 JCPDS-ICDD Copyright 1988 Quality: *
SiO2
Silicon Oxide Quartz, syn

Rad: CuKα1 wl: 1.540598 Filter: Mono. d-sp: Diffractometer
Cutoff: Int: Diffractometer I/Icor: 3.6
Ref: Natl. Bur. Stand. (U.S.) Monogr. 25, 18 61 (1981)

Sys: Hexagonal Space Group: P3221 (154)
a: 4.9133(2) b: c: 5.4053(4) A: C: 1.1001
α: β: γ: Z: 3
Ref: Ibid.
mp: Dx: 2.65 Dm: 2.66 SS/FOM: F(30)=76.6(.0126,31)

εα: nwβ: 1.544 εγ:1.553 Sign: + 2V:
Ref: Swanson, Fuyat, Natl. Bur. Stand. (U.S.), Circ. 539, 3 24 (1954)

Color: Colorless
Pattern at 25 C. Sample from the Glass Section at NBS, Gaithersburg, Maryland, USA, ground single-crystals of optical quality. Pattern reviewed by J. Holzer and G. McCarthy, North Dakota State University, Fargo, North Dakota, USA, JCPDS Grant-in-Aid ReportRG(1990).Agreeswellwithexperimentalandcalculated patterns. O2Si. Also called silica. Silicon used as internal standard.
PSC: hP9. To replace 5-490. Plus 6 reflections to 0.9089.

d A	Int	h	k	l	d A	Int	h	k	l
4.257	22	1	0	0	1.2285	1	2	2	0
3.342	100	1	0	1	1.1999	2	2	1	3
2.457	8	1	1	0	1.1978	1	2	2	1
2.282	8	1	0	2	1.1843	3	1	1	4
2.237	4	1	1	1	1.1804	3	3	1	0
2.127	6	2	0	0	1.1532	1	3	1	1
1.9792	4	2	0	1	1.1405	<1	2	0	4
1.8179	14	1	1	2	1.1143	<1	3	0	3
1.8021	<1	0	0	3	1.0813	2	3	1	2
1.6719	4	2	0	2	1.0635	<1	4	0	0
1.6591	2	1	0	3	1.0476	1	1	0	5
1.6082	<1	2	1	0	1.0438	<1	4	0	1
1.5418	9	2	1	1	1.0347	<1	2	1	4
1.4536	1	1	1	3	1.0150	1	2	2	3
1.4189	<1	3	0	0	0.9898	1	4	0	2
1.3820	6	2	1	2	0.9873	1	3	1	3
1.3752	7	2	0	3	0.9783	<1	3	0	4
1.3718	8	3	0	1	0.9762	1	3	2	0
1.2880	2	1	0	4	0.9636	<1	2	0	5
1.2558	2	3	0	2					

6-0710 JCPDS-ICDD Copyright 1988 Quality: i
FeS2
Iron Sulfide Pyrite, sy

Rad: CuKα1 wl: 1.5405 Filter: Ni d-sp:
Cutoff: Int: Diffractometer I/Icor:
Ref: Swanson et al, Natl. Bur. Stand. (U.S.), Circ. 539, 5 29 (1955)

Sys: Cubic Space Group: Pa3 (205)
a: 5.417 b: c: A: C:
α: β: v: Z: 4
Ref: Ibid.
mp: 642 C Dx: 5.01 Dm: 5.02 SS/FOM: F(24)=22.4(0.029,37)

Color: Black (in powder), brass-yellow (in crystals)
X-ray pattern at 26 C. CAS RN: 1309-36-0. Sample prepared as a fine precipitate and heated in a closed tube in S2 atmosphere for 4 hours at 700 C. Spectroscopic analysis: <0.1% Al, Ca, Mg, Si; <0.01% Co, Cu, Mo, Ni, Pb; <0.001% Cr, Ge, Mn; <0.0001% Ag. Validated by calculated pattern 24-76. Opaque mineral optical data on specimen from Tavistock, Devon, England: RR2Re=51.7, Disp.=16, VHN100=1505-1620, Color values=.327, .335, 51.8, Ref.: IMA Commission on Ore Microscopy QDF. Measured density and melting point by Dana's System of Mineralogy, 7th Ed.RG,1RG 238. FeS2. Also called pyrites; fools gold. PSC: cP12. To be deleted by Z-506, lower Fn, Bayliss, 11/90.

d A	Int	h	k	l	d A	Int	h	k	l
3.128	35	1	1	1	1.0060	8	2	5	0
2.709	85	2	0	0	0.9892	6	5	2	1
2.423	65	2	1	0	0.9577	12	4	4	0
2.2118	50	2	1	1	0.9030	16	6	0	0
1.9155	40	2	2	0	0.8788	8	6	1	1
1.6332	100	3	1	1	0.8565	8	6	2	0
1.5640	14	2	2	2	0.8261	4	5	3	3
1.5025	20	2	3	0	0.8166	4	6	2	2
1.4448	25	3	2	1	0.7981	6	6	3	1
1.2427	12	3	3	1					
1.2113	14	4	2	0					
1.1823	8	4	2	1					
1.1548	6	3	3	2					
1.1057	6	4	2	2					
1.0427	25	5	1	1					

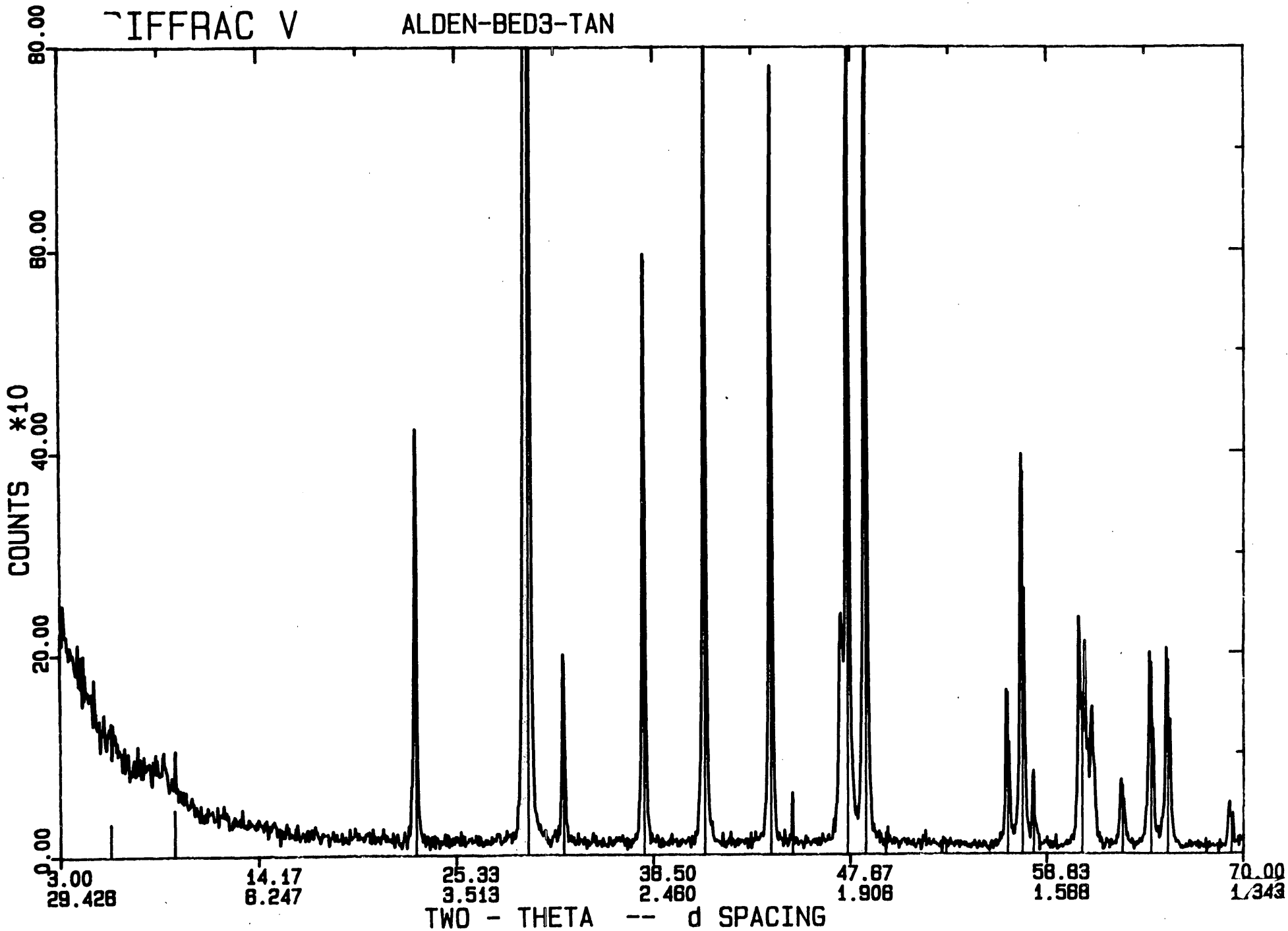

Figure 1, Appendix 1. X-ray diffractogram for Alden aggregate.

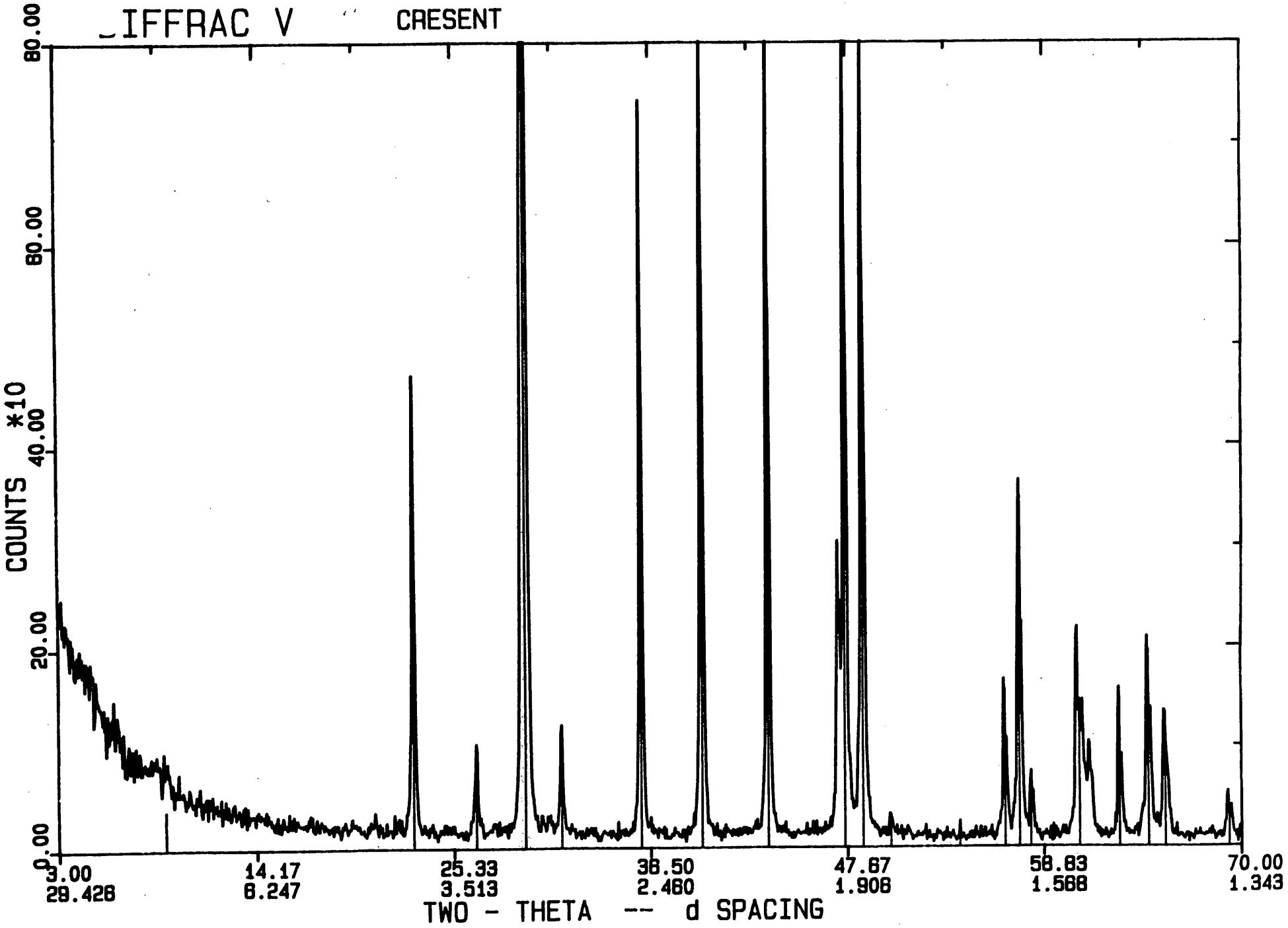

Figure 2, Appendix 1. X-ray diffractogram for Crescent aggregate.

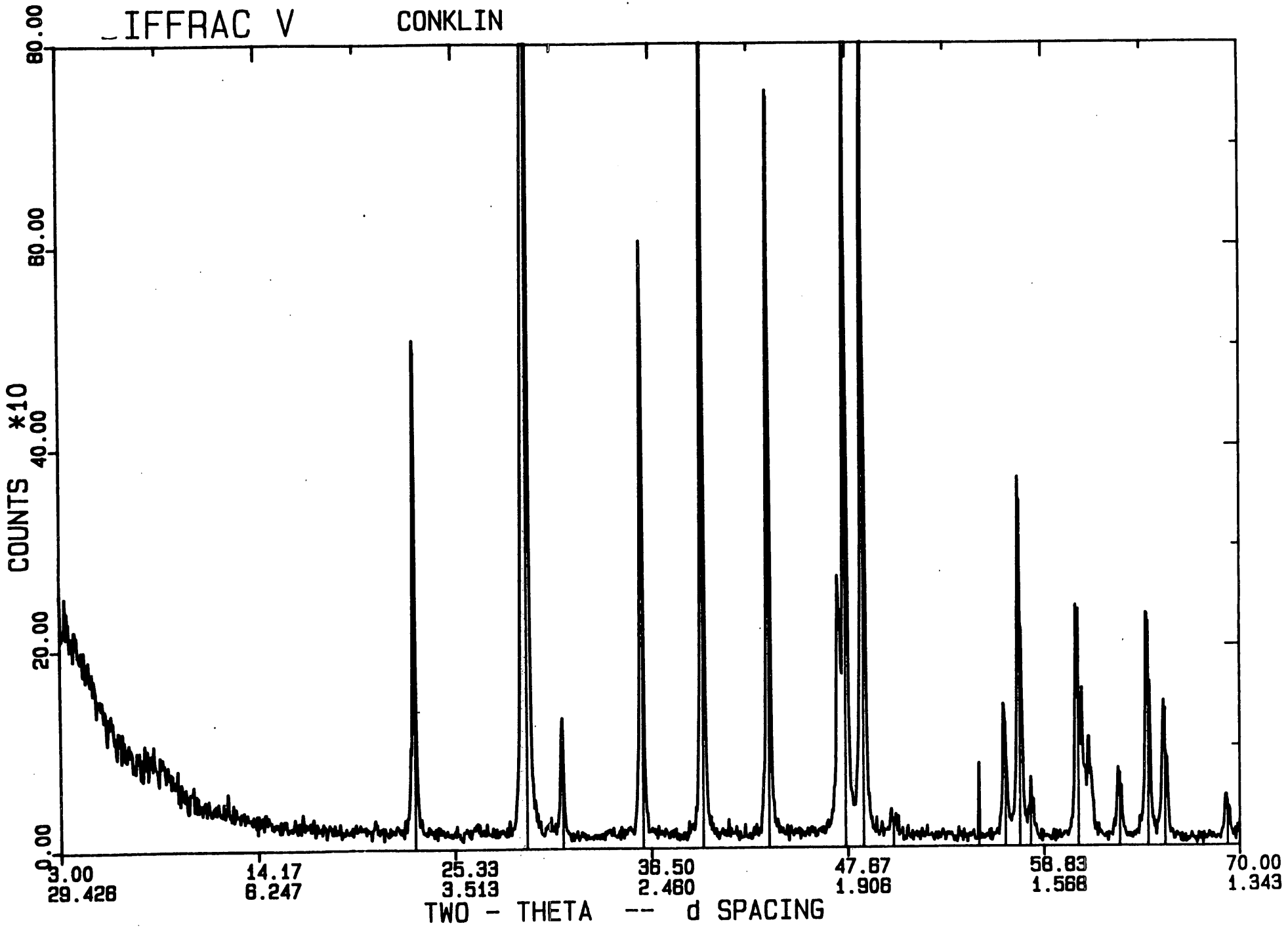

Figure 3, Appendix 1. X-ray diffractogram for Conklin aggregate.

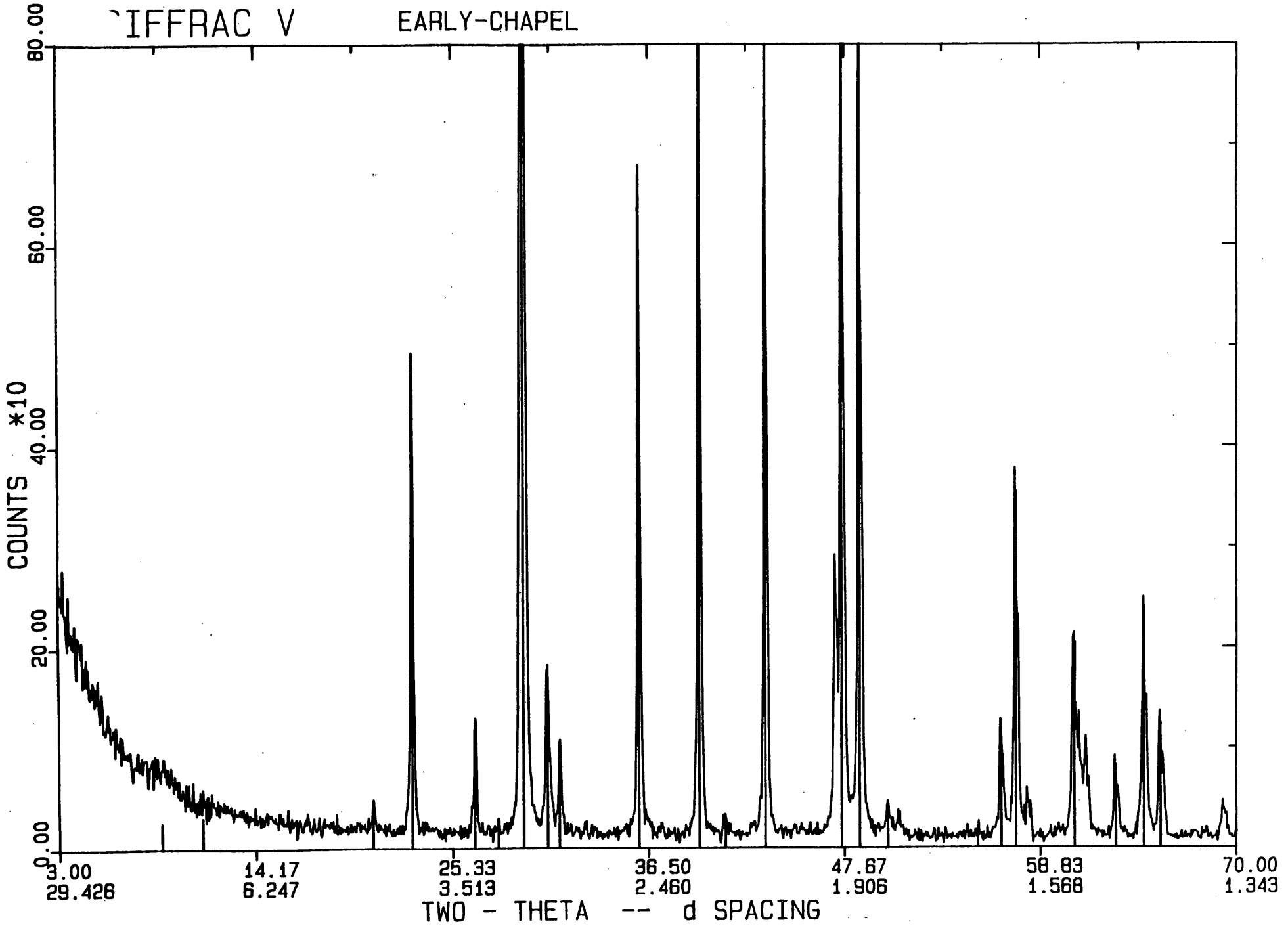

Figure 4, Appendix 1. X-ray diffractogram for Early Chapel aggregate.

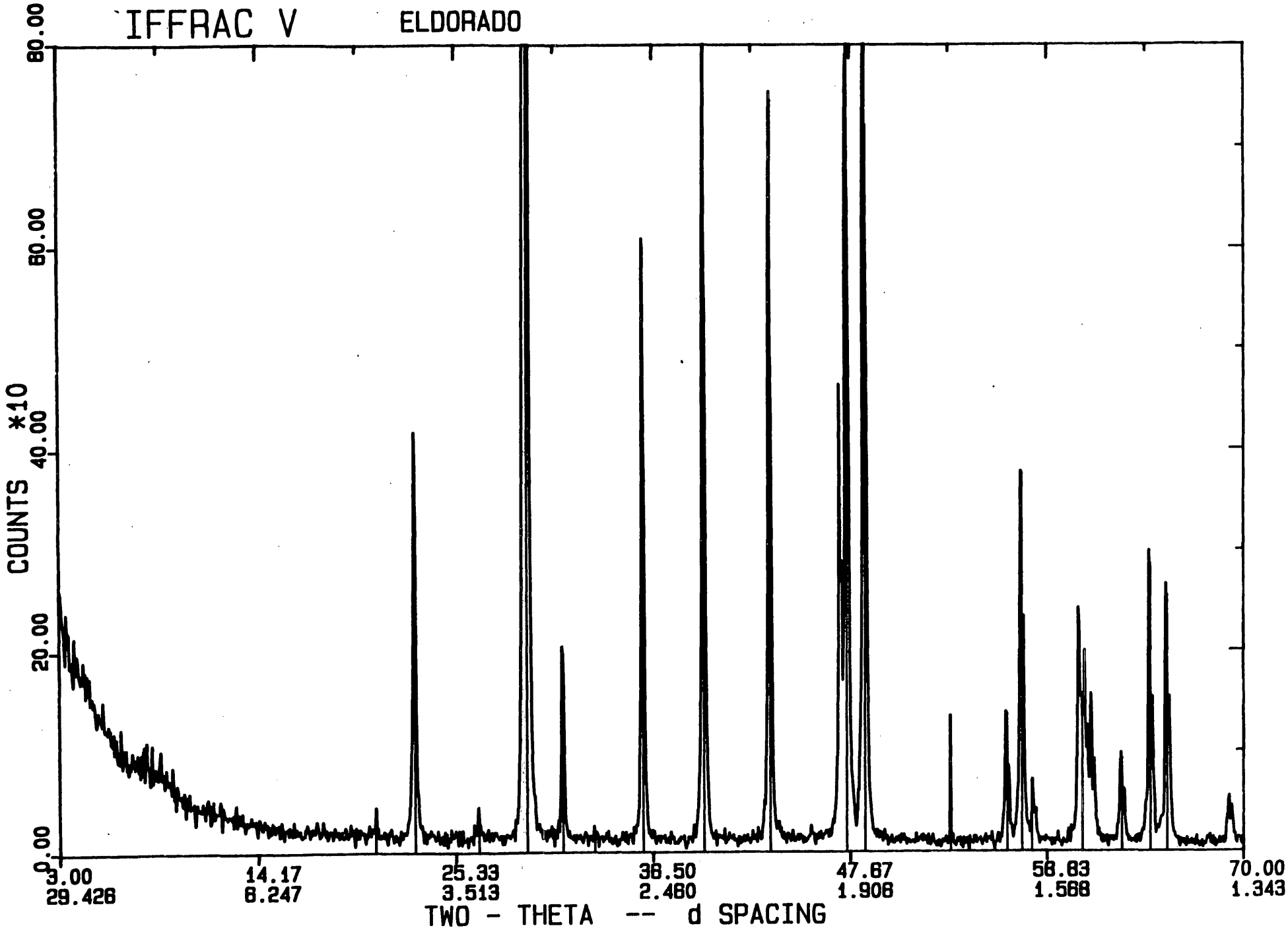

Figure 5, Appendix 1. X-ray diffractogram for Eldorado aggregate.

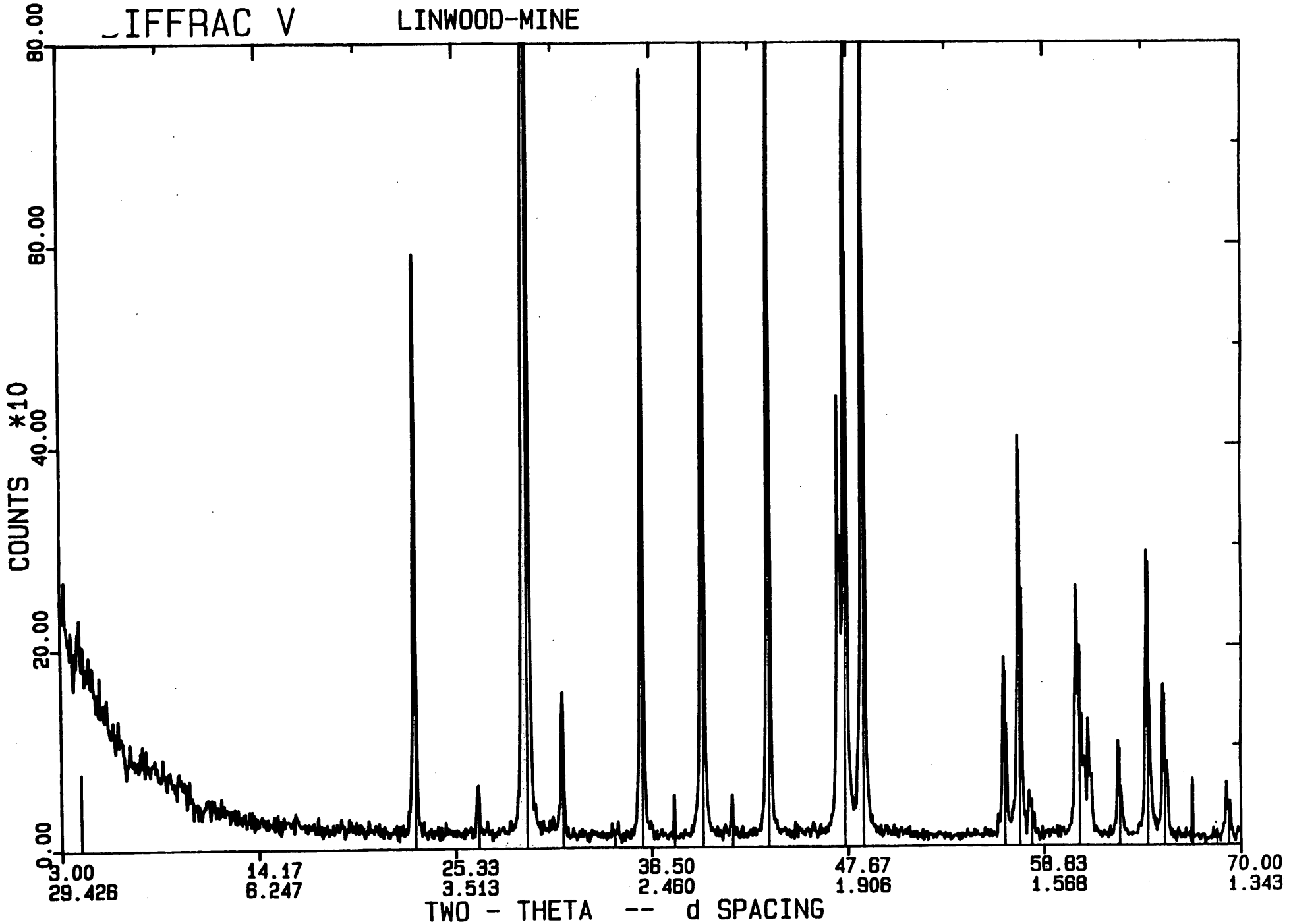

Figure 6, Appendix 1. X-ray diffractogram for Linwood aggregate.

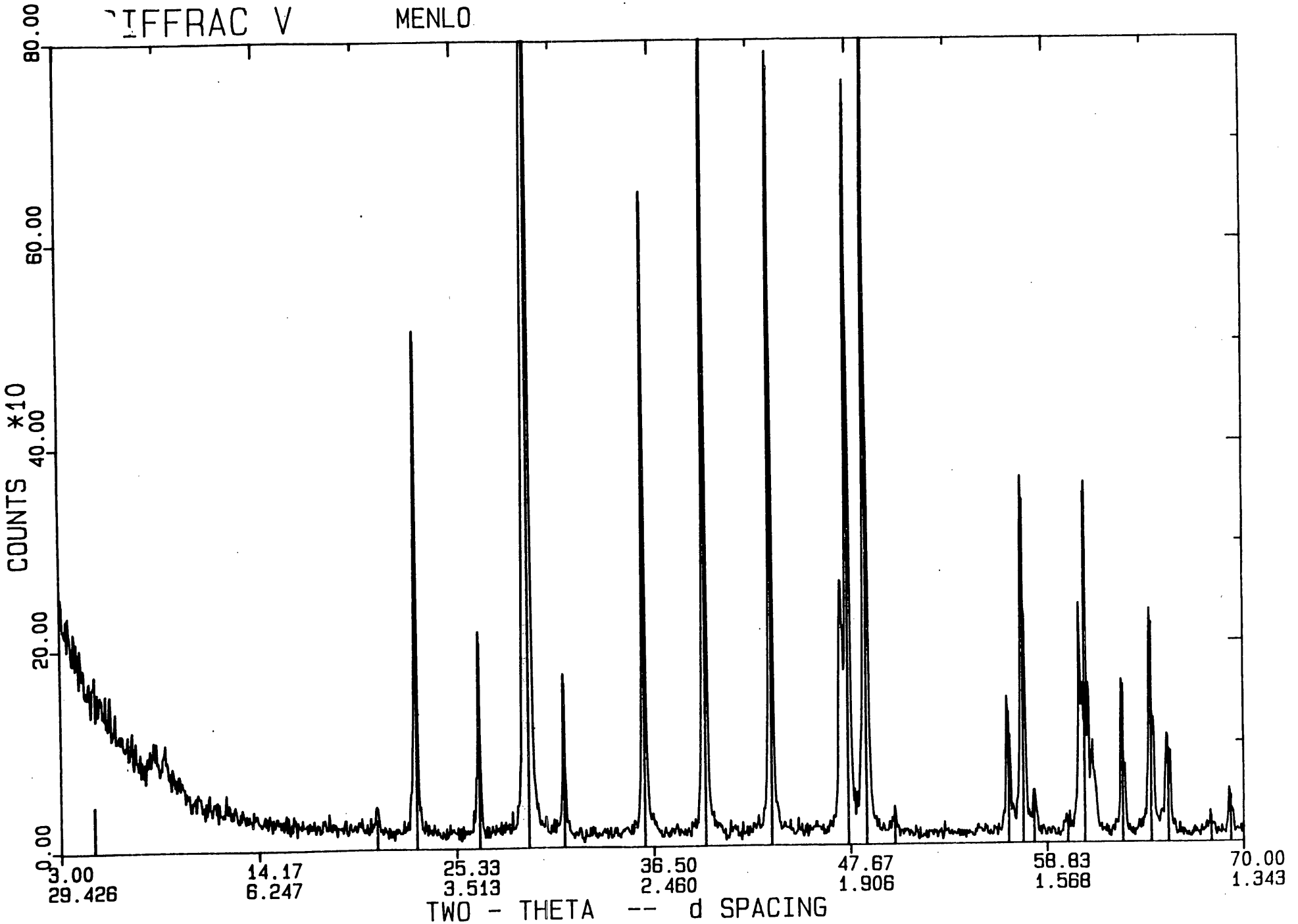

Figure 7, Appendix 1. X-ray diffractogram for Menlo aggregate.

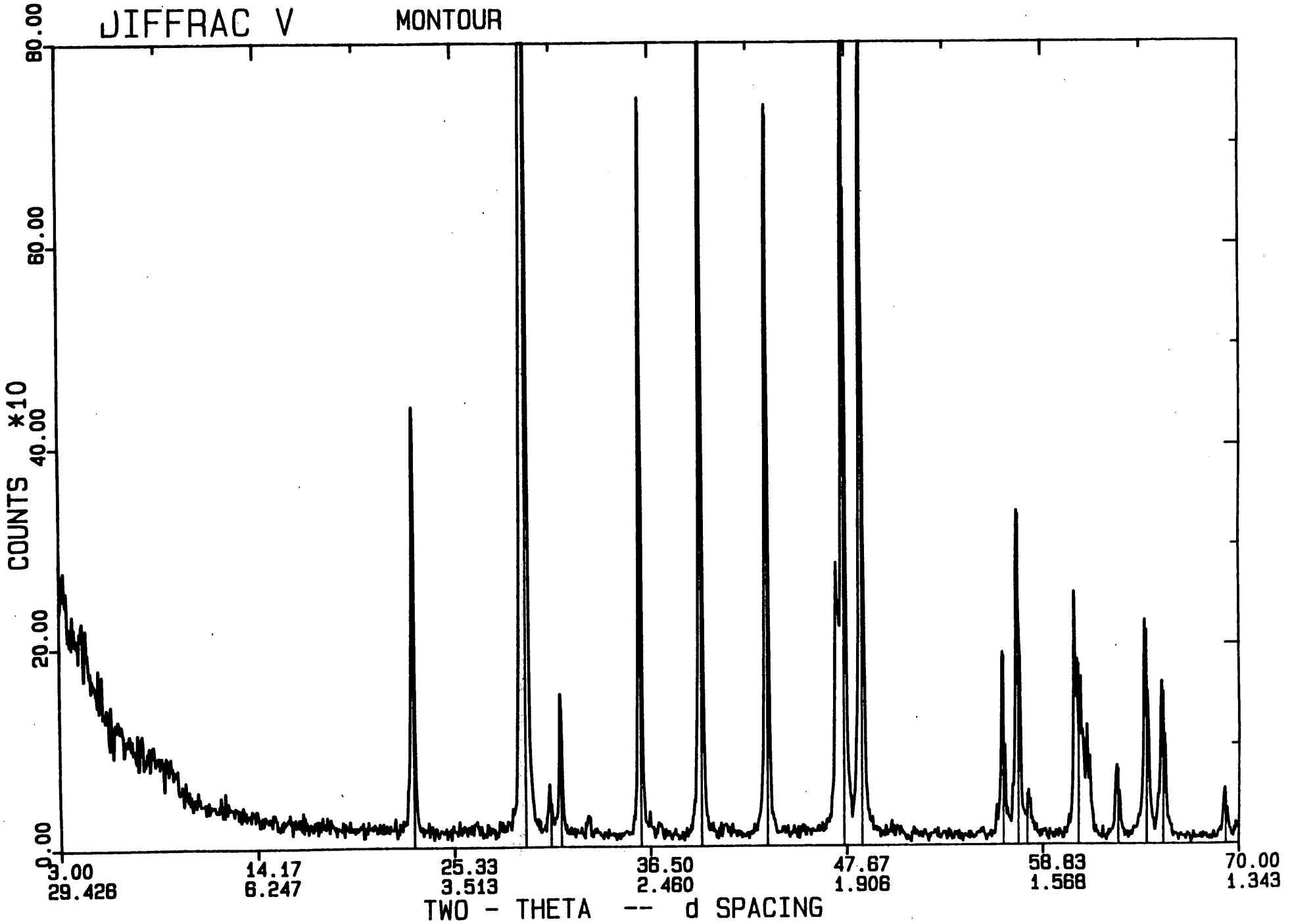

Figure 8, Appendix 1. X-ray diffractogram for Montour aggregate.

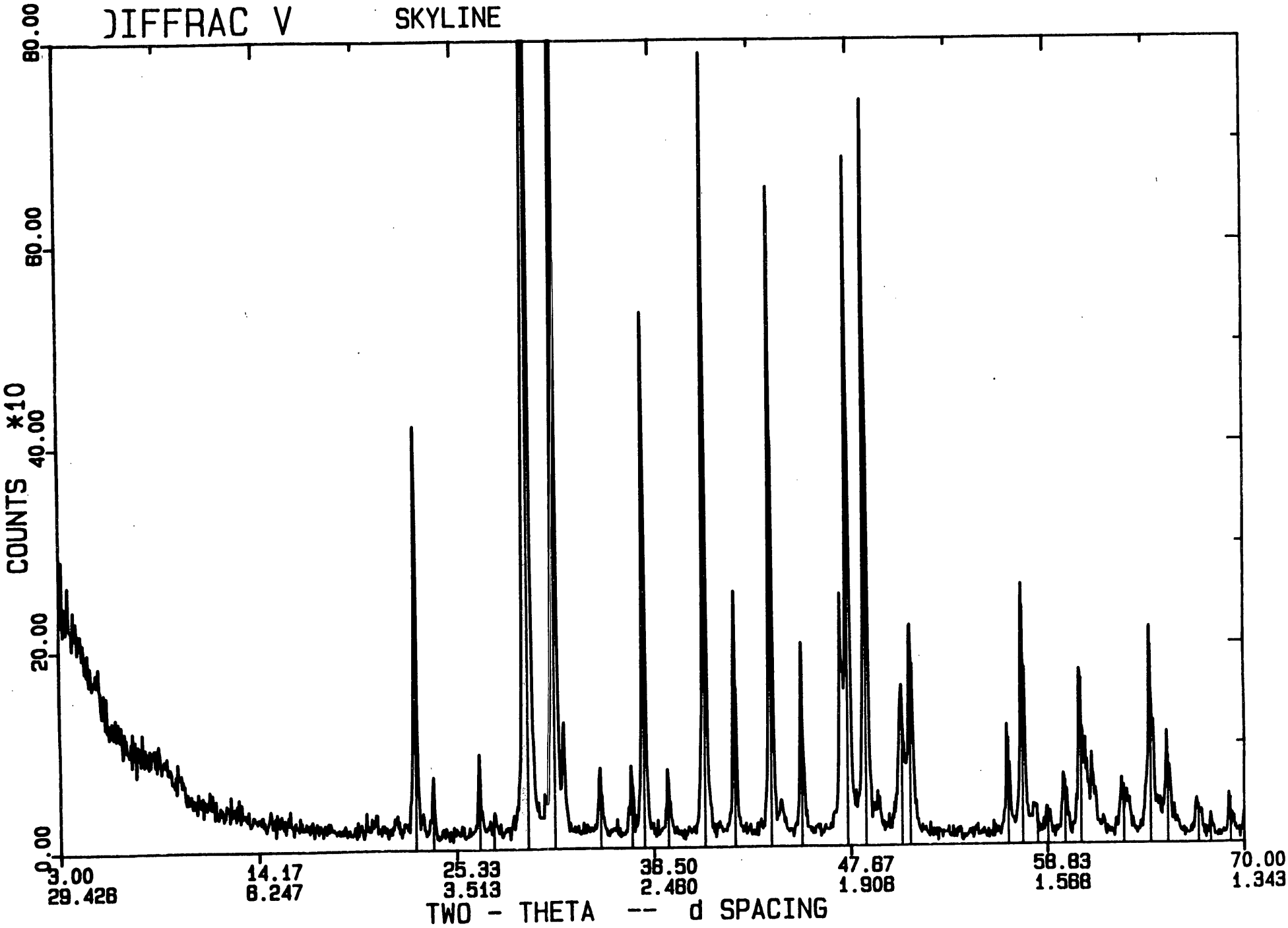

Figure 9, Appendix 1. X-ray diffractogram for Skyline aggregate.

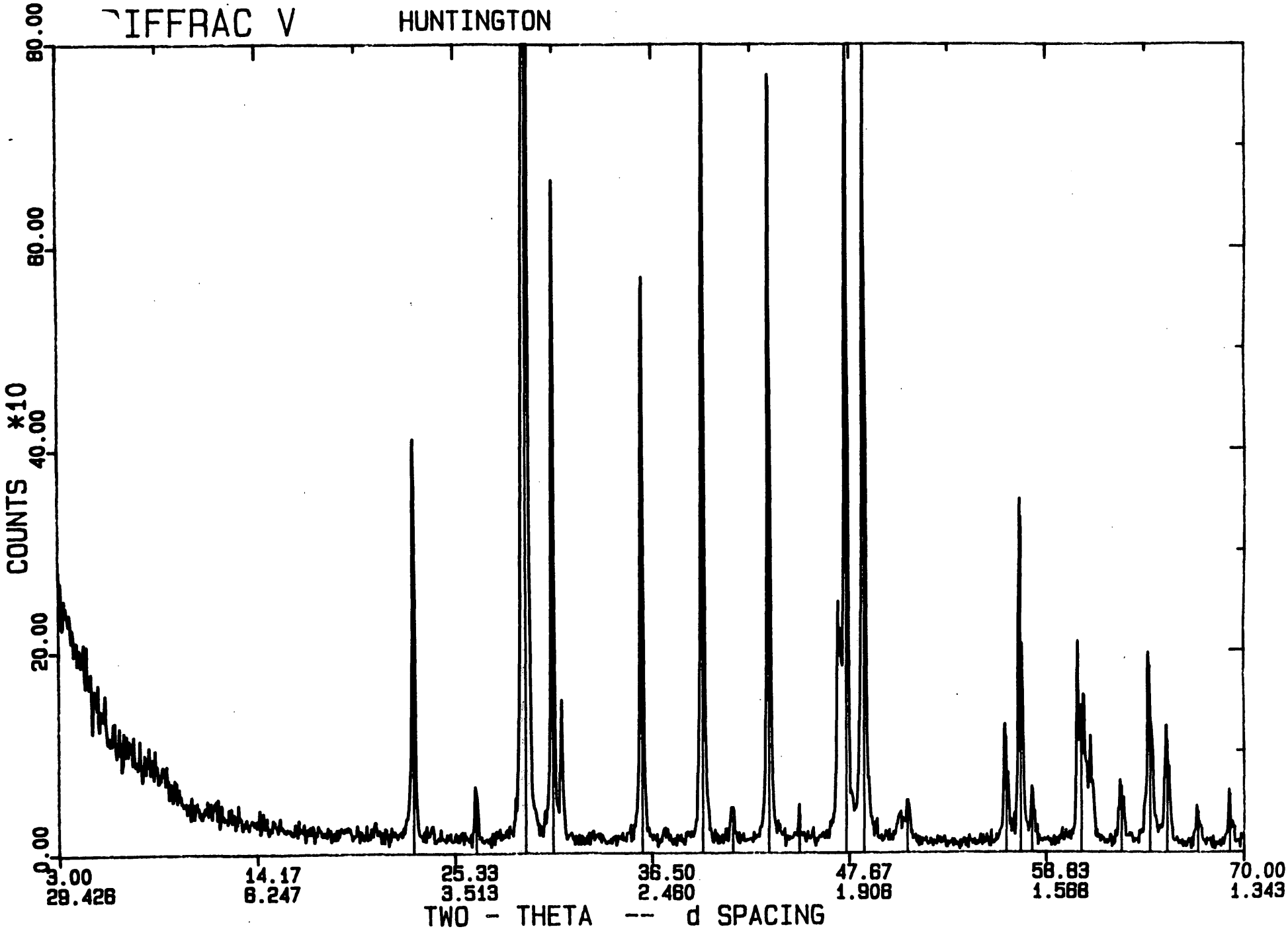

Figure 10, Appendix 1. X-ray diffractogram for Huntington aggregate.

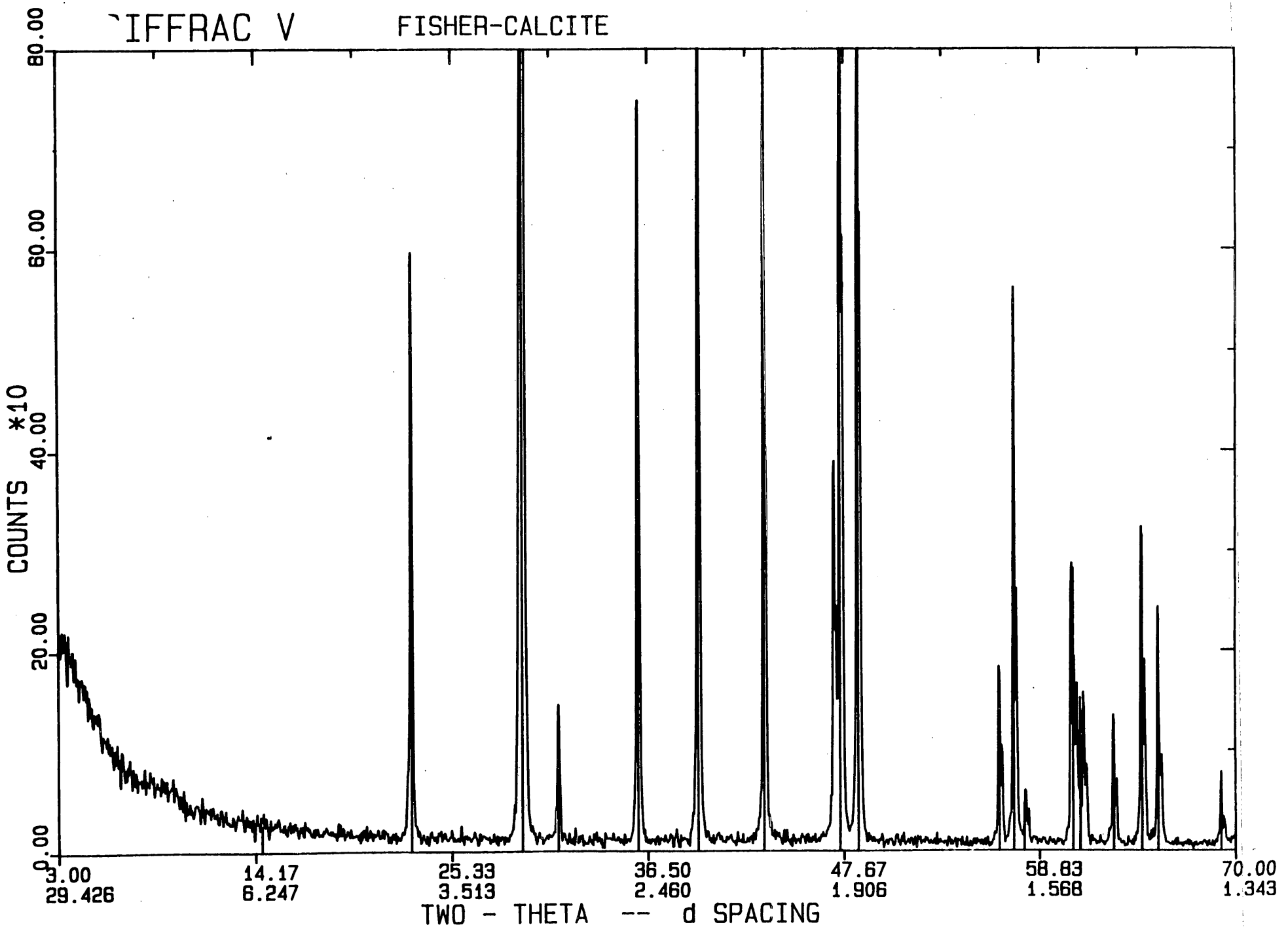

Figure 11, Appendix 1. X-ray diffractogram for Fisher Calcite.

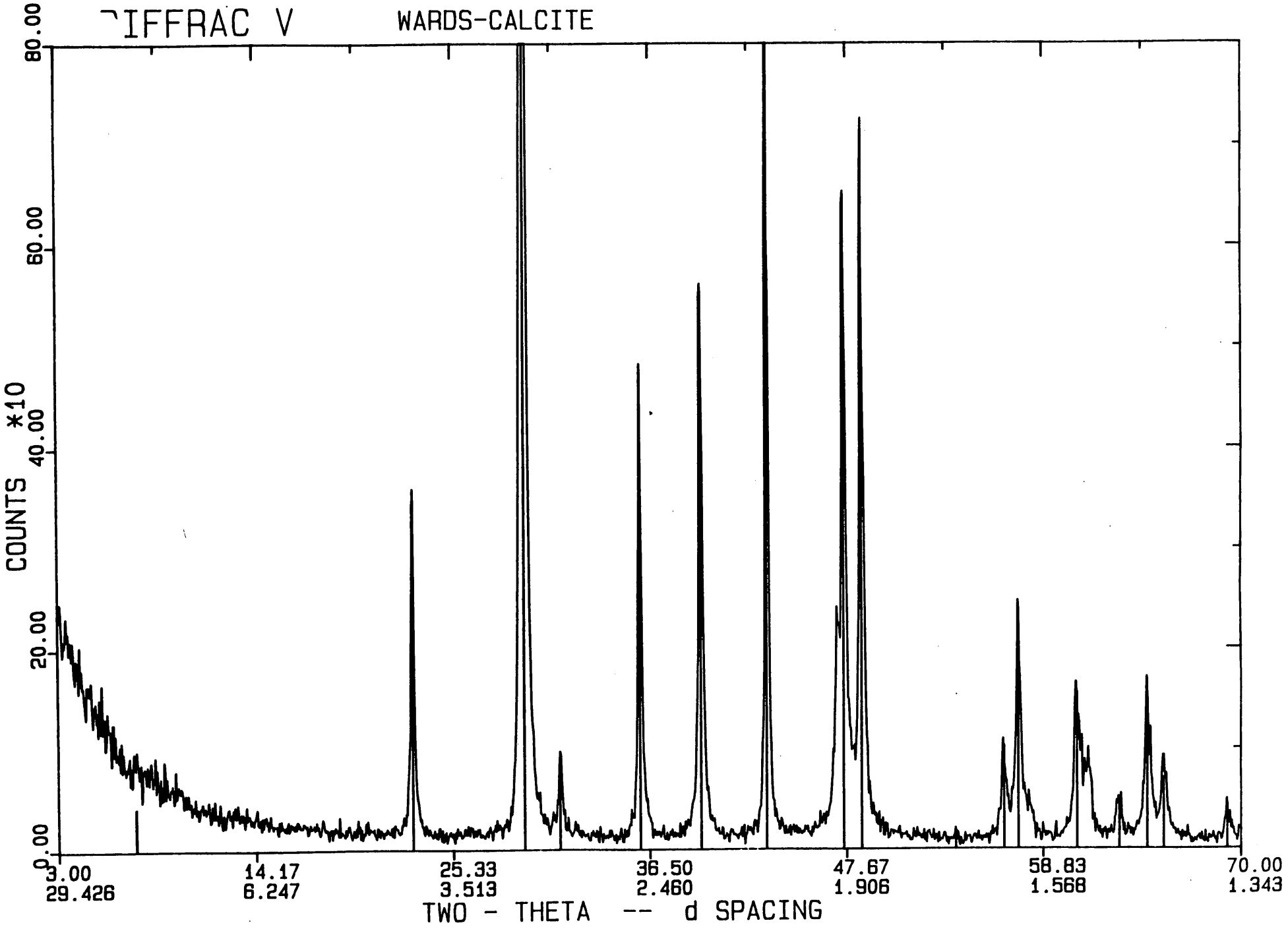

Figure 12, Appendix 1. X-ray diffractogram for Ward's Calcite.

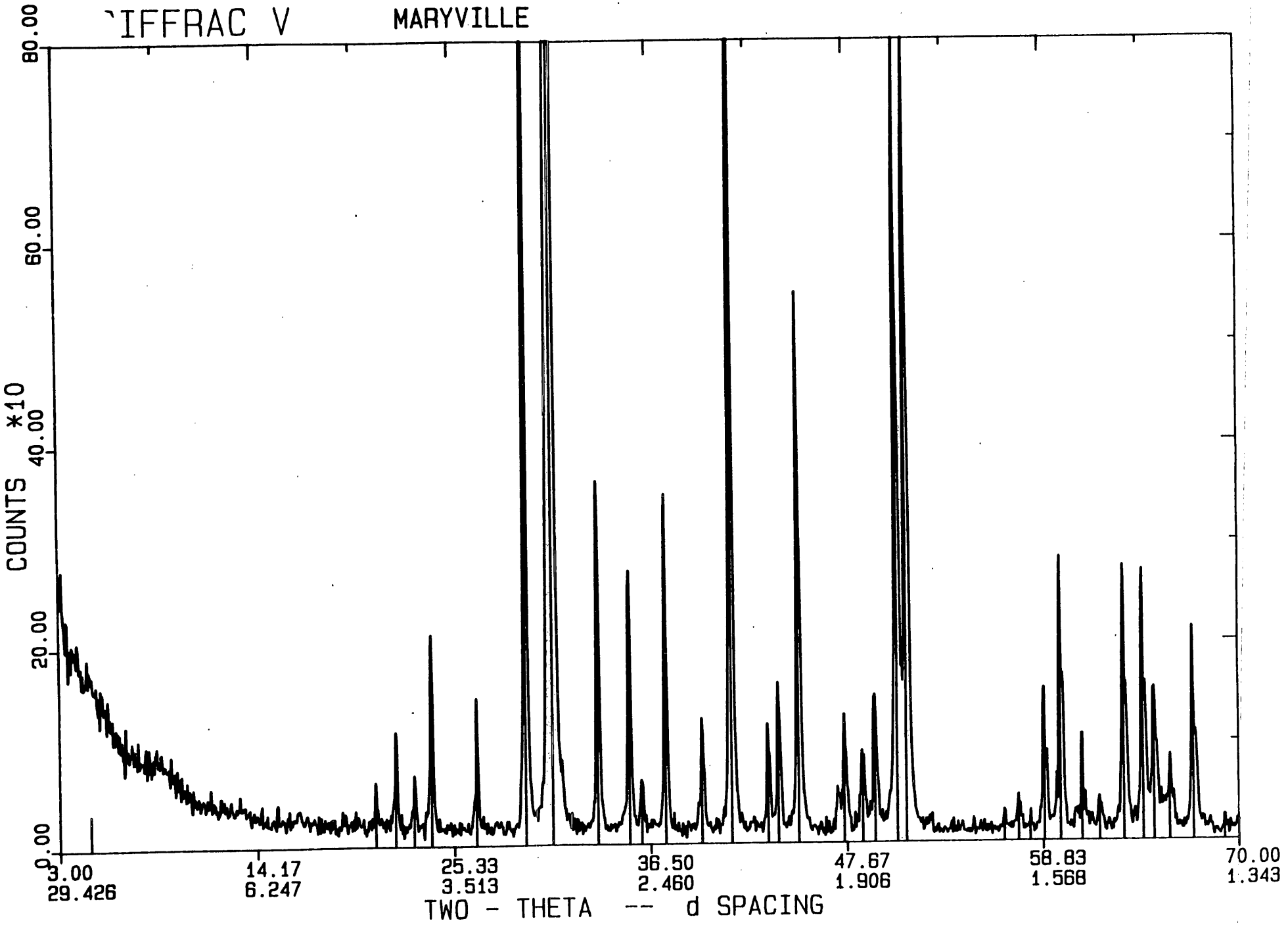

Figure 13, Appendix 1. X-ray diffractogram for Maryville aggregate.

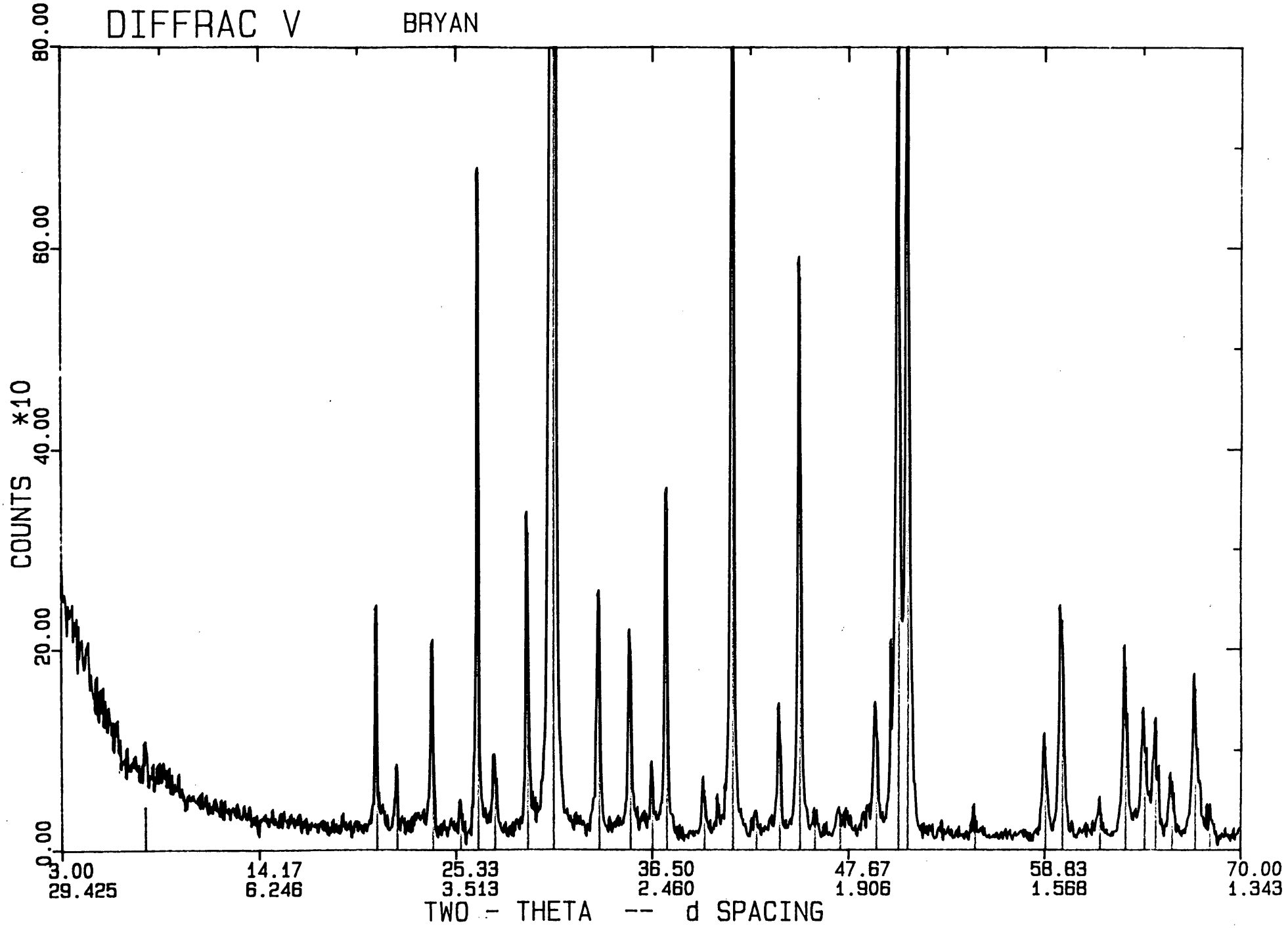

Figure 14, Appendix 1. X-ray diffractogram for Bryan aggregate.

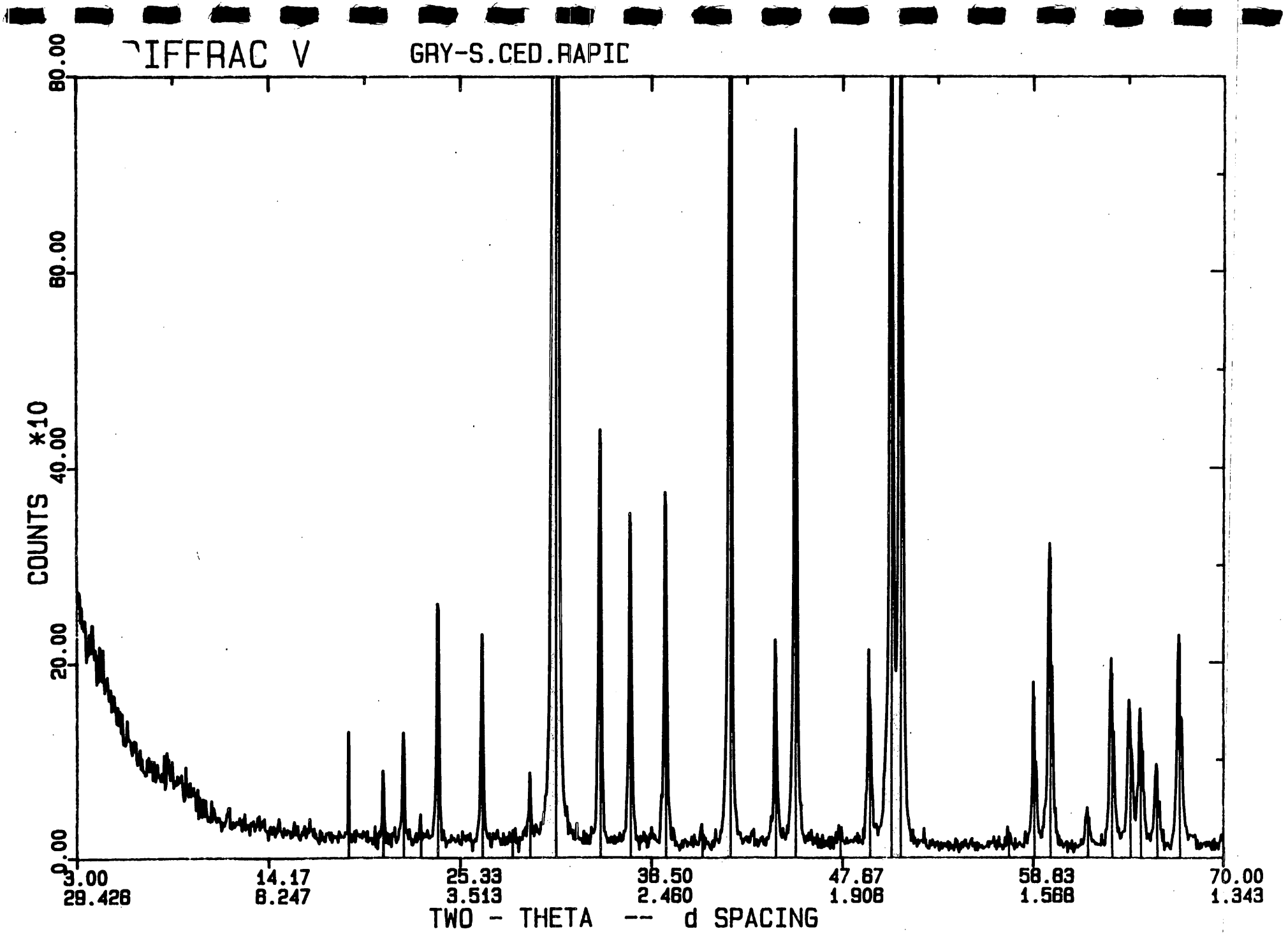

Figure 15, Appendix 1. X-ray diffractogram for Ced. Rap. Gray aggregate.

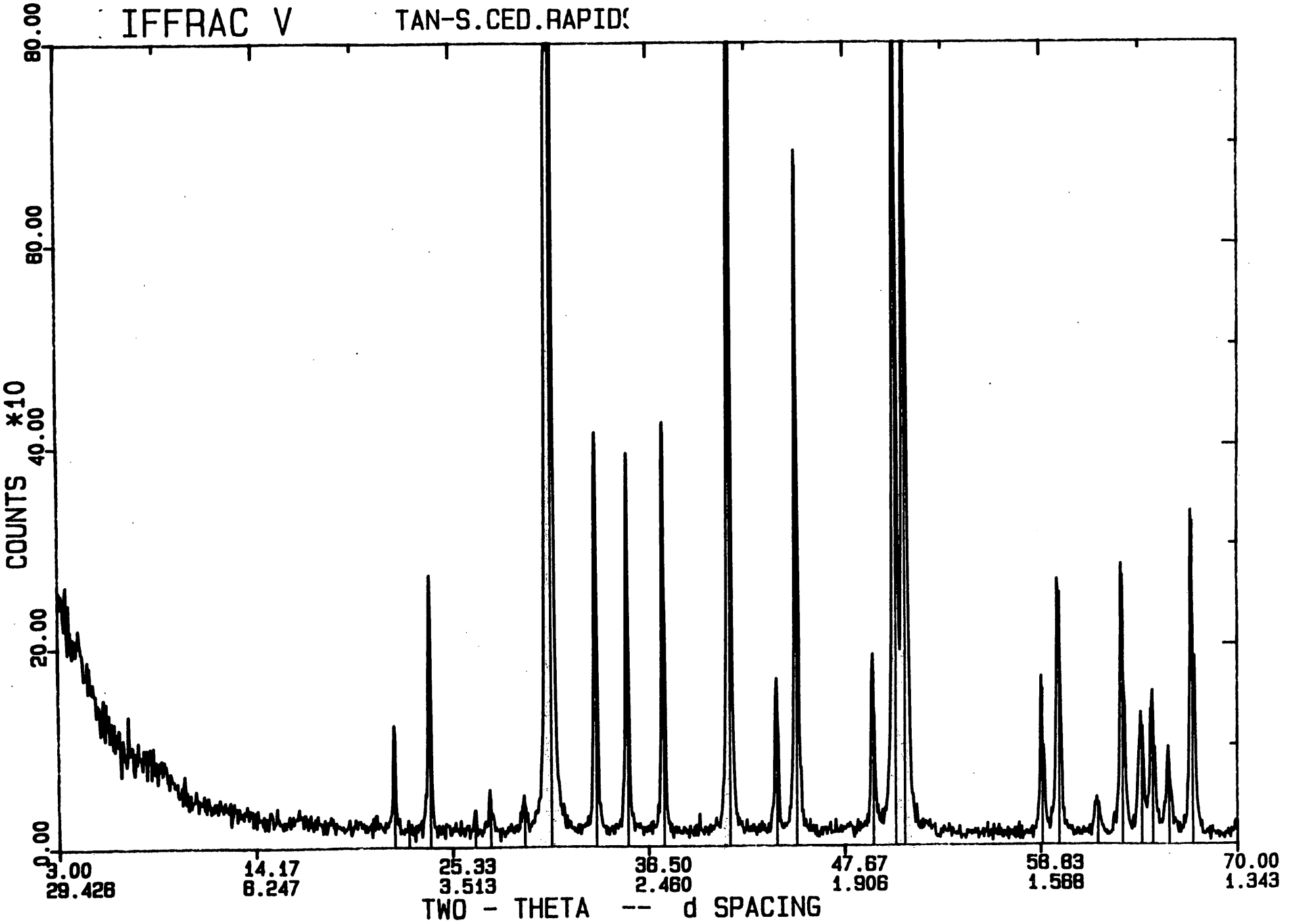

Figure 16, Appendix 1. X-ray diffractogram for Ced. Rap. Tan aggregate.

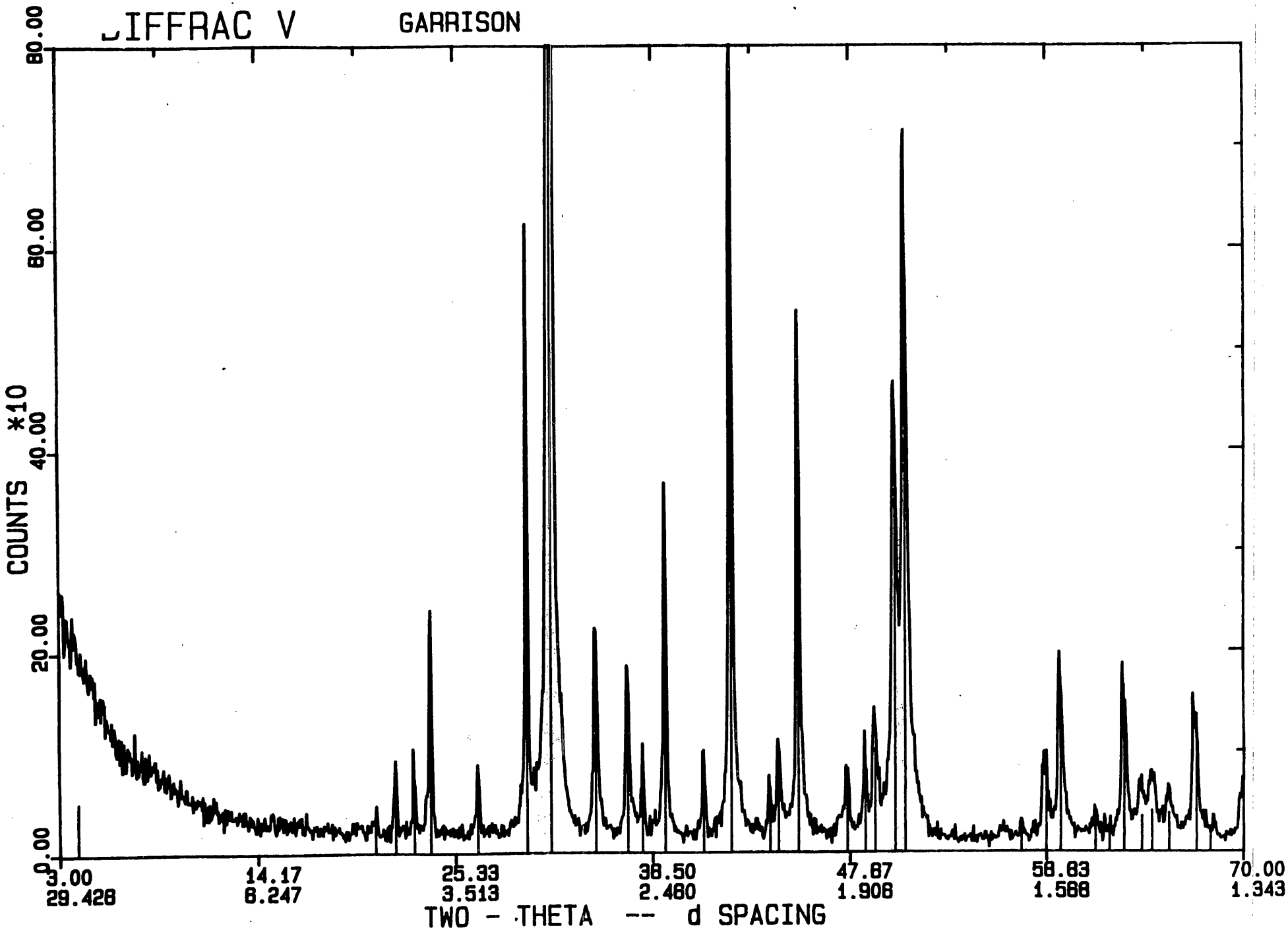

Figure 17, Appendix 1. X-ray diffractogram for Garrison aggregate.

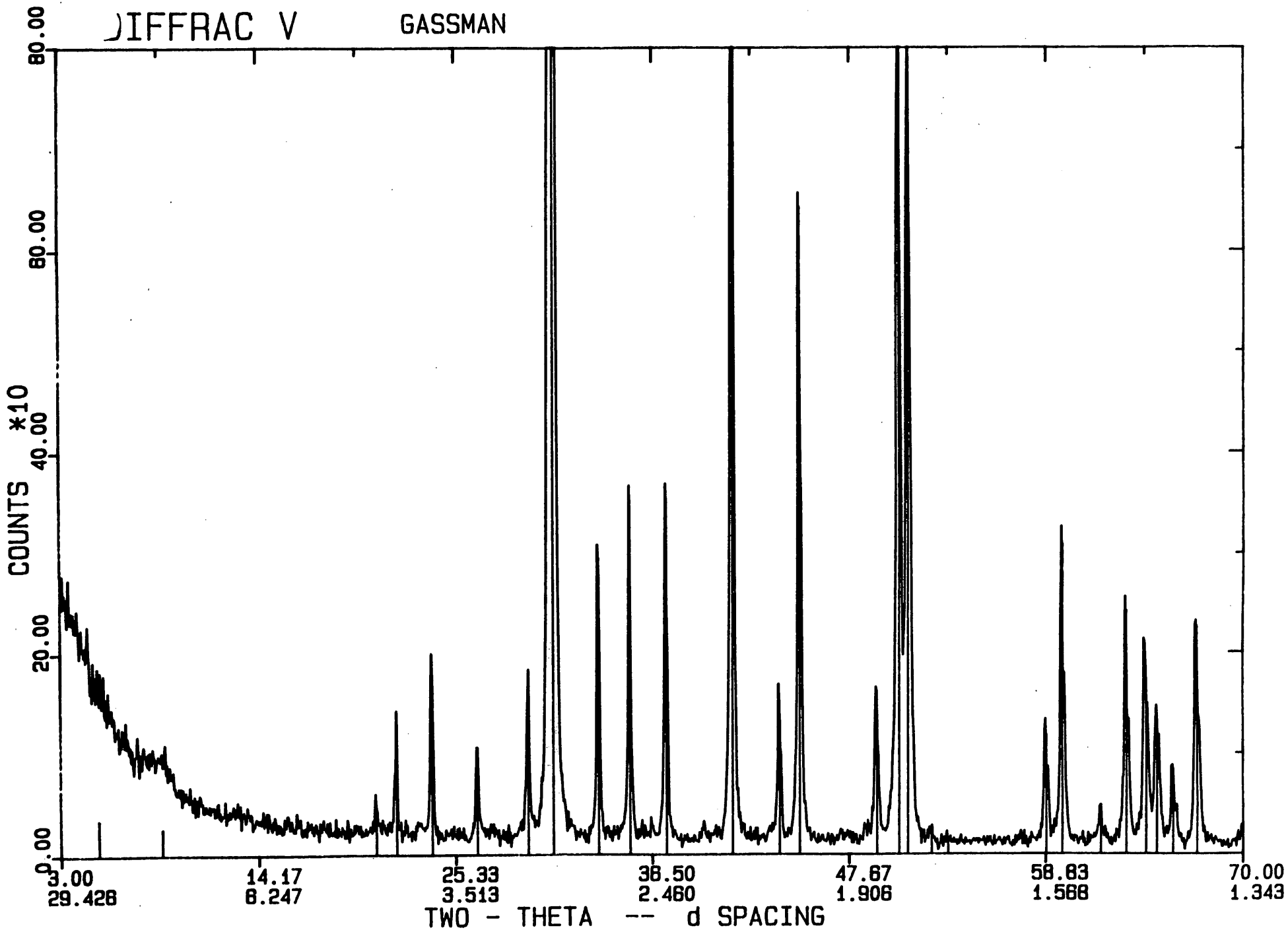

Figure 18, Appendix 1. X-ray diffractogram for Gassman aggregate.

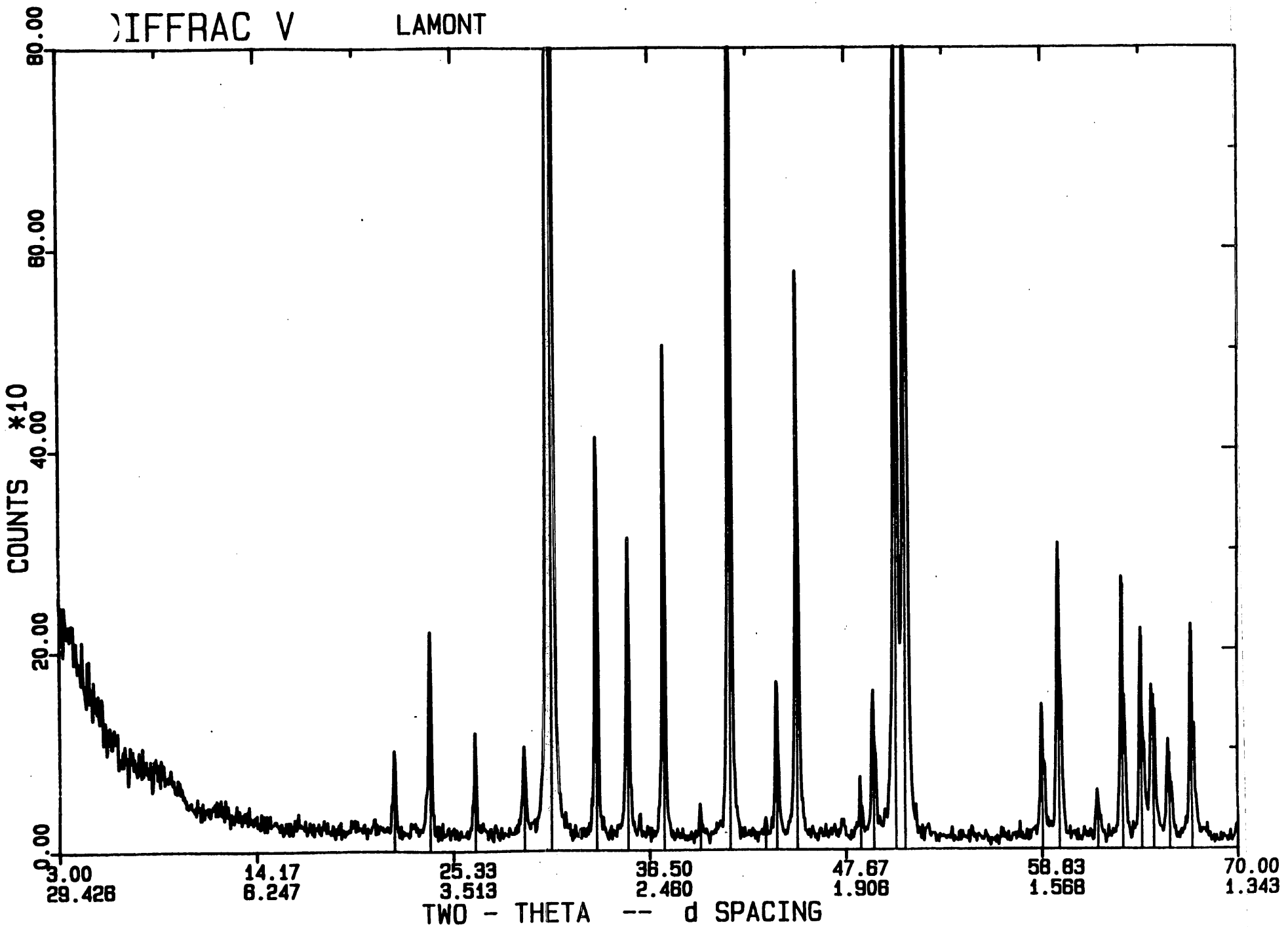

Figure 19, Appendix 1. X-ray diffractogram for Lamont aggregate.

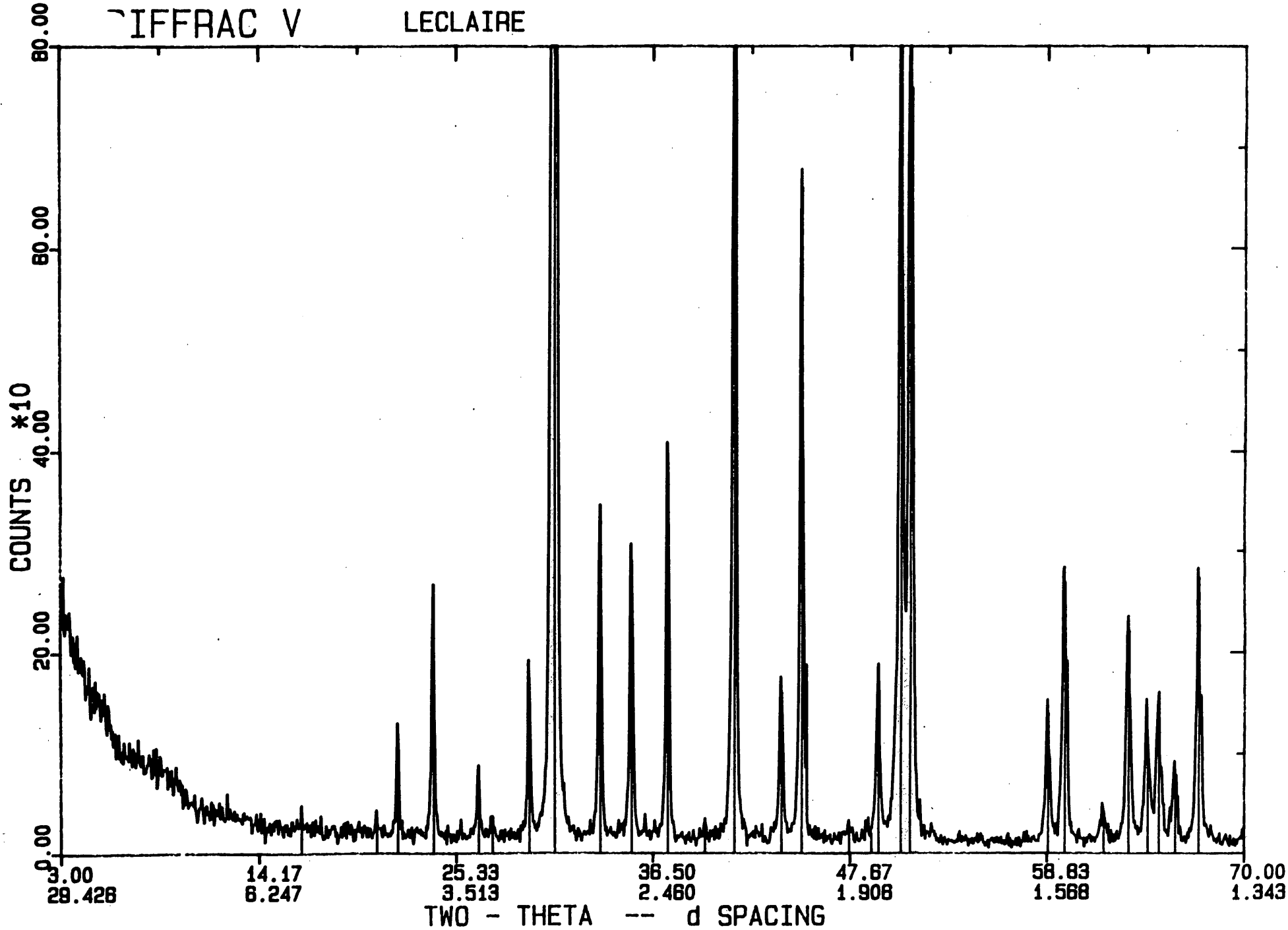

Figure 20, Appendix 1. X-ray diffractogram for LeClaire aggregate.

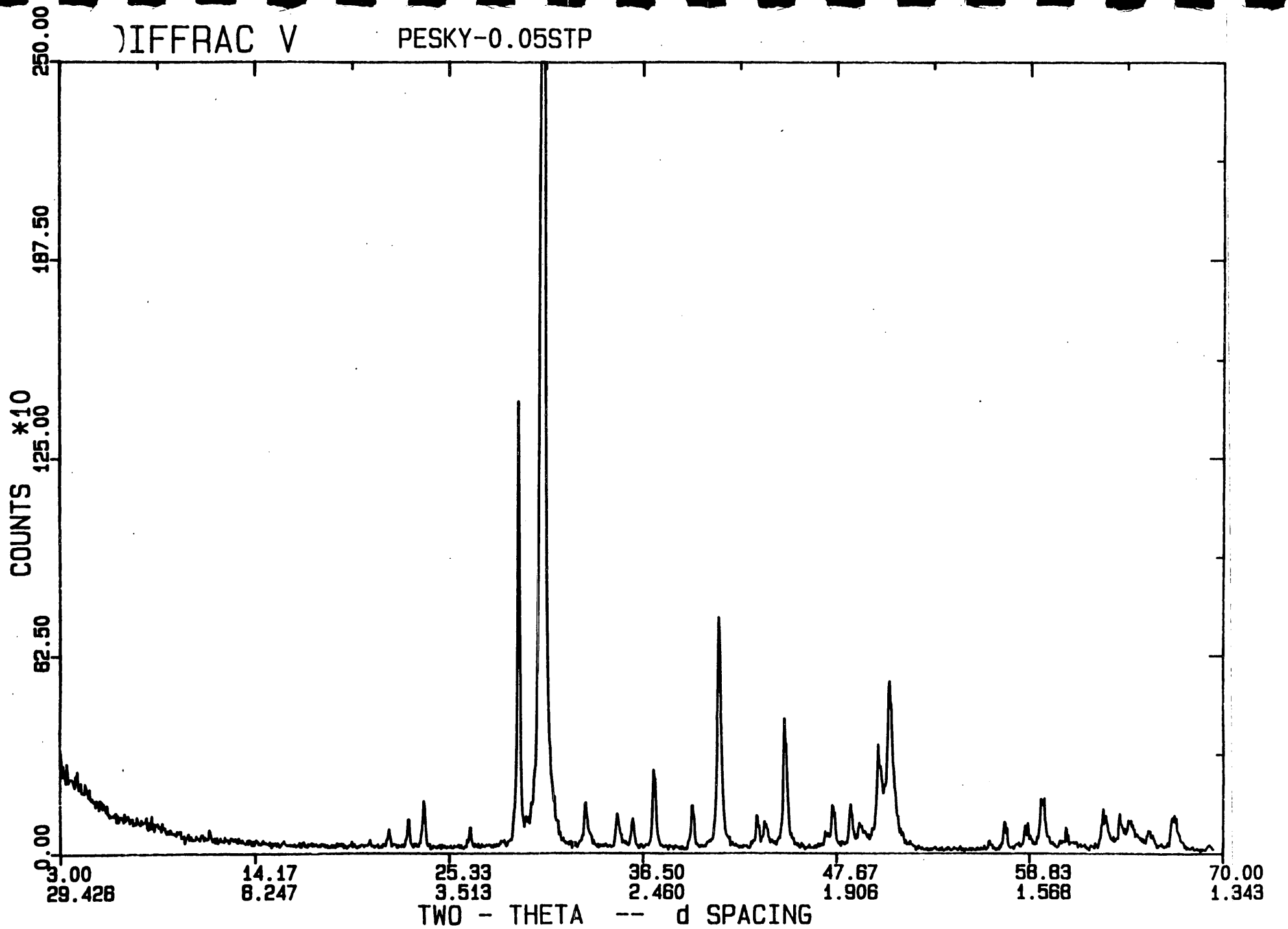

Figure 21, Appendix 1. X-ray diffractogram for Pesky aggregate.

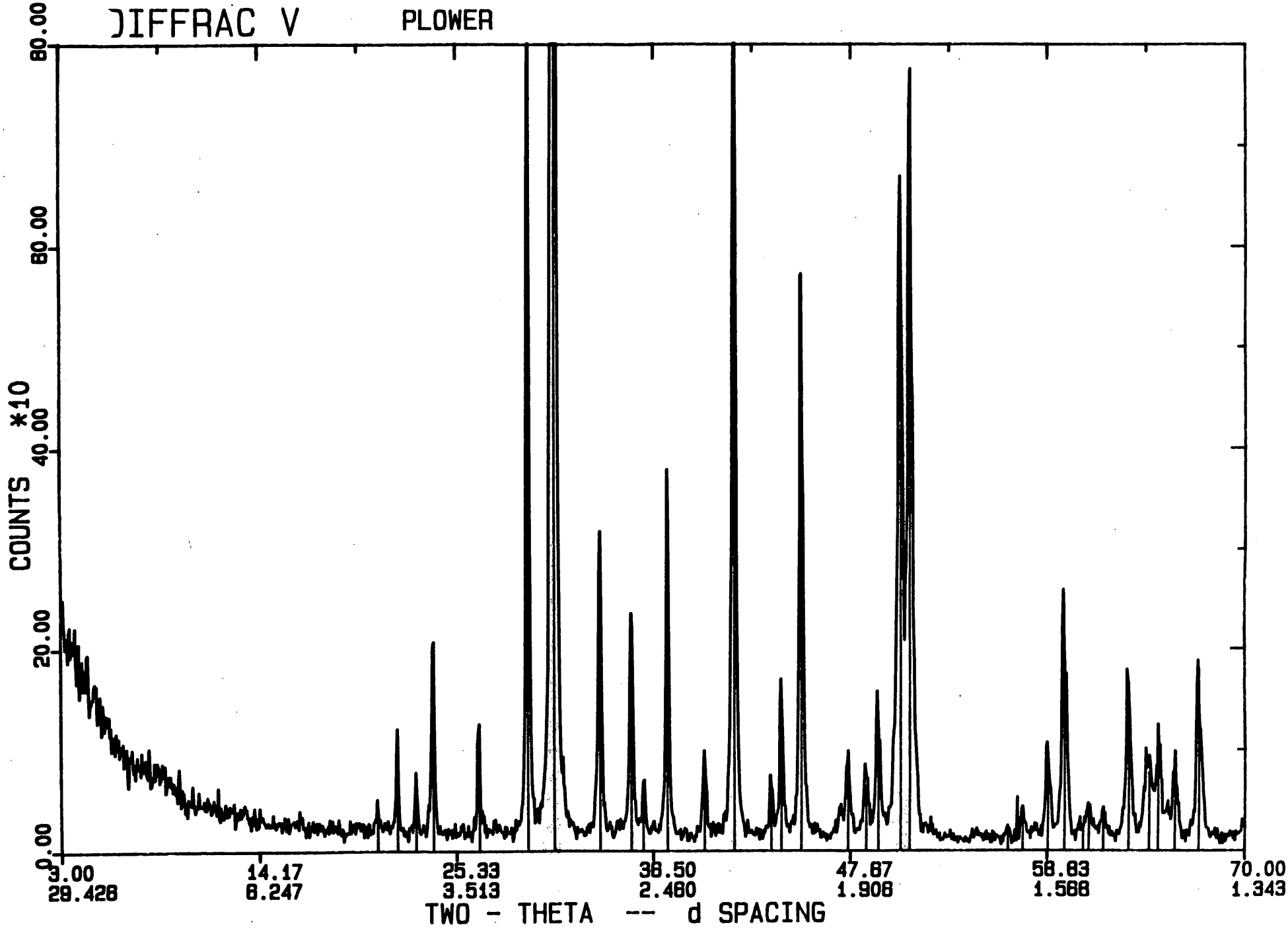

Figure 22, Appendix 1. X-ray diffractogram for Plower aggregate.

APPENDIX II

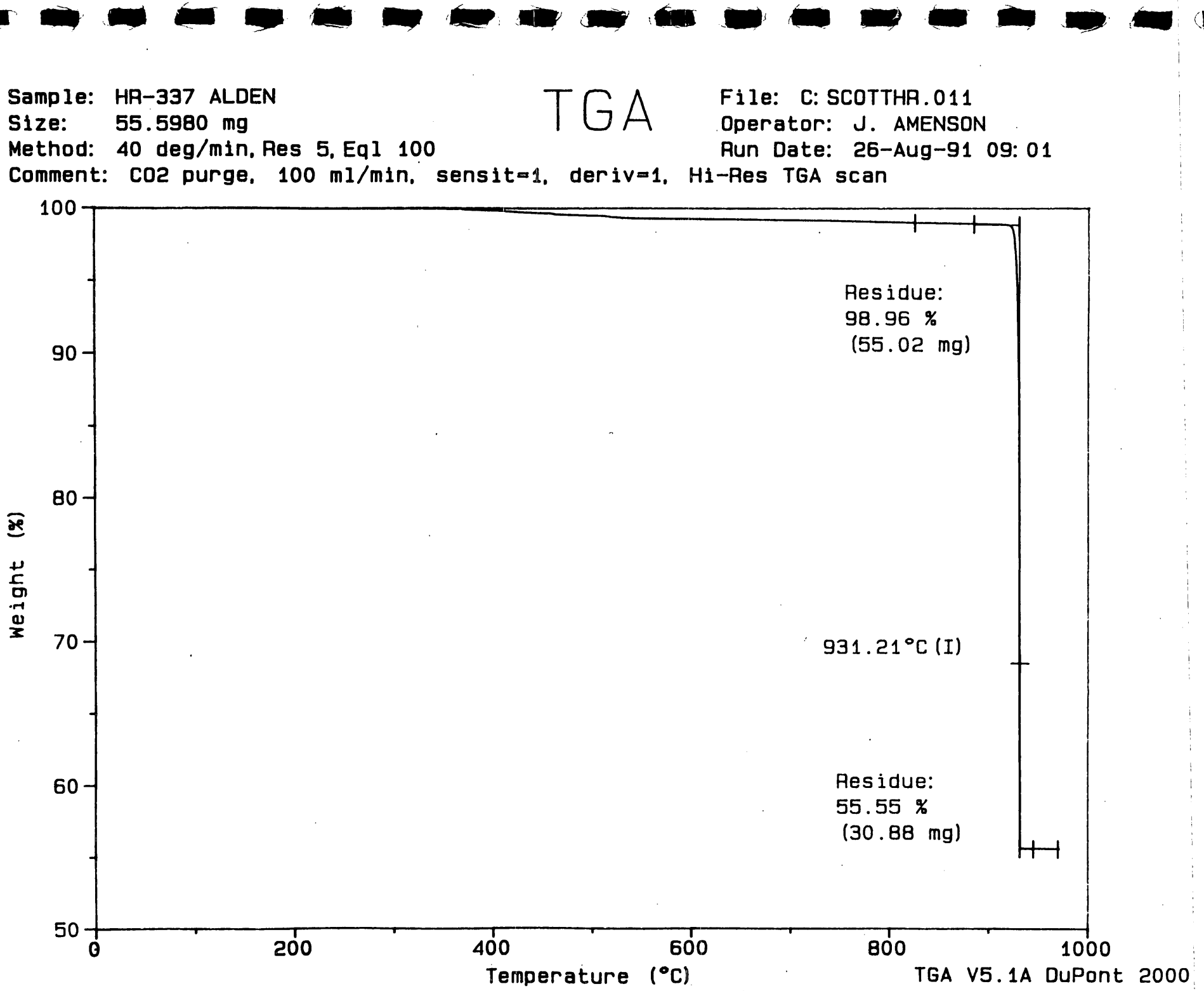

Figure 1, Appendix II. Thermal curve (CO_2 atmosphere) for Alden aggregate.

Sample: HR-337 CRESCENT
Size: 55.6220 mg
Method: 40 deg/min, Res 5, Eql 100
Comment: CO2 purge, 100 ml/min, sensit=1, deriv=1, Hi-Res TGA scan

TGA

File: C:SCOTTHR.002
Operator: J. AMENSON
Run Date: 23-Aug-91 11:30

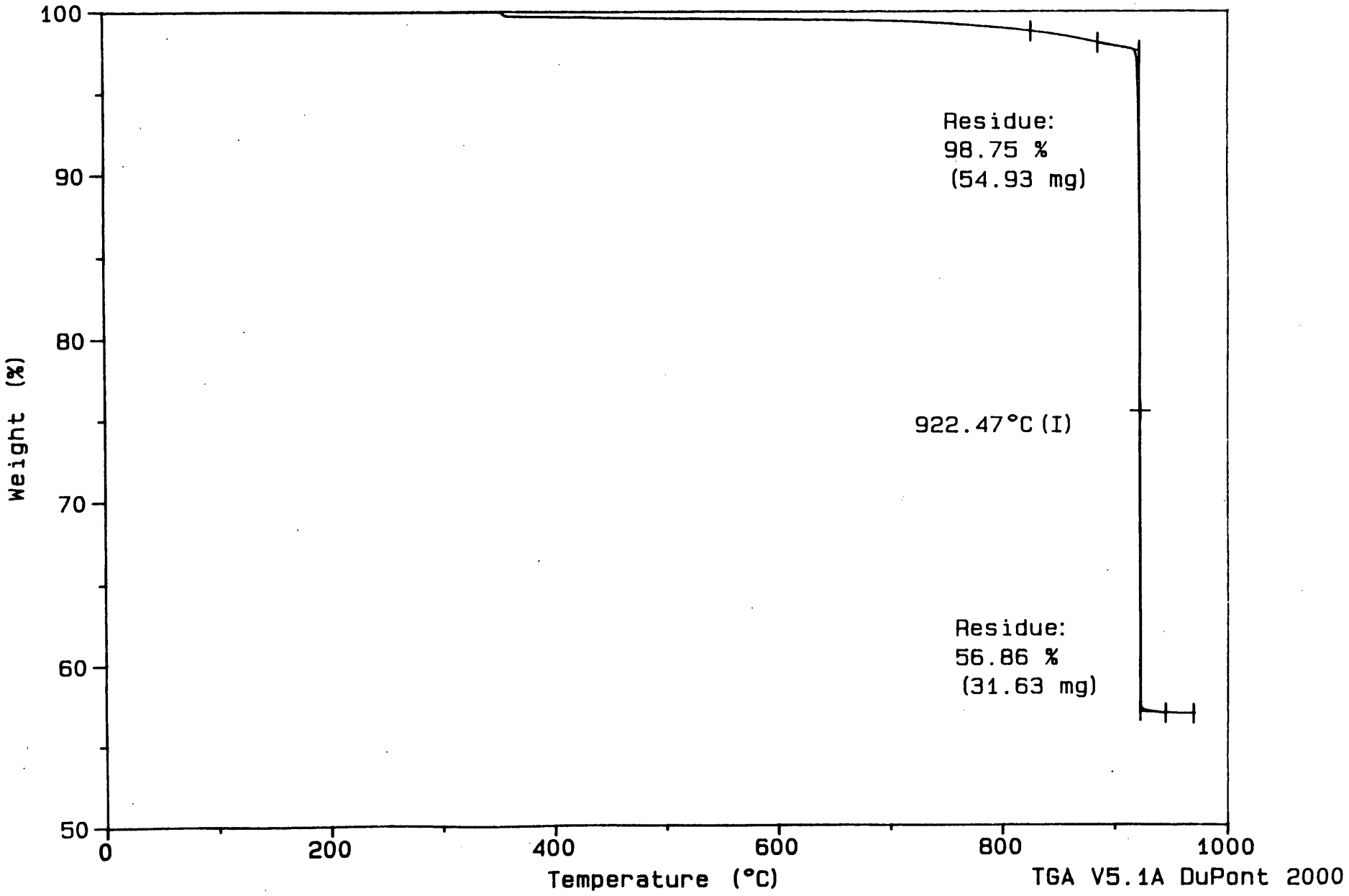

[redacted] Figure [redacted] Appendix II. [redacted] curve ([redacted] atmosphere) for Crescent aggregate. [redacted]

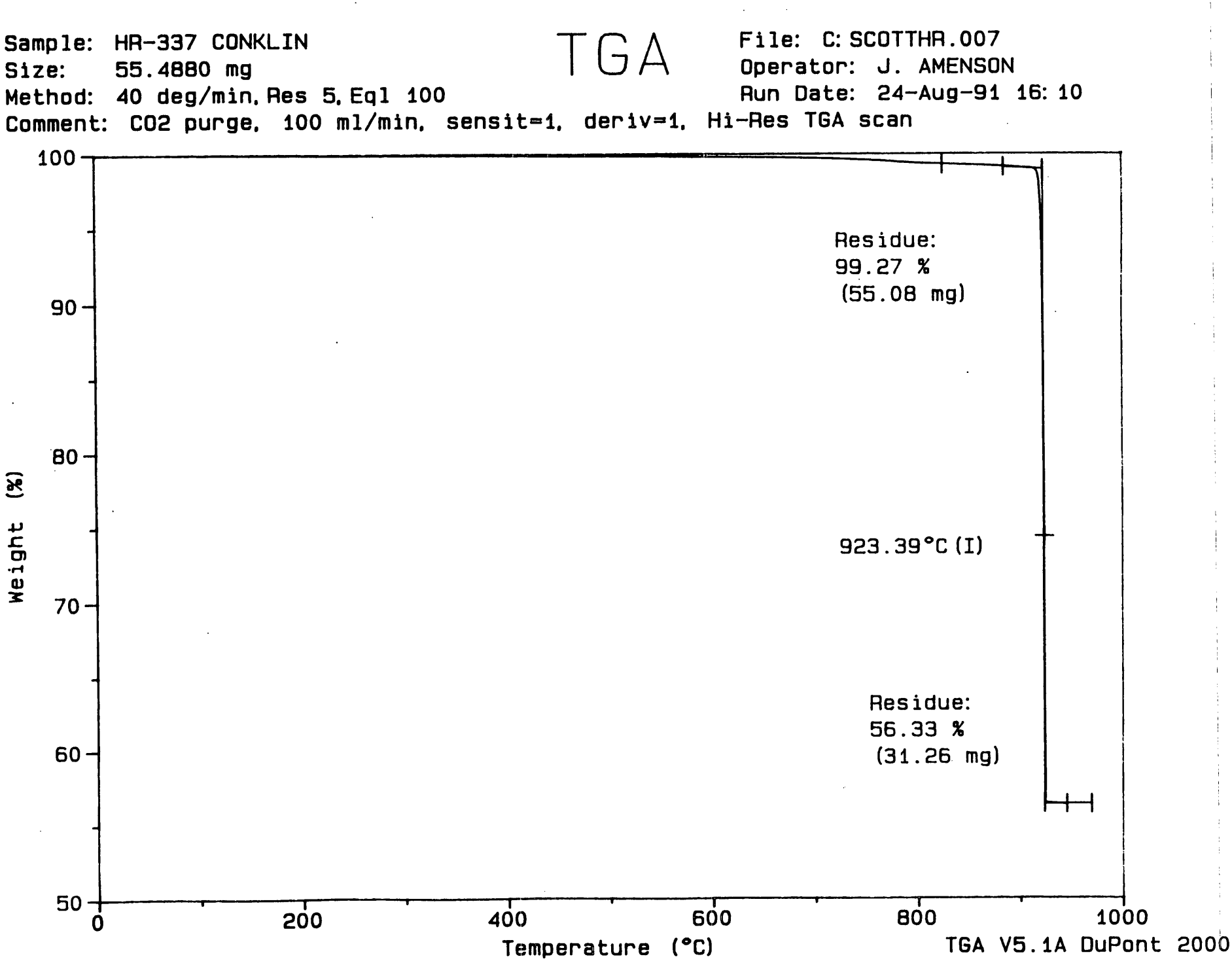

Figure 3, Appendix II. Thermal curve (CO_2 atmosphere) for Conklin aggregate.

Sample: HR-337 EARLY CHAPEL
Size: 55.6030 mg
Method: 40 deg/min, Res 5, Eql 100
Comment: CO2 purge, 100 ml/min, sensit=1, deriv=1, Hi-Res TGA scan

TGA

File: C: SCOTTHR.010
Operator: J. AMENSON
Run Date: 26-Aug-91 07:56

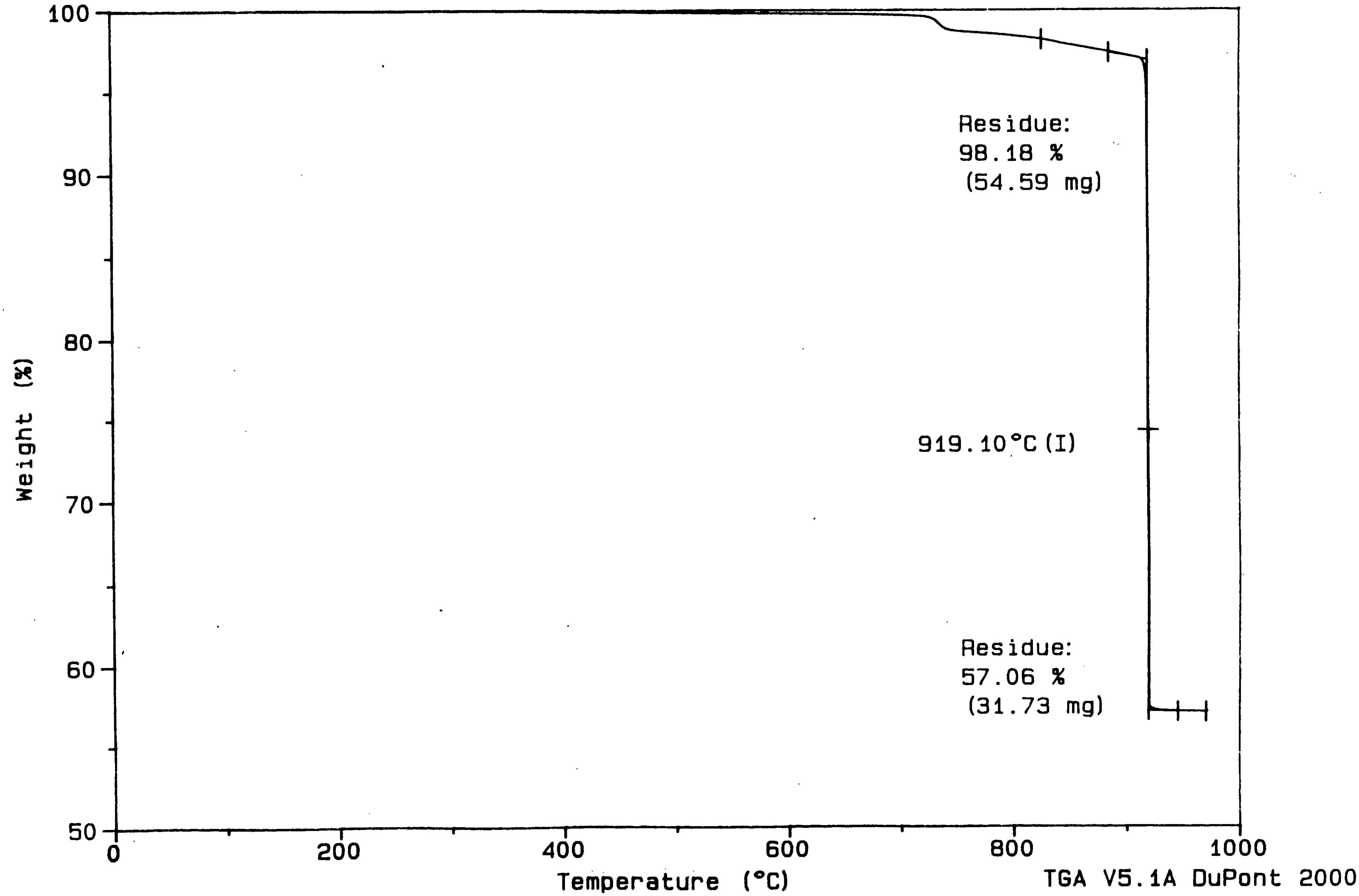

[redacted] [redacted] [redacted]ig[redacted] 4,[redacted]per[redacted] [redacted] T[redacted]mal[redacted]rv[redacted]CO2[redacted]mos[redacted]re[redacted]or [redacted]ly[redacted]ape[redacted]gg [redacted] [redacted] [redacted]

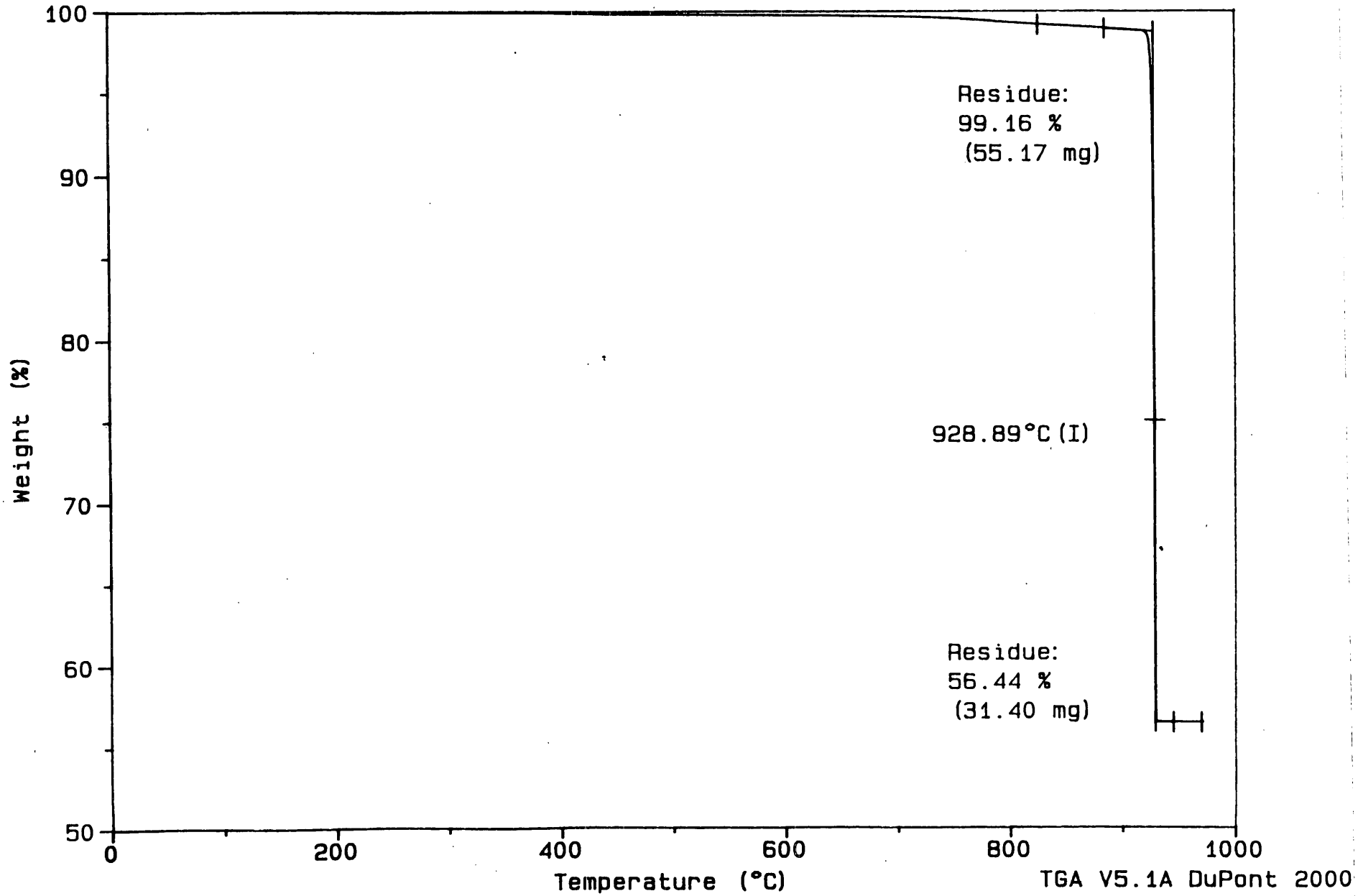

Figure 5, Appendix II. Thermal curve (CO_2 atmosphere) for Eldorado aggregate.

Sample: HR-337 LINWOOD
Size: 55.6240 mg
Method: 40 deg/min, Res 5, Eql 100
Comment: CO2 purge, 100 ml/min, sensit=1, deriv=1, Hi-Res TGA scan

TGA

File: C:SCOTTHR.012
Operator: J. AMENSON
Run Date: 26-Aug-91 10:00

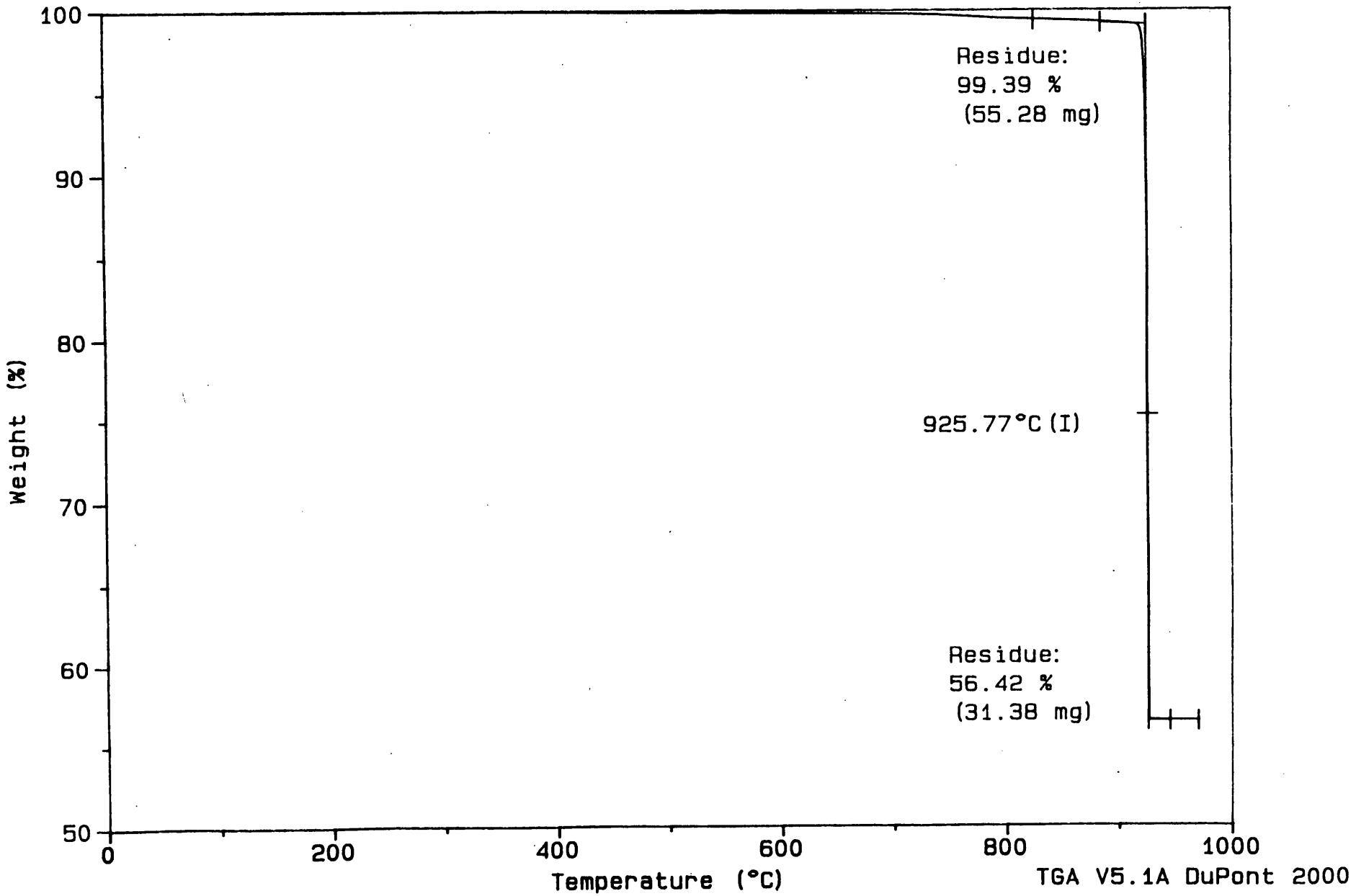

[redacted] Appendix II. [redacted] curve ([redacted] atmosphere) for Linwood aggregate. [redacted]

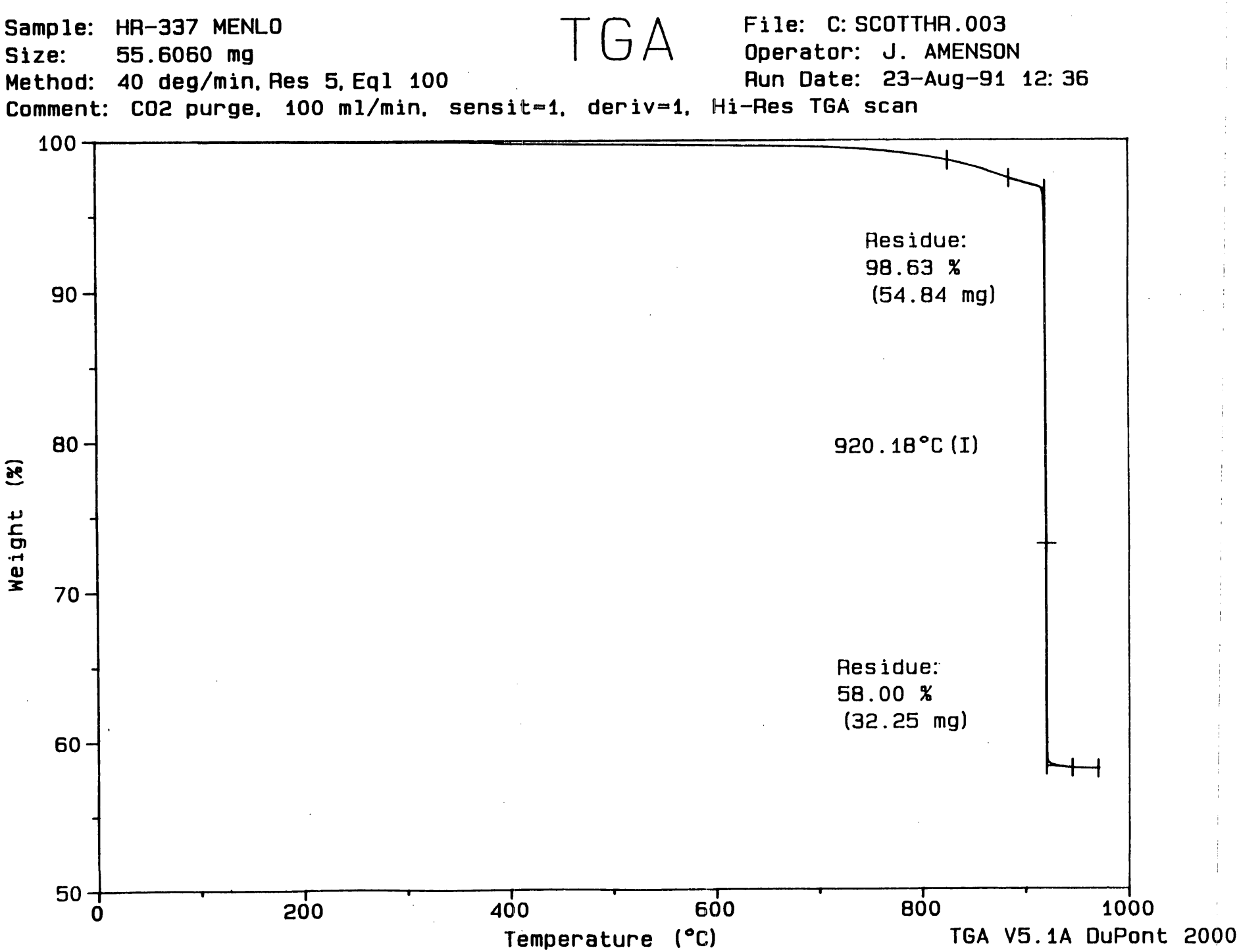

Figure 7, Appendix II. Thermal curve (CO_2 atmosphere) for Menlo aggregate.

Sample: HR-337 MONTOUR
Size: 55.8680 mg
Method: 40 deg/min, Res 5, Eql 100
Comment: CO2 purge, 100 ml/min, sensit=1, deriv=1, Hi-Res TGA scan

TGA

File: C:SCOTTHR.006
Operator: J. AMENSON
Run Date: 24-Aug-91 15:11

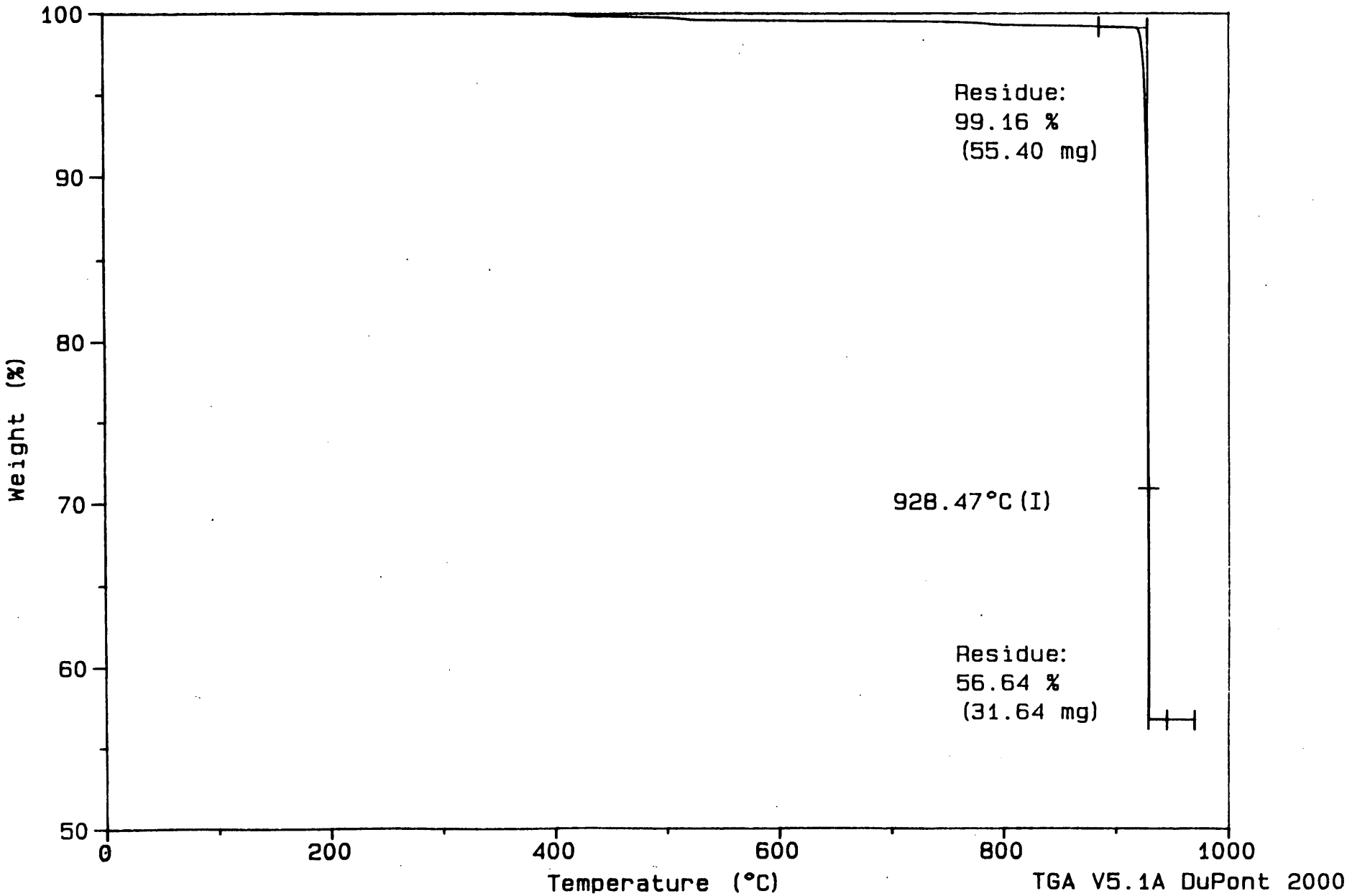

Figure 8, Appendix II. Thermal curve (CO_2 atmosphere) for Montmorillonite.

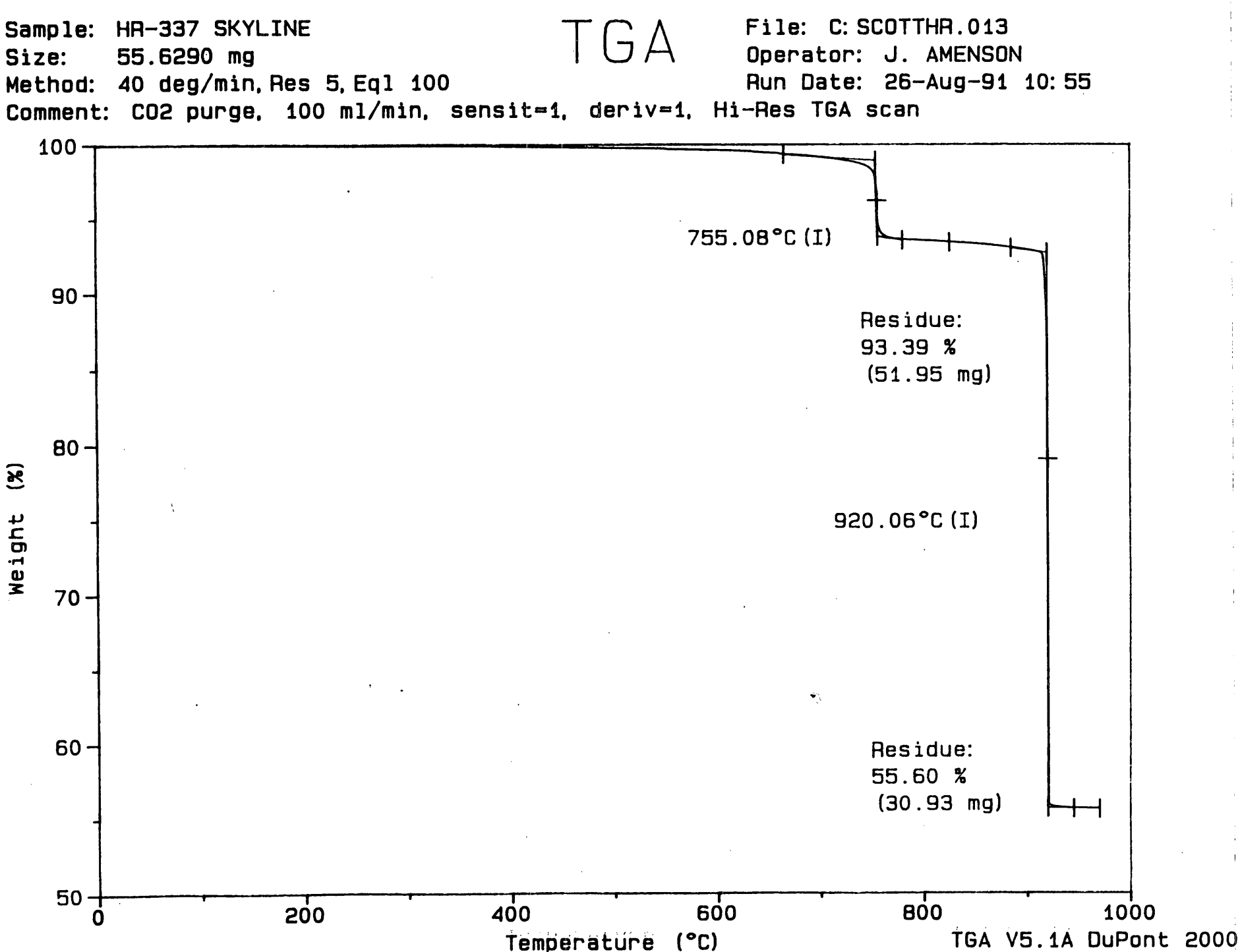

Figure 9, Appendix II. Thermal curve (CO_2 atmosphere) for Skyline aggregate.

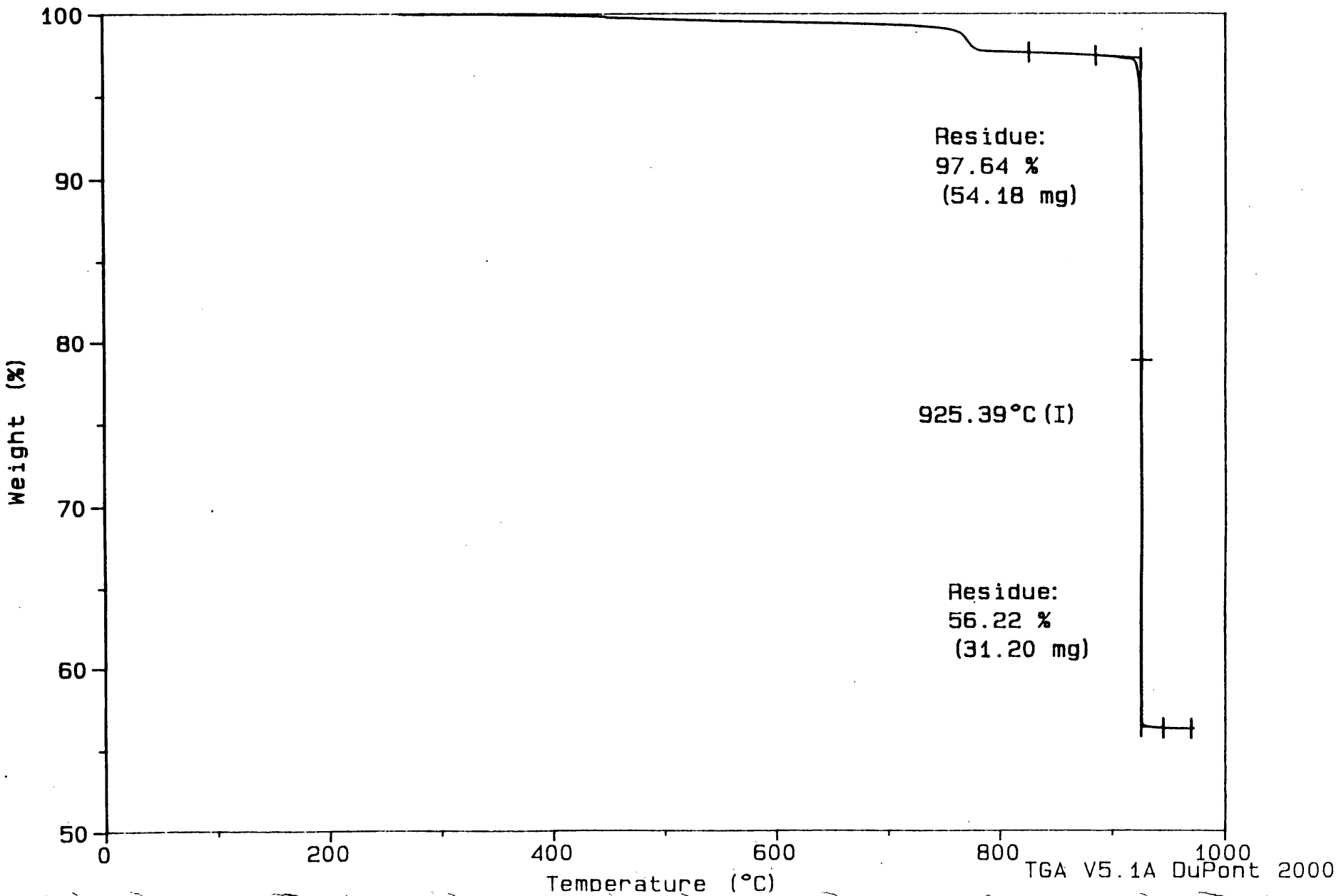

Figure 10, Appendix II. Thermal curve (CO_2 atmosphere) for huntington agg

Sample: HR-337 F5CO CALCITE
Size: 55.5370 mg
Method: 40 deg/min, Res 5, Eql 100
Comment: CO2 purge, 100 ml/min, sensit=1, deriv=1, Hi-Res TGA scan

TGA

File: C:SCOTTHR.024
Operator: J. AMENSON
Run Date: 22-Nov-91 09:34

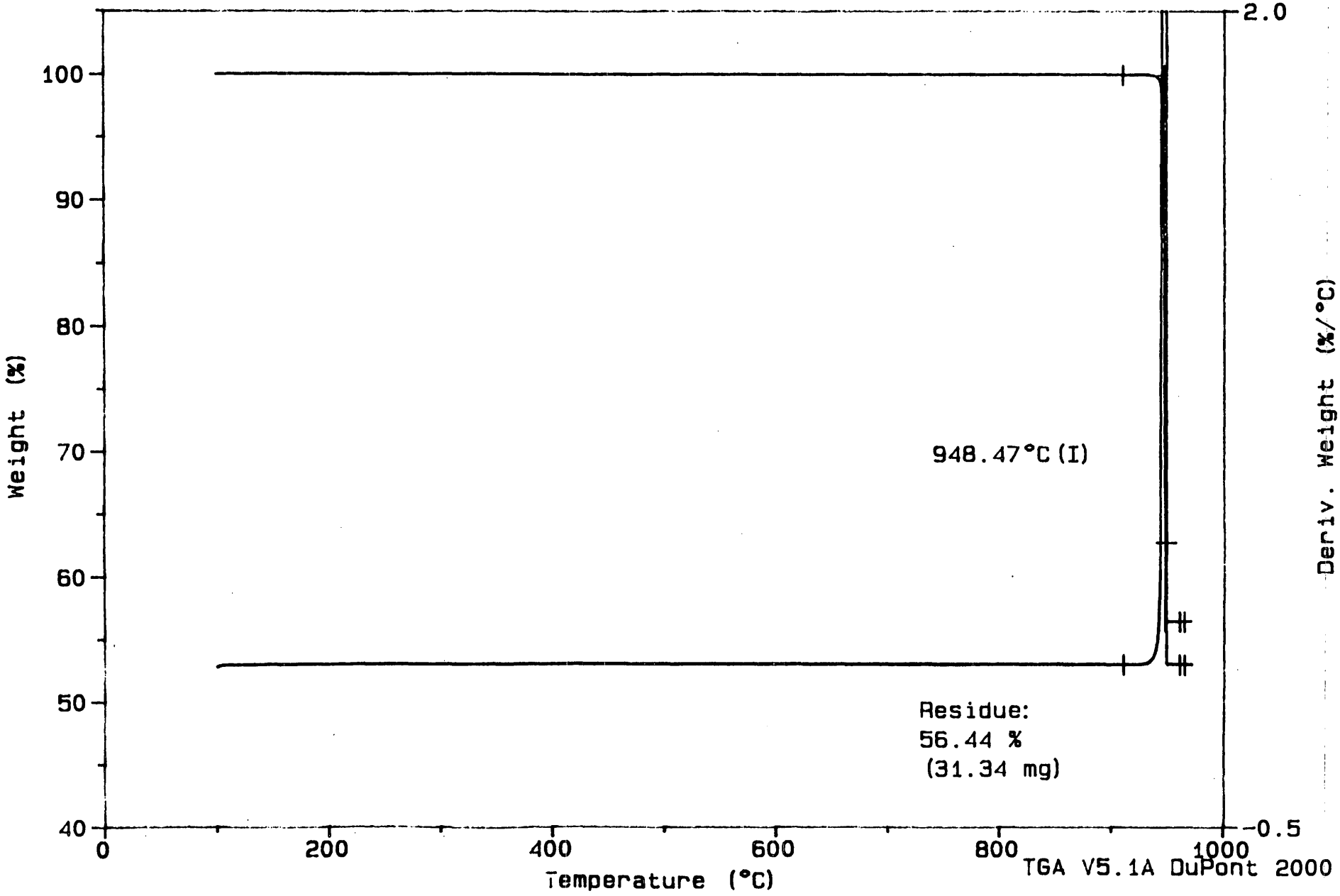

Figure 11, Appendix II. Thermal curve (CO_2 atmosphere) for Fisher Calcite.

Sample: HR-337 WARDS CALCITE (GROUND)
Size: 55.5370 mg
Method: 40 deg/min, Res 5, Eql 300
Comment: CO2 purge, 100 ml/min, sensit=1, deriv=1, Hi-Res TGA scan

TGA

File: C:SCOTTHR.036
Operator: J. AMENSON
Run Date: 4-Dec-91 11:46

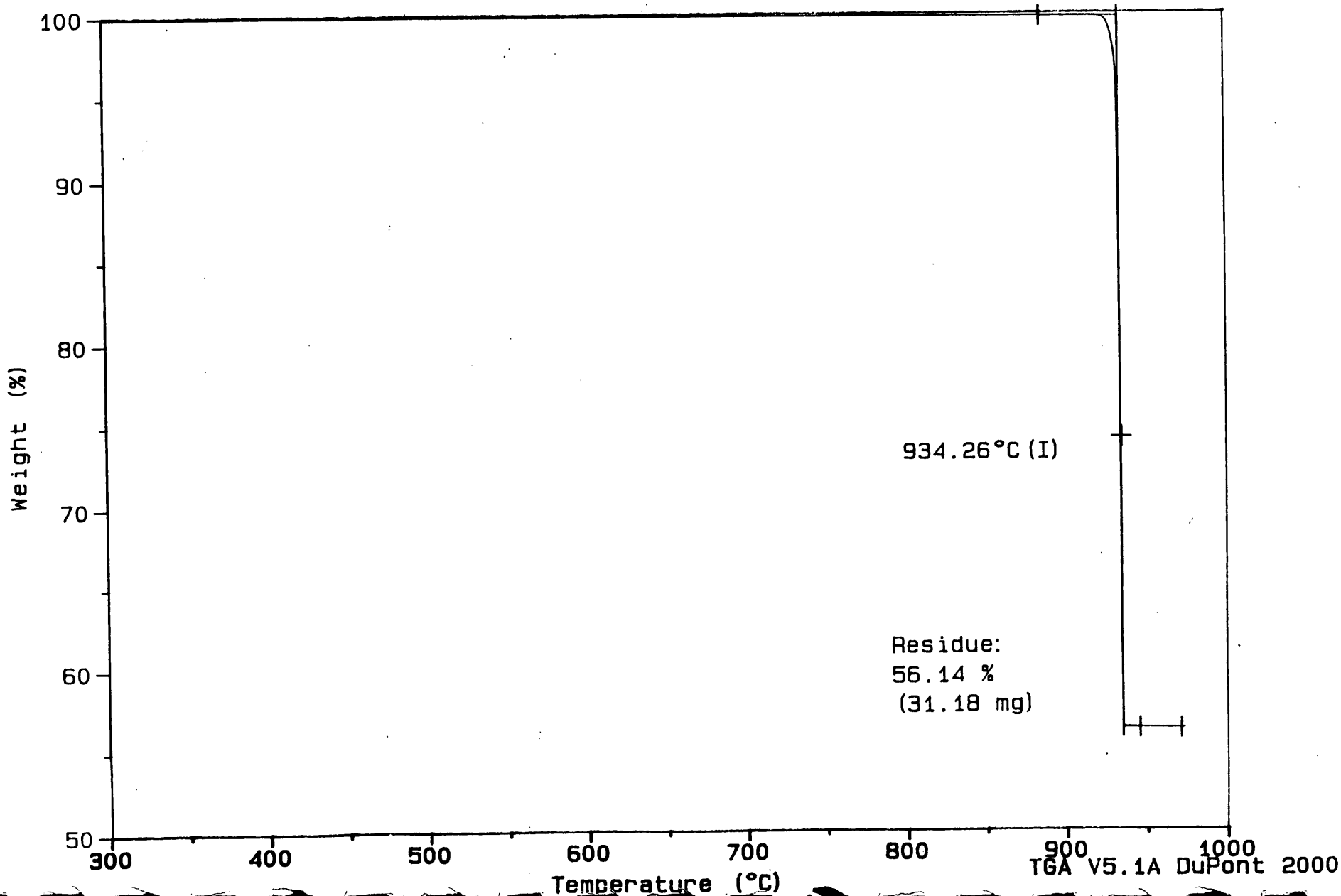

[redacted] Appendix II [redacted] (CO2 & [redacted]) [redacted] Wards [redacted]

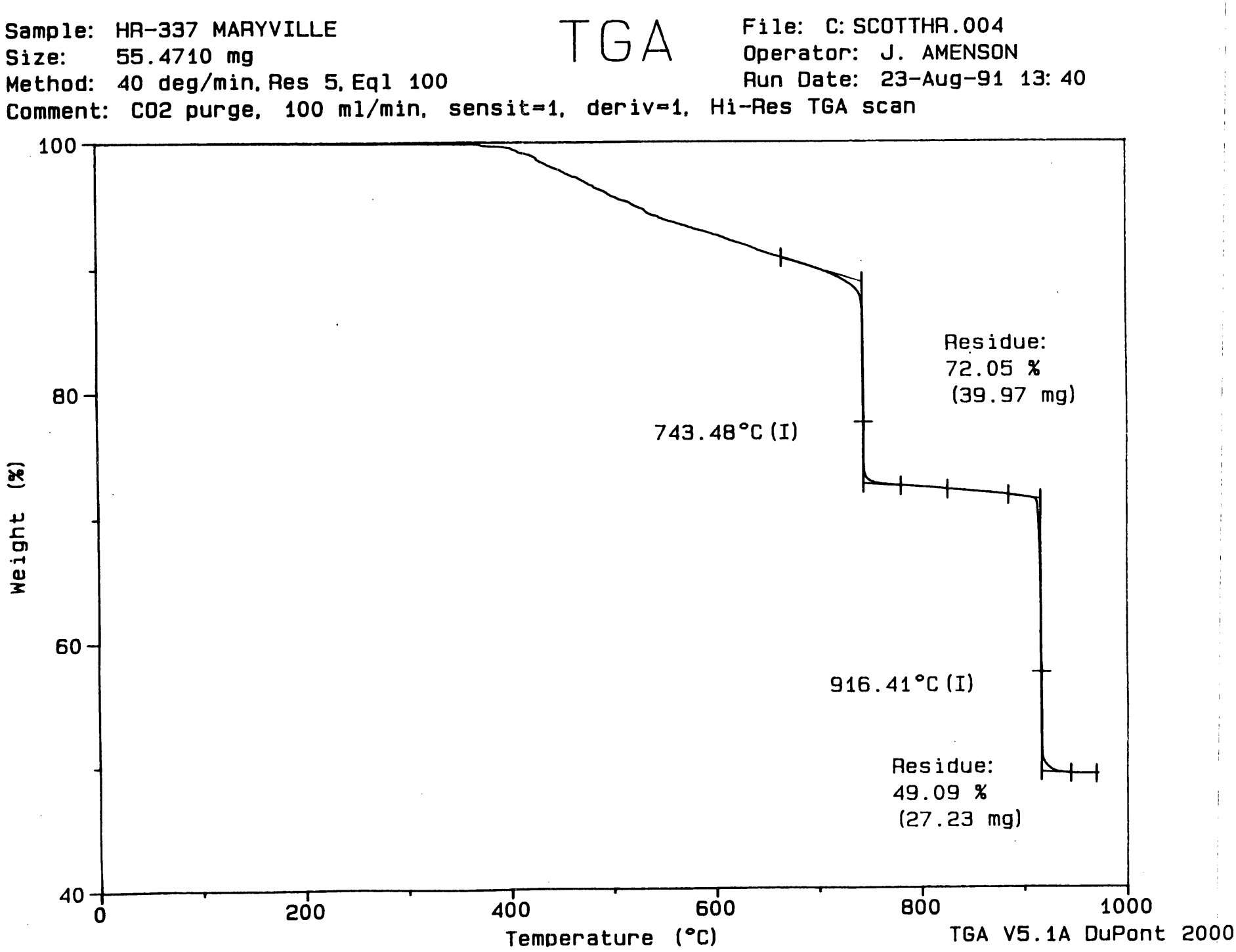

Figure 13, Appendix II. Thermal curve (CO_2 atmosphere) for Maryville aggregate

Sample: HR-337 BRYAN
Size: 55.4810 mg
Method: 40 deg/min, Res 5, Eql 100
Comment: CO2 purge, 100 ml/min, sensit=1, deriv=1, Hi-Res TGA scan

TGA

File: C:SCOTTHR.009
Operator: J. AMENSON
Run Date: 24-Aug-91 18:08

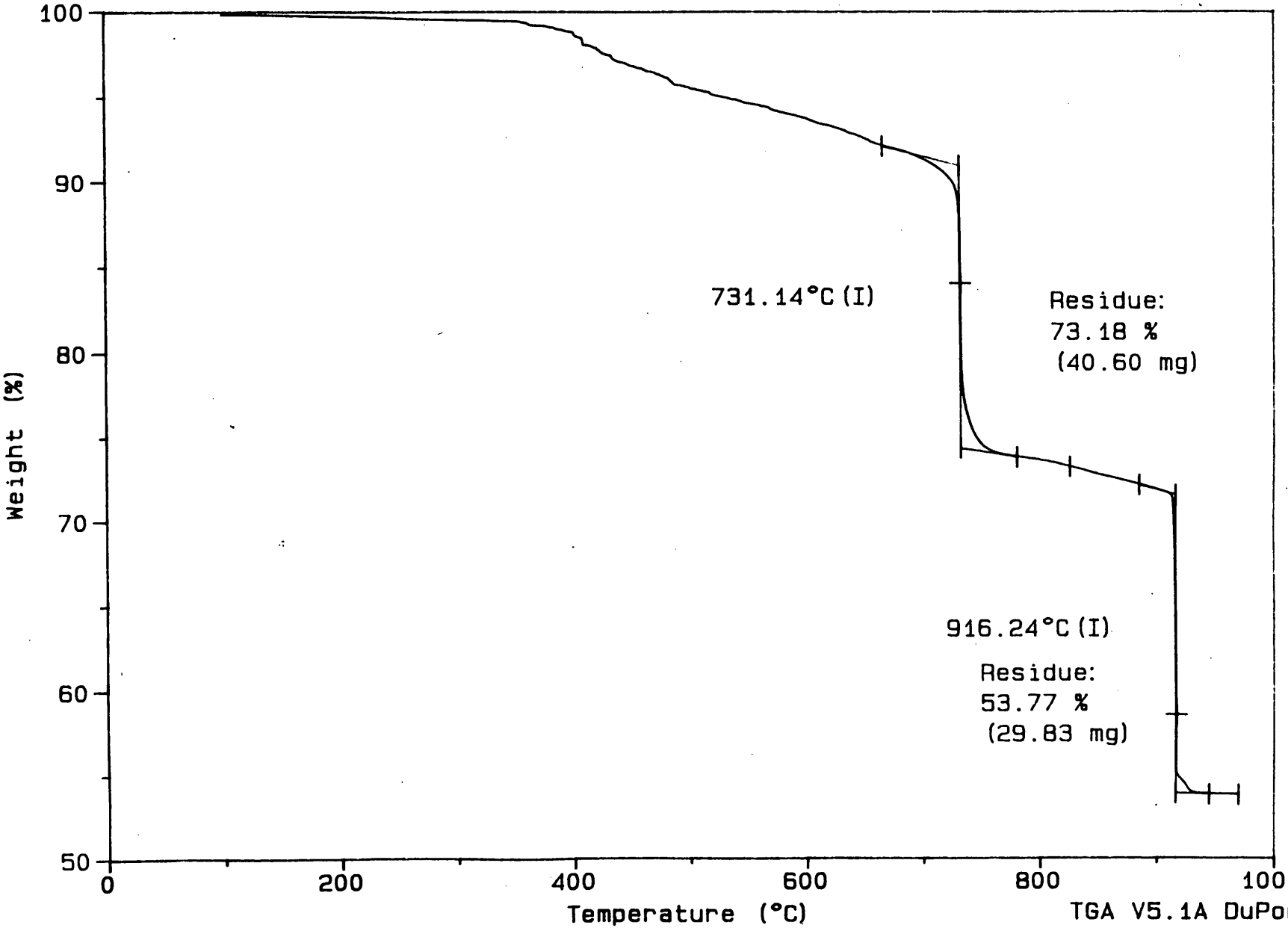

Sample: HR-337 CEDAR RAPIDS
Size: 55.4540 mg
Method: 40 deg/min, Res 5, Eql 100
Comment: CO2 purge, 100 ml/min, sensit=1, deriv=1, Hi-Res TGA scan

TGA

File: C:SCOTTHR.005
Operator: J. AMENSON
Run Date: 23-Aug-91 15:21

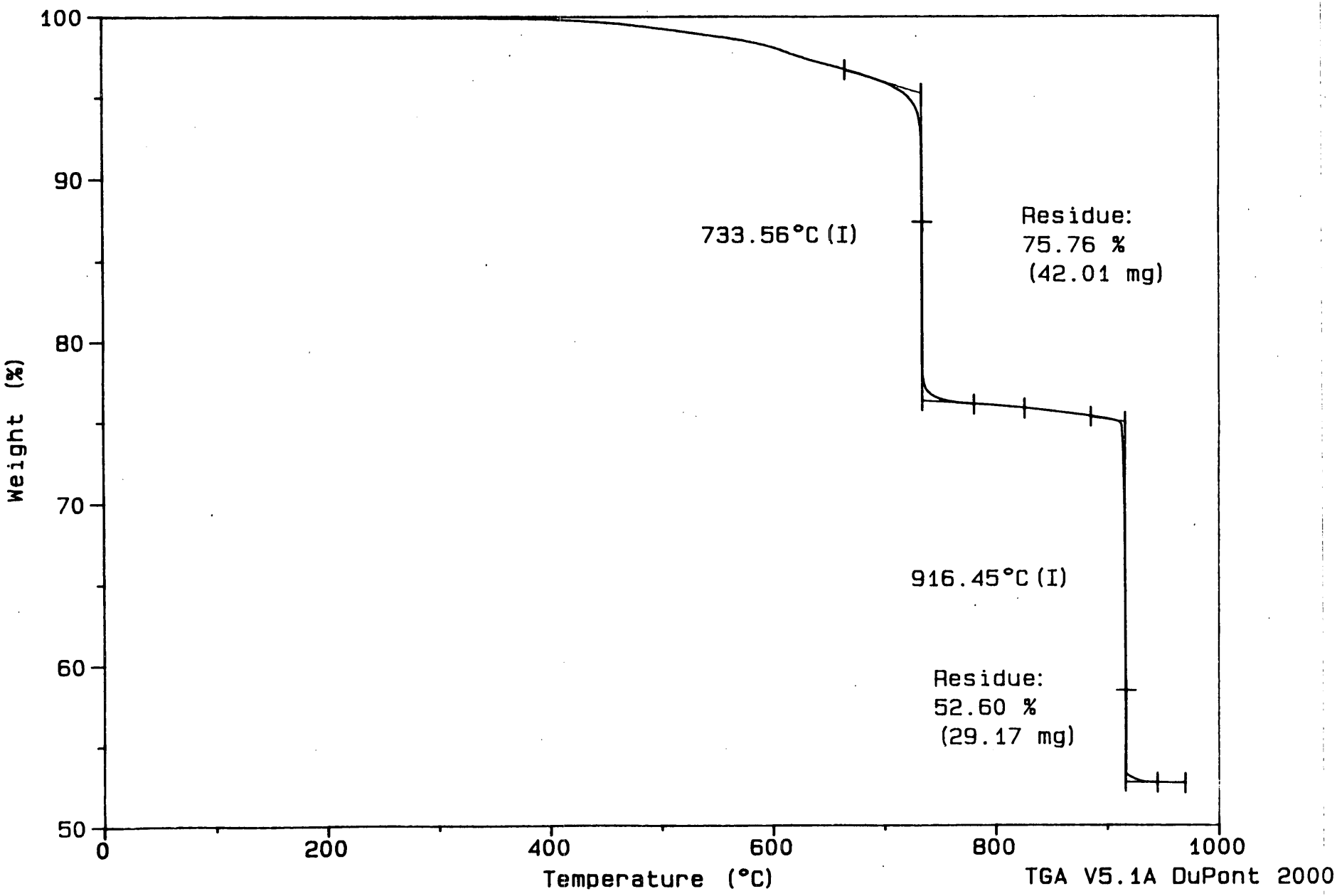

Figure 15, Appendix II. Thermal curve (CO_2 atmosphere) for Ced. Rap. Gray aggr

Sample: HR-337 TAN-SOUTH CEDAR RAPIDS
Size: 55.5050 mg
Method: 40 deg/min, Res 5, Eql 300
Comment: CO2 purge, 100 ml/min, sensit=1, deriv=1, Hi-Res TGA scan

TGA

File: C:SCOTTHR.019
Operator: J. AMENSON
Run Date: 27-Sep-91 13:27

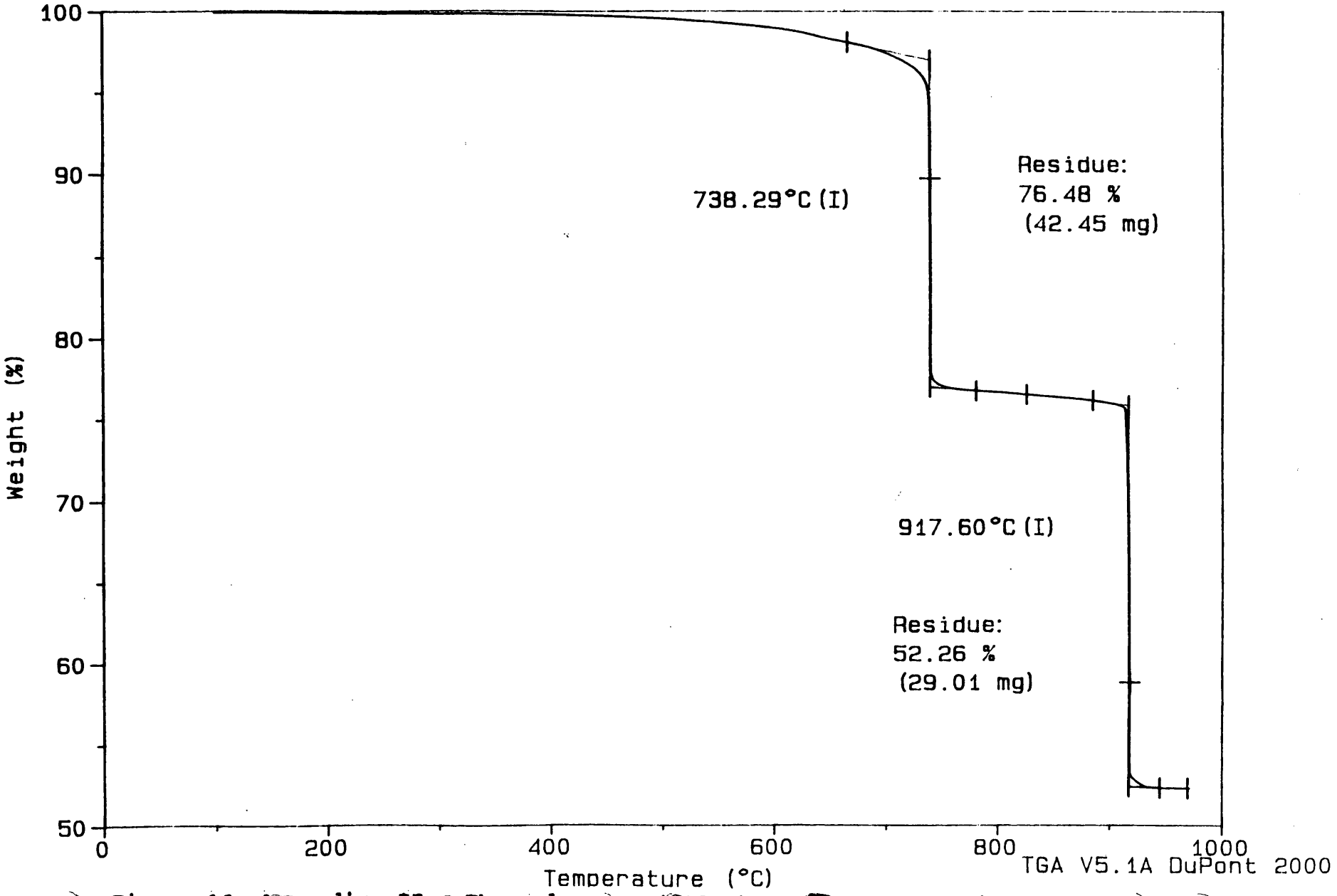

Figure 16, Appendix II Thermal curve (CO2 atmosphere) for Cedar Rapids Tar gr

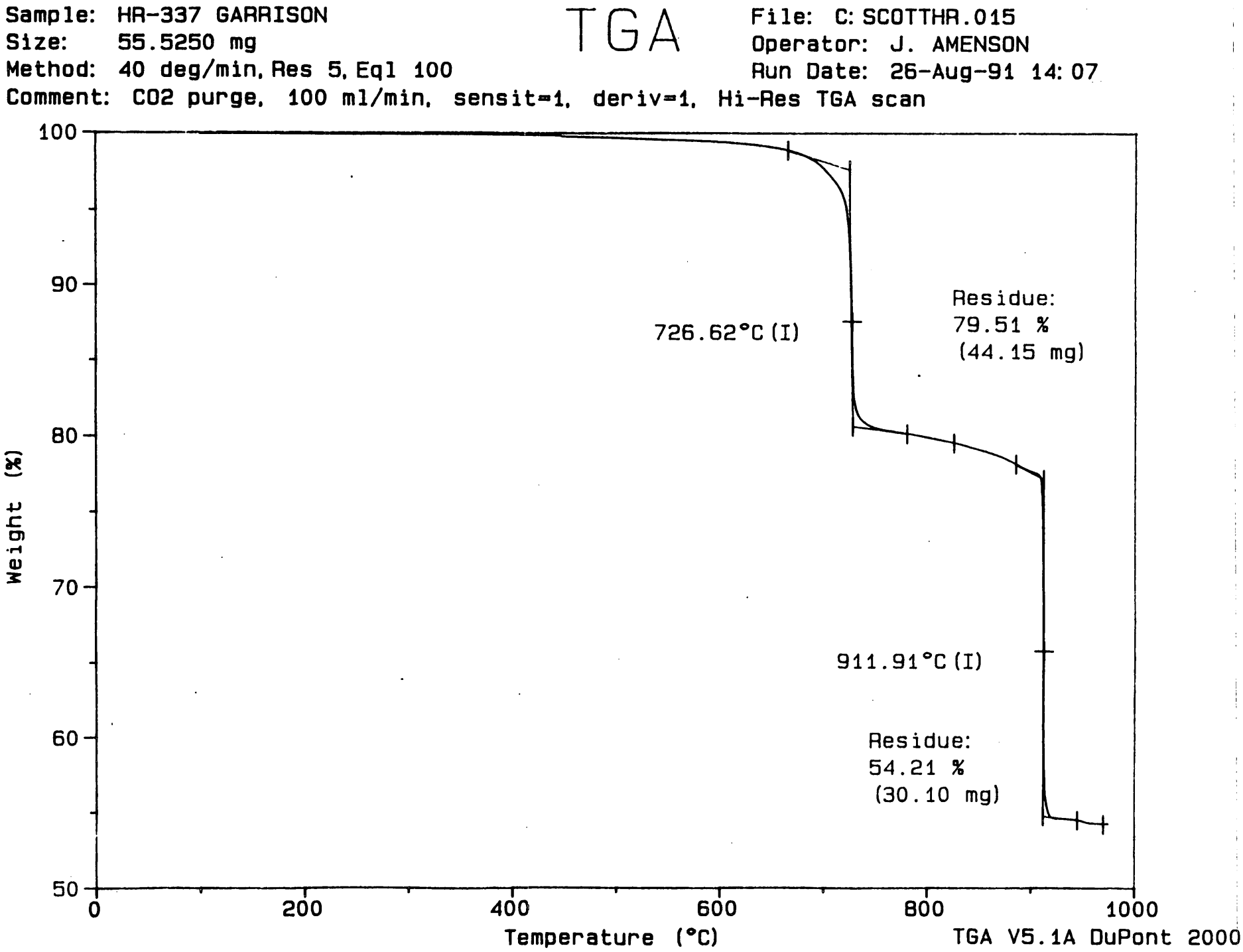

Figure 17, Appendix II. Thermal curve (CO_2 atmosphere) for Garrison aggregate.

Sample: HR-337 GASSMAN
Size: 55.4990 mg
Method: 40 deg/min, Res 5, Eql 300
Comment: CO2 purge, 100 ml/min, sensit=1, deriv=1, Hi-Res TGA scan

TGA

File: C:SCOTTHR.017
Operator: J. AMENSON
Run Date: 27-Sep-91 07:39

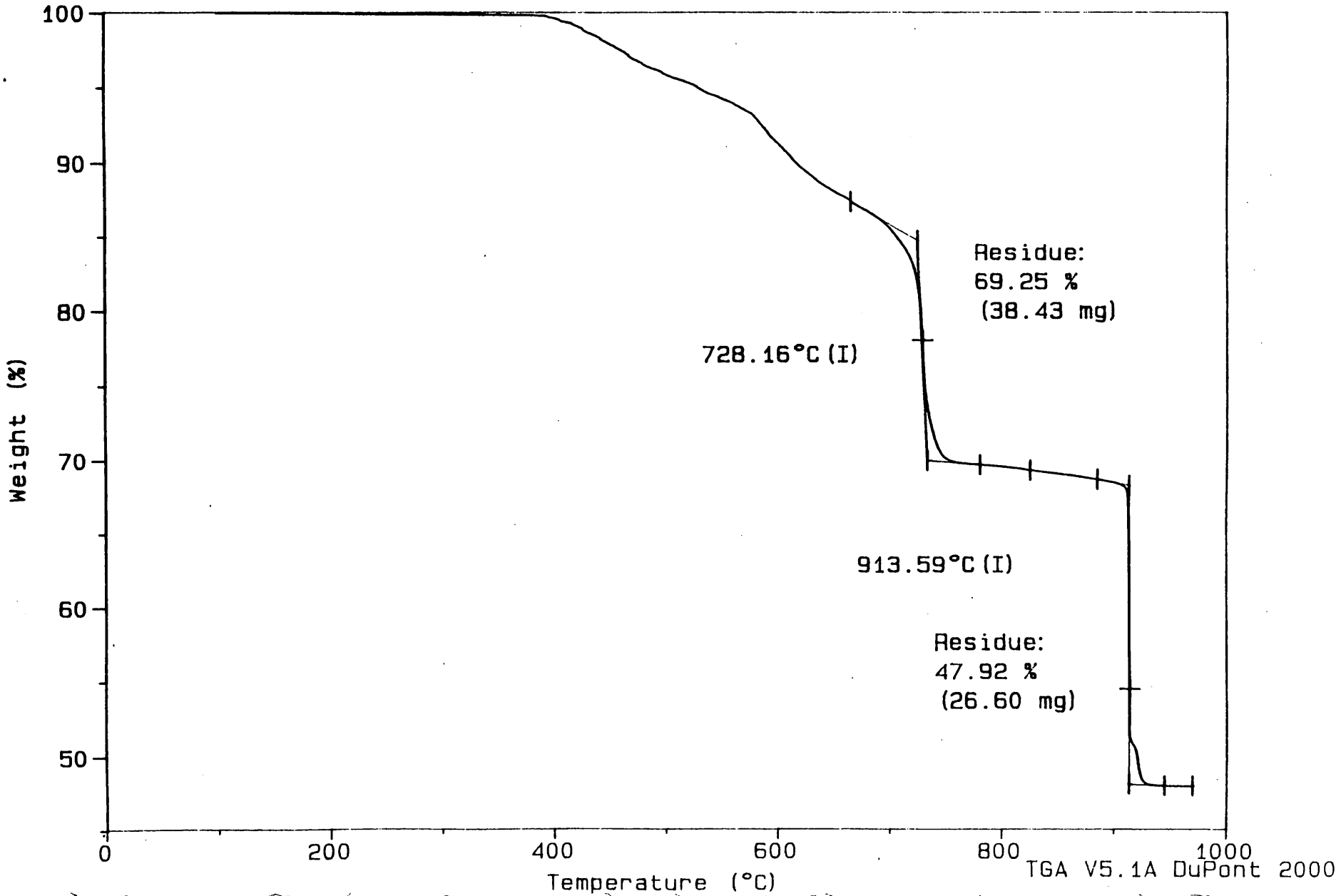

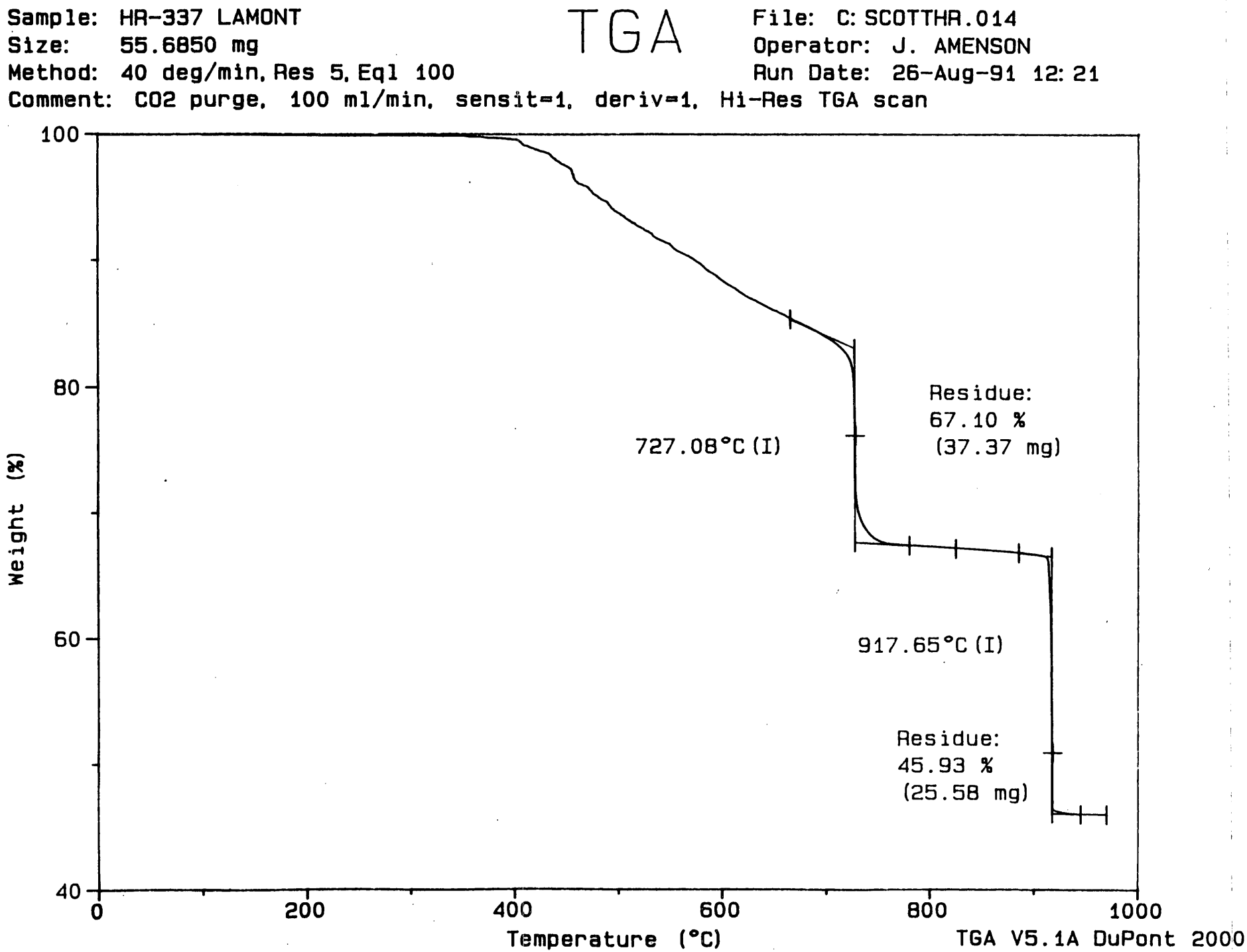

Figure 19, Appendix II. Thermal curve (CO_2 atmosphere) for Lamont aggregate.

Sample: HR-337 LE CLAIRE
Size: 55.4920 mg
Method: 40 deg/min, Res 5, Eql 300
Comment: CO2 purge, 100 ml/min, sensit=1, deriv=1, Hi-Res TGA scan

TGA

File: C:SCOTTHR.020
Operator: J. AMENSON
Run Date: 27-Sep-91 15:05

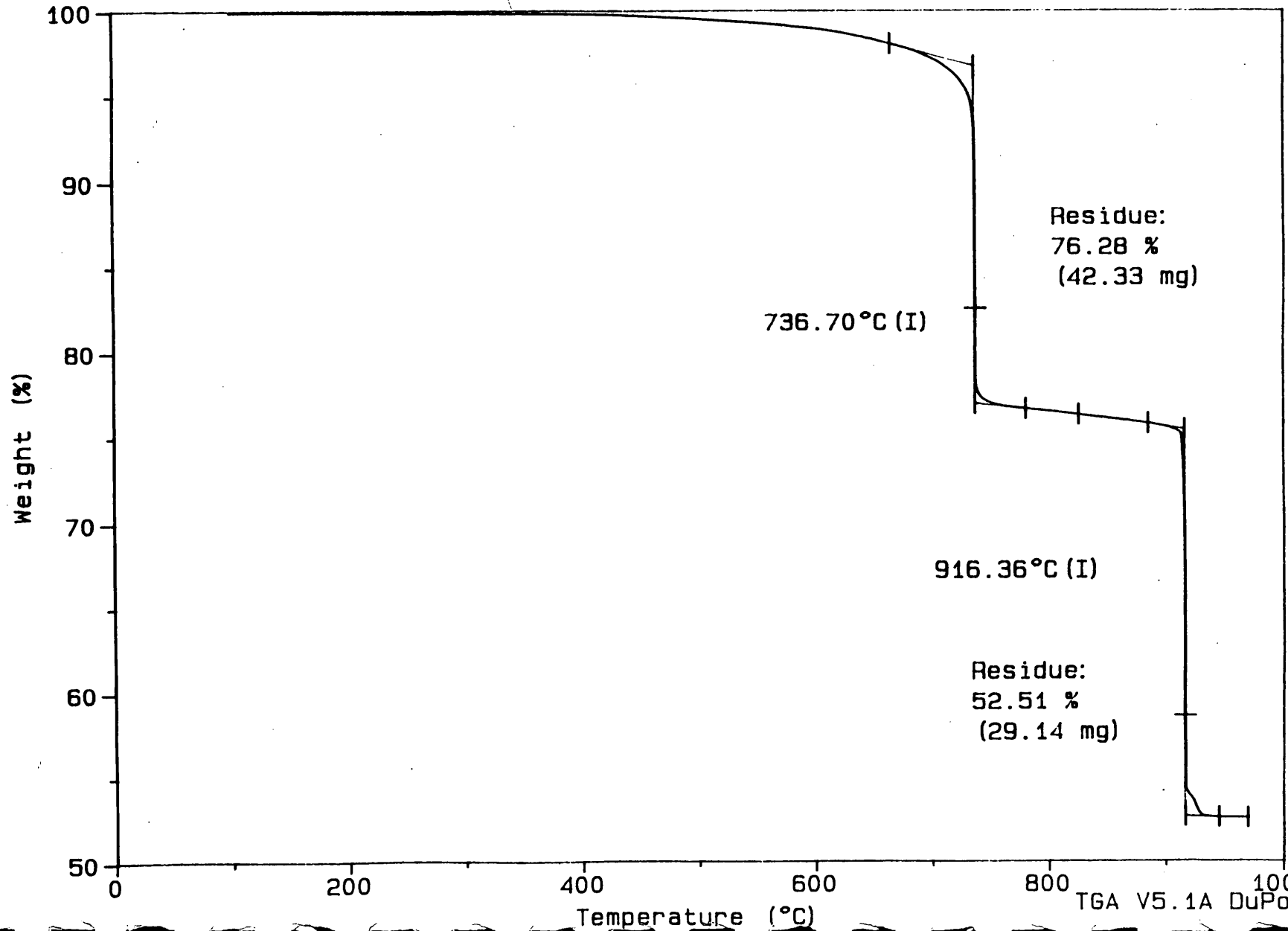

[redacted] Figure [redacted] Appendix [redacted] I. [redacted] thermal curve ([redacted] atmosphere) for [redacted] Lecture [redacted] aggregate. [redacted]

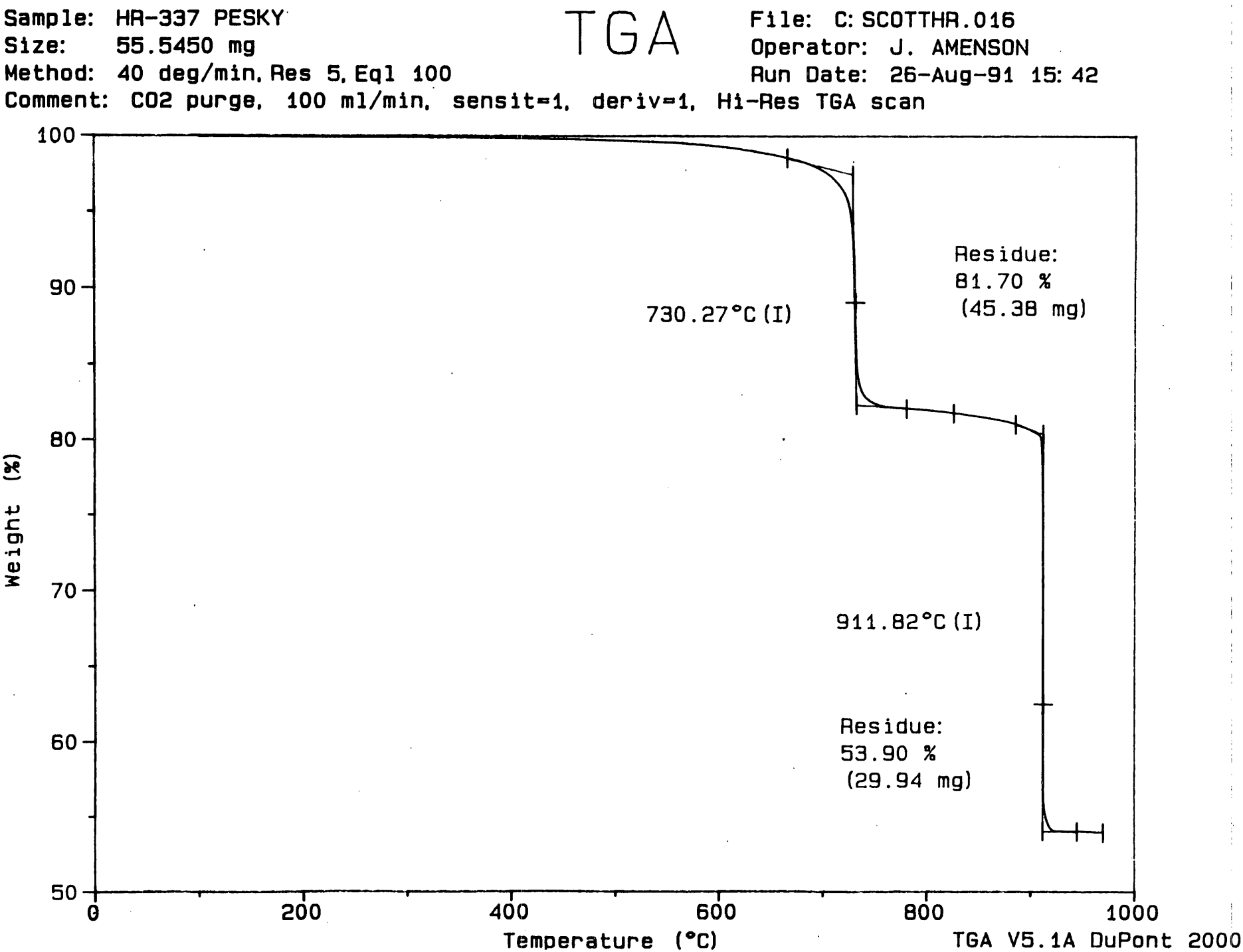

Figure 21, Appendix II. Thermal curve (CO_2 atmosphere) for Pesky aggregate.

Sample: HR-337 PLOWER
Size: 55.5040 mg
Method: 40 deg/min, Res 5, Eql 100
Comment: CO2 purge, 100 ml/min, sensit=1, deriv=1, Hi-Res TGA scan

TGA

File: C:SCOTTHR.001
Operator: J. AMENSON
Run Date: 23-Aug-91 09:40

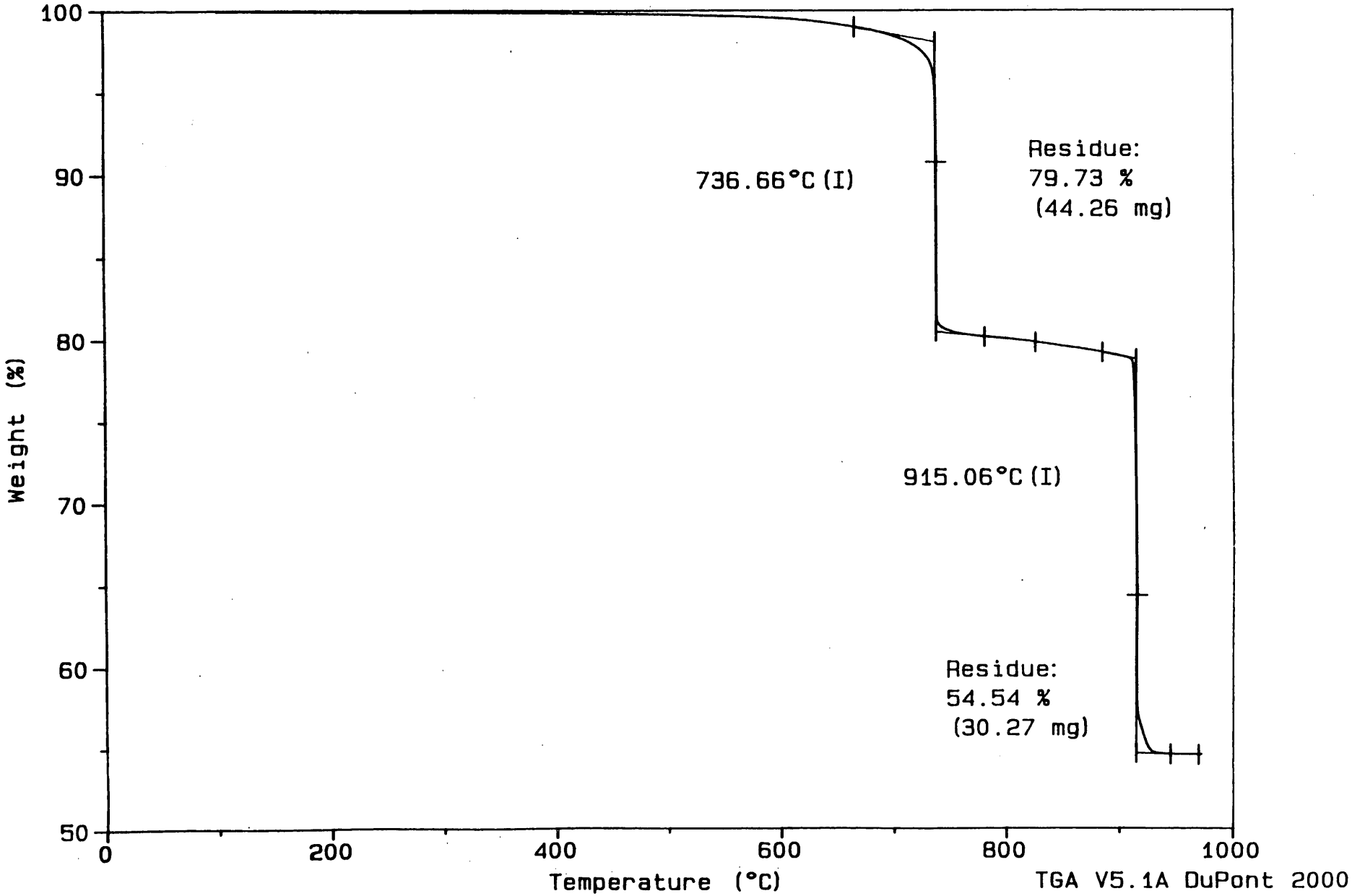

[redacted] Figure [redacted], Appendix II [redacted] The [redacted] 1 [redacted] e [redacted] 2 [redacted] sp [redacted] e) [redacted] P [redacted] r [redacted] reg [redacted].

APPENDIX III

Table 1, Appendix III. Correlation matrix for limestones and dolomites.

STAT. BASIC STATS	Correlations (hr337cor.sta) Marked correlations are significant at p < .05000						
Variable	SLIFE	DF	AINSOL	RELSIZE	DT_CAL_	LOSS	DT_DOL
SLIFE	1.0000 N=18 p= ---	.5271* N=18* p=.025*	-.5221* N=18* p=.026*	.7353* N=18* p=.001*	.4486 N=18 p=.062	-.7340* N=18* p=.001*	.4013 N=8 p=.324
DF	.5271* N=18* p=.025*	1.0000 N=18 p= ---	-.0886 N=18 p=.727	.5387* N=18* p=.021*	-.1037 N=18 p=.682	-.0879 N=18 p=.729	-.0051 N=8 p=.990
AINSOL	-.5221* N=18* p=.026*	-.0886 N=18 p=.727	1.0000 N=18 p= ---	-.1853 N=18 p=.462	-.4443 N=18 p=.065	.6901* N=18* p=.002*	-.1208 N=8 p=.776
RELSIZE	.7353* N=18* p=.001*	.5387* N=18* p=.021*	-.1853 N=18 p=.462	1.0000 N=18 p= ---	.2491 N=18 p=.319	-.4240 N=18 p=.079	.4966 N=8 p=.211
DT_CAL_	.4486 N=18 p=.062	-.1037 N=18 p=.682	-.4443 N=18 p=.065	.2491 N=18 p=.319	1.0000 N=18 p= ---	-.7361* N=18* p=.000*	.5166 N=8 p=.190
LOSS	-.7340* N=18* p=.001*	-.0879 N=18 p=.729	.6901* N=18* p=.002*	-.4240 N=18 p=.079	-.7361* N=18* p=.000*	1.0000 N=18 p= ---	-.5740 N=8 p=.137
DT_DOL	.4013 N=8 p=.324	-.0051 N=8 p=.990	-.1208 N=8 p=.776	.4966 N=8 p=.211	.5166 N=8 p=.190	-.5740 N=8 p=.137	1.0000 N=8 p= ---

Variables:

SLIFE	=	Service life in years
DF	=	Durability factor (ASTM C 666, method B)
AINSOL	=	Acid-insoluble residue (wt. %)
RELSIZE	=	Relative crystallite size (dimensionless)
DT_CAL	=	Calcite decomposition temperature (deg. C)
LOSS	=	Loss from 825 C to calcite decomposition temperature (wt. %)
DT_DOL	=	Dolomite decomposition temperature (deg. C)

Table 2, Appendix III. Correlation matrix for limestones (only).

STAT. BASIC STATS	Correlations (hr337cor.sta) Marked correlations are significant at p < .05000					
Variable	SLIFE	DF	AINSOL	RELSIZE	DT_CAL_	LOSS
SLIFE	1.0000 N=10 p= ---	.6841* N=10* p=.029*	-.8868* N=10* p=.001*	.6356* N=10* p=.048*	.7932* N=10* p=.006*	-.8738* N=10* p=.001*
DF	.6841* N=10* p=.029*	1.0000 N=10 p= ---	-.5895 N=10 p=.073	.6298 N=10 p=.051	.5613 N=10 p=.091	-.5065 N=10 p=.135
AINSOL	-.8868* N=10* p=.001*	-.5895 N=10 p=.073	1.0000 N=10 p= ---	-.6562* N=10* p=.039*	-.8266* N=10* p=.003*	.9355* N=10* p=.000*
RELSIZE	.6356* N=10* p=.048*	.6298 N=10 p=.051	-.6562* N=10* p=.039*	1.0000 N=10 p= ---	.7440* N=10* p=.014*	-.4969 N=10 p=.144
DT_CAL_	.7932* N=10* p=.006*	.5613 N=10 p=.091	-.8266* N=10* p=.003*	.7440* N=10* p=.014*	1.0000 N=10 p= ---	-.7421* N=10* p=.014*
LOSS	-.8738* N=10* p=.001*	-.5065 N=10 p=.135	.9355* N=10* p=.000*	-.4969 N=10 p=.144	-.7421* N=10* p=.014*	1.0000 N=10 p= ---

Variables:

SLIFE	=	Service life in years
DF	=	Durability factor (ASTM C 666, method B)
AINSOL	=	Acid-insoluble residue (wt. %)
RELSIZE	=	Relative crystallite size (dimensionless)
DT_CAL	=	Calcite decomposition temperature (deg. C)
LOSS	=	Loss from 825 C to calcite decomposition temperature (wt. %)
DT_DOL	=	Dolomite decomposition temperature (deg. C)

Table 3, Appendix III. Correlation matrix for dolomites (only).

STAT. BASIC STATS	Correlations (hr337cor.sta) Marked correlations are significant at p < .05000						
Variable	SLIFE	DF	AINSOL	RELSIZE	DT_CAL_	LOSS	DT_DOL
SLIFE	1.0000 N=8 p= ---	.5443 N=8 p=.163	-.4057 N=8 p=.319	.8960* N=8* p=.003*	.6887 N=8 p=.059	-.7173* N=8* p=.045*	.4013 N=8 p=.324
DF	.5443 N=8 p=.163	1.0000 N=8 p= ---	-.0966 N=8 p=.820	.3912 N=8 p=.338	.2357 N=8 p=.574	.0162 N=8 p=.970	-.0051 N=8 p=.990
AINSOL	-.4057 N=8 p=.319	-.0966 N=8 p=.820	1.0000 N=8 p= ---	-.1092 N=8 p=.797	.0596 N=8 p=.889	.5521 N=8 p=.156	-.1208 N=8 p=.776
RELSIZE	.8960* N=8* p=.003*	.3912 N=8 p=.338	-.1092 N=8 p=.797	1.0000 N=8 p= ---	.9011* N=8* p=.002*	-.7223* N=8* p=.043*	.4966 N=8 p=.211
DT_CAL_	.6887 N=8 p=.059	.2357 N=8 p=.574	.0596 N=8 p=.889	.9011* N=8* p=.002*	1.0000 N=8 p= ---	-.7242* N=8* p=.042*	.5166 N=8 p=.190
LOSS	-.7173* N=8* p=.045*	.0162 N=8 p=.970	.5521 N=8 p=.156	-.7223* N=8* p=.043*	-.7242* N=8* p=.042*	1.0000 N=8 p= ---	-.5740 N=8 p=.137
DT_DOL	.4013 N=8 p=.324	-.0051 N=8 p=.990	-.1208 N=8 p=.776	.4966 N=8 p=.211	.5166 N=8 p=.190	-.5740 N=8 p=.137	1.0000 N=8 p= ---

Variables:

SLIFE	=	Service life in years
DF	=	Durability factor (ASTM C 666, method B)
AINSOL	=	Acid-insoluble residue (wt. %)
RELSIZE	=	Relative crystallite size (dimensionless)
DT_CAL	=	Calcite decomposition temperature (deg. C)
LOSS	=	Loss from 825 C to calcite decomposition temperature (wt. %)
DT_DOL	=	Dolomite decomposition temperature (deg. C)